1. Report No.	2. Government Accession No.	3. Recipient's Catalog No.

4. Title and Subtitle	5. Report Date
FAST TRACK PAVING: CONCRETE TEMPERATURE CONTROL AND TRAFFIC OPENING CRITERIA FOR BONDED CONCRETE OVERLAYS Volume I - Final Report	
	6. Performing Organization Code

7. Author(s) B. Frank McCullough and Robert Otto Rasmussen	8. Performing Organization Report No.

9. Performing Organization Name and Address Transtec, Inc. 1012 East 38 ½ Street Austin, TX 78751	10. Work Unit No.
	11. Contract or Grant No. DTFH61-93-C-00106

12. Sponsoring Agency Name and Address Office of Engineering and Highway Operations R&D Federal Highway Administration 6300 Georgetown Pike McLean, VA 22101-2296	13. Type of Report and Period Covered Final Report - October 1993 to January 1998
	14. Sponsoring Agency Code

15. Supplementary Notes
Contracting Officer's Technical Representative: Stephen W. Forster, HNR-20

16. Abstract

It has been theorized that early-age behavior due to temperature and moisture changes can significantly affect the performance of a Portland cement concrete pavement (PCCP) or bonded concrete overlay (BCO) over its service life. During the first 72 hours following placement, the strength of PCC is relatively low in comparison to the strength that it will eventually achieve. During this "early-age" period, critical stresses can develop which may lead to pavement damage, and ultimately, a loss of performance.

This research focuses on modeling early-age behavior of both concrete pavements and bonded concrete overlays subjected to stresses from moisture and thermal changes. It includes the development of a two-part, versatile, comprehensive set of guidelines which provide direction in the proper selection of design and construction variables to minimize early-age damage to the PCCP and BCO. The first part of these guidelines is qualitative in nature and is based upon the results of this effort, past experience, and engineering judgment. They are intended to identify design and construction inputs which are most likely to lead to good behavior during the early-age period.

The second part of the guidelines is comprised of many complex models which have been developed to predict early-age behavior in jointed plain concrete pavements and bonded concrete overlays. These models are used to verify good behavior from the selection of inputs made using the qualitative guidelines. These models include a PCC temperature development model which accounts for heat generation from the hydrating paste, solar insolation, surface convection, irradiation, and dynamic specific heat and thermal conductivity values. Several mechanical properties are also modeled including thermal coefficient of expansion, drying shrinkage, creep, strength, and modulus of elasticity (using maturity methods). Finally, restraint to free movement due to slab-base friction and curling are modeled directly.

The end product from this research is a comprehensive software package termed HIgh PERformance PAVing (HIPERPAV). This package, which incorporates the complex models developed, can be used as a stand-alone product to verify the overall effect of specific combinations of design, construction, and environmental inputs on early-age behavior of a PCCP and BCO. This report serves as the final report for this project. This report is the first in a series. The other report in the series is:

FHWA-RD-98-###: HIPERPAV User's Manual

17. Key Words High Performance Concrete Pavements; Fast Track; Bonded Concrete Overlay; Jointed Concrete Pavement; Early Age; HIPERPAV; HIPERBOND; Mechanistic and Mechanistic-Empirical Models; Temperature; Heat of Hydration; Slab; Shrinkage; Relaxation Creep; Thermal Expansion; Slab Base Friction; Curling; Warping; Plastic Shrinkage; Cracking; JCP; JPCP; Delamination; BCO; PCCP; Debonding; Cement	18. Distribution Statement No Restrictions. This document is available to the public through the National Technical Information Service; Springfield, Virginia 22161

19. Security Classif. (of this report) Unclassified	20. Security Classif. (of this page) Unclassified	21. No. of Pages 204	22. Price

Form DOT F 1700.7 (8-72)   **Reproduction of completed page authorized**

TABLE OF CONTENTS

TABLE OF CONTENTS
(CONTINUED)

TABLE OF CONTENTS
(CONTINUED)

TABLE OF CONTENTS
(CONTINUED)

LIST OF FIGURES

LIST OF FIGURES
(CONTINUED)

LIST OF TABLES

SUMMARY

It has been theorized that early-age behavior due to temperature and moisture changes can significantly affect the performance of a Portland cement concrete pavement (PCCP) or bonded concrete overlay (BCO) over its service life. During the first 72 hours following placement, the strength of PCC is relatively low in comparison to the strength that it will eventually achieve. During this "early-age" period, critical stresses can develop which may lead to pavement damage, and ultimately, a loss of performance.

Most existing stress and strength models are too simplistic for practical application due to their inherent assumptions. These models generally fail to account for complex interactions between the numerous mechanisms involved, resulting in a significant loss of accuracy. A more accurate predictive tool for this type of pavement analysis would consider the large number of factors that determine stress and strength development, and allow easy entry of a range of inputs for each factor.

This research focuses on modeling early-age behavior of both concrete pavements and bonded concrete overlays subjected to stresses from moisture and thermal changes. It includes the development of a two-part, versatile, comprehensive set of guidelines which provide direction in the proper selection of design and construction variables to minimize early-age damage to the PCCP and BCO. The first part of these guidelines is qualitative in nature and is based upon the results of this effort, past experience, and engineering judgment. They are intended to identify design and construction inputs which are most likely to lead to good behavior during the early-age period.

The second part of the guidelines is comprised of many complex models which have been developed to predict early-age behavior in jointed plain concrete pavements and bonded concrete overlays. These models are used to verify good behavior from the selection of inputs made using the qualitative guidelines. These models include a PCC temperature development model which accounts for heat generation from the hydrating paste, solar insolation, surface convection, irradiation, and dynamic specific heat and thermal conductivity values. Several mechanical properties are also modeled including thermal coefficient of expansion, drying shrinkage, creep, strength, and modulus of elasticity (using maturity methods). Finally, restraint to free movement due to slab-base friction and curling are modeled directly.

The end product from this research is a comprehensive software package termed HIgh PERformance PAVing (HIPERPAV). This package, which incorporates the complex models developed, can be used as a stand-alone product to verify the overall effect of specific combinations of design, construction, and environmental inputs on early-age behavior of a PCCP and BCO.

CHAPTER 1   INTRODUCTION

As traffic on the highway system continues to increase, the need for durable pavements that minimize user costs during initial construction and throughout the service life has become more apparent. The need for durable pavements that minimize user costs during initial construction and throughout the service life is much greater under high traffic conditions. An effective way of minimizing user costs is through the application of principles for expediting ("fast tracking") the construction of PCC pavements. Expeditious construction techniques are especially applicable when an existing PCC pavement operating at or near traffic capacity is a candidate for a Bonded Concrete Overlay (BCO). It is important in these cases that the closure time be kept to a minimum. Considering the significance of expediting construction of PCC pavements and BCOs, a consolidation of knowledge that allows for an understanding of all the factors involved in this process is essential. This consolidation of knowledge becomes more important considering there is a growing body of information and experience that indicates that conditions during the initial construction and curing periods are critical in establishing the future performance characteristics of PCC pavements.

The goal of this study is to develop a set of tools which can be used to more effectively guide the engineer prior to and during construction. These tools include both a written set of guidelines as well as corresponding computer software that can assist in the design and construction of high performance PCCP. This chapter will highlight the background which led to the initiation of this study and outline the methods by which the goals of this study have been accomplished.

1.1   Background

The rapid traffic buildup on an aging highway system has resulted in a need for major rehabilitation at all functional levels of pavement, i.e., primary, secondary, and local. PCC pavement is capable of providing the long term durability and reduced maintenance costs needed to meet these growing demands and shrinking resources. The use of PCC pavement for upgrading the system includes building new pavements or placing BCOs directly over existing PCC pavements. In both cases, it is essential that "fast track" construction be executed in a rapid and efficient manner, without any compromise in pavement quality.

As a result of the increased attention being given to user delay cost and life cycle cost (LCC) analysis procedures, pavement rehabilitation strategies that require minimum closure time are selected more frequently. This offers a new challenge and opportunity for traditional concrete pavement construction practices. Traditionally, construction specifications have required a minimum curing period of 7 to 14 days before a concrete pavement can be opened to traffic, regardless of the concrete's strength. In areas where congestion is heavy, there is a great need to expedite the construction process to minimize traffic delay and user costs. However, expediting concrete pavement construction requires new research into concrete's response to curing conditions. This study represents a significant advance in this area.

The most detrimental effects of climatic conditions occur at extreme temperature conditions, specifically, greater than 32°C (90°F) in hot weather, and less than 4°C (40°F) in cold weather, commonly termed "hot weather concreting" and "cold weather concreting," respectively. It is at these extreme temperatures that the potential for large temperature changes in the pavement exist, which can lead to undesirable performance. The design and construction of PCC pavements should consider the possible effects of both lower and higher than normal curing temperatures on concrete properties and pavement behavior at early ages. Methods should be made available for evaluating pavement behavior due to these conditions. This report is confined primarily to examining "hot weather concreting" conditions, although consideration will also be given to "cold weather concreting" conditions. The emphasis on "hot weather concreting" is due to the rapid heat generation from cement hydration during the construction and curing period. These high slab temperatures then cause large temperature decreases during the first ambient temperature cycle. Large stresses are generated throughout the PCC slab from the large slab temperature differentials and the compounding effect of increased moisture changes (i.e., shrinkage). With this approach, it will also be possible to accurately model PCC slab temperature changes experienced during the curing period by predicting the slab temperature at final set.

1.2   Research Approach

This section outlines the research undertaken for this project. The objectives that served as the focus of the work accomplished are first identified. The significance of the work is then highlighted, followed by an outline of the research plan.

1.2.1   Research Objectives

The primary objectives of this research project are as follows:

1. To provide practical and implementable guidelines for the control of concrete temperature during the curing process of PCC pavement,

2. To provide guidelines for monitoring bond stresses and bond strength criteria to prevent pavement delamination and for the determination of the time for opening to traffic of newly constructed BCOs, and

1.2.2   Research Significance

In order to construct high quality pavements, measures must be taken to minimize the negative effects of many different factors including environmental, materials, design, and construction related items. Portland Cement Concrete pavements are especially vulnerable during early-ages due to the nature of the materials used in the concrete. Since the potential for

2

early-age damage of these types of pavements is significant, the need exists for a tool to predict PCCP behavior. In the past, rules-of-thumb and other general design and construction guidelines have been, at best, inconsistent in decreasing the potential for early-age damage. Such guidelines should include the ability to account for each of the factors affecting PCCP behavior, and make reliable and accurate recommendations to minimize early-age damage.

1.2.3   Research Plan

The scope of this research project involves two important areas for expediting construction and rehabilitation of PCC pavements. The first of these refers to temperature management during the initial curing period prior to opening the pavement to traffic. The objective is to either maintain, increase or decrease the concrete's early age setting and curing temperature within acceptable limits to obtain the desired results. The second area of this research focuses on the development and maintenance of bonding between an existing concrete pavement and a BCO. The objective here is to develop new techniques or refine existing techniques for measuring bond strength in both the laboratory and field. The intent of this study is to develop guidelines for engineers on the design and construction of concrete pavements and bonded concrete overlays.

The research undertaken for this project involved the development and assembly of models which can predict each of the subsystems involved in the development of stresses and strength in early age PCC pavements. Each of the models is described in detail along with the reasons for their respective selection among other alternatives. The models were integrated into user-friendly computer software that maximizes the potential benefits of utilizing the selected models. Guidelines for the selection of appropriate inputs to the comprehensive model as well as a framework for an early-age PCCP construction monitoring system are described.

In order to accomplish the primary study objective, the following tasks were executed during this research project:

1. *Select the Important Distress Types* - Different areas of the country may be more susceptible than others to certain distress types. If a particular area has experienced a negligible level of one particular distress type, little emphasis needs to be placed on controlling that distress type during construction. Some distresses are more prevalent than others overall, therefore the most common distresses should be investigated in more detail.

2. *Predict the Occurrence of the Distress via Modeling* - Models which can be used to predict the occurrence and manifestation of the selected distress types must be selected. In order for these models to be accepted universally, they should be mechanistic-empirical in nature. This ensures flexibility and adaptability for local conditions. The selected models should also be robust enough to capture the important elements leading to the selected distress.

3. *Reverse Procedure for Analysis* - In order to determine how to design and construct a high performance PCCP or BCO, the steps outlined immediately above must be reversed. In other words, a desired level of performance is selected first. This performance level then becomes the target to be achieved by the models. If a particular set of selected conditions (inputs)

produce results that meet or exceed the desired level of performance through modeling, they are flagged as being a possible set of conditions to use for design and construction. If the opposite is true and the trial set of conditions are predicted to cause poor performance, the set of inputs is rejected as a potential candidate.

4. *Guideline Formulation* - The final step in accomplishing the goal of achieving high performance pavements is to incorporate the above steps into an easy-to-use and robust set of guidelines. The results of this study are presented in the form of a set of written general guidelines and a computerized set of verification guidelines.

1.3   Report Objectives

The following are objectives for the development of this report:

1. *Document the Research Effort* - This research includes the development of both qualitative guidelines as well as quantitative verification guidelines including models related to the early-age behavior of PCCP and BCO.

2. *Document Software Development and Use* - Two software packages, HIPERPAV (HIgh PERformance PAVing) and HIPERBOND (HIgh PERformance BONDed concrete overlays), were also developed as part of this project. Their development and proper application is also documented.

3. *Document Calibration and Validation Efforts* - In order to ensure reliability of the final product, calibration and validation efforts related to this research are documented.

4. *Provide an Implementable Product* - In order to ensure implementability, efforts have been made at each stage of the guideline and report development to maintain readability and clarity.

1.4   Report Scope and Format

The intent of this report is to fulfill the objectives described in the previous section. To accomplish this, the report has been structured in a modularized format so that each chapter can serve as a stand-alone document. The continuity of the report, however, has not been diminished.

Chapter 2 will present the basic principles of PCCP and BCO behavior in the early-age period. The detrimental effects of climatic conditions on pavement performance will be discussed. Specific distress types and their causes will be introduced in addition to a description of the hydration process that occurs during the early-age period. A discussion of the properties affecting PCCP and BCO performance will then follow. This section will include the behavior effects due to heat development, moisture loss, and aggregate type in the early-age PCCP and

BCO. Finally, the effect of environmental influences on PCCP and BCO behavior and performance will be described. This discussion will include a characterization of all of the primary environmental-related factors as well as modeling basics.

The qualitative written guidelines for minimizing damage to early-age PCCP and BCO are found in chapter 3. The guidelines are divided into four areas. The first is a set of PCC materials-related guidelines in which recommendations are made regarding the proper selection of aggregates, cement, admixtures, and mix design proportioning. The impact on behavior and performance from the selection of various alternatives is discussed. The second type of guidelines is related to environmental factors. Temperature, relative humidity, and other critical environmental factors are discussed concerning their impact on an early-age PCCP or BCO. Construction-related guidelines are also included, with sections related to the opening age criteria of fast-track PCCP and BCO, the curing method used, time of day of construction, and initial mix temperature. Finally, guidelines specific to the design of a PCCP and BCO including surface type, thickness, and subbase type are described. These guidelines should be used to minimize the potential for early-age damage, and a subsequent loss in overall performance. They may be used as a stand-alone document from which final recommendations can be made for PCCP and/or BCO design and construction. They also may be used in order to develop a set of trial inputs to enter into either the HIPERPAV or HIPERBOND verification guidelines.

Chapter 4 describes in detail the theory used in developing the HIPERPAV and HIPERBOND systems. Models for various components characterizing the early-age behavior of PCCP and BCO are described along with the logic for their selection among other alternatives. The models described include an early-age temperature prediction model for PCCP accounting for heat of hydration as well as other environmental effects. A thermal coefficient of expansion model for early-age PCC is also described as well as a model to predict drying shrinkage strains. Stress models related to both axial restraint due to slab-base friction as well as curling are then described. Relaxation creep is also included by adjusting the modulus of elasticity value. A strength model is then outlined, and the procedure by which the resulting values are compared to the critical stress levels is discussed. BCO bond stress and strength prediction models are derived. Finally, calibration of the models is discussed.

Chapter 5 describes conclusions derived from this study as well as recommendations for future improvements to the guidelines and the models within the HIPERPAV and HIPERBOND systems.

Several appendices follow which elaborate on many of the concepts described throughout this report as well as present the findings from the laboratory and field evaluations undertaken during this project.

CHAPTER 2   PRINCIPLES OF EARLY-AGE PCCP AND BCO BEHAVIOR

This chapter discusses some of the principal concepts regarding the early-age behavior of PCCP and BCO. These concepts relate to the design, construction, materials, and environmental parameters associated with these types of pavements.

2.1   Detrimental Effects of Climatic Conditions on Pavement Performance

A study of the detrimental effects of slab temperature and gradient on PCC pavements due to curling stresses and thermal shock must begin by defining the distress types associated with their occurrence. The problem should be further specified by identifying the critical period during which the distresses may originate. Since the primary reason for early distress is that the stress on the pavement exceeds its strength, the mechanical state of stress producing the distress mechanism must also be outlined.

2.1.1   Associated Distress Types

The scope of this project is confined to those factors and variables occurring during the concrete curing period that affect long term pavement performance. For example, fatigue cracking, corner breaks, and punchouts are distresses that occur as a result of loads applied after full concrete strength has been achieved. Therefore, these distresses are not of major concern in this study. Obviously, fast track construction scheduling should limit early application of loads resulting in early age stress to avoid a negative impact on pavement life. Therefore, this type of load is not of direct concern in this study.

A wide body of information has been developed relative to the behavior of PCC during its early curing stages, and this information is drawn upon for this study. However, it is recognized that BCOs are a special case and the nature of their performance may compound the problems.

The authors' inspection of various types of PCC pavements, i.e., Jointed Concrete Pavements (JCP), Continuously Reinforced Concrete Pavements (CRCP), and Prestressed Concrete Pavements (PCP), on construction projects in various parts of the United States and in foreign countries provides a wide variety of experience from which to draw. Also, when inspecting concrete pavements throughout the world, it has become apparent that in many cases there are long sections that perform exceptionally well directly adjacent to areas where extensive early age distress occurs using the same aggregates, mix designs, etc. On recent projects in Texas, similar observations on all three concrete pavement types during the early curing and their subsequent service life have resulted some interesting occurrences.

Figure 1 describes, in general, some observations collected during early curing period, service period, and failure period by presenting a graphical description of the detrimental effects

of slab temperature and moisture changes. The horizontal axis is time, with three periods represented: the initial curing period, the good performance period, and the marginal to poor performance period (failure). The curing period in this instance is defined as the first 72 h after placement, and the good performance period is defined as the time from the initial traffic opening until excessive deterioration is experienced. This may be from 10 to 40 years depending on various factors. The marginal or poor performance period occurs when extensive repairs and overlays are being performed.

In the vertical direction, the distress severity increases, moving from top to bottom of the figure. Figure 1a presents a condition where excellent control or "favorable climatic circumstances" exist during the early curing period. In this case, no detrimental cracking is observed. The joints are sawed as represented in the second phase, and no distress is observed. During the third phase, typical distresses might be observed on a rigid pavement that has extended beyond its structural life. However, the pavement is still satisfactory from a functional standpoint, i.e., serviceability or riding quality.

Figure 1b presents a plan view where poor control and/or extreme environmental conditions exist. In this case, plastic shrinkage cracks occur due to rapid drying of the fresh concrete, since the rate of water loss from the surface exceeds the rate of available bleed water. A variety of causes may contribute to plastic shrinkage cracking such as segregation-induced bleeding, poor mix design or loss of water to the subgrade. It is assumed most of these cases can be corrected by proper mix design. The primary concern here is to quantify the external factors resulting in plastic shrinkage cracking in terms of temperature and moisture changes. During the "good service period," the plastic shrinkage cracking may not be detrimental, but surface deterioration may still occur. In the "wearout period," patching will probably be required.

Figure 1c demonstrates a situation where very poor control is exercised or extreme conditions of temperature change and moisture loss result in thermal shock to the pavement. In this case, random, or "craze," cracking occurs over the surface of the pavement prior to the time when joints are sawed. These cracks are generally very narrow in width, but can still be observed by the naked eye. On some projects, the extreme climatic conditions can dominate all other variables which contribute to this random cracking. For example, on a recent project in Houston, Texas where various experimental test sections with varying steel percentages and aggregate types were used, the cracking due to thermal shock was independent of all other pavement variables. It was dependent only on the moisture and temperature changes. During the second or "good service period" phase, there is rapid deterioration of the pavement when traffic is applied. Many areas experience corner breaks, cracks, and punchouts requiring extensive patching and providing reduced service life. Generally, by the third phase, an overlay is required.

Figure 1d illustrates another set of poor control or detrimental climatic conditions that affect the pavement. In this case, an edge view of the pavement is provided. As studies have shown, very fine horizontal cracking occurs at random depths below the surface.[1] This is not visible to the naked eye, and can be discovered only by coring. In the second phase, the impact is not readily apparent, but during the third phase extensive spalling is experienced at the joints and at cracks that extend down to the horizontal cracks. In these cases, extensive repairs or an overlay may be required.

Not to Scale

(a) *Plan View Good Temperature & Moisture Control*

Pavement Edge

Transverse Joints

Figure 1a. Excellent Control and Good Service Life.

(b) *Plan View Plastic Shrinkage Cracking*

Plastic Shrinkage Cracking

Patches

Figure 1b. Poor Control and Fair Service Life.

Legend

▨	Failures
▢	Patches
▨	ACP Overlay

(c) *Plan View Thermal Shock Cracking*

ACP Overlay

Failures

Patches

Figure 1c. Very Poor Control and Poor Service Life.

(d) *Edge View Horizontal Cracking*

Horizontal Micro Cracks

Spalls

Figure 1d. Very Poor Control and Poor Service Life.

Initial Curing Period	Good Service Period	Wearout Period
First 72hours after placement	72 hrs to 10 - 40 years	10 - 40 years to 15 - 45 years

Figure 1. Detrimental effects of slab temperature and moisture changes on the service life of Portland cement concrete pavement.

Figure 2 is a graphical description of the additional detrimental effects of slab temperature and moisture changes applicable only to the service life of BCOs. Again, figure 2a shows a scenario where full bond is obtained at the interface, and no distress is observed during the curing period. In this case, the pavement provides excellent service life. In figure 2b, climatic or surface conditions exist such that the concrete overlay separates from the existing pavement, i.e., delamination. This condition generally starts at the edge and follows cracks or joints in the pavement. During the initial life of the pavement, the impact is not detrimental, but eventually failures will be noted and patches will be required as shown on the right side of figure 2b.

Figure 3 presents typical distress histories for new PCC pavements and BCOs for varying conditions of field control. Figure 3a may be associated with figures 1a, 1b and 1c, etc. The gray line in this figure shows the cracking, whereas the solid line shows the failures and patches. For the excellent control conditions, there is no cracking, but for the poor and very poor conditions, various levels of cracking occur during the first 72 h after placement as indicated by the gray lines. The pavement experiencing thermal shock, fails prematurely, and requires patching very rapidly. The pavement constructed under good control conditions provides a long service life and does not develop failures until after the design life is achieved. 72 h has been shown from experience to be the time period during which early-age distresses usually develop. After the first 72-h period, it has been found (both from experience and from modeling) that the early-age effects (hydration and rapid strength gain) become minimal.

Figure 3b presents the information that may be associated with the horizontal cracking shown in figure 1d. In this case, the gray line represents horizontal cracking, and the solid line represents spalling and repairs. Again, where good control conditions exist, no horizontal cracking is experienced; whereas if cracking is experienced during poor control and environmental conditions then spalling occurs during the entire life of the pavement, requiring extensive repairs. Alternatively, during good control and environmental conditions, spalling may or may not occur in the pavement. Figure 3c presents delaminations and failures at all levels of quality control on a BCO.

In summary, when conditions labeled as "poor quality control or extreme climatic conditions" are experienced during the curing period, poor to very poor performance may result during the life of the pavement. When "good control or favorable environmental conditions" exist at the time of placement, then excellent performance is achieved that may extend well beyond the design life. It is, therefore, imperative that a complete understanding of the pavement's response, resulting from these conditions, be identified and mathematically modeled. After this understanding is defined, meaningful guidelines can be established to minimize the potential for early-age PCCP damage.

2.1.2   *Critical Period*

Figure 4a, presents a plot of structural rigidity or degree of set for the PCC as a function of time, and may be used to describe the critical period. In the field, the term "initial set" and

Cross Sections

Plan Views

(a)

Concrete Overlay

Existing Pavement

Subbase

Transverse Joints

Figure 2a. Good Control and Service Life.

(b)

Delamination

Concrete Overlay

Existing Pavement

Subbase

Edge of Delamination

Delamination

Patches

Figure 2b. Poor Control and Poor Service Life.

Figure 2. Detrimental effects of slab temperature and moisture changes on the service life of bonded concrete overlays.

11
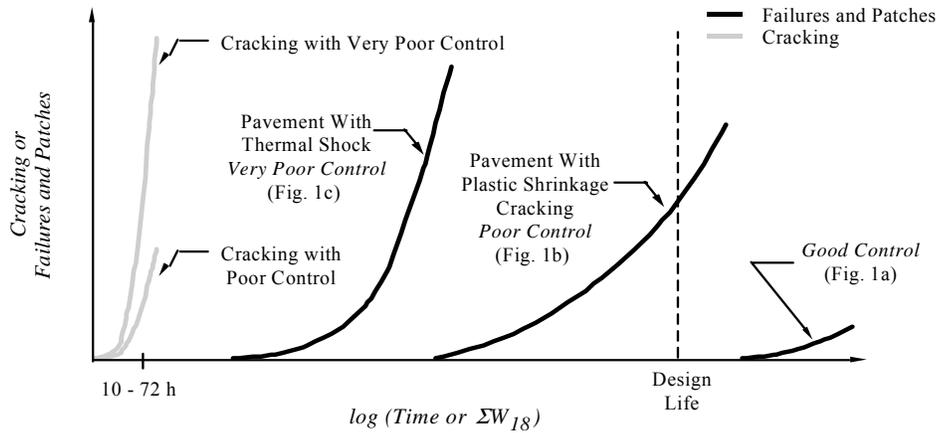
Figure 3a. Cracking History for Very Poor, Poor, and Good Control Conditions from Figure 1.
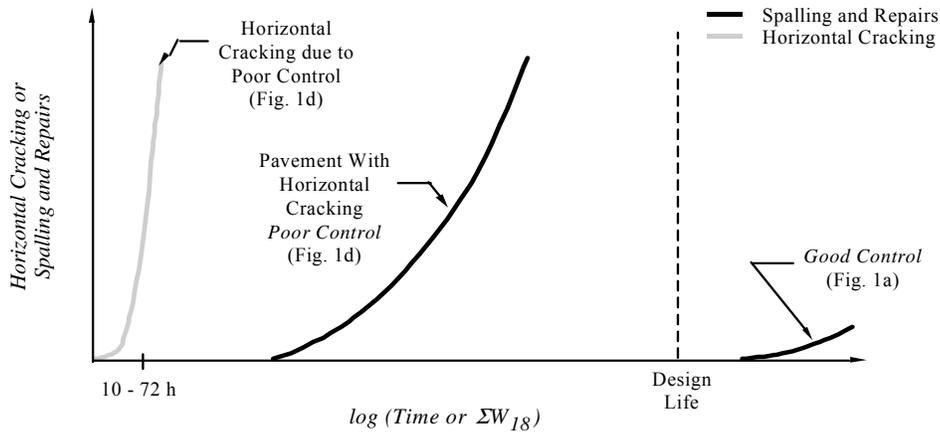
Figure 3b. Horizontal Cracking History for Very Poor, Poor, and Good Control Conditions from Figure 1.
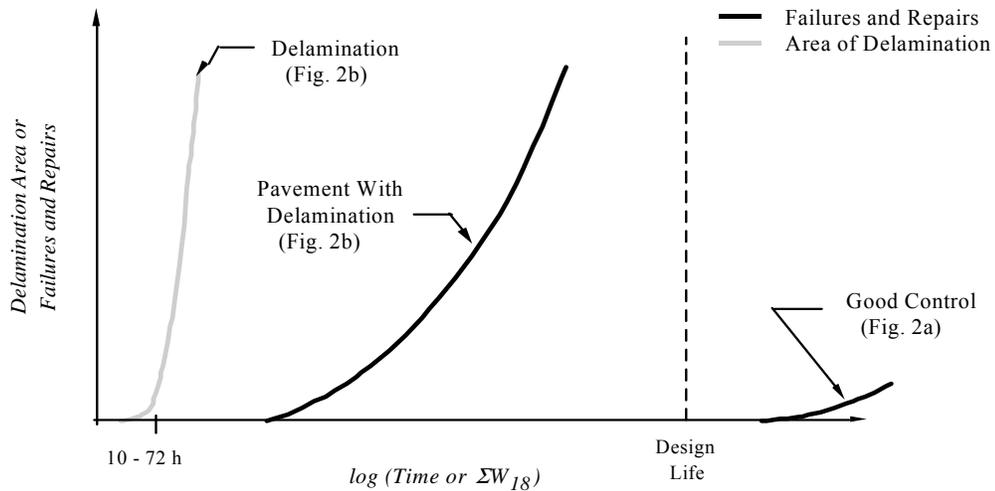
Figure 3c. Delamination, Failures, and Repairs History for Poor and Good Control Conditions from Figure 2.

Figure 3. Distress histories of Portland cement concrete pavement and bonded concrete overlays for various conditions of field control.

12
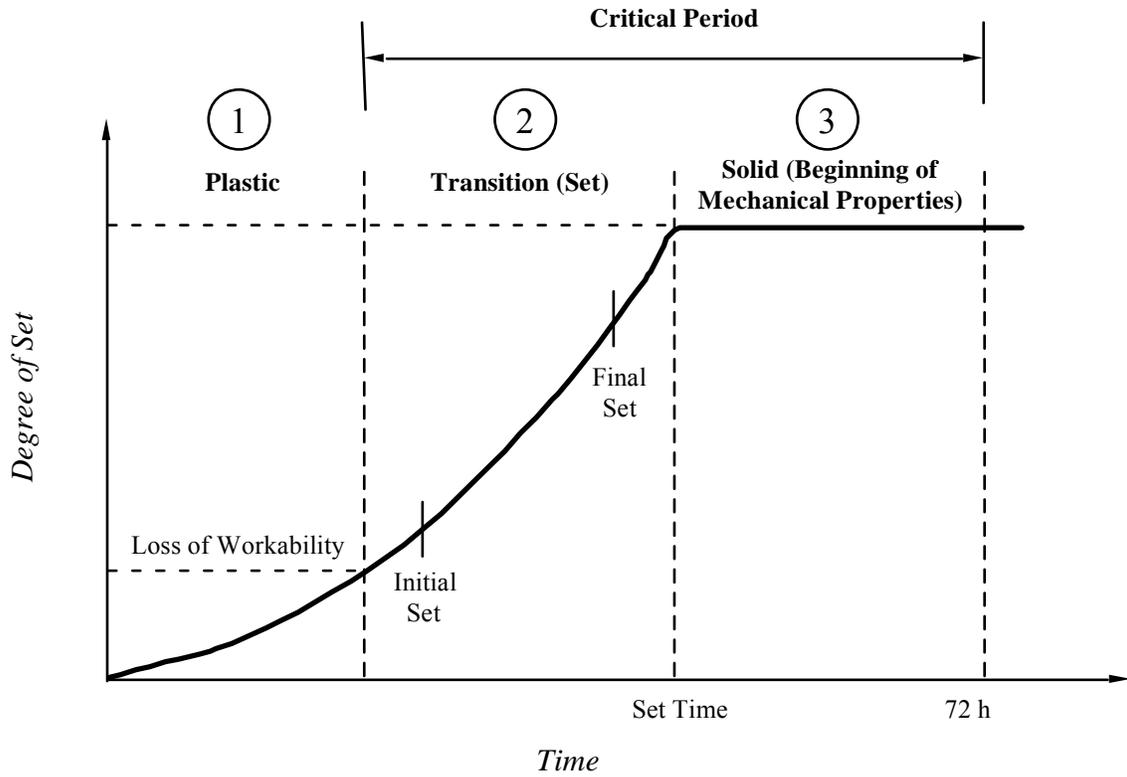
Figure 4a. Definition of Set Time in Terms of the Degree of PCC Set.
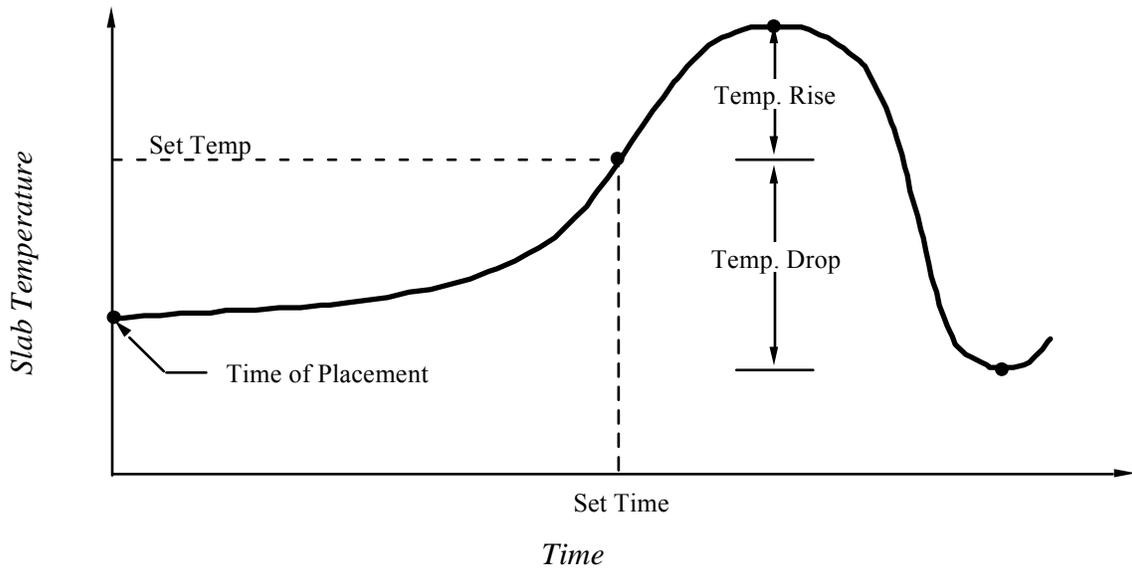
Figure 4b. Definition of Set Temperature in Terms of Set Time.

Figure 4. Definition of critical period using progress of concrete placement
from plastic to solid.

13

"final set" are commonly used, and figure 4a may be used to illustrate this concept. If the graph is examined in the time direction, when the concrete is first placed it is in a semi-fluid or plastic state. Prior to initial set, there is a transition from the plastic state to the solid state. Examining the figure in the vertical direction, the plastic state ends when the workability of the concrete is lost as indicated by the dashed horizontal line. This corresponds to the approximate time of "initial set". Next is the transition period. After the final set, the mechanical strength begins to increase and stresses immediately begin to develop in the pavement. This point in time is defined as the set time. The concrete pavement temperature at which the set time occurs is then defined as the set temperature. This is the reference temperature, and any increase above this value will be defined as a temperature rise. Conversely, any temperature below it will be defined as a temperature drop. These concepts are illustrated in figure 4b.

The subsequent discussion pertains to the initial curing period even though the curing compound may remain on the pavement until traffic wears it off. This period coincides with the occurrence of thermal shock, resulting in cracking, and horizontal cracking as illustrated in figure 3.

2.1.3   *Mechanical State of Stress*

Since concrete is weak in tension relative to its compressive strength, early age tensile stresses can result in the cracking shown in figure 1. Hence, the modeling must primarily pertain to the critical conditions resulting in tensile stress. Since the problem is three dimensional, the state of stress due to volume changes in both the vertical and in the two horizontal axial directions must be taken into consideration.

Many factors influence the overall state of stress in a pavement system. The factors are too numerous to consider them all in a mathematical model. However, by reducing the number of factors through elimination of those which, in most cases, are relatively insignificant, a model can be developed which is relatively accurate. The additional factors which are not directly considered by the model can be indirectly accounted for by incorporating variability and reliability calculations into the overall mathematical model.

Therefore, in order to simplify the modeling process, volume changes that will be considered during the construction process are reduced to only those caused by temperature changes and moisture loss. Moisture loss is generally characterized as concrete drying shrinkage. The thermal characterization of the concrete material is also important. The state of stress in both the vertical and horizontal direction must be modeled for the movement conditions shown in figure 5. The general mathematical model takes the form of the following function:

$$\sigma(t,x) = f\left[\alpha_c(t), \Delta T(t,x), Z_c(t,x), E_c(t,x), \nabla T(t,x), \nabla M(t,x), \cdots\right] \qquad (1)$$

where,

σ   = stress in the concrete due to restrained movements,

t   = time variable,

x   = space variable,

α_c = thermal coefficient of expansion of concrete,

Z_c = shrinkage due to moisture loss,

E_c = modulus of elasticity,

ΔT = temperature decrease from concrete set temperature,

∇T = temperature gradient in pavement, and

∇M = moisture gradient in pavement.

Axial Deformation

Full Restraint
(Zero Movement)

L

ΔL

L

Δ L - Partial Restraint

Δ L - Unrestrained

Vertical Deformation

Unrestrained

Partial Restraint

Full Restraint

Dry/Cool

Wet/Warm
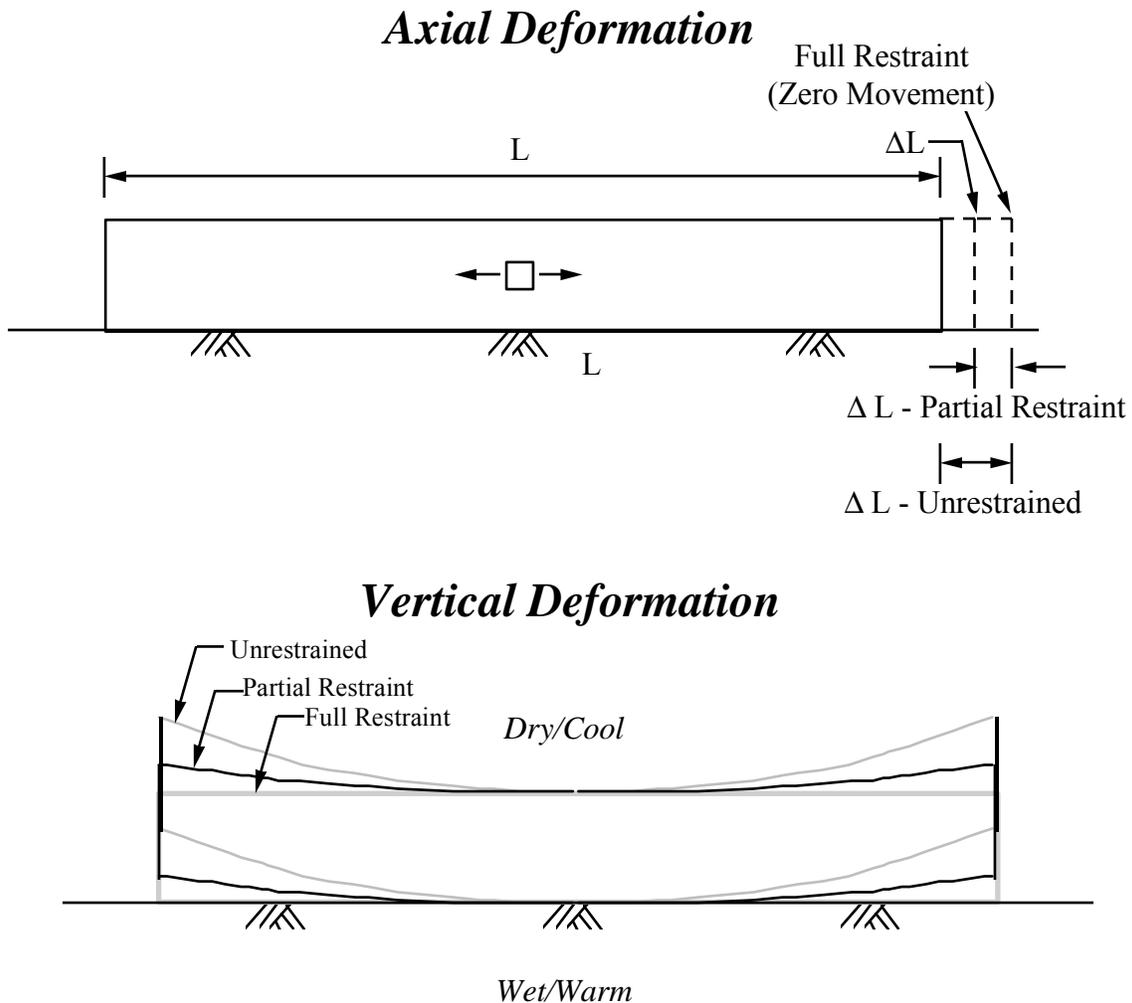
Figure 5. Axial and vertical deformation characteristics to be modeled for the critical period defined in figure 4.

15

For both the axial and vertical conditions shown in figure 5, the stresses in the concrete are zero if unrestrained movement occurs. Conversely, the stresses are at a theoretical maximum if full restraint or zero movement occurs. The stress levels for the actual conditions are between the zero restraint condition and the full restraint condition. Therefore, the stress relationship is complex, and must be solved by an iterative procedure. The complexity is further increased since each of the inputs in equation 1 has a functional relationship that is demonstrated in subsequent sections.

For conceptual purposes, the tensile stresses in the concrete may be described as a function of the thermal coefficient multiplied by the decrease in temperature plus the concrete moisture loss, i.e., drying shrinkage. The thermal coefficient represents the coefficient of the solid which consists of a weighted average of the two components, i.e., aggregate and cement paste. In contrast, the shrinkage is primarily a function of the cement paste (although restrained by the aggregate).

The information contained in section 4.1 of this report describes the effort to characterize those factors that affect the thermal coefficient and concrete moisture loss. As can be seen in the various subsections of section 4.1, these factors are complex and require considerable study. Nevertheless, models must be developed in order to predict the properties, and then they can be calibrated for a range of input conditions, temperature changes, material properties, etc., to develop the guidelines. In essence, each of the distress types shown in figures 1 and 2 is modeled with various factors that influence equation 1.

The stress equations developed from the functional relationship of equation 1 are applicable to the solid state in figure 4.

2.2   Properties of Concrete Affecting Early-Age Pavement Behavior

Referring to figure 4, significant heat generation is initiated in the plastic phase and continues through transition and into the early phases of the solid stage. The rate and duration of heat generation depends on factors related to the cement and climatic conditions. The purpose of this section is to provide a summary of various processes inherent in an early-age concrete pavement or overlay. First, an overview is presented, then a discussion pertaining to the paste and aggregate is given.

2.2.1   Overview

As indicated previously from a macroscopic viewpoint, the two components of PCC are the aggregate particles and the binder medium composed of the hydrated cement paste. Any properties exhibited by the PCC must be a weighted combination of the properties of these individual components. Equation 2 is a conceptual formulation of this concept that uses the individual constituent properties to obtain the mix properties.

$$P_{concrete}(t,T,x) = \frac{P_{paste}(t,T,x) \bullet V_p + \sum\limits_{i=1}^{n}\left[P_{agg,i} \bullet V_{agg,i}\right]}{V_{mix}}$$ (2)

where,

$P_{concrete}$ = any inherent property of the mix being investigated,

V_{mix} = total volume of the mix,

P_{paste} = paste property of interest,

V_p = volume of the paste,

P_{agg} = aggregate property of interest per each of the individual aggregates used,

V_{agg} = volume of the aggregate, and

(t,T,x) = function of time, temperature, and space.

The conceptual notation shows that the properties of the mix may vary with time, temperature, and space. In other words, any or all three of the factors may be of interest for a specific property.

Chapter 4 will describe the specific models used for each of these properties and how they vary in order for the temperature of the concrete to be predicted as shown in the following equation:

$$T_{mix}(t,T,x) = f\left[P_{m,i}, P_{m,2}, \cdots P_{m,i}, \cdots P_{m,n}\right](t,T,x)$$ (3)

where,

T_{mix} = the predicted temperature of the mix for any point in time and ambient temperature,

$P_{m,i}$ = the ith specific property of the mix that affects heat generation,

$P_{m,n}$ = the nth number of specific properties considered, and all other terms as previously defined.

Figure 6 is a plot of the mix temperature as a function of time, and may be used to demonstrate the concepts incorporated in equation 3. The solid line represents a typical air temperature cycle over a three day period with clear skies. The dashed and dotted lines represent two different patterns that may be predicted by equation 3 from various properties developed as part of equation 2. Using the concepts described in chapter 4, the gray line represents the temperature of the mix that might result with a finely ground Type III Cement. In contrast, the dashed line represents the placement of a Type II Cement with very coarse grind.

17

The temperature regimes for these two mixes result in different performance trends during the curing period as presented for the various conditions in figure 1. For example, the dashed line may result in the performance shown for figure 1a, whereas the gray line may result in a performance as demonstrated by figures 1b, 1c and/or 1d. The intent of the equation is to predict mix temperatures for various placement conditions as illustrated in figure 6.
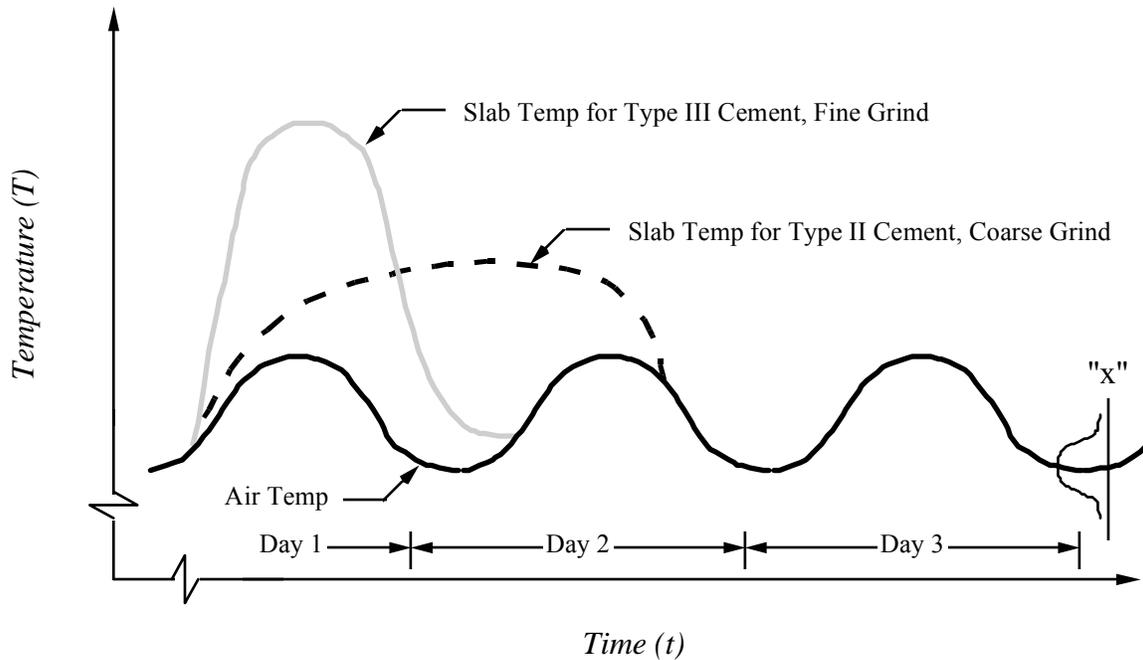
Figure 6. Temperature of the concrete mix as a function of air temperature, time, and material variability.

Obviously, the ambient air temperature will also affect the pattern as demonstrated by figure 6 and characterized in equation 3. The graph also shows how the temperature varies with time within a 24 h cycle and between cycles for the days after construction. On the right side of the figure, variability during the third cycle is shown. At a given point in time, a distribution of temperature is shown to represent the variability (normal curve shown). In the subsequent sections of this report, several of the key properties represented by equation 2 are presented and described.

2.2.2   Effect of Hydration

The hydration of Portland Cement involves a sequence of chemical reactions between the cement components, calcium sulfate, and water leading to stiffening and hardening of the cement paste. This hardening process is illustrated in figure 4 for the critical period between plastic and solid states. As table 1 depicts, there are four stages in the hydration process: the initial few minutes, the induction period, the acceleration stage, and the post acceleration stage. For each of

these stages, there are ongoing chemical and physical processes that result in the generation of heat. The last three of these stages can be seen graphically by the circled numerals in figure 4.

Table 1. Description of the processes and relevance of various stages during the hydration of Portland cement. (2)

Reaction Stage	Chemical Processes	Physical Processes	Relevance to Mechanical Properties
First Minutes	Rapid dissolution of alkali sulfates and aluminates, initial hydration of C_3S[1], formation of AF_4[2]	High rate of heat evolution	Changes in liquid phase influences setting time
First hours (induction period) *Period 1 from figure 4a*	Formation of CH[3] and C-S-H[4] nuclei begins	Formation of early hydration products, low rate of heat evolution, continuous increase in viscosity	Hydration of calcium silicates determines initial set at end of induction period
Approx. 3-12 h (acceleration stage) *Period 2 from figure 4a*	Rapid chemical reaction to form C-S-H and CH	Rapid formation of hydrates leads to solidification and decrease in porosity, high rate of heat evolution	Change from plastic to rigid consistency (initial to final set), early strength development
Post-acceleration stage *Period 3 from figure 4a*	Diffusion controlled formation of C-S-H and CH, recrystallization of ettringite to monosulphate, hydration of C_2S[5] becomes significant	Decrease in heat of evolution, continuing decrease in porosity, particle to particle and paste to aggregate bond formation	Continuous strength development, decrease in creep, porosity and morphology of hydrated system determines ultimate strength, volume stability and durability

Note: [1] Tricalcium Silicate (C_3S) [2] Ettringite (AF_4) [3] Calcium Hydroxide (CH)
[4] Calcium Silicate Hydrate (C-S-H) [5] Dicalcium Silicate (C_2S)

During the acceleration stage, hydration products form that influence the rate of hydration. These products, with respect to chemical composition of the cement, are calcium hydroxide, calcium silicate hydrate, and ettringite. For the physical process, the magnitude of the water-to-cement ratio and the current ambient conditions will affect the rate and degree of hydration.

In addition to the key chemical components, the major material properties required are the thermal conductivity and the specific heat. The thermal conductivity is defined as the rate of heat flow through a known thickness of material between two phases of uniform areas which are subjected to a major temperature difference. The thermal conductivity of the cement paste has generally been found to have a small range and is generally invariant with temperature in the normal ranges of curing. However, it is significantly affected by moisture content. In general, an increase in moisture content within the cement leads to an increase in thermal conductivity. The specific heat is defined as the number of calories required to raise the temperature of one gram of material 1°C.

Thermal conductivity is important for the prediction of the profile of temperature at any point in time with depth. An understanding of the climatic and curing factors is also important, since concrete near an exposed surface will transfer more heat and undergo a greater change in temperature than the interior concrete. Furthermore, the subbase upon which the PCC pavement is placed is very important due to the fact that the initial temperature at the bottom of the PCCP may be influenced by it. For example, a black-base could result in a very high initial temperature if the PCCP is constructed during the daylight hours, whereas a cement treated base would remain much cooler resulting in a lower initial temperature.

The specific heat is considered to be important relative to the temperature change of the concrete material. It is affected by the aggregate in the mixture (both in content and type). It is also dependent on the temperature of the cement paste.

2.2.3. *Effect of Moisture Loss and Gradients*

Moisture in the concrete may be classified into one of two types. The first type is referred to as structural water, chemically bound within the cement paste. The second type is water contained in the pore structure. The sum of these portions equals the total water content in the paste. One effect of the moisture on the concrete pavement is the drying shrinkage and creep behavior. These behavioral characteristics are of concern with the respect to the concrete slab deformation, formation of cracks, and/or development of delamination in BCOs as shown in figures 1b and 1c.

It is necessary to predict humidity and water diffusion when considering moisture or warping-induced stresses in PCC pavement. This characteristic is inherently related to a material property referred to as the moisture diffusivity (D), which is dependent on the pore water content of the paste. Moisture diffusivity is generally characterized as the rate of moisture movement through concrete materials in terms of the mass of evaporable water passing through a unit area perpendicular to the direction of flow. Important terms or variables in characterizing diffusivity are permeability and porosity. Permeability is a function of humidity and temperature. The moisture loss in drying specimens will be much greater in regions of high permeability such as near exposed surfaces resulting from a late application of curing compound.

The characterization of diffusivity is important in order to accurately model moisture flow in hardening concrete. Generally, diffusivity changes very little with time in a hardened concrete. However, dramatic changes occur in diffusivity during the plastic and early hardening stages, i.e., the first 24 h after the placement of the concrete or the critical period defined in figure 4. The characterization of diffusivity will permit quantification of varying moisture loss at an early age (equation 2). Therefore, it can be used as an input in the calculation of drying shrinkage for use in connection with the stress analysis illustrated in equation 1. Diffusivity may also be used to represent the effectiveness of surface curing (curing compound, polyethylene sheeting, cotton mats, etc.) to retain the moisture at the pavement surface. Thus, an additional property to be used in the concept described in equation 3 is moisture diffusivity.

2.2.4. Aggregate Properties

The key aggregate properties include the thermal coefficient of expansion, thermal conductivity, and specific heat. These properties must be characterized, and used in equations 1, 2, and 3. Because aggregates constitute the largest portion of PCC in terms of both volume and mass, their properties will dominate the overall properties of the mix. The general guidelines outlined in chapter 3 will describe in detail the properties of aggregates which are beneficial to a PCC mix. The most important property, from a stress development perspective, is the thermal coefficient of expansion. All else being equal, pavements constructed with aggregates of low thermal coefficients of expansion will generally perform better than those constructed with aggregates of a higher thermal coefficient of expansion. Other properties of the aggregates, however, should not be overlooked, but are beyond the scope of this study. These include size, shape, texture, and soundness. The user of these guidelines should be well versed in the design of PCC mixes. The PCA has published a well accepted source of information related to these areas.[3]

2.2.5 Joint Sawing

An important factor which can determine the potential for early-age cracking in newly constructed PCCP is the timing of the joint sawing operations. The purpose of joints in a jointed concrete pavement is to control the location of the cracking that will naturally occur during the life of the pavement. The majority of this cracking will occur during the early-age period as a result of restraint to volumetric changes. If the joints are not sawed early enough, uncontrolled cracking can result, which may lead to undesirable long-term performance due to poor load transfer and spalling. Sawcutting operations should therefore be performed as soon as possible following construction in order to minimize the potential for uncontrolled cracking. However, the start-time of sawcutting is also constrained by the time required to gain sufficient PCC strength to support the weight of the equipment (and operator) as well as the forces introduced by the cutting blade during the cutting operations. The complexity of this problem has led to numerous research efforts, and is beyond the scope of this project. However, provisions are made in these guidelines to simulate the effect of varying sawing times on the overall behavior of the early-age PCCP. This is done by simulating an increase in the stresses due to a long joint spacing until the time of sawing.

2.3 Influence of Ambient Temperature Conditions and Thermal Shock on PCC Pavements

The necessity of having an understanding of the effect of ambient temperature on a PCC pavement is apparent from the previous discussion. However, this concept must be expanded to not only include temperature, but also moisture and time. Figure 7 is a conceptual illustration of the complete system that must be considered in order to model the influence of ambient climatic conditions on the PCC pavement as expressed in equation 3. The effects of convection (loss of

heat due to the wind), irradiation (loss or gain of heat due to differences in temperature between the slab and the air), solar radiation (gain in heat due to the sun's energy), and conduction (loss of heat into the support layers) are observed in figure 7.
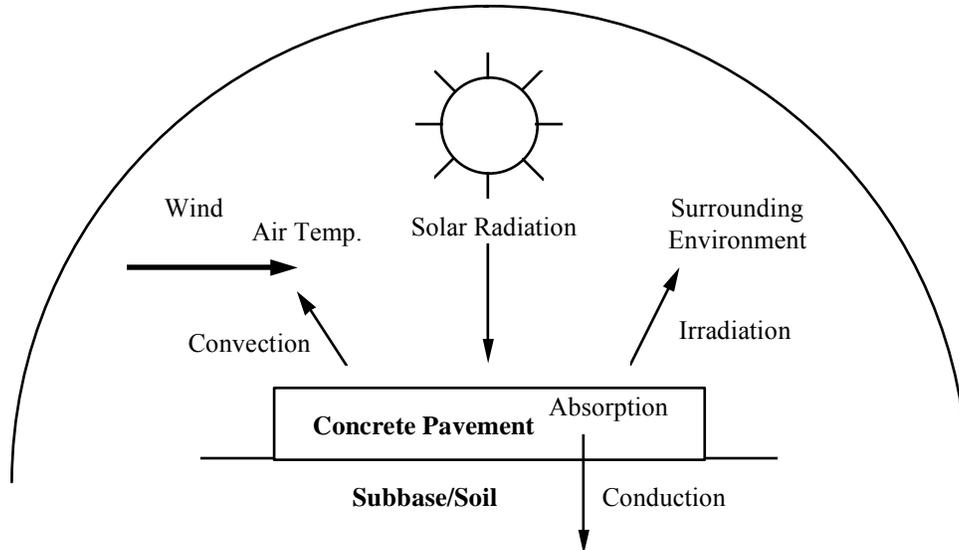
Figure 7. Heat transfer between concrete surface and environment.

In the next section, other factors external to the concrete pavement will be reviewed. First, the external factors are identified and described. This is followed by concepts for their modeling. Next, existing models will be discussed. The concluding subsection will provide preliminary guidelines that reflect the present state of knowledge for construction practices and methods to control concrete temperature.

2.3.1   Characterization of Factors

The governing equation of heat transfer (see section 4.1) shows that heat transfer is a function of the thermal conductivity, density, specific heat, and heat generated by the hydrating cement. The heat energy is transferred between the concrete surface and the environment through convection and the absorption of solar radiation. At the bottom of the concrete layer, the heat transfer is affected by conduction of the subbase type. Thus, the heat transfer conditions for a granular subbase, cement-stabilized subbase, asphalt-stabilized subbase or PCC pavement will be different, as discussed previously.

Heat transfer by convection between the environment and the pavement surface is a complex function that depends on the relative humidity and temperature of the air and the roughness of the concrete surface. Wind velocity is also a major factor in the rate of heat

transfer. The roughness of the concrete surface is a relatively constant variable for typical pavements being placed.

Another heat transfer mechanism between the concrete surface and the environment is irradiation. This is a different heat transfer mechanism from conduction or convection, and it occurs even if the bodies are isolated in a vacuum. In general, this factor is a function of the surface diffusivity of the concrete which depends on both the air temperature and surface temperature. Generally, this factor does not vary considerably within the normal range of climatic conditions.

The absorption of solar radiation is partly a function of the rate at which thermal energy is incident upon a concrete surface. The solar radiation which is absorbed directly by the concrete surface causes the concrete surface to warm more rapidly than the interior region of the concrete pavement. Other factors affecting this parameter include time of day, day of year, latitude of the project site, and cloudiness. The incident rate is maximum if the surface is perpendicular to the rays, but approaches zero as the sun is setting. Cloudiness also has a major effect on the absorption of solar radiation with the maximum occurring on a clear day. During a very cloudy day or at night, the absorption approaches zero. Thus, on a cloudy day, the pavement experiences small thermal changes due to solar radiation effects. Although this factor is important, it is difficult to quantify. The absorptivity of the surface can also vary significantly with black surfaces being five times as absorptive as white surfaces.

2.3.2   Modeling Concepts

In chapter 4, extensive information is compiled that may be used for developing the concepts of a complete model. A great majority of the previously developed models for temperature distribution through a slab use a linear relationship of temperature versus depth. Field observations have shown, however, that a non-linear temperature distribution occurs in the slab under most conditions.

It has been suggested that the best approach for considering a non-linear temperature distribution in the cross section of a concrete slab is based on dividing the distribution into three components:[4]

1. A uniform temperature, T_{axial} which causes axial displacement (expansion or contraction).

2. A linear gradient T_{curl}, which causes bending.

3. A non-linear temperature distribution, $T_{non-linear}$.

The computer model developed for this project has the capability to predict the true non-linear distribution of temperature in the pavement.

2.3.3   Existing Models

Section 4.1.1 provides a detailed discussion of one potential model for predicting temperature distributions through a pavement slab. In this model, the pavement system is idealized as a combination of two dimensional, finite elements to predict the temperature distribution due to heat of hydration, ambient heat of the environment, and radiant heat from the sun. Table 4.1 lists input parameters and provides a general overview of the detail that is required to correctly model the problem. A total of 18 parameters are shown, all of which have been discussed previously and that indicate the complexity of the model.

2.3.4   Preliminary Guidelines to Control Temperature

Chapter 3 describes, in detail, current materials, construction practices and methods that influence temperature gradients and may be considered as a set of preliminary guidelines. Essentially, these factors are a general reflection of the parameters required for models discussed in the previous sections and in chapter 4.

The process of temperature management should consider the main factors that affect stress and strength development of the concrete. Like factors affecting stress development, the factors that affect strength development, in most instances, are also related to temperature. As a result, there is a natural correlation between these two parameters encompassed within maturity relationships which can be used during construction. When PCCPs are cured by different methods or are exposed to changes in temperature, it is expected that the rate of hydration of the cement will be affected. Alternatives such as modifying the temperature of the mixing water or methods of curing to insulate the pavement from the environment may be used to control the pavement temperature. Since the activation energy is a measure of the energy needed for the reaction (hydration) to occur, cement type is a major variable affecting its value. For example, Type III Cement requires less activation energy than Type I. Thus, on warm days, Type I Cement may be more appropriate, whereas, on cold days, Type III may be more appropriate. Energy can also be provided to the mix by increasing the temperature of the concrete constituents or by using different curing methods.

2.4   Effects of Early-Age Loading on the Bond of BCO

Most of the current information, as presented in this report, is focused on the effect of early-age loading. This information emphasizes that a BCO adds directly to a pavement's load carrying capacity by creating a monolithic pavement structure of increased structural stiffness and thickness. Furthermore, the use of BCOs can be a cost-effective pavement rehabilitation approach for existing concrete pavements and is ideal for fast track technology.

It was found that the majority of debonding problems (delamination), occur in the first 12 to 48 h of the overlay's life. The causes can be grouped into two categories. The first category is related to the early-age BCO characteristics which include all the factors affecting overlay behavior (strength gain, shrinkage, temperature, etc.) prior to opening the pavement to traffic.

24

The second category includes the effect of early-age traffic and material behavior of the pavement system until failure. Studies have shown that the failure of a BCO at early ages is initiated when the combination of tensile and/or shear stresses at the interface exceed the available bond strength. Stresses due to volumetric changes occur due to either the temperature differentials and/or shrinkage/swelling as discussed in previous sections. Stresses due to traffic will be discussed further below.

2.4.1   Effect of Traffic Loading on Pavement Stress

Obviously, the application of live traffic loads adds to the stress caused by environmental factors. Thus, the traffic loads will compound conditions in the slab and increase stresses within the pavement system. It will also change as cracks form, joints are sawed, the concrete fatigues, and load transfer decreases over time. The season of placement determines the curing temperature rate, rate of strength and modulus gain, and the minimum and maximum temperatures to which the overlay is subjected during the initial period after construction. Thus, the loadings due to traffic application at early-ages should be added to the factors shown in equation 1.

2.4.2   Traffic Loading and Failure Criteria in BCO

The failure of a bonded system can be defined as the time in which the pavement is either unsafe to use or has had adverse effects on the users of the facility due to the physical loss of the overlay. Obviously, from the descriptions in figures 2 and 3, structural failure as defined by delamination is much more important. The overall stress at which delamination occurs may be much lower than the environmental conditions suggest since the analysis must consider various fatigue mechanisms. The literature has suggested fatigue mechanisms that impact BCOs may be flexural, compressive, shear, and/or tension fatigue. All or any one of these different stresses as a total must not exceed the interfacial bond strength if the overlay is to remain bonded.

2.5   Interface Bond Strength Development

Few attempts have been made to measure bond strength development in the early ages of the BCO's life. Thus, a primary objective of this study is to develop techniques to measure early bond strengths in-situ and correlate these strengths with selected conventional and/or non-destructive testing results. The information obtained during the literature review regarding the effects of early age and rate of bond strength development in BCOs is presented in the following subsections.

Numerous curing factors have a major effect on both the rate of strength gain and on the ultimate strength that a concrete material may achieve. Thus, fast track BCOs may require thorough curing protection under some climatic conditions and also the restriction of heavier truck types during early ages. The special curing conditions may be needed in the first few days to retain the moisture and heat which is conducive to high early strength development. Based on

maturity concepts (discussed in chapter 4), high temperatures during the early stages of curing result in greater early concrete strength gain. However, this can also add to the stresses.

At early ages, it has been found that the strength of concrete relative to its ultimate strength measured with respect to its splitting tensile and compressive strengths are approximately equal. The strength of concrete relative to its ultimate value in terms of pullout bond strength and modulus of elasticity, however, develops more rapidly than the compressive and tensile relative strengths. In this respect, the more rapid development of bond strength may permit the possibility of early-age traffic loading as required in fast track scheduling. Furthermore, in a fully bonded concrete structure, the elements in the upper layer of the pavement are in compression due to wheel loadings, and consequently, its shear strength is increased and less susceptible to debonding. If steps are taken to insure that delamination does not occur at an early age, it is quite possible to add traffic at earlier ages than previously thought possible.

2.6   Field and Laboratory Tests to Monitor Bond Strength

Chapter 3 presents the engineering strength parameters, correlations, and test procedures related to bond development. Bond strength is commonly divided into two categories; shear strength and tensile strength at the interface. Several test methods have previously been investigated to assess both the shear and the tensile strength. Research has indicated that at least five material properties of concrete are significant in the development of interfacial stresses at early-ages of the BCO. These include:

1. Concrete modulus,

2. Coefficient of thermal expansion,

3. Rate and amount of ultimate drying shrinkage,

4. Rate of development of interfacial tensile and shear strength, and

5. Temperature associated with the time at which the concrete begins to set or develop stress.

A testing protocol has been developed as part of this study to consistently and accurately assess the bond strength of a BCO. A key to the successful establishment of a testing protocol is characterization of the bond strength of concrete at a bond interface and the correlation of bond strength to testing methods that can be readily implemented in the field. Typically, the type of test methods that meet this criteria are non-destructive in nature. This approach inherently focuses on bond strength across an interface undamaged by relative displacement between the overlay and the existing concrete surface. Consequently, the BCO construction guidelines presented here address techniques to sufficiently limit relative overlay displacements to ensure the integrity of the bond/non-destructive testing relationship.

The maturity method has been investigated in this project as a surrogate test. A combination of laboratory tests and field measurements of temperature during the curing period have been undertaken to accomplish this goal. The placement of temperature devices in the pavement permit a direct history of the curing temperatures during the initial stages of the pavement life. Using a mix-dependent, time-temperature relationship developed prior to project construction, the exact time for allowing traffic can be determined. These criteria can vary for both construction traffic as well as regular vehicle traffic.

Modified versions of the pullout and breakoff tests have also been investigated in the field. With regard to laboratory tests, two kinds of shear tests have been considered. These include the slant shear test and the direct shear test. The specimens required for these tests are difficult to obtain from the pavement and generally have to be cast either at the jobsite or in the laboratory. These procedures will be discussed in more detail in chapter 3.

2.7   Summary Observations

The information presented in this chapter demonstrates that the critical period which establishes the performance characteristics (i.e., good or bad) for a PCC pavement or BCO is the first 72 h after placement. This observation emphasizes the need to fully understand, through modeling, the effect of concrete temperature and moisture changes on the pavement stresses and their relation to the strength of an early-age PCCP or BCO.

This study has resulted in the development of a framework for PCC pavement performance optimization with fast-track concrete paving. Guidelines for this optimization have been developed on the basis of sound mathematical models calibrated with actual field data, and not from the extrapolation of limited field data that would lead to marginal or very conservative guidelines.

CHAPTER 3   GENERAL GUIDELINES FOR PCCP AND BCO   DESIGN AND CONSTRUCTION

The purpose of this chapter is to discuss inputs which influence the early age behavior of PCCP and BCOs and to outline general guidelines for the design and construction of PCCP. Inputs to these guidelines are divided into the following four basic categories which are discussed in subsequent sections.

- **Materials and Mix Design** - The materials of PCC include the aggregate, cement, and mix-water. Each of these constituents may be modified in various ways in order to achieve desirable results. This section will identify the means by which these factors can be modified.

- **Environmental** - These inputs are often the most unpredictable and uncontrollable of all the inputs to the guidelines. Some control can be established through the selection of specific paving times. The user must keep in mind, though, the high degree of variability associated with predicting weather conditions.

- **Construction** - Construction inputs are often quite adjustable to meet the users needs. Specifications for fast-track PCCP can take advantage of the significant effects that these inputs have on the overall performance of the pavement. In addition, these inputs usually can be modified less expensively than modifying other non-construction related variables.

- **Pavement Design** - The inputs associated with this category are often selected prior to the use of these guidelines in the pre-construction process. The selection of these inputs is usually based on other factors such as structural capacity requirements. However, if adjustment of these inputs is still possible at the time of analysis, modification of these inputs can often prove to be beneficial.

The following sections detail the specific recommendations and guidelines for inputs selection associated with each of the four categories. Because these guidelines provide only general guidance with the selection of the input parameters in these categories, it is the responsibility of the user to utilize engineering judgment in the final selection of the inputs in the verification guidelines described in chapter 4. Other factors such as economics, materials availability, and ease of construction should be considered when making the final decision. The guidelines presented here do not optimize the decision process, but provide a means by which to predict the success or failure of a particular combination of inputs to the overall performance of a PCCP or a BCO.

3.1 Materials Inputs

Portland Cement Concrete consists of three basic constituents: aggregate, cement, and water. In addition to these basic components, additional admixtures may be added to enhance or reduce a particular characteristic of PCC. These admixtures include, but are not limited to: pozzolans, fly ash, and other mineral admixtures; chemical admixtures which can act as superplasticizers, water reducers, and retarders; and reinforcements in the form of fibers made of either polymers or metal. The use of various admixtures can significantly affect the behavior of PCC during the hydration period, especially in fast-track mixes which have a greater behavior susceptibility to even small variations in the mix design. However, modification to the three basic PCC components both in type and content can also affect the overall PCC performance.

The following sections will highlight the influence of the basic materials parameters on basic PCCP behavior, with emphasis placed on the influence on fast-track mixes and Bonded Concrete Overlays. These general guidelines should be used to formulate the inputs to the guidelines.

3.1.1 Aggregates

Aggregates are, both volumetrically and by mass, the largest component of a PCC mix. Because of this, the behavior of the aggregate can significantly affect the PCC behavior, and, in the long term, PCC performance. Equation 2 from section 2.2.1 demonstrates the quantitative effect on various concrete properties as a function of the volume of the PCC mix constituents. Coarse aggregate, in general, is more influential than fine aggregate on PCC behavior. Aggregates consist of one or more minerals and are most often naturally formed, but can also be manmade (such as slags). Most aggregates can be divided into two very general categories: calcareous aggregates which include limestones and dolomites, and siliceous aggregates which include granites and quartzes. Some aggregates, particularly sands and gravels may be a "blend" of these general categories. For these guidelines, aggregates will be classified as either calcareous or siliceous.

At early-ages, the cement mortar is often the "weak zone" in which a failure will occur. Because of this, the strength of the aggregate does not greatly affect the early age behavior.

It has been observed that, all other factors being equal, PCCP constructed with aggregates with a low thermal coefficient of expansion (i.e. calcareous aggregates) perform better in marginal thermal situations than those built with aggregates with a high thermal coefficient of expansion (i.e. siliceous aggregates). Since concrete made with siliceous aggregates expands and contracts more than concrete made with calcareous aggregates, higher stresses in the pavement can result with siliceous aggregates. These higher stresses lead to lower performance.

If the user decides to use a siliceous aggregate, measures should be taken to minimize the thermal influence of the aggregate type. These measures will be discussed in more detail in the following sections.

It is also recommended that bonded concrete overlays be constructed with an aggregate which is of equal or lower thermal coefficient. In other words, an existing PCCP constructed with a limestone aggregate should not be overlaid with a BCO containing a siliceous aggregate. However, an existing a siliceous aggregate pavement may be overlaid with a PCC containing a calcareous aggregates. In addition, an existing pavement of any type can be overlaid with a PCC of the same coarse aggregate type. Table 2 demonstrates this decision making process graphically. The reason for this is that the bottom layer of a pavement (in this case, the existing PCCP) is not subjected to as large of a temperature change as the top layer (in this case, the BCO). In addition, the temperature differential a short distance from the BCO and the existing PCCP is small, thus the differential stresses across the interface are small. Because of this, the bottom layer can be of a higher thermal coefficient of expansion and respond (strain) similar to the top layer. This table should be used with caution, however, since many of the aggregate classifications listed have a range of thermal coefficients. The thermal coefficients of the two pavement layers may be different than the layers made with concrete of "typical" aggregates.

Table 2. Coarse aggregate use in BCO versus existing pavement.

| | | Bonded Concrete Overlay Coarse Aggregate Type | | | | |
		Sandstone	Siliceous Gravel	Granite/ Gneiss	Basalt	Limestone/ Dolomite
Existing Pavement Coarse Aggregate Type	Sandstone	Yes	Yes	Yes	Yes	Yes
	Siliceous Gravel	Yes	Yes	Yes	Yes	Yes
	Granite/ Gneiss	No	No	Yes	Yes	Yes
	Basalt	No	No	Yes	Yes	Yes
	Limestone/ Dolomite	No	No	No	Yes	Yes

In the final selection of aggregate type, other factors such as availability and cost should be included in the decision making process. If siliceous river gravel is the only locally available material, other precautions should be taken in order to minimize early-age damage.

The proportion of aggregate in the mix design can also influence the early-age behavior, although it can be secondary when compared with other factors. However, it should be noted that by increasing the relative proportion of aggregate in the mix design (as compared to the

other constituents), the stiffness of the mix in either the plastic or solid state will be higher (see section 4.1.4), therefore the stresses will be greater, and thus the potential for early-age damage is higher. It should be emphasized again, however, that this effect is in most cases a secondary one, and it is therefore recommended to first attempt to modify other inputs in order to lessen the potential for early-age damage.

3.1.2   Cement

As opposed to aggregate properties, cement paste properties change as a function of time. This is particularly true during the early-age period. Because of the complexity of the hydration process, the general guidelines given here should be used with caution. Improper selection of the cement type can lead to a poor performing PCCP. The following list includes the five basic types of cement:[3]

- **Type I**   Normal cement
- **Type II**   Moderate Sulfate Resistance
- **Type III**   High Early Strength
- **Type IV**   Low Heat of Hydration
- **Type V**   High Sulfate Resistance

Of these, Types I and III are most commonly used for fast-track mixes, with Types II and V being used occasionally for other PCCP construction including BCOs, especially in areas with high sulfate contents either naturally in the soil or due to deicing salts or saline environments near the sea. Type IV cement is rarely used in pavements. Each type of cement reacts differently when exposed to water. Cement reacts chemically with water resulting in the generation of heat, and different types of cement release different quantities of heat at different rates. The strength of a Portland cement concrete has been found to be directly related to the amount of heat generated by this chemical reaction. These concepts are discussed in more detail in chapter 4. In general, however, a Type III cement releases its heat earlier than other types of cement, and therefore is defined as a High Early Strength cement. Type IV (although noted as not being used in pavements) is the other extreme, releasing its heat very slowly and thus slowly gaining strength.

Type III cement is often identified as a key "ingredient" to fast-track mixes, however, serious detrimental effects can occur with its use. Because of the high heat associated with Type III use, the stresses in the pavement at early-ages can be quite significant. This is especially true when the "cooling" of the concrete after the maximum cement hydration has occurred coincides with an environmental cooling such as sundown. Therefore, the use of Type III cement for fast-track paving purposes should be carefully considered. Type I cements have been used successfully for fast-track mixes. By carefully constructing the PCCP and taking other measures

32

to maximize strength gain, a Type I cement can be used successfully for all but the shortest opening criteria.

Type III cement is often more expensive than Type I cement, and as mentioned herein, is more prone to early-age PCCP damage. Therefore, it is recommended that Type I cement be used as the cement for all but the shortest opening-age criteria. If, after modifying the other inputs, the strength gain of using a Type I cement is still not adequate, a Type III may be used.

If a Type III cement is used, it is recommended that the construction time be such that the maximum hydration temperature does not coincide with the air temperature maximum. In many cases, this requires that the construction take place in the late afternoon or evening h. Night paving is recommended for environments that are subject to extreme high temperatures such as the southwest deserts (during the summer months).

Cement Types II and V can be treated similar to Type I cements, although the heat of hydration is often even lower for these types. Early-age damage due to the use of these types of cement is therefore minimal; however, strength gain of the mix may not be satisfactory to achieve the selected opening-age criteria.

The cement content in a PCC mix will also influence the overall early-age behavior. PCC mixes with large cement contents are, in general, more susceptible to shrinkage problems. In addition, a high cement content can lead to significant heat development in the slab, which can lead to undesirable effects. The benefits of a higher cement content can include better workability and a higher strength, however, adjustment in other factors such as the water-cementitious materials (w/cm) ratio and the use of admixtures may be better suited to achieving these mix properties.

The w/cm ratio is defined as the mass of mix water (including free moisture on the aggregates) divided by the combined mass of the cement and any additional cementitious mineral admixtures including some fly ashes, silica fume, and slags. This ratio is important in determining the overall strength of the mix as well as other mechanical properties including creep and shrinkage. In general, increasing the w/cm will decrease the strength of the mix. The w/cm should be selected so that it is as low as possible while still maintaining a workable mix. Additional information related to proper mix design concepts can be found in the literature.[3]

3.1.3 Admixtures

Several types of admixtures are used in PCCP. The following is a list of the various types of admixtures, and the effects of their use in fast-track PCC mixes and BCOs.

- **Accelerators** - These admixtures yield similar thermal effects to using Type III cement. They can increase the strength gain at early-ages. The same cautions are noted in using these types of admixtures as are noted in the previous section on the use of Type III cements. Accelerators can be used in place of Type III cement if the Type III cement is

not available or is too expensive. Calcium Chloride is a common accelerator, although its use can lead to other problems related to long-term durability.

- **Air Entrainers** - This type of admixture is used in almost all PCC pavements. Most construction specifications mandate a minimum level of air entrainment. Air entrainment has been shown to increase the long-term durability of the mix as well as to increase workability. However, air-entrainment does cause a decrease in strength and therefore, care should be used in the use and control of an air-entraining agent.

- **Mineral admixtures** - Pozzolans are the most common of these type of admixtures. Fly ash, Diatomaceous earth, silica fume, and ground slag are often used in PCC mixes. When used correctly, they have been shown to increase strength and/or durability of PCC mixes.

- **Retarders** - These admixtures retard (extend) the setting time of the PCC. Although retarders can be useful in areas which are subjected to long haul times between the batch plant and the pour, they can also be detrimental to the pavement structure. Fast-track pavements rarely use retarders due to their reduction in the strength gain rate. Their use is not recommended in BCO applications.

- **Superplasticizers** - If used properly, these admixtures can reduce the amount of water necessary to achieve workability of a PCC mix. They, therefore, can be used to reduce the w/cm ratio, and thus increase the strength as well as expedite the strength development. Superplasticizers are very commonly used in fast-track mixes because of their beneficial effects.

- **Water Reducers** - These admixtures perform the same function as the superplasticizers, but to a lesser extent. They can be used successfully in both fast-track mixes and BCO.

In general, a fast-track mix will contain an air entrainer, superplasticizer, and possibly mineral admixtures or accelerators. Many mix designs can be developed using these materials, and the design should consider past experience with their use, availability, and economics. It should be noted that the verification guidelines in chapter 4 have provisions for superplasticizers, mineral admixtures, and accelerators (by treating them similar to Type III cements). Air entrainers are considered to be an essential element of PCC (where applicable), and therefore is not explicitly used as an input to the guidelines.

3.1.4   Concrete Mix Design

Concrete mix designs should be optimized for workability and strength prior to use of these guidelines. Many "fast-track" mixes have been developed. As discussed previously, many contain Type III cement or other admixtures to accelerate the strength gain. However, other factors should be considered in the mix design.

One key factor is the 28-day strength. The ultimate strength of the mix will directly influence the strength during the early-age. The 28-day strength of the mix should be selected so

34

as to satisfy the pavement design including the long-term effects of fatigue and other traffic-induced cracking. It is recommended that the strength be selected as high as possible while still controlling the adverse effects that may result from such a design including high shrinkage and rapid heat generation. This will reduce the potential for early-age damage.

Other factors should also be accounted for during the mix design process. Shrinkage cracking, for example, can occur if the water content of the concrete is too high. Coarse aggregate can be substituted, in some cases, for a portion of the fine aggregate in order to achieve a lower water content and increase the strength of the mix. In the current model (see chapter 4), the content or type of cement does not affect the shrinkage of the mix, but does affect the strength gain and thermal stresses associated with the heat gain (as discussed previously). Some admixtures, especially accelerators as well as many superplasticizers and water reducers can increase the level of shrinkage.

Because many of the PCC constituents have both positive and negative effects associated with them, it is recommended that the initially engineered mix first be verified via the numerical guidelines in the following chapters. If the mix fails the guideline criteria, modifications to the mix can be made based on engineering judgment and the criteria outlined herein.

3.2   Environmental Inputs

Although the user does not have direct control over the environmental inputs that will occur during construction, they do have some indirect control via selection of the season and time of day of construction. Six key parameters are identified here which directly influence the performance of PCCP during early-age:

- Average Air Temperature
- Air Temperature Range over a 24 h period
- Solar Radiation (a function of overcast conditions)
- Windspeed
- Average Relative Humidity
- Relative Humidity Range over a 24 h period

The first four inputs affect the temperature of the pavement, and thus the stresses that occur will be due to thermal expansion and contraction. The last two parameters (as well as the first four to a lesser degree) influence the drying shrinkage potential of the pavement, and thus must be directly considered.

In order to use the verification guidelines in the following chapter, the user must estimate the daily maximum and minimum temperature and humidity. The average values are readily available from the National Weather Service, or they can be obtained from a Weather Almanac from a local bookstore or from the meteorology department of the local media.

The environmental parameters are in many cases the most variable of the input parameters. Because of the unpredictability of the actual weather, it is recommended to use

35

caution in the proper selection of the inputs. "Average" values of the environmental variables may be satisfactory in most simulations, but the user may also want to test extreme conditions.

The overcast conditions are also an input to the guidelines. The user's best estimate of the weather conditions present at the construction time should be used. This value can be based upon the knowledge of the indigenous weather patterns during the season construction will take place. The critical value is usually the sunny condition; therefore, if there is concern over the proper selection, this value can be used as a conservative alternative.

Windspeed can also influence the early-age behavior. Wind can lead to convective cooling of an unprotected or minimally protected pavement which can possibly lead to undesirable behavior. In addition, high windspeeds can lead to moisture loss from the surface of the pavement, resulting in the potential for excessive shrinkage. Measures can be taken to reduce this effect via curing methods using blankets or polyethylene sheeting.

It should be stressed that average values for the weather conditions should be tried. Reliability can be factored into the stress and strength calculations (discussed in later sections). Therefore, the addition of a factor of safety to these inputs may result in too conservative an analysis. It is left to the judgment of the engineer as to the environmental factors used in the analysis. This decision should be based upon the facility in question. If minimization of early-age damage to the facility is critical, then some factor of safety should be incorporated into the environmental parameters. In addition, the local variability of the environmental parameters should be used as a decision criterion of the proper selection.

3.3   Construction Inputs

Some of the most critical inputs to proper fast-track PCCP Paving and BCO construction are encompassed in the category of construction parameters. These factors can often be modified on-site as conditions permit. This allows for flexibility in the design of the PCC mix, and in most cases ensures prevention of early-age damage. Three general construction parameters which are inputs to the guidelines will be discussed here.

3.3.1   Opening Age Criteria

The selection of the opening-age criteria is often based on regulatory constraints. For example, urban highway reconstruction guidelines in many Metropolitan Political Organizations (MPOs) require that construction occur during only off-peak times. These constraints may restrict the opening-age criteria to a low value such as 8 h, or possibly even as little as 4 h. The mix design of the very early-age strength PCC pavements may be different from a more conventional fast-track mix of 12 or 24 h opening criteria. The difference in the opening-age criteria will govern the strength gain of the concrete. It will also govern the associated heat released during this process, and consequently the stress development. Because of the tighter window of strength gain, PCC mixes of very early-strength are more sensitive to variations in the

input parameters. It is therefore recommended that the longest opening age criteria possible be used. This will prevent any unnecessary early-age damage.

3.3.2   Curing Method

Several curing methods are readily available for PCCP construction. The most common curing method is the application of a liquid membrane, which is often wax-based and white in color. The purpose of this type of curing compound is to minimize shrinkage cracking by minimizing excess moisture-loss through evaporation. One of the two common methods of applying this type of compound is the use of a sprayer bar which traverses the width of the pour and applies the membrane by sprayer jets evenly spaced across the pavement width. The second method is with a wand or other hand-held device which is directed by human control. Neither of these application methods is fail-safe. The application rate is usually uneven, thus subjecting some areas of the pavement to greater moisture loss than others. A liquid membrane has been found to be beneficial in minimizing moisture loss when used correctly. A double application of liquid membrane can lead to an even lower potential for moisture-loss-related distresses (e.g. plastic shrinkage cracking). This effect is documented further in appendix A.

A second type of curing method which may be used is polyethylene sheeting. If used properly, this type of curing method is very beneficial in retaining moisture. By applying the sheeting, the moisture is trapped beneath the nearly impervious layer. This minimizes evaporation, and thus drying shrinkage. However, if the sheeting is not securely fastened to the surface by edge weighting, wind can enter through the openings and increase the potential for early-age damage. In addition, because the sheeting cannot be placed until the PCC has hardened enough to sustain the disturbance from the sheeting application, an application of liquid membrane is usually first applied, with the sheeting applied later. Polyethylene sheeting also acts as a thermal insulator. This property can be beneficial if the construction site is subjected to rapid cooling following construction. However, it can be detrimental if used improperly. The insulation, in concert with the excess heat produced by fast-track PCC mixes can result in too great a curing temperature, and thus cause damage following placement.

Cotton mats are the third most common curing method used on PCC pavements. The benefits of this type of curing method are similar to that of polyethylene sheeting. However, in addition to acting as a block to moisture loss, the cotton mats are usually wetted and therefore provide free moisture which may counter the negative effects of drying on the surface of the slab. The cotton mats also serve as thermal insulators, so they are subject to the same benefits and drawbacks described for polyethylene sheeting.

The selection of the proper curing method is key to the construction of a high performance pavement. Because of the complexity of the pavement construction process, engineering judgment should be used in addition to the general recommendations made herein.

Because of the relatively small thickness of a BCO, the curing method is crucial in its successful construction. The effects of drying shrinkage are limited to the surface; therefore, the large surface area of BCO (as compared to the volume of concrete) subjects it to a greater sensitivity towards moisture loss than full depth paving. This, coupled with the greater heat loss,

leads to an increased probability of delamination or other types of early-age distress. The use of an insulating curing method such as polyethylene sheeting or cotton mats can minimize these distresses in many instances.

3.3.3 *Time of Day of Construction*

As discussed in section 3.2, the environmental parameters can create a high level of uncertainty as to the construction outcome. However, one strategy to address some of the adverse effects of climate is to adjust the construction times. By doing this, the temperature buildup in the PCC can be controlled in order to maximize strength gain and minimize early-age damage. This type of control is especially critical for fast-track mixes.

In general, if the ambient temperature is expected to be very warm (greater than 32°C (90°F)), paving in the early evening and into the night is recommended. This strategy takes advantage of the cooling during the evening to buffer the heat gain from hydration, and then takes advantage of the warming during the following day to counter any thermal shock effects due to decreased heat of hydration, thus minimizing early-age damage. In addition, this strategy generally has construction coinciding with off-peak traffic periods and therefore minimizes the user costs associated with the construction.

If the weather conditions are consistently cool (less than 10°C (50°F)), then paving in the early morning will take advantage of the solar radiation during the day to increase strength gain. During the cool evenings, however, insulatory curing methods such as cotton mats and/or polyethylene sheeting should be used in order to minimize early-age damage.

In many cases, other factors such as traffic will dictate the time of construction, but consideration should be given to adjusting the construction time as a relatively inexpensive means to minimize early-age damage to fast-track PCCP paving and early-age delamination to BCO.

3.3.4 *Initial Mix Temperature*

Because careful temperature control of the concrete is crucial in constructing high performance PCCP, the initial mix temperature can be an important input. Several methods have been used in the past to reduce the concrete temperature. These techniques can be used in conditions where the ambient air temperature is expected to be very high and random cracking or cracking due to excessive thermal expansion can occur:

- **Cooling Concrete with Chilled Mixing Water** - One method of cooling concrete is to use chilled mixing water. Since the amount of chilled water can not exceed the amount of mix water in the batch, this method can reduce the concrete's temperature a maximum of 5°C (9°F). Implementing this technique requires a sizable initial investment in mechanical refrigeration equipment and insulated water storage tanks unless other chilled water sources are available such as groundwater sources.

- **Using Liquid Nitrogen to Cool Mix Water** - Another effective method of cooling mix water is to inject either the water storage tank or the water feed line with liquid nitrogen. This method is capable of reducing the concrete's temperature by as much as 10°C (18°F). However, the costs of installing and supplying a liquid nitrogen supply vessel must be considered.

- **Cooling Mixed Concrete with Liquid Nitrogen** - A related technique for cooling concrete is to directly inject the concrete mixture with liquid nitrogen. This technique requires the installation of a liquid nitrogen supply vessel and an injection nozzle for central mixers. This method is one of the most effective in utilizing the cooling capacity of the liquid nitrogen and is capable of chilling the concrete temperatures by up to 10°C (50°F). This method of controlling concrete temperature is relatively expensive where the benefits of using this technique in fast-track concrete pavement projects must be carefully weighed against the cost.

- **Cooling Concrete with Ice** - This method is also capable of reducing the concrete's temperature by as much as 10°C (18°F). However, the actual temperature reduction will be limited by the amount of cooled mixing water the concrete batch can accommodate. Due to the difference in specific gravity of ice and water, it must be weighed separately prior to adding it to the concrete mixer. Block ice is a suitable alternative. However, it must be crushed prior to its addition to the batch plant. Although effective at reducing concrete temperature, the use of ice to cool concrete requires a large capital investment and may only be applicable to ready-mix concrete where some mixing may occur during transit.

- **Cooling of Coarse Aggregate** - Another commonly used method of cooling concrete is to cool the coarse aggregate. This has been achieved by spraying cool or chilled water on the aggregate as it passes along a conveyor belt. Simple lawn sprinklers have also been used to provide a continuous source of moisture for aggregate stock piles. To implement the former method, equipment must be available to chill the necessary water to meet concrete production requirements. By reducing the coarse aggregate temperature by 1°C (2°F), the concrete temperature can be reduced by 0.5°C (1°F). A special effort must be made when using this technique to ensure that the coarse aggregate is uniformly saturated to avoid large variations in slump from batch to batch. In addition, by simply protecting the aggregate stockpiles from direct sunlight, the aggregate temperature can be reduced significantly.

Fast-track mixes rarely require heating of the concrete except for paving in cold weather conditions. BCO construction may require heating of the mix, especially in cooler climates due to the faster heat loss in a BCO as opposed to new construction. Some of the techniques currently used for this are as follows:

- **Heating Mixing Water** - Heating mixing water is one of the simplest and most cost effective techniques for increasing concrete temperature. Because the specific heat of water is four to five times that of most aggregate, its capacity to contain heat is much greater. The temperature of the mixing water can be easily increased by simply mixing

the hot and cold feed water lines. This allows for more uniform control of the concrete temperature delivered to the jobsite. At paving temperatures below 10°C (50°F), it may be more appropriate to use heated mixing water rather than admixtures to achieve an accelerated set in the paving mixture.

- **Heating Aggregate** - Aggregate can also be heated to increase the temperature of the concrete. Although this technique is less efficient than preheating the mixing water, it may be necessary in the extreme cases of cold weather where increased strength gain is required. In this process, the aggregate must be fed through a large heater and stored in a heated silo to maintain the temperature. Because of the large content of aggregate in the mix, increasing the temperature of the aggregate can have a significant effect on the mix temperature. Steam heating of the aggregate has also been used extensively in cold weather concreting operations.

For purposes of the verification guidelines, the initial concrete temperature should be estimated, based upon past experience. If one of the methods for heating or cooling the mix is used, the initial mix temperature should be adjusted accordingly.

3.3.5   *Joint Sawing*

In order to minimize the potential for uncontrolled cracking in a PCCP, proper joint sawing procedures should be established. In general, the time of joint sawing should consider the following limiting criteria:

1. The joint sawing should be performed prior to the development of stresses in the pavement that are large enough to cause cracking to occur. These stresses are the result of restrained volumetric changes from both temperature and moisture changes in the young pavement.

2. The joints must not be sawed until the pavement is strong enough to support the weight of the sawing equipment and operator, and also strong enough to avoid excessive raveling due to the forces introduced by the cutting blade.

Various research efforts have been undertaken which may provide the user with additional guidance in regard to this particular aspect of PCC construction. One such research effort was undertaken by the FHWA in 1994 which resulted in a set of guidelines for timing contraction joint sawing and the earliest loading for concrete pavements. [5]

3.4   Pavement Design Inputs

Although the design parameters have little direct effect on the early-age behavior of the PCC, they do have a significant influence on the pavement stress development, and thus the

behavior of the pavement. The type of pavement, joint spacing (if applicable), and the subbase type each affect the pavement performance both in early-age and mature stages.

3.4.1   Pavement (Surface) Type and Thickness and Joint Spacing

Four general types of PCCP are constructed today. Jointed Plain Concrete Pavement (JPCP) is the most common type having transverse joint spacings of typically 4.5 to 6 m (15 to 20 ft) with no slab reinforcement. If a crack occurs at mid-slab in this type of pavement, only the aggregate in the pavement can prevent a fault from occurring. Jointed Reinforced Concrete Pavement (JRCP) also has transverse joints, but at longer spacings typically 12 to 30 meters (40 to 100 ft). This can be done due to the presence of mid-slab reinforcement. Cracks in many cases will occur mid-slab, but are held together with the reinforcement and thus faulting is minimized. Continuously Reinforced Concrete Pavement (CRCP) does not have transverse contraction joints. It is heavily reinforced and therefore holds the cracks closed that will form. Prestressed Concrete Pavement (PCP) is constructed with the same ideology as prestressed concrete girders: by applying a compressive stress via post-tensioned cables, the pavement can resist greater loads, and thus may be constructed thinner.

Of these four types of pavements, the jointed type pavements comprise the great majority of the existing pavements. CRCP is increasing in popularity, but still only accounts for a small fraction of the lane-miles of concrete pavement.[6] PCP is rarely used, and will not be discussed in these guidelines.

Each type of pavement reacts to environmental and external loading differently. Although only JPCP will be considered for this study, pavement restraint concepts (see section 4.6.1) could be utilized to account for each of the other pavement types. Because each of the pavement types is different, the mode of "failure" is different as well. It should be noted that although it is beyond the scope of this report to determine which type of pavement should be constructed, it should be recognized that the pavement type does affect the early-age performance.

The thickness design of a PCCP is usually based on long-term performance requirements. Traffic-induced loading can lead to fatigue and other forms of cracking, spalling, and faulting. Each of these distress types can be controlled to different degrees by specifying a thicker cross section of PCCP. In general, a thicker pavement will lead to a lower potential for early-age damage as well.

3.4.2   Subbase Type

Subbase type has a greater influence on the restraint level in a concrete pavement than any other factor. By selecting an appropriate subbase, with minimal friction at the surface-subbase interface, the restraint will be minimized, and therefore the stress development in the pavement will be minimized (see section 4.2.1).

It is therefore recommended to use a subbase with minimal friction such as an asphalt treated aggregate or the use of an asphalt concrete bond-breaker. The use of a bituminous bond-breaker will minimize the restraint in the new pavement as well as minimize any reflective cracking from underlying layers. Typical values of slab-subbase friction for various subbase types can be found in table 14 in chapter 4.

3.4.3   Reliability

Reliability stems from the field of industrial process engineering. It is a measure of the effectiveness of a design to succeed given the variability associated with a particular system. Each of the early-age behavior inputs identified in this study have different degrees of variability associated with them. Reliability is a means by which this complexity can be reduced. By selecting a certain level of reliability, the user is, in essence, selecting the confidence interval of the analysis results. For example, if a reliability (confidence level) of 95 percent is selected, the user is willing to accept a 1 in 20 chance (5 percent), that the results of these guidelines will be incorrect. By selecting a higher level of reliability, these odds are reduced, however, the conservativeness of the associated design may become cost prohibitive.

Selection of the optimum reliability level should be a function of the importance of a facility to the user. For low-end facilities such as secondary or tertiary highways, a lower degree of reliability may be chosen (50 percent to 85 percent), while a higher degree of reliability should be selected for primary or interstate highways (90 percent to 99.5 percent). A more thorough discussion of reliability can be found in chapter 4.

3.5   Summary of Fast-Track PCCP Guidelines

Many different input parameters have been discussed in this chapter. Selection of input parameters to be used in the construction of a PCCP should not be arbitrary but in consideration of the complex relationships between these input parameters. Table 3 summarizes some of the input parameters that have been discussed in this chapter, divided into the four general categories outlined previously: materials, environmental, construction, and design.

For the designer, the pavement design and mix design parameters would probably be of most interest. These input categories include many of the parameters which the designer may have control over. Each of these parameters would influence the overall behavior of the pavement system.

For the contractor or the agency, the most relevant parameters would probably be in the construction category. This is due to the fact that these inputs can be adjusted in real time in order to minimize the potential for early-age damage, while minimizing costs. Curing methods, for example, can be adjusted day to day depending on the expected weather conditions. If weather conditions are favorable, minimal curing effort may be satisfactory. Conversely, if the weather is expected to be unfavorable for a given day, extra precautions can be taken to minimize early-age damage.

Table 3. Summary table of early-age PCCP input parameters.

Construction Parameters	Materials Parameters
Curing Method	Cement Type
Time of Day of Construction	Cement Content
Initial Mix Temperature	Aggregate Type
Time of Joint Sawing	Coarse Aggregate Content
Design Parameters	Fine Aggregate Content
Pavement Type	Water/Cementitious Materials Ratio
Reliability	28-Day Strength
Subbase Type	Admixtures
Opening Age Criteria	*Environmental Parameters*
Thickness	Ambient Air Temperature
Joint Spacing	Ambient Air Temperature Range
	Overcast Conditions
	Ambient Relative Humidity
	Ambient Relative Humidity Range
	Windspeed

3.6   Additional Guidelines for Avoiding BCO Delamination

Delamination of a BCO from the existing pavement surface is a result of bond exceeding bond strength. High bond stresses can result from large volumetric changes, which can be controlled using the general guidelines established in sections 3.1 through 3.5. The primary source of delamination stress is caused by restrained thermal stress and restrained shrinkage stress. The recommendations outlined in chapter 2 which pertain to the HIPERPAV guidelines are also applicable for controlling stresses in a BCO. These include modification of the materials, environment, construction, and design. Section 3.6.1 will highlight some of the more critical inputs and prioritize them based upon practicality, economics, and relative benefits (as compared to the overall costs).

The second potential source of delamination is low bond strength. Laboratory and field testing have shown that bond strength development can be correlated well with the strength development of the PCC. Section 3.6.2 will describe methods to maximize the bond strength both directly and indirectly.

3.6.1   Bond Stress Minimization

Bond stresses can occur either parallel to the bond surface in the form of shear stresses or perpendicular to the bond surface in the form of tensile stresses. Stress in excess of either of the corresponding strengths (tensile or shear) can lead to delamination. In general, both of these stresses occur simultaneously, and therefore precautions must be taken to minimize both. Parameters in each of the four categories can be modified in order to minimize the bond stress, especially at early-ages. The recommendations made in this chapter regarding these four types of parameters are applicable for both BCO as well as PCCP new construction. Some additional general guidelines are outlined herein related specifically to BCO construction.

3.6.2   Bond Strength Maximization

The strength of the bond between the existing pavement and the BCO is a function of two key parameters; these include the surface preparation used prior to overlay construction and the type of bonding agent used during construction. The following sections will explore various options for these categories and their effect on the overall performance of the BCO system.

3.6.2.1 Surface Preparation

Proper surface preparation is important in maximizing the bond strength and therefore minimizing the potential for early-age delamination in BCO. Several surface preparation techniques have been used in the past including:

- **No Surface Preparation** - A sweeping of the existing surface is usually performed. Generally, poor performance can be expected using this method due to the possibility of the presence of deleterious material on the existing pavement surface which can act as a bond breaker. In addition, in some cases, trafficking of the existing pavement could lead to a polished condition which would further decrease the bonding potential.

- **Cold Milling** - This process involves the removal of a surface layer of the existing pavement via mechanical means such as a roto-miller to provide a rough surface. This process breaks the aggregate as well as the mortar. Cold milling often fractures the aggregate along the surface which can subsequently result in a weak zone of concrete near the bond interface. Because of this, this method is not recommended unless local experience has demonstrated satisfactory past performance.

- **Sandblasting** - This method applies sand via pneumatic means. The sand successfully eliminates some surface contamination and removes some of the mortar, but is generally ineffective in preparing a sound bonding surface, and is therefore not highly recommended.

- **Air Blasting** - Air is generally not used as the sole surface preparation technique, but is usually used in conjunction with another preparation type. However, high pressure air can be used to remove some surface contamination and deleterious material. This

44

method is not recommended for most facilities due to its failure to develop a coarse bonding surface.

- **Water Blasting** - This technique is relatively new in the pavements field. High pressure water can be used to remove the cement mortar and expose the coarse aggregate. This technique has been used in structural applications and in hydrodemolition projects. Although preliminary performance evaluations of BCOs constructed using this technique have shown promise, a recommendation is not made as to its potential benefits as compared to other surface preparation techniques. The cost of using this technique should also be considered since in initial trials, it was comparable to other traditional alternatives.

- **Shotblasting** - This process involves firing steel balls at the pavement surface via mechanical or pneumatic means. Traditional shotblasting does produce a clean surface, but the surface roughness is often not adequate. It is recommended that a heavy shotblasting be used instead.

- **Heavy Shotblasting** - Although similar to the standard shotblasting process, heavy shotblasting produces a very desirable surface for BCO. It is produced by using standard shotblasting techniques but for a longer time, or by using larger shot. This method of surface preparation has demonstrated excellent performance in the past, and is highly recommended.

- **Mechanical Fasteners** - This method of surface preparation is also relatively new to the pavements area. It has been used successfully in the past for bridge deck overlays as well as structural applications. It involves the application of mechanical fasteners such as nails to the existing pavement at critical areas such as the pavement corners and edges. The nails then resist the delamination stresses both in shear and in tension. This method of surface preparation should be used in conjunction with one of the traditional methods listed above. Although the installation of fasteners can be expensive initially, if they prove to be effective in the long-term, the benefits of their use in BCO construction may prove to be substantial. However, since their use is still in the experimental stage, no recommendation is given here as to their use.

The final selection of a preparation technique must include many factors. Economics should be considered as a primary variable. The most beneficial surface preparation techniques are more expensive than the less beneficial ones. Of those listed, the best alternative includes the use of heavy shotblasting. Although still in the experimental stages, both water blasting (ultra-high pressure) and mechanical fasteners seem to be excellent methods if used properly. Cold milling tends to destroy the aggregate surface, and thus lessens the bonding potential. In addition, cold milling creates a weak zone by fracturing the surface of the existing pavement. This can lead to spalling and delamination. Air blasting, sandblasting, and standard shotblasting may not develop an adequate surface for BCO construction.

3.6.2.2 Bonding Agent

Consideration of a bonding agent to be used at the interface of the existing pavement and the BCO is also important. Several types of bonding agents have been used in the past on BCO projects with varying degrees of success. The following sections discuss the various options that have been used in the past as well as some recommendations as to their application.

- **No Bonding Agent** - Constructing BCOs without bonding agents has been done successfully in the past. The key to this approach is good surface preparation and a dry surface. No loose debris or dust should be present prior to construction of the BCO. In addition, this method should not be used if the pavement surface is moist, as this has led to debonding in some instances.[7] The use of no bonding agent should be weighed against the cost of additional surface preparation.

- **PC Grout** - This type of bonding agent is the most commonly used in BCO construction today. The mix design of the grout should maintain a relatively low w/c ratio. Types I, II, and III cement have also been used successfully in the past, although a Type III is recommended under conditions which may lead to premature delamination (due to environmental factors). The grout should be applied directly in front of the paving operations because if the grout is allowed to dry prior to concrete placement, the grout may act as a debonding layer between the existing pavement and the BCO.

- **Latex** - Latex has been used on some BCO projects in the past with varying success. The strength of latex is approximately the same as that of grout. However, the performance of some projects constructed using latex have had undesirable performance; therefore, unless successful employment of the method has been achieved, it is not recommended.

- **Epoxy** - Some BCO projects have been constructed in the past using epoxy as a bonding agent. The performance of projects using epoxy has demonstrated some delamination problems. The bond strength of projects using epoxy has been found to be approximately one-half to two-thirds that of those constructed with PC grout. It is, therefore, not recommended for use without prior experience.

3.7   Recommendations for Bond Strength Monitoring

It is important in many cases to monitor and predict the actual BCO bond strength in order to determine the time at which the facility may be opened to traffic. This section will describe some detailed procedures by which the bond strength may be determined. These procedures can be used in conjunction with the HIPERBOND guidelines, or may be used as a basis for policy concerning opening criteria for BCOs.

These recommendations are for the monitoring of bond strength both in the field and in the laboratory including test methods to monitor both shear and tensile bond. Guidance as to limits of these measured values will also be given.

Table 4 summarizes the recommended testing procedures for the laboratory and the field. The subsequent sections describe each of the recommended testing procedures in detail. Further research is recommended to determine the optimum sampling and testing frequency to establish a satisfactory confidence level for the bond strength. It is recommended, however, that the in-situ tests be performed near the corners and edges of the pavement since this is where the highest delamination stresses occur, and is therefore the location at which delamination is most likely to occur.

Table 4. Recommended testing procedures for BCO bond strength.

Failure Mechanism	Recommended Field Testing Procedure	Recommended Laboratory Testing Procedure
Shear Stress	Torsional Shear Test	Iowa Shear Test
Tensile Stress	Break-off Test	Break-off Test on Prepared Test Slabs

Torsional Shear Test. In order to expedite the monitoring of BCO shear strength, the torsional shear test was selected as the optimum field testing procedure. The equipment required for this test is minimal. The four primary elements required for the test are: a cylindrical plastic sleeve, which is required to separate the test specimens from the surrounding PCCP; heavy grease, to lubricate the plastic sleeve to expedite its removal prior to testing; a torsional transfer device, which is a simple machined device constructed of steel or aluminum; and a torque wrench with adequate range and accuracy for the test (an electronic torque wrench with the capability of recording the maximum torque is recommended, but not required). In addition to these, additional tools such as a tamping rod (to ensure adequate PCC consistency in the vicinity of the testing apparatus) and lock-jaw pliers (for sleeve extraction) may be necessary to improve the use of this testing method. The test begins by inserting the plastic sleeve and the torsional transfer device into the fresh PCCP until in contact with the bond interface. Any concrete which is disturbed during this process should be reconsolidated using the tamping rod. Figures 8 and 9 demonstrate the device and their correct placement into the PCCP. Measurement is then conducted at various time intervals in order to determine the bond shear strength. The measurement process is performed by first removing the plastic sleeve (using the pliers if necessary). Next, the torque wrench is used to rotate the fins until failure. The maximum torque before failure is recorded and used to calculate the maximum shear stress at the interface. Typical 28-day shear strength values for a BCO range from 1.5 MPa (220 lbf/in^2) for a poorly bonded surface to 4.5 MPa (650 lbf/in^2) for a well bonded surface.

Figure 8. Torsional shear test apparatus (shear fins and PVC sleeves).

Figure 9. Torsional shear testing in operation.

Break-off Test.   Of the many nondestructive testing procedures available, the Break-off test is a direct measure of strength. The stress at failure is then related to the compressive or the flexural strength of the concrete using a predetermined relationship for the particular concrete mix. The test procedure consists of breaking off a cylindrical specimen of in-place concrete. The test specimen is created in the concrete by means of a disposable tubular plastic sleeve, which is cast into the fresh concrete, and then removed at the time of testing. A force is applied through a load cell by means of a hydraulic pump mechanism. The force required to break-off a test specimen

48

is measured by a mechanical manometer. The Break-off test provides a more effective means of monitoring the curing conditions of concrete. This test procedure is applied here to measure the tensile bond strength of the BCO. Figure 10 is a close-up of the specimen and sleeve after testing has been completed. Figure 11 shows the test being undertaken. Typical 28-day tensile strength values for a BCO range from 0.7 MPa (100 lbf/in^2) for a poorly bonded surface to 2.2 MPa (320 lbf/in^2) for a well bonded surface.

Iowa Shear Test.   The Iowa Shear test is a laboratory method of measuring the shear strength of a bonded concrete specimen. The testing apparatus consists of a two-part collar which allows a 4 inch diameter core to be inserted so that the bonded plane is positioned between the two collars. A tensile force is then applied to one collar with the other collar fixed. The force at failure of the bond is recorded. The shear strength is calculated as the force at failure divided by the surface area of the bonded surface.

3.8   Summary of BCO Guidelines

The previous two sections have highlighted some guidelines which are specific to the design, construction and monitoring of bonded concrete overlays. These guidelines should be used with the other sections of this chapter for BCOs. The objective of these guidelines is to provide the user with a direction in the proper selection of the various parameters which can affect the overall performance of BCOs. The HIPERBOND system described in the next chapter should be used to verify the selection of the various parameters made in this chapter. The combination of these qualitative guidelines and the quantitative guidelines in the HIPERBOND system will improve the overall reliability of the design. The potential for early-age damage (delamination) can be identified, and precautions and alternative measures can be taken in order to reduce this possibility. Table 5 summarizes the various inputs which were described in this chapter and which are used directly in the HIPERBOND.

Figure 10. Break-off test sleeve and sample.

Figure 11. Break-off testing in operation.

Table 5. Summary table of early-age BCO input parameters.

Construction Parameters	Materials Parameters
Curing Method	Cement Type
Time of Day of Construction	Cement Content
Initial Mix Temperature	Aggregate Type (Existing Pavement and BCO)
Design Parameters	Coarse Aggregate Content
Pavement Type	Fine Aggregate Content
Reliability	Water/Cementitious Materials Ratio
Joint Spacing	28-Day Strength (Existing Pavement and BCO)
Subbase Type	Admixtures
Opening Age Criteria	*Environmental Parameters*
Thickness (Existing Pavement and BCO)	Ambient Air Temperature
Bond Tensile Strength, and	Ambient Air Temperature Range
Bond Shear Strength	Overcast Conditions
or	Ambient Relative Humidity
Surface Preparation, and	Ambient Relative Humidity Range
Bonding Agent	Windspeed

CHAPTER 4 EARLY-AGE PCCP AND BCO BEHAVIOR MODEL DEVELOPMENT

This chapter will describe in brief some of the technical background of the models used in this study. These models are the key elements in a set of guidelines which can be used to verify adequacy of performance of a specific subset of design, environmental, construction, and materials inputs. The verification guidelines for early-age PCCP have been termed the HIgh PERformance PAVing (HIPERPAV) guidelines, and the early-age bonded concrete overlay guidelines are termed HIgh PERformance BONDed concrete overlays (HIPERBOND). A computer software package termed HIPERPAV containing both of these guidelines has been developed in order to simplify their use.

The HIPERPAV and HIPERBOND guidelines directly address the following PCCP and BCO properties during the early-age period as characterized by figure 4:

- PCC Temperature Development including:
    - Heat Generation (i.e. Heat of Hydration - Internal)
    - Solar Insolation
    - Surface Convection
    - Irradiation
    - Age Dependent Specific Heat
    - Age Dependent Thermal Conductivity
- PCC Mechanical Properties including:
    - Age Dependent Thermal Coefficient of Expansion
    - Drying Shrinkage
    - Creep Relaxation
    - Strength Development using Maturity Methods
    - Modulus of Elasticity Development using Maturity Methods
    - Bond Strength Development using Maturity Methods
    - Very Early-Age Moisture Loss (Plastic Shrinkage)

- Restraint to Free Movement including:

  ☞ Restraint of Slab Temperature and Moisture Gradients (Curling and Warping)

  ☞ Axial Restraint due to Slab-Base Friction

  ☞ Overlay Bond Interface Restraint

Models were developed, and are described herein, which characterize each of these properties. These models are used by the software to predict the critical stresses and strengths in the PCCP and BCO which will then be compared in order to determine the potential for early-age damage. The critical stresses are defined here as the largest stresses within the pavement structure that can lead to pavement damage (i.e. tensile stresses in PCCP and delamination stresses in BCO systems). Figure 12 shows the overall framework for the HIPERPAV and HIPERBOND applications.

Section 4.1 discusses the concepts behind the development of the PCCP/BCO Temperature Prediction Model. Sections 4.2 and 4.3 explore two critical models - thermal coefficient of expansion development and drying shrinkage development. Section 4.4 combines the aforementioned models to predict the critical strains in the early-age PCCP and BCO. Section 4.5 then introduces the development of the elastic properties of the PCC by predicting the modulus of elasticity, which is corrected to account for relaxation creep. Section 4.6 presents appropriate models to predict the restraint in a PCC slab which leads to stress development. These restraint models are combined with the elastic modulus model and the critical strains in order to predict the critical PCCP stresses. Section 4.7 then demonstrates a model to predict the PCCP strength. Section 4.8 details the models used by HIPERBOND to assess the bond stresses and strength development. Section 4.9 will discuss the principles behind the early-age damage prediction models for PCCP and BCO. Finally, section 4.10 will demonstrate some of the calibration and validation efforts that were undertaken as part of this project.

4.1   Early-Age Temperature Prediction Model

Early-age variations in temperature can have a significant effect on the behavior and the resulting distress level of the pavement. Because the strength of young concrete can be significantly lower than the final strength, lower levels of stress can cause the same level of damage as higher levels of stress in a mature pavement structure. Therefore, controlling the stresses caused by temperature and moisture fluctuations is key in minimizing early-age damage to PCC pavements and bonded concrete overlays.
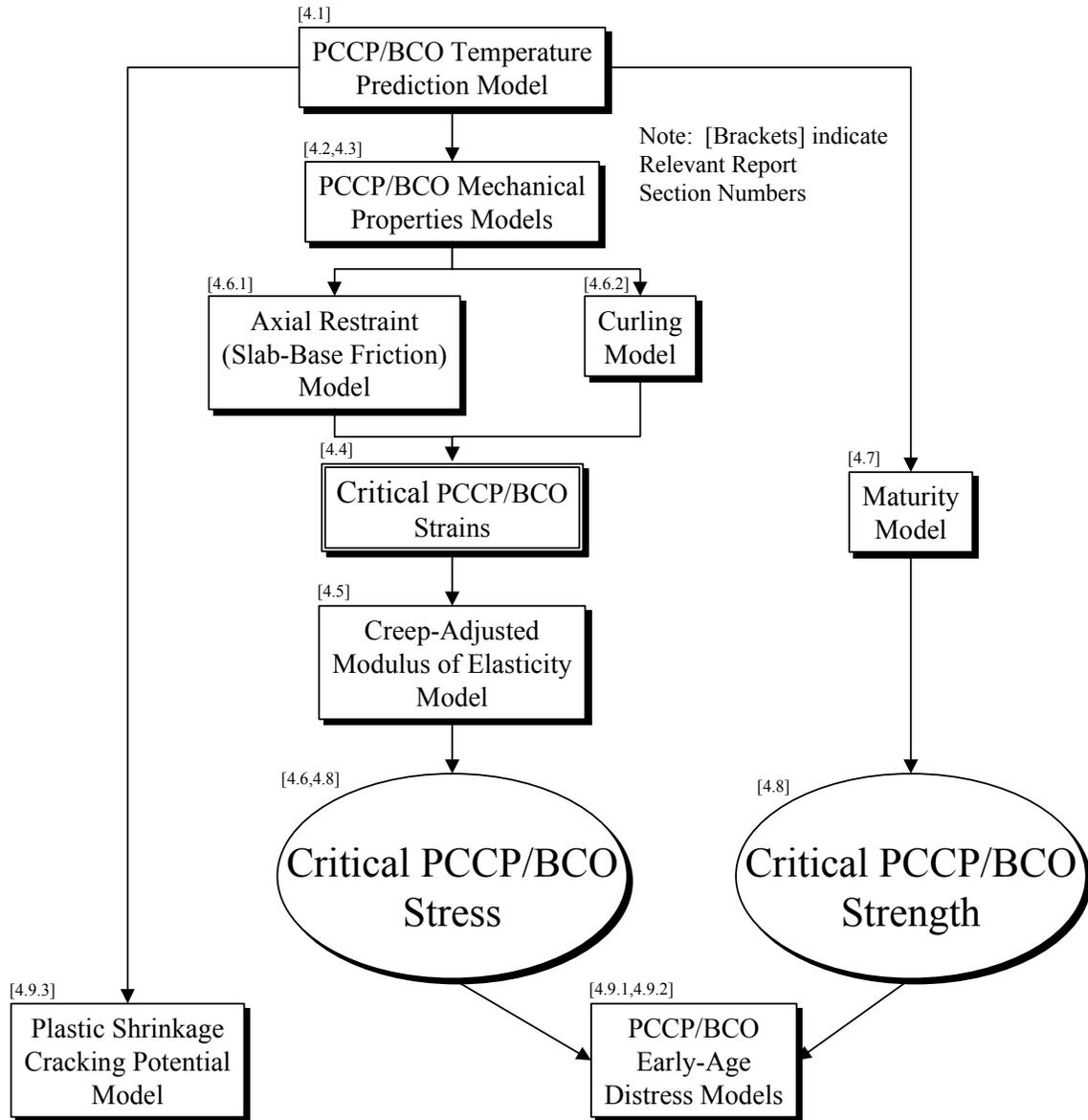
Figure 12. Framework for HIPERPAV guideline models.

Several models are in existence which can predict the effects of temperature on concrete, however very few of them can account for the early-age effects of the heat of hydration. In addition, many of the existing models fail to characterize the complex boundary condition mechanisms such as convection, irradiation, and solar radiation absorption. The project which developed these guidelines used innovative models in order to better assess this behavior specifically for early-age PCC. The following sections briefly describe the theory behind these models.

4.1.1 Overview of Temperature Effects

In order to account for temperature effects in PCCP and BCOs, a model was developed which predicts the free (unrestrained) strain caused by thermal fluctuations in concrete pavement. Temperature effects can be divided into two general categories. The first category is axial movements and their related stresses, and the second is vertical movements due to thermal gradients and their related stresses in the pavements, both linear and non-linear. The first category will cause uniform movements in the pavement, the most critical of which is caused by cooling which leads to tensile stresses in the slab. In the second category, curling can also develop tensile stresses in the slab, and must, therefore, be accounted for in a comprehensive analysis of the slab.

Some of the calculated free strain will cause movement of the slab, while the remaining strain will cause stress development. The calculation of free strain due to thermal effects requires two models: a model to predict the pavement temperature distribution; and a model to predict the thermal coefficient of expansion. These models can then be used to calculate the free strain values. The following sections describe each of these models and how they interact.

4.1.2 Temperature Model Basis

Temperature development in concrete due to hydration and ambient temperature conditions can be determined from the general differential equation for heat transfer. The governing model of heat transfer in two dimensions can be expressed below: [8]

$$k_x \bullet \frac{d^2T}{dx^2} \ + \ k_y \bullet \frac{d^2T}{dy^2} \ + \ Q_h(t,T) \ = \ \rho \bullet C_p \bullet \frac{dT}{dt} \tag{4}$$

where,

k_x, k_y = thermal conductivities of concrete (W/m·°C),
ρ = concrete density (kg/m³),
C_p = specific heat (J/kg·°C),
Q_h = generated heat from heat of hydration of cement and external sources (W/m³),
T = nodal temperature (°C), and
t = time (s).

All the thermal parameters included in the above equation are basic material properties which can be characterized by laboratory tests, backcalculated, or correlated to more common values such as the types and amounts of the concrete constituents.

4.1.3 Heat of Hydration

The heat of hydration of the maturing concrete is characterized by the Q_h term in equation 4. The heat of hydration is the amount of heat that is released into the PCC system due to the hydration processes of the cementitious materials. It is mathematically defined as follows: [9]

$$Q_h = H_u C \psi \frac{\lambda_1 \kappa_1}{t_1} \bullet \frac{\left[\ln(\tau)\right]^{-(1+\kappa_1)}}{\tau} \bullet e^{\left[-\frac{\Phi}{R}\left(\frac{1}{T+273} - \frac{1}{T_r + 273}\right)\right]} \tag{5}$$

where,

H_u = total heat of hydration (J/g),
C = cementitious materials content (g/cm²),
λ_1, κ_1, t_1 = hydration shape and time parameters,

τ = age parameter, defined as: $1 + \left\{ \dfrac{\displaystyle\sum_{t=0}^{age}\left[\dfrac{e^{\left[-\frac{\Phi}{R}\left(\frac{1}{T+273} - \frac{1}{T_r+273}\right)\right]}}{} \bullet \Delta t \right]}{t_1} \right\}$ $\tag{6}$

ψ = degree of hydration, defined as: $e^{-\lambda_1 (\ln \tau)^{-\kappa_1}}$ $\tag{7}$
Φ = activating energy (J/mol),
R = universal gas constant, 8.3144 J/mol/°C,
T = nodal temperature (°C), and
T_r = reference temperature, 20°C.

The total heat of hydration can also be estimated directly from the cement chemistry. Although the precise chemical composition of Portland Cement is quite complex, it can be simplified by combining chemical components of a similar nature into categories. These categories are often termed Bogue Compounds. These compounds include:

- C_3S (Tricalcium Silicate)
- C_2S (Dicalcium Silicate)
- C_4AF (Tetracalcium Aluminoferrite)
- C_3A (Tricalcium Aluminate)
- C (Free Lime)
- MgO (Magnesium Oxide)

In addition to these compounds, Portland Cement contains other chemical compounds including various metals and their oxides. Magnesium Oxide is a common compound which can be found in large enough quantities to affect the heat of hydration.

Each cement constituent has been found to have a unique heat of hydration. One method to estimate the total heat of hydration of a cement is to determine the percentages of the total mass of each constituent and multiply these by the heat of hydration of the respective components. This is shown mathematically by:

$$H_u = p_{C_3S}H_{C_3S} + p_{C_2S}H_{C_2S} + p_{C_3A}H_{C_3A} + p_{C_4AF}H_{C_4AF} + p_CH_C + p_{MgO}H_{MgO} \qquad (8)$$

where,

H_u = total heat of hydration (J/g),
H_{C_3S} = heat of hydration of C3S (J/g),
H_{C_2S} = heat of hydration of C2S (J/g),
H_{C_3A} = heat of hydration of C3A (J/g),
H_{C_4AF} = heat of hydration of C4AF (J/g),
H_C = heat of hydration of C (J/g),
H_{MgO} = heat of hydration of MgO (J/g),
p_{C_3S} = fraction by mass of C3S,
p_{C_2S} = fraction by mass of C2S,
p_{C_3A} = fraction by mass of C3A,
p_{C_4AF} = fraction by mass of C4AF,
p_C = fraction by mass of C, and
p_{MgO} = fraction by mass of MgO.

The values for the heat of hydration of the various Bogue Compounds can be seen in Table 6. The typical mass fractions for the various cement types can be seen in Table 7.

Table 6. Heat of hydration of Bogue compounds.

Compound	*Heat of Hydration (J/g)*
C3S	500
C4S	260
C3A	850
C4AF	420
C	1165
MgO	850

Table 7. Typical compound composition of cements.

Cement Type	Typical compound composition, %			
	C_3S	C_2S	C_3A	C_4AF
I	55	19	10	7
II	51	24	6	11
III	56	19	10	7
IV	28	49	4	12
V	38	43	4	9

4.1.4   Boundary Conditions

The boundary conditions associated with the heat transfer model are critical to accurately determining the pavement temperature. Boundary conditions associated with a concrete pavement consist of conditions associated with both the pavement top surface and bottom surface conditions. At the pavement surface, heat transfer is effected by all the heat mechanisms associated with environmental factors characterized by convection, irradiation, and solar absorption. At the bottom of the concrete layer, heat transfer is affected by conduction as a function of the subbase thermal properties (for new-construction PCCP), and the existing pavement (for BCO). These conditions are summarized as follows: [9]

$$-k\widetilde{\nabla}T \bullet \tilde{n} + q_c + q_r - q_s = 0 \ on \ pavement \ surface \tag{9}$$

$$k\widetilde{\nabla}T \bullet \tilde{n} = 0 \ on \ pavement \ bottom \tag{10}$$

where,

k	=	thermal conductivity (W/m•°C),
q_c	=	heat flux due to convection (W/m³),
q_r	=	heat flux due to irradiation (W/m³),
q_s	=	solar radiation absorption (W/m³),
$\widetilde{\nabla}$	=	gradient notation,
$\tilde{n}$	=	unit direction of heat flow by vector notation, and
T	=	nodal temperature (°C).

The model above (equation 10), which represents the physical mechanism of conduction, may be used to analyze the heat transfer between a concrete pavement and the atmosphere above and the subbase layers below. Thermal conductivity, k, is an important material property. It has been found from previous studies to be a function of the degree of hydration at early ages.[10] Heat energy is also transferred between a

concrete surface and the environment through convection, irradiation, and solar absorption as described in the following paragraphs.

Convection   Heat transfer takes place where a concrete surface is exposed to wind which is at a different temperature than that of the concrete pavement. This type of heat transfer is known as convection (q_c from equation 9), and can be modeled using equation 11. This equation contains a convective heat transfer coefficient (h_c) which is a function of both the curing method used and the windspeed. Table 4.1 contains the formulae which are used to estimate the value of h_c.[9]

$$q_c = h_c \bullet \left(T_s - T_e \right) \tag{11}$$

where,

h_c = convective heat transfer coefficient (W/m²•°C) (see table 8),
T_s = PCCP or BCO surface temperature (°C), and
T_e = air temperature, (°C).

Table 8. Heat transfer coefficients as a function of curing method.[11]

Curing Method	Heat Transfer Coefficient (h_c)
None or Liquid Membrane	-0.0022×w² + 0.6522×w + 1.9521
Polyethylene Sheeting	-0.0072×w² + 0.4152×w + 1.8526
Cotton Mat	0.223×ln(w) + 1.1132
Polyethylene Sheeting and Cotton Mat	0.0425×ln(w) + 0.5913

Note: w = windspeed in mi/h

Irradiation   The concrete surface is also affected by irradiation heat transfer which is accomplished by electromagnetic waves between a concrete surface and its surroundings. This parameter is defined as q_r in equation 9. The Stefan-Boltzmann equation is often used for this type of heat transfer. The general form of this equation is: [8]

$$q_r = \varepsilon\sigma\left(T_s^4 - T_\infty^4 \right) \tag{12}$$

where,

ε = surface emissivity of concrete,
σ = Stefan-Boltzmann constant, 5.67×10^{-8} W/(m²·°C⁴),
T_s = concrete surface temperature, (°K), and
T_∞ = surrounding temperature, (°K).

However, due to the high degree of non-linearity that this equation inherently implies due to the fourth order, a simplified equation has been derived which can be used in place of the original equation. The simplified equation is: [9]

$$q_r = \varepsilon\left[4.8 + 0.075\left(T_e - 5\right)\right]\left(T_s + T_e\right) \tag{13}$$

where,

ε = surface emissivity,
T_e = air temperature (°C), and
T_s = concrete surface temperature (°C).

The surface emissivity is highly a function of surface color. An ideal black-body would have a value of 1. Most PCC, however, have values ranging from 0.8 to 0.9.

Insolation (Solar Absorption)   Insolation, q_s, is the final boundary condition considered in equation 5. This type of heat transfer is due to the exposure of the pavement surface to the sun. This factor has been shown to be quite significant. A simplified model to predict this value is as follows: [9]

$$q_s = \beta_s q_{solar} \tag{14}$$

where,

β_s = solar absorptivity, and
q_{solar} = instantaneous areal solar radiation (J).

The solar absorptivity of PCCP or BCO is a function of the surface color, with typical values ranging from 0.5 to 0.6. An ideal white-body would have a value of 0.0, and an ideal black-body would have a value of 1.0. The solar radiation is highly a function of cloud cover. Table 9 contains the values used as defaults in the HIPERPAV and HIPERBOND guidelines. Note that solar radiation is still present with an overcast sky due to longer wavelength radiation which can penetrate the cloud cover. The solar radiation at night is negligible.

Table 9. Default solar radiation values used in HIPERPAV and HIPERBOND.

Sky Conditions	Solar Radiation (kW/m²)
Sunny	1.0
Partly Cloudy	0.7
Cloudy (Overcast)	0.3

A schematic of the processes relative to pavement temperature interaction with the environment is illustrated in figure 13.

4.1.5   Model Specifics and Inputs

The heat transfer model is in the form of a finite element model. The geometry of the models is shown in figure 14. The concrete substrate and its underlying pavement layers are bordered on the bottom by a soil mass.

The important parameters for a thermal analysis of a hardening concrete pavement include 1) thermal properties of early-aged concrete, 2) heat of hydration characteristics, 3) pavement geometry, and 4) weather data.[12,13,14] These parameters serve as input data in the temperature prediction analysis. Table 10 summarizes some of the typical values of the input data for the computer models. Analytical results are given in terms of temperature variation in a concrete pavement at early ages.
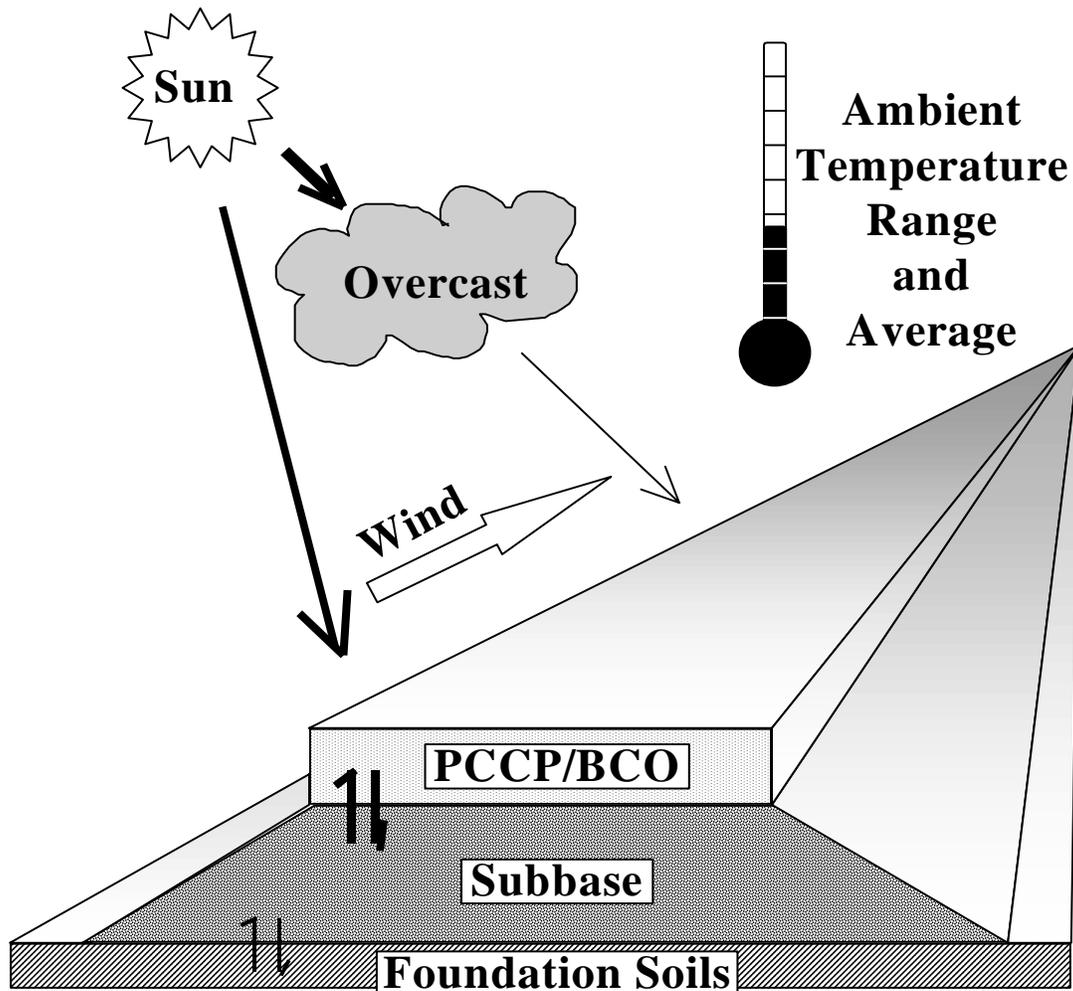
Figure 13. Heat transfer between a concrete pavement and the environment.

10 Support Elements @ 2",3.9",6.3",7.5",9.1"   12 PCCP Elements @ (D/6)"

HIPERPAV

2 Elements @2"

10 Support Elements @ 2",3.9",6.3",7.5",9.1"   12 PCCP Elements @ (D_e/6)"   8 BCO Elements @ (D_o/4)"

HIPERBOND

2 Elements @2"
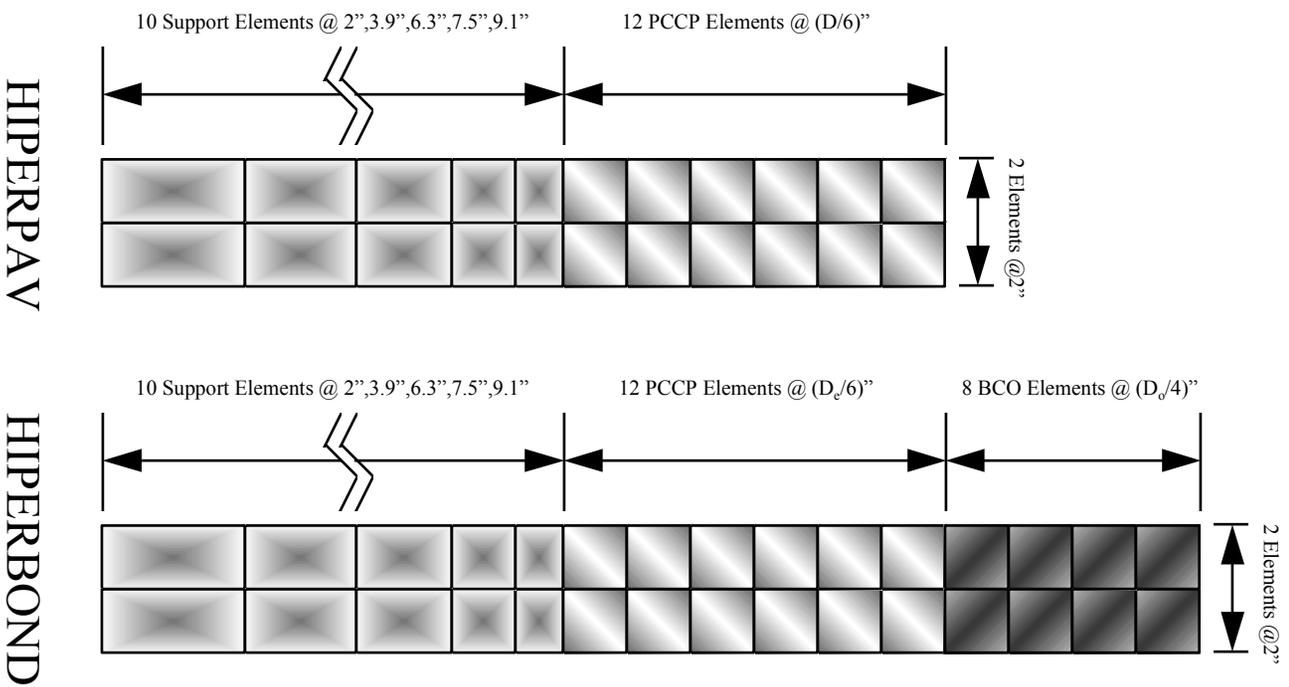
Figure 14. Geometry of concrete pavement system for heat transfer modeling.

63

Table 10. Inputs for temperature prediction model in HIPERPAV and HIPERBOND.

Data Category	Input Data	Typical Value
Concrete Properties	Thermal conductivity, k_x, k_y, (W/m•°C)	Varies with Age @ t = ∞: 0.612
	Density, ρ, (g/cm³)	2.3325
	Specific heat, C_p, (J/g•°C)	Cement - Varies with Age Aggregate - See Table 11
	Emissivity, ε	0.88
	Solar Absorptivity, β_s	0.55
Soil Properties	Thermal conductivity, k_x, k_y, (W/m•°C)	0.30
	Density, ρ, (g/cm³)	1.6000
	Specific heat, C_p, (J/g•°C)	0.80

Heat of Hydration					
Cement Type or Constituent	Total Heat of Hydration, H_u (J/g)	Activating Energy, Φ (J/mol)	Hydration Parameter λ_1	Hydration Parameter t_1	Hydration Parameter κ_1
Type I	460	41750	2.42	2.12	0.85
Type IP	410	41715	2.42	2.12	0.85
Type II	406	39050	3.16	2.06	1.07
Type III	468	44150	3.52	1.10	0.97
Type V	373	36350	3.90	2.0	1.29
C_3S	500	-	-	-	-
C_2S	260	-	-	-	-
C_3A	850	-	-	-	-
C_4AF	420	-	-	-	-
C	1165	-	-	-	-
MgO	850	-	-	-	-

Table 11. Specific heat for various aggregates.

Aggregate Type	Specific heat @ time ∞ C_p, (J/g•°C)
Limestone/Dolomite	0.91
Sandstone	0.77
Granite/Gneiss	0.78
Siliceous Gravel	0.77
Basalt	0.90

Thermal conductivity, k, and the specific heat, c_p, of the young concrete have been found to be a function of the degree of hydration.[10] The general formulae for these relationships are as follows:

$$c_p = c_{p\infty}(1.25 - 0.25\psi)$$ (15)

$$k = k_\infty(2 - \psi)$$ (16)

where,

$c_{p\infty}$ = specific heat of mature concrete,
k_∞ = thermal conductivity of mature concrete, and
ψ = degree of hydration (defined in equation 7).

4.2   Thermal Coefficient of Expansion Prediction Model

One of the keys to characterizing the effects of thermal properties of hardening concrete on a concrete pavement structure is accounting for thermal movements in relation to the coefficient of thermal expansion (CTE). Accurate values of the CTE are needed to predict potential thermally-induced movements of the concrete pavement. The CTE of early-age concrete is a function of both the concrete age and relative humidity. These effects are illustrated in figures 15 and 16 respectively.

Contrary to the CTE of the cement paste, the CTE for the aggregate is independent of the concrete age. Therefore, the CTE of the cement paste typically governs the overall expansion of the concrete mix during the hardening process. It is also noted that the CTE of concrete in a hardened state is typically larger than the aggregate CTE.

4.2.1   Thermal Coefficient of Expansion of the Cement Paste

The CTE of fully cured cement paste ranges from approximately 18 to 20 μ/°C. This property is a function of several factors such as the cement fineness, age, moisture content, and the chemical composition of the cement.[15,17] It has been noted that the CTE of cement paste can increase as the cement fineness increases.[18] Figure 15 shows age dependency of the CTE, where the CTE at very early ages decreases markedly.[15]
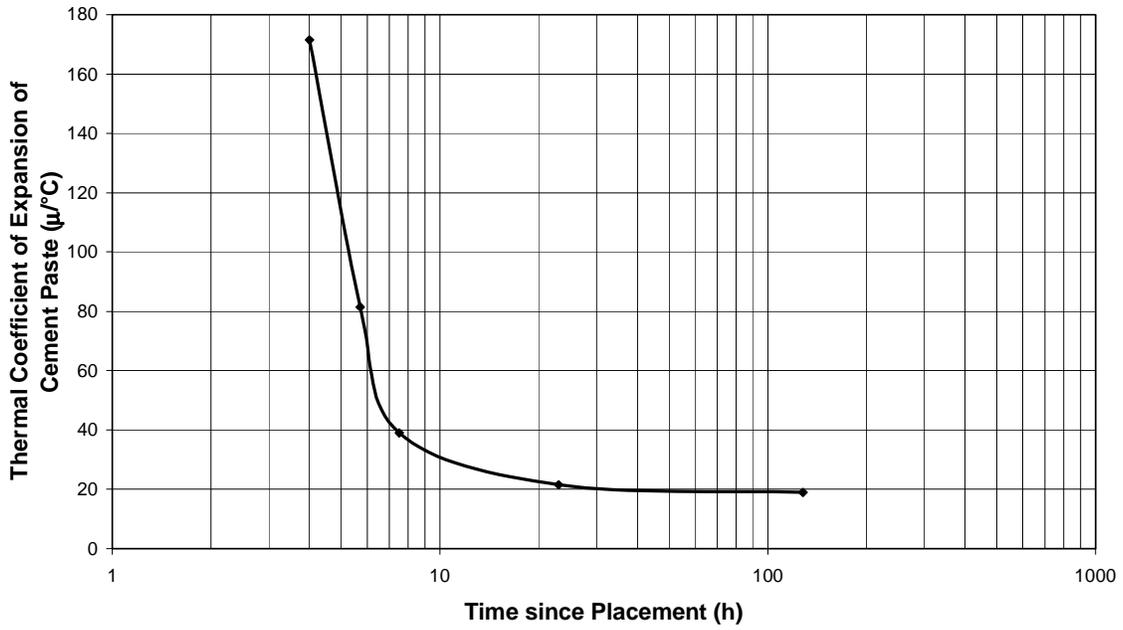
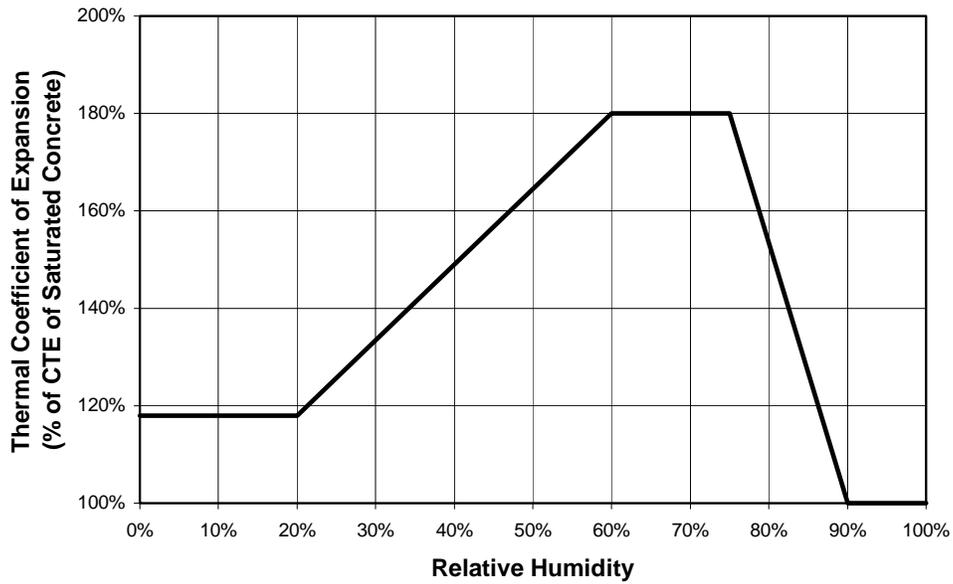*Figure 15. Age dependency of the coefficient of thermal expansion of cement paste.(15)*

Figure 16. Relative humidity dependency of the coefficient of thermal expansion of Concrete.[16]

4.2.2 Thermal Coefficient of Expansion of the Aggregate

Generally, the coefficients of thermal expansion (CTE) for aggregates are not as large as the CTE is for a hardening Portland cement. It is typically believed that the aggregate CTE is not a function of aggregate temperature within the ranges of temperature to which a pavement structure is typically subjected.[19] It has been shown that the coefficient of thermal expansion appears to be dependent upon the chemical and mineral composition of the aggregate.[18] It has been shown that limestone has an average coefficient of about 4-8 $\mu\varepsilon$/°C while siliceous gravel has approximately 7-12 $\mu\varepsilon$/°C.[20]

The thermal expansion characteristics exhibited by hardened concrete are largely controlled by the aggregate type, since approximately 50 percent of the volume of concrete is comprised of coarse aggregate.

4.2.3 Thermal Coefficient of Expansion of the Concrete Mix

Past research has indicated that the CTE of hardened concrete can be estimated from the volumes of coarse aggregate and mortar.[15] This is the approach used in the development of this model for the guidelines. By using the cement type, aggregate type, and mix design provided by the user, a weighted average can be made and an estimate of the CTE as a function of age is made. In addition, it has been shown that the CTE can vary as a function of the moisture content of the concrete.[16] This relationship is shown in figure 16. The following mathematical model is therefore used to assess the CTE, α_{conc}, of the mix:

$$\alpha_{conc} = C_m \left[\sum_{i=1}^{\# \, of \, aggs} \left(\alpha_{agg,i} \frac{V_{agg,i}}{V_{conc}} \right) + \alpha_{paste} \frac{V_{paste}}{V_{conc}} \right] \tag{17}$$

where,

C_m = moisture correction factor (derived from figure 16),
$\alpha_{agg,i}$ = CTE of ith aggregate ($\mu\varepsilon$/°C), (see table 12),
α_{paste} = CTE of cement paste ($\mu\varepsilon$/°C), (derived from figure 15),
V_{agg} = volume of aggregate in mix (m³),
V_{paste} = volume of paste in mix (m³), and
V_{conc} = total volume of concrete mix (m³).

Table 12.   Thermal coefficient of expansion of select aggregates.

Aggregate Type	Range of α_{agg}	α_{agg} used in HIPERPAV/HIPERBOND
Sandstone	8-13 $\mu\varepsilon/°C$	11.0 $\mu\varepsilon/°C$
Siliceous Gravel	7-12 $\mu\varepsilon/°C$	10.0 $\mu\varepsilon/°C$
Granite/Gneiss	6-10 $\mu\varepsilon/°C$	7.5 $\mu\varepsilon/°C$
Basalt	5-9 $\mu\varepsilon/°C$	7.0 $\mu\varepsilon/°C$
Limestone/Dolomite	4-8 $\mu\varepsilon/°C$	7.0 $\mu\varepsilon/°C$

As will be demonstrated in section 4.4, the CTE of the concrete mix is a critical factor in the accurate determination of the thermal strains in the pavement.

4.3   Drying Shrinkage Prediction

The effects of moisture loss can be significant to the overall behavior of a PCCP system. In extreme climates such as the southwestern deserts of the United States, the magnitude of strain due to drying shrinkage can be quite significant due to the evaporation caused by low humidity, high temperatures, and wind.

Drying shrinkage is caused by the loss of moisture from the surface of a pavement at a rate greater than it can be replenished by the free moisture present in the slab. Because of this, in the majority of cases, drying shrinkage strains affect only those regions of the slab subject to the greatest moisture loss (i.e. the exposed surfaces).

The drying shrinkage profile can be predicted by combining the predicted ultimate shrinkage with reasonable assumptions concerning the pavement moisture profile. These modeling concepts are discussed in the following subsections. The end result is an additional strain gradient in the pavement which can sometimes aggravate stress levels due to curling and axial restraint.

4.3.1   Ultimate Drying Shrinkage

The ultimate drying shrinkage potential of a PCC pavement is a function of many parameters. A proposed RILEM model, termed B3, has been used for this determination.[21] The model is a function of the mix design of the concrete as well as the strength and elastic modulus of the concrete at 28 days. The general equation for the ultimate drying shrinkage ($\varepsilon_{sh\infty}$) is as follows:

$$\varepsilon_{sh\infty} = \varepsilon_{s\infty} \frac{E(7+600)}{E(t_\circ + \tau_{sh})} \tag{18}$$

where,

$E(t)$ = elastic modulus (lbf/in^2) of the concrete at age t (days), estimated using:

$$E(t) = E_{28\text{-days}} \sqrt{\frac{t}{4+0.85t}} \tag{19}$$

t_o = age of the concrete when drying begins (days),
$\varepsilon_{s\infty}$ = $C_1 C_2 [26w^{2.1}(f'_c)^{-0.28} + 270]$, and $\tag{20}$
τ_{sh} = shrinkage half-time (days) = $k_t (k_s D)^2$, $\tag{21}$

where,

$$C_1 = \begin{cases} 1.0 & \text{for type I cement} \\ 0.85 & \text{for type II cement} \\ 1.1 & \text{for type III cement} \end{cases}$$

$$C_2 = \begin{cases} 0.75 & \text{for steam cured specimens} \\ 1.0 & \text{for specimens cured in water or at 100\% relative humidity} \\ 1.2 & \text{for specimens sealed during curing} \end{cases}$$

w = water content of concrete (lb/ft^3),
f'_c = 28-day compressive strength of concrete (lbf/in^2),
k_s = cross-section shape factor (approximately 1.00 for slabs),
D = thickness of the slab (in), and
k_t = $190.8 t_o^{-0.08} f'_c{}^{-0.25}$ (days/in²). $\tag{22}$

Table 13 contains the values of C_2 used in the HIPERPAV and HIPERBOND systems as a function of the curing method.

Table 13. Values of C_2 used in HIPERPAV/HIPERBOND ultimate shrinkage model.

Curing Method	C_2
None	0.70
Liquid Membrane	0.90
Double Liquid Membrane	0.95
Triple Liquid Membrane	1.0
Polyethylene Sheeting	1.0
Wet Cotton Mat	1.1
Polyethylene Sheet + Cotton Mat	1.2

Although all of the models investigated for drying shrinkage were based predominantly upon longer-term shrinkage values (on the order of 10 to 1000 days), the B_3 model did have some calibration data at very early ages. It was therefore believed to be the ideal model for this project.

The ultimate drying shrinkage calculated from this model can be used as a basis for the actual shrinkage in the PCC. The actual shrinkage will be based upon this value as well as the geometry of the slab, curing method, and the other factors which influence the moisture profile, as discussed previously. Section 4.4 will describe the logic used in identifying the actual shrinkage strains in the PCCP and BCO.

4.3.2   Pavement Moisture Profile

An attempt initially was made in this project to quantitatively assess the moisture profile in an early-age PCCP and BCO. The model required to do this was also to be finite element in nature (similar to the temperature prediction model). One of the primary inputs to this type of model is a property known as moisture diffusivity. Until very recently, moisture diffusivity has never been explored for use in pavements. Although laboratory and field data were collected as part of this study in order to better quantify the moisture diffusivity for PCCP, the status of the quantitative modeling of the moisture profile was felt to be too preliminary for inclusion into the final product of this study. Chapter 5 contains an outline of additional work which can be undertaken in order to better prepare this model for inclusion in the HIPERPAV/HIPERBOND systems. In addition, appendix A describes the status quo of the moisture model.

However, based on previous work, it could be reasonably assumed that the maximum strain due to drying shrinkage occurs at the surface of the pavement.[19] In addition, it is assumed that the shrinkage strains significantly decrease through the depth of the pavement, to near zero at the center of the slab and below. Although this assumption may seem imprecise, it should be noted that at very early-ages, the shrinkage strains were found to be relatively small when compared to temperature-induced strains. The resulting error was therefore assumed to be small when compared to the overall stress prediction.

4.4   PCCP/BCO Strain Prediction

As figure 12 denotes, a critical junction of the models described is the development of the strain levels present in the PCCP. The strain levels are comprised of strains due to thermal movements such as curling and axial movements as well as strains due to moisture loss (drying shrinkage). The following subsections describe the methods used to determine the strain levels in the pavement. It should be noted that the strain models that are developed in the following sections are for theoretically unrestrained pavements. The stress development due to restraint will be discussed in subsequent sections in more detail.

4.4.1 Thermal Strain Models

Using the results of the temperature prediction model from section 4.1 and the thermal coefficient of expansion model from section 4.2, the free thermal strains (the strain that an unrestrained slab would undergo) may be calculated. The general model for this calculation is as follows:

$$\nabla \varepsilon_T = \nabla T \bullet \alpha_{conc} \tag{23}$$

where,

$\nabla \varepsilon_T$ = Thermal Strain Gradient ($\mu\varepsilon$/mm)
∇T = Temperature Gradient (°C/mm)
α_{conc} = Thermal Coefficient of Expansion ($\mu\varepsilon$/°C)

This general model was divided into two specific models: a curling model and an axial model. These models are discussed in the following subsections.

4.4.1.1 Curling Strain Model

Westergaard developed a model to predict the deflections, strains, and stresses in a rigid pavement due to a uniform (linear) temperature gradient.[22] The resulting model was a closed form solution and was found to be reasonably accurate. Bradbury enhanced Westergaard's original model by accounting for the varying restraint as a function of the pavement geometry and relative stiffnesses.[23] The resulting model is used in the HIPERPAV and HIPERBOND systems as the curling stress/strain model. The following equations characterize the curling stress prediction using Bradbury's model:

$$\sigma_{curl,critical} = \frac{\alpha_{conc} \bullet \nabla T \bullet E}{2(1-v^2)}(C_{max} + vC_{min}) \tag{24}$$

where,

$\sigma_{curl,critical}$ = critical PCCP or PCCP/BCO curling stress (located in the interior of the slab) (Pa),

$\alpha conc$ = thermal coefficient of expansion of the PCC ($\mu\varepsilon$/°C),

∇T = difference in temperature between the PCCP or PCCP/BCO surface and bottom (°C),

v = Poisson's ratio, and

C_{max}, C_{min} = maximum and minimum values of the Curling Restraint Factor(derived from figure 17), using the slab length (L) in meters, and the following definition for the radius of relative stiffness (l):

71

$$l = \sqrt[4]{\frac{Eh^3}{12(1-v^2)k}}$$

(25)

where,

E = modulus of elasticity of PCC (Pa),
h = thickness of PCCP or PCCP/BCO (m), and
k = modulus of reaction of the support layers (Pa/m).
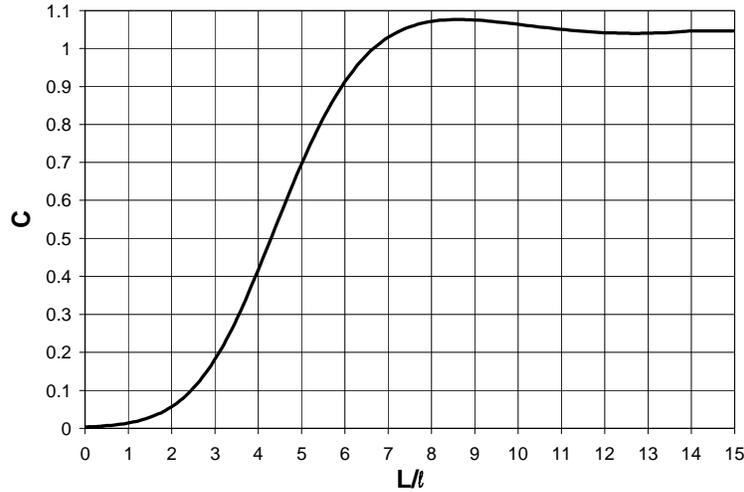
Figure 17. Curling restraint factor distribution.[23]

As observed, the previous equations predict the curling stress, as opposed to the strain values calculated from the other models. The "strain" value for curling is calculated by dividing the stress (σ_{curl}) by the creep-adjusted modulus of elasticity, E_{adjust}. Although this σ/E value does not have physical meaning, per se, it does allow for the incorporation of the creep-adjusted modulus of elasticity later in the modeling process.

It should be noted that the restraint from the weight of the slab to the curling movement is inherent in this model. The "C" correction factor accounts for the slab geometry and stiffness as compared to that of the support layers. The restraint of the axial thermal movements will be derived separately in section 4.6.

The temperature gradient used for this model is based on a datum of the temperature gradient at final set. Therefore, any permanent upward or downward curling of the unloaded slab is directly accounted for by this method. This method is characterized by the following equation:

$$\nabla T \left(from\ Equation\ 23 \right) = \nabla T_{current} - \nabla T_{set} = \left(T_{top,current} - T_{bottom,current} \right) - \left(T_{top,final-set} - T_{bottom,final-set} \right)$$

(26)

Figure 18 graphically demonstrates the concept of this model. The solid line in figure 18a shows the actual temperature gradient in the PCCP at the time of final set (which is defined as the PCC temperature when the degree of hydration is equal to 0.43 times the water-cementitious materials ratio). The dashed line represents the temperature gradient at the time for which the curling is currently being analyzed. The horizontal lines represent the difference in temperature (ΔT) at various depths of the PCCP between the final set and the current temperature. Figure 18b demonstrates the approximations that are sometimes made when determining the actual temperature gradient. If a constant set temperature is assumed (uniform throughout the cross-section), then the differences in temperature for each layer will be different (denoted as ΔT_{iA} instead of ΔT_i, where i is the layer number). In figure 18c, the differences in temperature for each layer are set equal to the actual values, thus the shape of the gradient is quite different than that in figure 18b. The maximum difference in temperature in the old model is found in the bottom layer (number 19A), while the new model predicts the maximum difference in temperature to occur closer to mid-slab (in layer 14). This difference in the gradient approximation becomes more significant if the gradient at final-set is larger than demonstrated here.

4.4.1.2 Axial Thermal Strain Model

The axial thermal strains are calculated by first deriving the average temperature difference between the current slab temperature and the slab temperature at final set. The following equation is used to perform this operation:

$$\Delta T = \frac{\sum_{z=0}^{h}\left[\left(T_{z,current} - T_{z,final-set}\right)\Delta z\right]}{h} \tag{27}$$

where,

ΔT = temperature difference used by axial thermal strain model (°C),
h = total slab thickness (mm),
T_z = slab temperature at depth z (°C), and
Δz = depth increment used in summation (mm).

The unrestrained PCCP strains can then be calculated by multiplying the value of ΔT from equation 27 with the thermal coefficient of expansion (α_{conc}).

18a
Actual
Temperature
Gradients

Slab Temperature

Top

Depth

Bottom

Current
Temperature
Gradient
($\nabla T_{current}$)

ΔT_1
ΔT_2
ΔT_3
ΔT_4
ΔT_5
ΔT_6
ΔT_7
ΔT_8
ΔT_9
ΔT_{10}
ΔT_{11}
ΔT_{12}
ΔT_{13}
ΔT_{14}
ΔT_{15}
ΔT_{16}
ΔT_{17}
ΔT_{18}
ΔT_{19}

Actual Temperature
Gradient at
Final Set
($\nabla T_{final-set}$)

18b
Approximate
Temperature
Gradient from
Previous Analyses

Slab Temperature

Top

Depth

Bottom

Current
Temperature
Gradient
($\nabla T_{current}$)

ΔT_{1A}
ΔT_{2A}
ΔT_{3A}
ΔT_{4A}
ΔT_{5A}
ΔT_{6A}
ΔT_{7A}
ΔT_{8A}
ΔT_{9A}
ΔT_{10A}
ΔT_{11A}
ΔT_{12A}
ΔT_{13A}
ΔT_{14A}
ΔT_{15A}
ΔT_{16A}
ΔT_{17A}
ΔT_{18A}
ΔT_{19A}

Previously Assumed
Constant Temperature
at Final Set
($\nabla T_{constant-final-set}$)

18c
Approximate
Temperature
Gradient from
This Analysis

Slab Temperature

Top

Depth

Bottom

Equivalent
Temperature
Gradient
($\nabla T_{current}$)

ΔT_1
ΔT_2
ΔT_3
ΔT_4
ΔT_5
ΔT_6
ΔT_7
ΔT_8
ΔT_9
ΔT_{10}
ΔT_{11}
ΔT_{12}
ΔT_{13}
ΔT_{14}
ΔT_{15}
ΔT_{16}
ΔT_{17}
ΔT_{18}
ΔT_{19}

Figure 18. Idealization of equivalent temperature gradient.

4.4.2 Shrinkage-Induced Strain Model

The general form of the model to predict free shrinkage strains is as follows:

$$\nabla\varepsilon_{sh} = f(\nabla M, \varepsilon_{sh\infty}) \tag{28}$$

where,

$\nabla\varepsilon_{sh}$ = shrinkage-induced strain gradient (profile),
∇M = moisture gradient (see section 4.3.2), and
$\varepsilon_{sh\infty}$ = ultimate drying shrinkage (see section 4.3.1).

This strain gradient can be superimposed on the strain gradient due to thermal changes, and the resulting gradient can then be used in predicting the stress development in the PCC slab.

However, as discussed in section 4.3.2, the moisture model was not mature enough in its development to be used reliably in this project; therefore reasonable assumptions concerning the moisture profile were made. Figure 19 represents the distribution of the shrinkage strains used by the HIPERPAV and HIPERBOND models. The maximum value of shrinkage is observed to be at the surface of the pavement (z=0), linearly decreasing to zero at the center of the PCCP slab (or BCO), and continuing to be negligible to the bottom of the PCCP slab (or BCO). This profile is believed to be reasonable until a more refined moisture model can be developed and possibly later incorporated into the HIPERPAV and HIPERBOND systems.
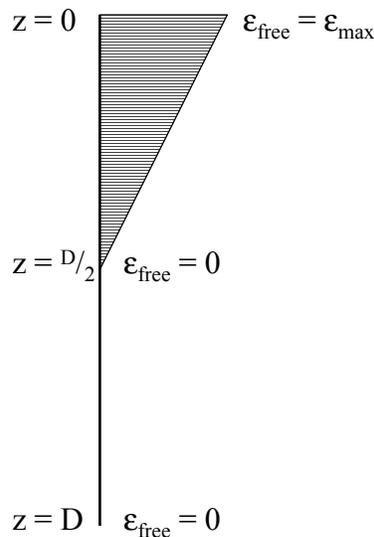
Figure 19. Assumed distribution of normalized shrinkage strain gradient.

75

4.4.3 Total Free Strains

Each of the models described in the preceding sections are represented by boxes in the second column of figure 20. The third column represents the two types of free strain calculated by the models (see sections 4.4.1 and 4.4.2). The summation of the strain profiles results in the critical strain values required to calculate the PCCP and BCO critical stresses. The missing elements, namely the modulus of elasticity and the restraint will be discussed in the following sections.

Note: Items in **BOLD** are variables which can be adjusted by the user for various construction scenarios. Items in [BRACKETS] are model variables derived from the user variables.
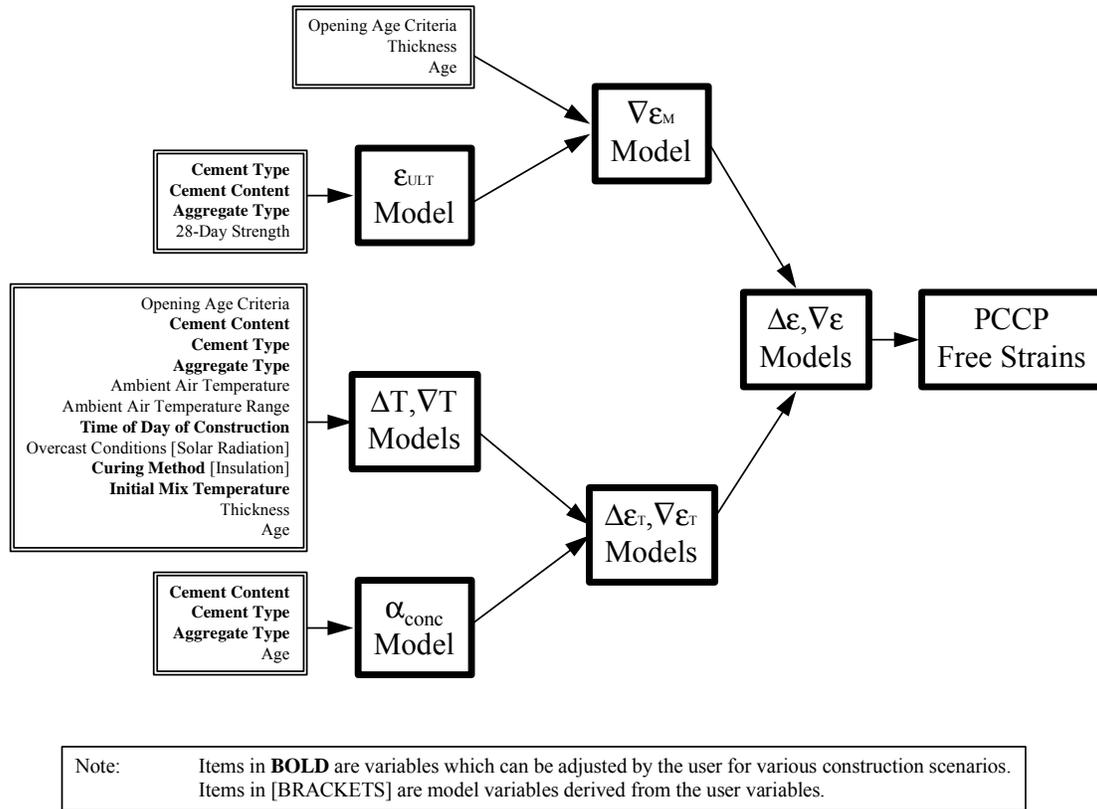
Figure 20. Flowchart of free strain model logic.

4.5 Elastic Modulus Development and Relaxation Creep Effects

The modulus of elasticity of the PCC is a critical factor in determining the overall stress level present. In order to simplify the overall modeling process, two early-age characteristics will be combined into a single model. The first is prediction of the actual modulus of elasticity using maturity methods (similar to the prediction of concrete strength - see section 4.7). The second characteristic is relaxation creep, or the tendency for PCC under load to demonstrate a decrease in the internal stress level over time. The following subsections will describe the models used to characterize these phenomena.

76

4.5.1 Predicting Modulus of Elasticity using Maturity Methods

Maturity methods have been used extensively in recent years to predict the in-place strength of PCC.[19] The basis for this method is simple: the strength (and modulus of elasticity) of a PCC specimen are directly related to the quantity of heat developed from the hydrating cement. The practical benefit of this method is that field evaluations of in-place strength can be predicted from simple temperature measurements of the concrete over time. The theoretical benefit is the ability to accurately predict both the strength and modulus of elasticity of PCC over a wide range of conditions based simply on the temperature development in the modeled pavement (see section 4.1).

The two models that have been used the most in characterizing maturity are the Nurse-Saul model and the Arrhenius model.[24] The Nurse-Saul model is simplistic in nature and is based upon the integration of the time-temperature history of a PCC. Theory states that for the same mix, equivalent areas under the time-temperature curve (with a lower-bounds datum) represent identical strengths. Arrhenius theory, however, is more complex mathematically, and has been demonstrated to better predict the actual processes present in a maturing PCC.

The basis of Arrhenius theory is the prediction of the equivalent age, t_e. The equivalent age can then be used to calculate the degree of hydration of the concrete. The degree of hydration is then used to predict the concrete strength or modulus of elasticity. The equivalent age, t_e, is equal to the numerator of equation 6, or redefined here as:

$$t_e = \sum_{t=0}^{age} \left[e^{\left[-\frac{\Phi}{R}\left(\frac{1}{T+273} - \frac{1}{T_r+273} \right) \right]} \bullet \Delta t \right] \tag{29}$$

where,

t_e = equivalent age (h),
Φ = activating energy (J/mol) (see typical values in table 10),
t = time (h),
R = universal gas constant, 8.3144 J/mol/°C,
T = nodal PCC temperature (°C), and
T_r = reference temperature, 20°C,

which can be reduced to:

$$t_e = \sum_{t=0}^{age} \left[e^{\left[-\frac{\Phi}{8.3144}\left(\frac{1}{T+273} - \frac{1}{293} \right) \right]} \bullet \Delta t \right] \tag{30}$$

The degree of hydration, ψ, is then defined as:

$$\psi = e^{-\lambda_1 (\ln \tau)^{-\kappa_1}} \tag{31}$$

where,

τ = age parameter, defined as: $1 + \left(\dfrac{t_e}{t_1}\right)$, and $\tag{32}$

λ_1, κ_1, t_1 = hydration shape and time parameters (see typical values in table 10).

The prediction of the modulus of elasticity requires a benchmark value. This value is entered manually by the user as the 28-day mean laboratory value (cured under standard conditions and methods). In order to calculate the early-age modulus of elasticity, the degree of hydration is used with the following equation:

$$E_{current} = E_{28-day} \left(\frac{\psi_{current} - \psi_{critical}}{\psi_{28-day} - \psi_{critical}}\right)^{2/3} \tag{33}$$

where,

$\psi_{current}$ = degree of hydration at specific time,

$\psi_{critical}$ = degree of hydration at final set of PCC = $0.43 \times {}^{W}/_{CM}$, $\tag{34}$

ψ_{28-day} = degree of hydration at 28-days (assuming PCC remains at reference temperature), defined mathematically as:

$$\psi_{28-day} = e^{-\lambda_1 \left[\ln\left(1 + \frac{672.}{t_1}\right)\right]^{-\kappa_1}} \tag{35}$$

${}^{W}/_{CM}$ = water-cementitious materials ratio of the concrete mix.

4.5.2 Relaxation Creep Fundamentals

Creep is a characteristic of many materials, including PCC, which, if not accounted for correctly, can result in an erroneous response prediction. This has been found to be especially true for PCC during the early-age period.[19] In the HIPERPAV and HIPERBOND systems, creep effects are accounted for by using a creep-adjusted modulus of elasticity. The following subsections describe the basic mechanisms of creep in PCC and demonstrate the rationale behind the adjusted modulus of elasticity model.

Creep in materials can have two distinct effects, depending on the loading and restraint conditions. The first effect occurs under a constant stress condition that results in a deformation of the specimen with time. The second effect occurs under a constant

strain condition that causes a decrease in stress results over time. This second effect is often termed "relaxation."

PCC at early-age has been shown to demonstrate viscoelastic behavior. This behavior can be characterized in the same manner as that of asphalt, but with different levels of viscoelastic response.

4.5.3 Relaxation Creep Adjusted Modulus of Elasticity

The effective or creep-adjusted modulus of elasticity, E_{eff}, is defined by the following general equation: [25]

$$E_{eff} = \frac{E_\circ}{|1 + J_t E_\circ|} \tag{36}$$

where,

$\quad E_o \quad$ = elastic modulus at the time of load application (age of set),
$\quad J_t \quad$ = adjusted creep compliance factor (mm²/N), defined as:

$$J_t = J_t' \delta_t \xi_t \phi_t \tag{37}$$

where,

$\quad J_t' \quad$ = creep compliance factor (mm²/N), defined as:

$$J_t' = \left[28.74\left(1 - e^{-0.801t}\right) + 8.13\left(1 - e^{-45.38t}\right) + 4.468t\right] \times 10^{-6}, \tag{38}$$

$\quad \delta_t \quad$ = stress intensity correction factor, defined as:

$$\delta_t = 0.017\sigma + 0.701, \tag{39}$$

$\quad \xi_t \quad$ = loading time correction factor, defined as:

$$\xi_t = -1.107\ln(\tau) + 1.538, \text{ and} \tag{40}$$

$\quad \phi_t \quad$ = temperature correction factor, defined as:

$$\phi_t = 0.0257T + 0.487 \tag{41}$$

where,

$\quad t \quad$ = age of PCC (days),
$\quad \sigma \quad$ = average PCC stress (N/mm²),
$\quad \tau \quad$ = elapsed time since start of loading (days), and
$\quad T \quad$ = average cross-sectional PCC temperature (°C).

Although the formulation of the effective or creep-adjusted modulus is rather complex, the simplicity of the model is maintained by providing the user with a single modulus value for a given age. This value for E can be used in the overall stress calculations.

4.6   Slab Restraint and Stress Development

In an early-age pavement subjected to strain-induced loading (such as shrinkage and thermal movements), stresses cannot develop without some degree of restraint. These principles were initially discussed in section 2.1.3, "Mechanical State of Stress" and conceptually illustrated in figure 5. The objective of this section is to quantify these concepts previously discussed. In order to assess the critical stress conditions in a pavement, an accurate determination of the degree of restraint must be determined. The following subsections discuss the concepts of slab restraint and outline the details of the models developed for use in the HIPERPAV and HIPERBOND systems.

4.6.1   Slab Axial Restraint Concepts

One method of representing the level of axial restraint due to slab-base friction is via a unitless variable. This variable is termed the restraint factor, R_F. The concept of the restraint factor is graphically represented in figure 21. The upper bound of the restraint factor is a value of 1.0. For axial movement, this level of restraint would represent a base course with infinite friction, so that no free movement can occur. If no movement occurs, the free strain would fully translate into an internal stress equal to the free strain multiplied by the modulus of elasticity. The other extreme would be a frictionless base with a friction coefficient of 0.0. This would then translate into a restraint factor of 0.0. Because of the frictionless surface, the free strain subjected to the pavement is translated into movement of the slab along the base, and no stresses develop. The length of the slab after subjecting to the strain is equal to the original length multiplied by the quantity of one minus the free strain.

The conditions represented by the extremes of the restraint factor are in fact never experienced in practice. In all cases, the actual level of restraint is some level between these extremes. In addition, the restraint factor will vary along the length of the slab. For an uncracked slab subjected to axial loading (e.g. due to shrinkage or a uniform drop in slab temperature), the critical restraint factor would be at the center slab, and would decrease with distance from the center of the slab. For a restraint factor between 0.0 and 1.0, the maximum internal stress developed in the slab would be equal to the product of the free strain, modulus of elasticity, and the restraint factor. The resulting length of the slab would be equal to the product noted on the last drawing of figure 21.

The restraint factor is primarily a function of the base type (i.e. friction level), but is also, to a lesser degree, a function of the joint spacing, thickness of the slab, and the modulus of elasticity (making the model a circular form since the modulus is also used in

the stress calculation). A cement treated base, for example, has a significantly higher restraint factor than an asphalt concrete base. Similarly, a thicker slab has a greater restraint factor than a thinner slab.

Slab Fully Restrained (Full Friction - No Sliding)

$$L_o \quad \{R_F = 1.0\}$$

$$\sigma = \varepsilon_{FREE} \times E$$

FRICTION = ∞

No Slab Restraint (No Friction - Unrestricted Sliding)

$$L_{FREE} = L_o \times (1 - \varepsilon_{FREE}) \quad \{R_F = 0.0\}$$

$$\sigma = 0.0$$

FRICTION = 0.0

Some Slab Restraint (Some Friction - Some Sliding)

$$L_{ACTUAL} = L_o \times [1 - \varepsilon_{FREE} \times (1 - R_F)] \quad \{0.0 < R_F < 1.0\}$$

$$\sigma = \varepsilon_{FREE} \times E \times R_F$$

0.0 < FRICTION < ∞
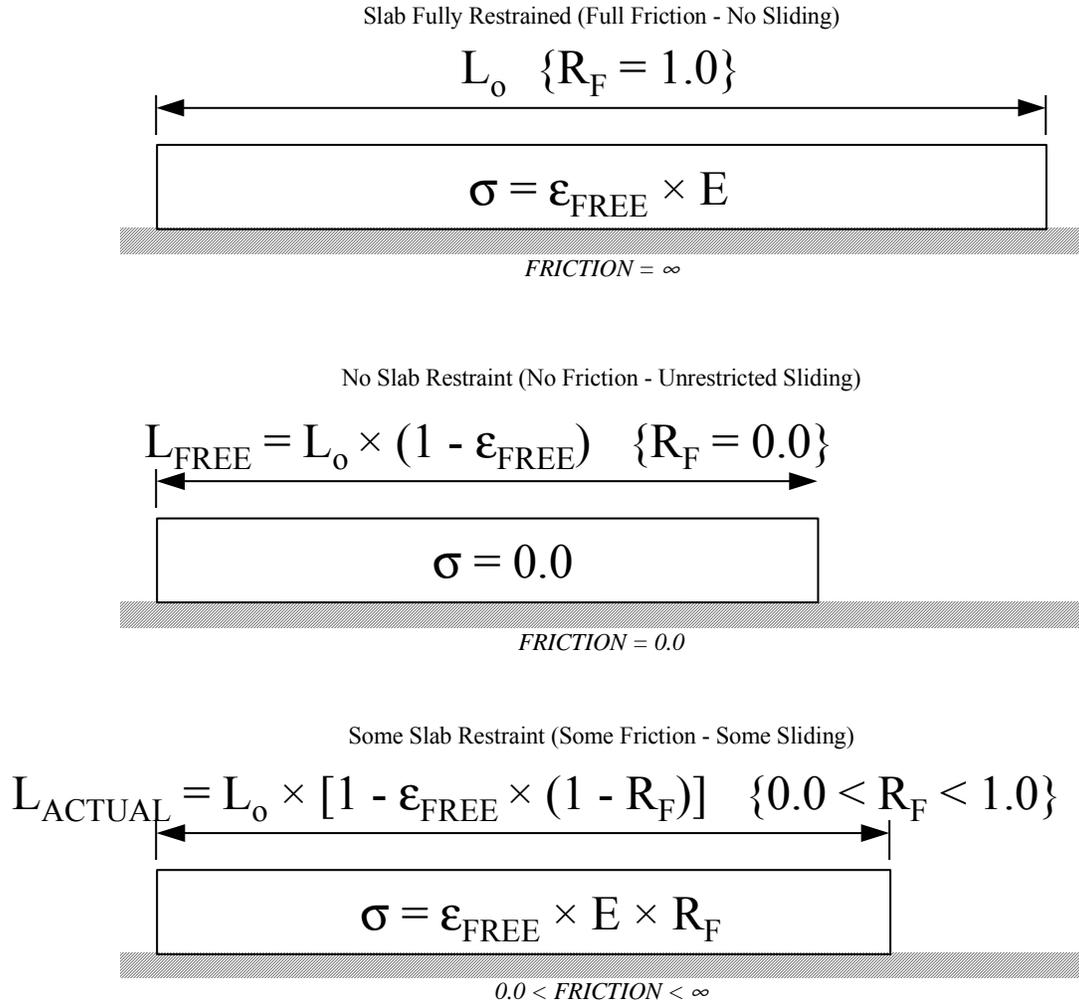
Figure 21. Schematic of slab restraint concept.

Joint sawing is considered in this model by modifying the effective slab length used during the analysis. Prior to sawcutting operations, the joint spacing is assumed to be infinite, and the stresses are calculated based on this assumption. Following the time of sawcutting, the joint spacing is reduced to the value which is entered by the user. A decrease in the stress at this time is therefore observed as a result of this effect.

In order to calculate the restraint factor due to slab-base friction, a model has been selected which was originally developed for CRCP, but has been adapted for JCP for this project.[26] The basis for the model is the following differential equation:

$$\frac{d^2 u_c}{dx^2} - \left(\frac{b}{E_c A_c} \right) \tau_f = 0 \tag{42}$$

where,

u_c = PCC axial displacement (m),
x   = coordinate in direction of axial movement,
b   = pavement width (m),
E_c = modulus of elasticity of PCC (kPa),
A_c = cross sectional area of pavement (m²), and
τ_f = friction stress (kPa) (see figure 22).

The shape of the curve in figure 22 is a function of the base type beneath the PCCP. Table 14 contains the coefficients which define the shape of the friction stress curve for various subbase types. In addition, the user may enter measured values of the friction characteristics directly (C_2 and τ_f from figure 22).
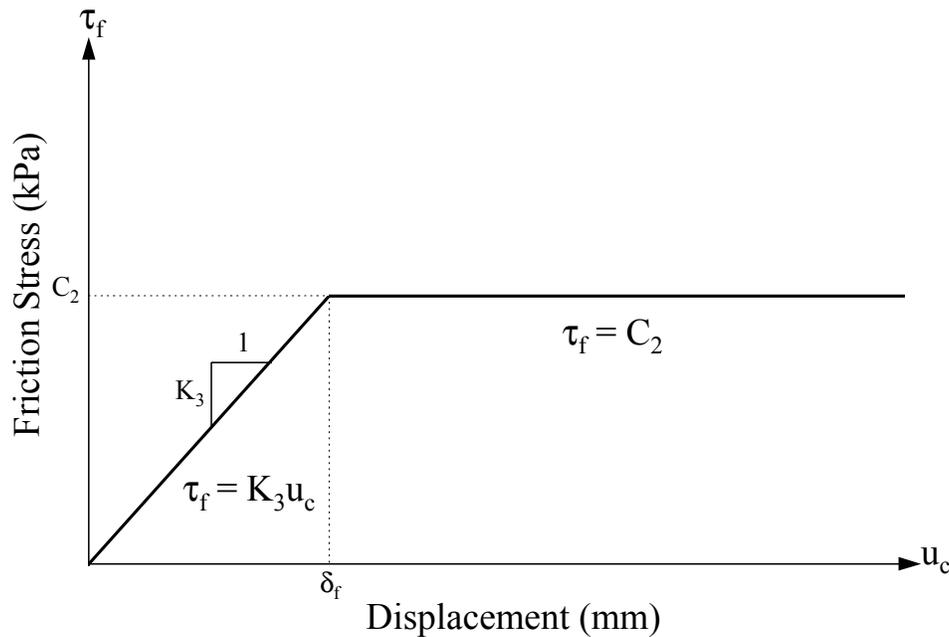
Figure 22. Friction stress function used in axial restraint model.

Solving the original differential equation, the stress in the concrete due to slab-base friction can be calculated. In addition, the free movement of the slab can be calculated using the same equations. These are then combined using the concepts set forth in figure 21 in order to calculate the restraint factors. The axial restraint factor calculation procedure has been demonstrated in this section to be rather complex. Because the restraint factor values are a function of several dynamic variables, specific factors cannot be tabulated here.

Table 14. Friction stress characteristics of subbase types.(27)

Subbase Type	C_2 in kPa (lbf/in^2) (max. friction)	δ_f in mm (in.) (displ. @ sliding)	K_3 in kPa/mm (lbf/in^2/in) (friction slope)
Asphalt Concrete	16 (2.3)	1.27 (0.05)	13 (46)
Asphalt Stabilized	13 (1.9)	0.86 (0.034)	15 (56)
Cement Stabilized	106 (15.4)	0.025 (0.001)	4200 (15000)
Lime Treated Clay	11 (1.65)	0.29 (0.0115)	38 (140)
Natural Clay	6 (0.85)	1.04 (0.041)	6 (21)
Granular	17 (2.5)	0.76 (0.03)	22 (83)

4.6.2 Slab Curling Restraint Concepts

Section 4.4.1.1 described in detail the concepts behind the restraint of slab curling. The stresses due to curling were calculated directly and separately using the "C" values from figure 17.

4.6.3 Critical Stress Determination

Two sources of stresses are modeled in the HIPERPAV system. The first is due to axial movements caused by uniform changes in temperature or moisture. The second is due to non-uniform temperature and moisture distributions (gradients), both linear and non-linear. The uniform movements will cause tensile stresses only if they tend to decrease the volume of the slab (i.e. temperature decrease or moisture loss). However, thermal and moisture gradients always lead to tensile stress development in the slab. To simplify the modeling process, these stresses can be assumed to be superimposed on each other. The location of the critical (maximum) value of stress will actually change during the early-age life of the pavement. Although it will be in the interior of the slab, the vertical position will change with time as the slab curls upward and downward through diurnal cycles.

Although the position of the critical stress fluctuates, the stress in the pavement structure can be determined using the following general formula:

$$\sigma_{critical} = MAX_{TENSILE} \begin{cases} \left(\varepsilon_{axial,top} + \varepsilon_{sh}\right) \times R_F \times E_{eff} + \sigma_{curl,top} \\ \varepsilon_{axial,mid} \times R_F \times E_{eff} \\ \varepsilon_{axial,bottom} \times R_F \times E_{eff} + \sigma_{curl,bottom} \\ 0 \end{cases} \qquad (43)$$

This process is demonstrated graphically in figure 23.
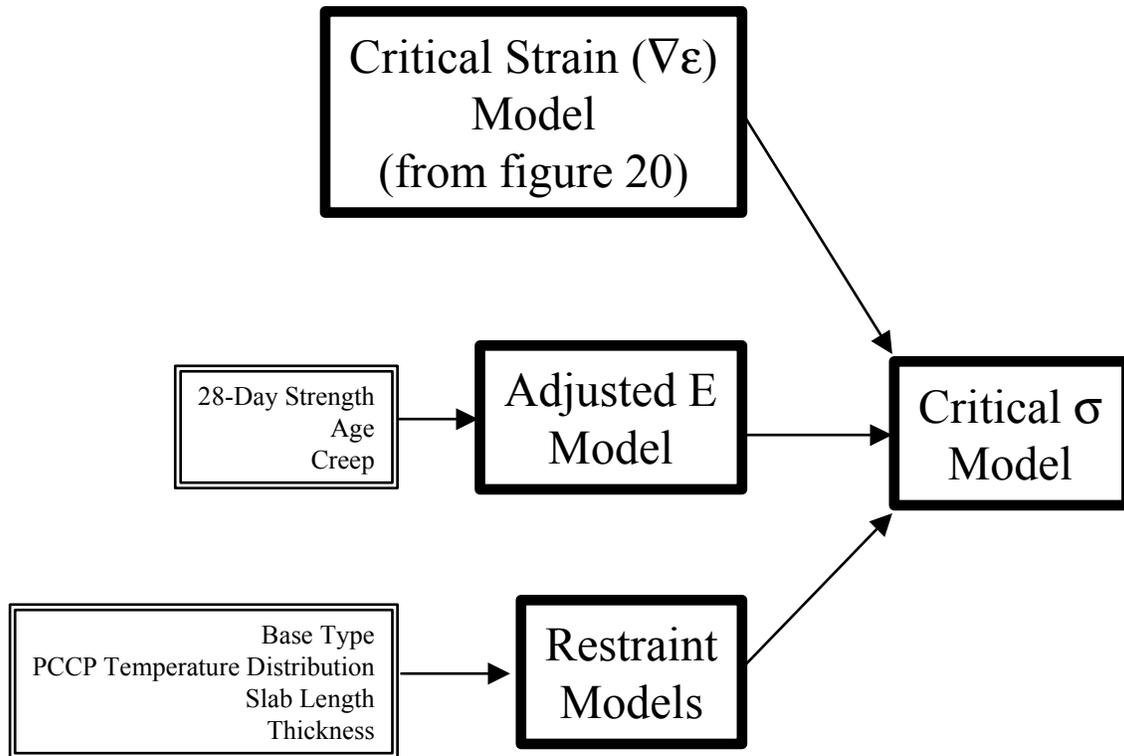
Figure 23. Schematic of critical stress model logic.

4.7   Strength Modeling for Full-Depth PCCP

In order to have the ability to assess the potential for early-age PCCP damage, models must be developed in order to accurately predict the strength of the PCC and, for BCOs, the bond between the existing PCCP and the BCO. This section will discuss the former, while the latter will be discussed in detail in section 4.8. The reliability concepts discussed in section 4.7.2 are applicable to both PCC strength development as well as the bond strength development of BCOs discussed in the next section.

Several forms of PCC strength prediction models have been developed. Some models simply apply an empirical closed-form equation to predict the strength as a function of the 28-day strength. However, these models are not sensitive enough to capture the relationship between temperature development in the early-age slab and the strength gain. The type of model which mechanistically defines this relationship is commonly referred to as the maturity method. The following sections will describe this method in more detail and demonstrate its application in the HIPERPAV system.

4.7.1 Strength Prediction using Maturity Methods

In order to determine the possibility of distress in the early-age PCCP, a measure of strength must be developed. PCC strength is a function of many factors. Apart from the mix design, the strength development is a function of time and temperature.

As mentioned previously, the strength development is a critical factor in determining the behavior of the pavement. One method which is widely accepted as a method to predict PCC strength is the maturity concept.

As discussed in section 4.5, maturity is a measure of the thermal history of a PCC specimen. If a concrete is cured in an environment which is insulatory and prevents heat loss to the environment, it will gain strength faster than that of a specimen which is exposed. The detriment of a high heat cure is that the environmentally induced stresses in the PCCP, when exposed at a later age, could ultimately be higher, thus making the PCCP more vulnerable to premature distress.

Strength of PCC develops due to hydration. Hydration is a complex chemical process which transforms the basic cementitious minerals into a semi-crystalline matrix. The matrix provides the dynamic element of the strength gain in PCC, while the strength of the other component, aggregate, remains constant. Because of this, if one wishes to predict the strength gain phenomena in PCC, the cement paste matrix should be of primary concern.

In addition to the maturity concepts mentioned herein, simplified models have been developed which can assess the strength of a PCC mix as a function of time. These models are usually developed based upon empirical regression models fit through experimental data from actual PCC specimens. These simplified models do not directly account for the temperature dependence of the hydration process, and therefore may not be sensitive enough to predict the early-age strength gain.

The strength of the PCC is calculated using the degree of hydration. For a detailed formulation of the degree of hydration calculations, refer to section 4.5.1. The general formula for the early-age strength, $S_{current}$, is:

$$S_{current} = S_{28-day}\left(\frac{\psi_{current} - \psi_{critical}}{\psi_{28-day} - \psi_{critical}}\right) \tag{44}$$

where,

$\psi_{current}$ = degree of hydration at specific time,
$\psi_{critical}$ = degree of hydration at final set (see equation 34), and
ψ_{28-day} = degree of hydration at 28-days (see equation 35).

Equation 44 is very similar to equation 33 (calculating the modulus of elasticity). Both equations require a 28-day benchmark value, and both have a correction factor for

the age of the PCC. However, note that the exponent on the strength equation is 1, while it is 2/3 for the modulus of elasticity. It should be noted that, although not used in HIPERPAV, for compressive strength gain, this exponent would equal approximately 1.5. These relationships between the concrete strength and elastic parameters versus the degree of hydration have been documented by laboratory and field research.[28]

4.7.2 Reliability Analysis and Threshold Determination

In order to account for the variability associated with the materials in a typical construction project, reliability concepts are incorporated into the identification of the strength development. Reliability is a statistical term which is defined as the percent chance that the failure criteria will not be violated. For example, if the reliability is determined to be 95 percent, on the average, only 1 instance out of 20 (5 percent) will fail.

A large reliability has higher associated construction costs due to the additional precautions that must be taken to minimize early-age damage such as more stringent curing methods, or limitations on the construction times. Conversely, a lower reliability increases the chance of a premature failure, which itself has a direct cost associated with it. Generally, the greater the importance of a facility, the higher the reliability which is selected for the guidelines. For example, an urban freeway may require a reliability of 99 percent due to the impacts associated with disrupting traffic for reconstruction, whereas a local road may be satisfactory with a reliability of 75 percent.

Reliability is incorporated into the HIPERPAV system by adjusting the stresses and strengths by using the following formulae:

$$s = s_{actual} \times \left[1 - \left(\frac{z(R) \times CV_s}{\sqrt{2}} \right) \right] \qquad (45)$$

$$\sigma = \sigma_{actual} \times \left[1 + \left(\frac{z(R) \times CV_\sigma}{\sqrt{2}} \right) \right] \qquad (46)$$

where,

s = the strength for input into the HIPERPAV system,
s_{actual} = the average strength used for modeling,
σ = the stress to compare to the strength value,
σ_{actual} = the average stress calculated by HIPERPAV
$z(R)$ = the normally distributed z-value for the given reliability (see table 15),
CV_s = the coefficient of variation of the strength, and
CV_σ = the coefficient of variation of the stress.

Typically, the coefficient of variation of PCC strength is in the range of 10 percent to 20 percent. If the user feels that this variation is too large or small for the materials being used, they may adjust the reliability so as to account for the difference in variability. For example, if the user knows that the CV is closer to 10 percent for their mix, they may reduce the required reliability from 99 percent to 95 percent.

Table 15. Table of normally distributed z-values versus reliability.

Reliability, R (%)	Normally Distributed z-value
50	0.000
60	0.253
70	0.524
75	0.674
80	0.841
85	1.037
90	1.282
92	1.405
95	1.645
97	1.881
98	2.054
99	2.327
99.9	3.090
99.99	3.750

4.8   Bonded Concrete Overlay (BCO) Delamination Models

Delamination is the primary mode of distress in most BCO projects. Because of this, one of the principal objectives of the project for which these guidelines were developed is to recommend measures which can be taken to minimize this distress type. Delamination is simply the separation of the BCO from the existing pavement. This separation can then lead to secondary distress types such as cracking, punchouts, and spalling.

Two mechanisms can lead to delamination, namely, bond shear failure, and bond tensile failure. These failure mechanisms can work independently or simultaneously. The end result is the same, namely the separation of the PCC layers. The first mechanism, bond shear failure, is caused by a potential for differential lateral movement between the two PCC layers. If the potential differential movement is great enough, the shear stress at the bond interface will exceed the bond shear strength, and a failure will occur in shear along the interface. The second failure mechanism, bond tensile failure, is caused by a potential differential movement in the vertical direction. If the potential differential movement is great enough, the tensile stress at the bond interface can exceed

87

the tensile strength of the bond. A graphical representation of these failure modes can be seen in figure 24.

The stresses at the bond interface can be predicted quantitatively using various analytical tools. The bond strength can be assessed using the maturity methods described in previous sections related to strength and modulus of elasticity gain in a maturing concrete. The following sections will describe the models used in the HIPERBOND system to characterize these phenomena.

BCO

EXISTING PCCP
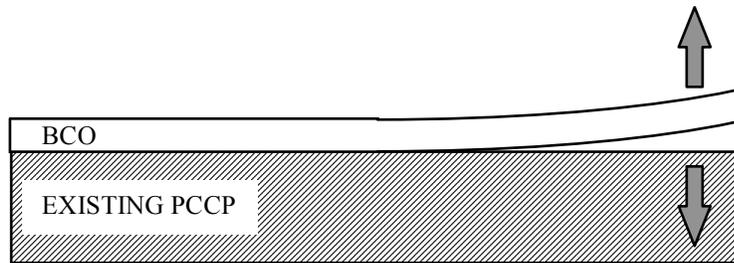
Bond Tensile Failure

BCO

EXISTING PCCP
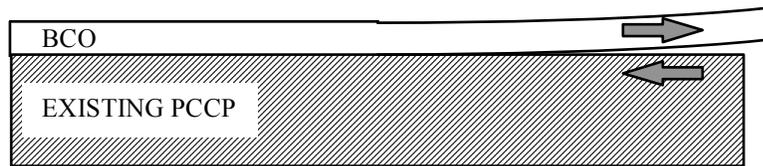
Bond Shear Failure

Figure 24. Shear and tensile BCO bond failure mechanisms.

4.8.1 Overlay Stress Model Development

The United States Forest Service Laboratory has developed a comprehensive model for predicting stresses in a system of laminated beams.[29] The model consists of a three layer system with two different materials fastened together by a thin adhesive layer. The model is based on elastic beam theory and requires an eigenvalue-based solution due to its complex nature. In reviewing several potential models for predicting interface stresses, including finite-element based solutions, this model was believed to be superior because of its quick computation time, robustness, and accuracy.

Figure 25 represents the ideal system from which this model is developed. Each of the three layers is characterized by a modulus of elasticity (E), thermal coefficient of expansion (α), thickness (h), and Poisson's ratio (ν). The total length of the beam is 2 ℓ.
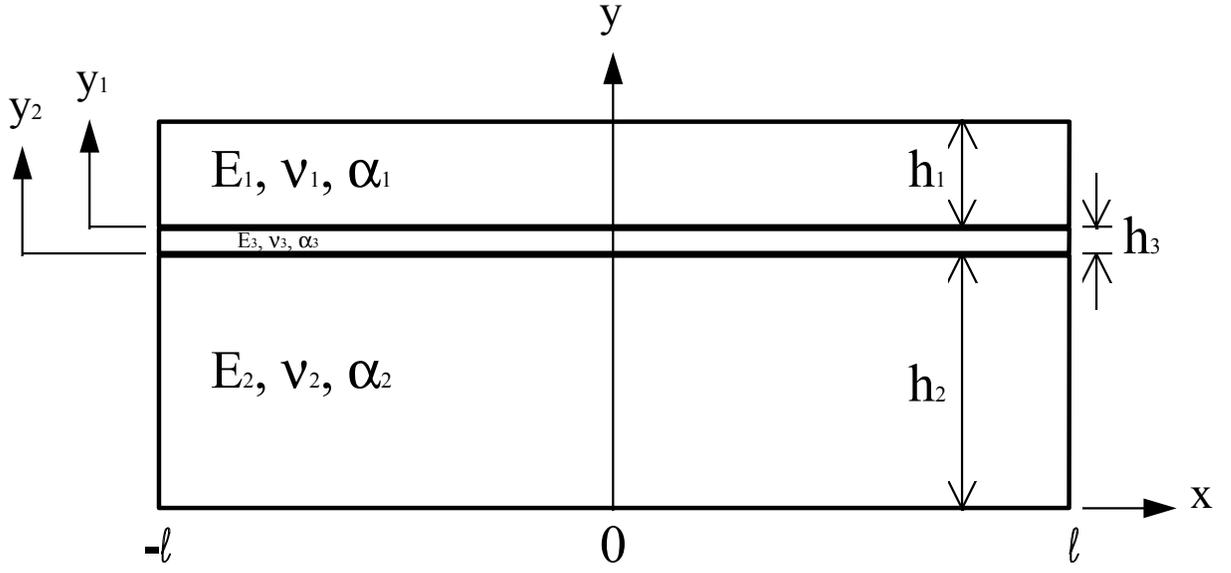
Figure 25. Idealized elastic layer system used in HIPERBOND.

The model is presented here in a simplified form. A full definition of the model can be found in the original source.[29] The general governing equations for the stress analysis are as follows:

$$\left[C_1 \frac{d^4}{d\xi^4} + C_2 \frac{d^2}{d\xi^2} + C_3 \right] \frac{\sigma_1}{E_1} + \left[C_4 \frac{d^4}{d\xi^4} + C_5 \frac{d^2}{d\xi^2} + C_6 \right] \frac{\sigma_1^*}{E_1} = C_{10} \tag{47}$$

$$\left[C_4 \frac{d^4}{d\xi^4} + C_5 \frac{d^2}{d\xi^2} + C_6 \right] \frac{\sigma_1}{E_1} + \left[C_7 \frac{d^4}{d\xi^4} + C_8 \frac{d^2}{d\xi^2} + C_9 \right] \frac{\sigma_1^*}{E_1} = C_{11} \tag{48}$$

where,

$C_1, C_2, ... C_{11}$ = elastic coefficients = $f(E, h, \nu, \alpha, \ell)$
(not defined here due to their complexity),[29]

ξ = normalized x-coordinate of slab ($\xi = -1$ @ $x = -\ell$; $\xi = 1$ @ $x = \ell$; see figure 25),

σ_1 = primary stress function, and

σ_1^* = secondary stress function.

After solving these differential equations for σ_1 and σ_1^*, the following equations can be used to solve for the tensile and shear stresses at the bond interface:

$$\tau_{xy} = \frac{\partial \sigma_1}{\partial x} \bullet h_1 + \frac{\partial \sigma_1^*}{\partial x} \bullet \frac{h_1}{2} \tag{49}$$

$$\sigma_y = \frac{\partial^2 \sigma_1}{\partial x^2} \bullet \frac{h_1^2}{2} + \frac{\partial^2 \sigma_1^*}{\partial x^2} \bullet \frac{h_1^2}{3} \tag{50}$$

where,

τ_{xy} = shear stress in x-y plane at interface,
σ_y = tensile stress normal to interface surface,
h_1 = overlay thickness (see figure 25).

4.8.2 *Overlay Bond Strength Model Development*

Although some evidence has arisen during the course of this research that bond strength may develop faster than tensile strength of the PCC, the same relationship was used in predicting each strength type. This may build into the model some degree of conservativeness. This model is recommended until further evidence is developed demonstrating a greater acceleration of bond strength during the early-age period. Bond strengths, therefore, are developed using the same model as was presented in section 4.7. The general form of this equation is as follows:

$$\widetilde{S}_{current} = \widetilde{S}_{28-day} \left(\frac{\psi_{current} - \psi_{critical}}{\psi_{28-day} - \psi_{critical}} \right) \tag{51}$$

where,

$\widetilde{S}_{current}$ = bond strength (tensile or shear) for current time (age) (kPa),
$\widetilde{S}_{28-day}$ = bond strength (tensile or shear) at 28-days (kPa),
$\psi_{current}$ = degree of hydration at specific time,
$\psi_{critical}$ = degree of hydration at final set (see equation 34), and
ψ_{28-day} = degree of hydration at 28-days (see equation 35).

The bond strengths developed by this model are subsequently adjusted (lowered) to account for variability. This process is described in section 4.7.2.

4.9   Early-Age Distress Models

The ultimate objective of the HIPERPAV and HIPERBOND guidelines is to predict the potential for early-age damage. Figure 26 depicts the three primary forms of distress which are investigated in this study.   The first distress type is plastic shrinkage

		Distress Type	Critical Stress Locations	Critical Period

(a) *Plan View Plastic Shrinkage Cracking*

Plastic Shrinkage Cracking

First 3 to 12 h
or until Curing Method
Application

(b) *Plan View Thermal Shock Cracking*

First 72 h

(c) *Profile View Bonded Concrete Overlay Delamination*

First 72 h
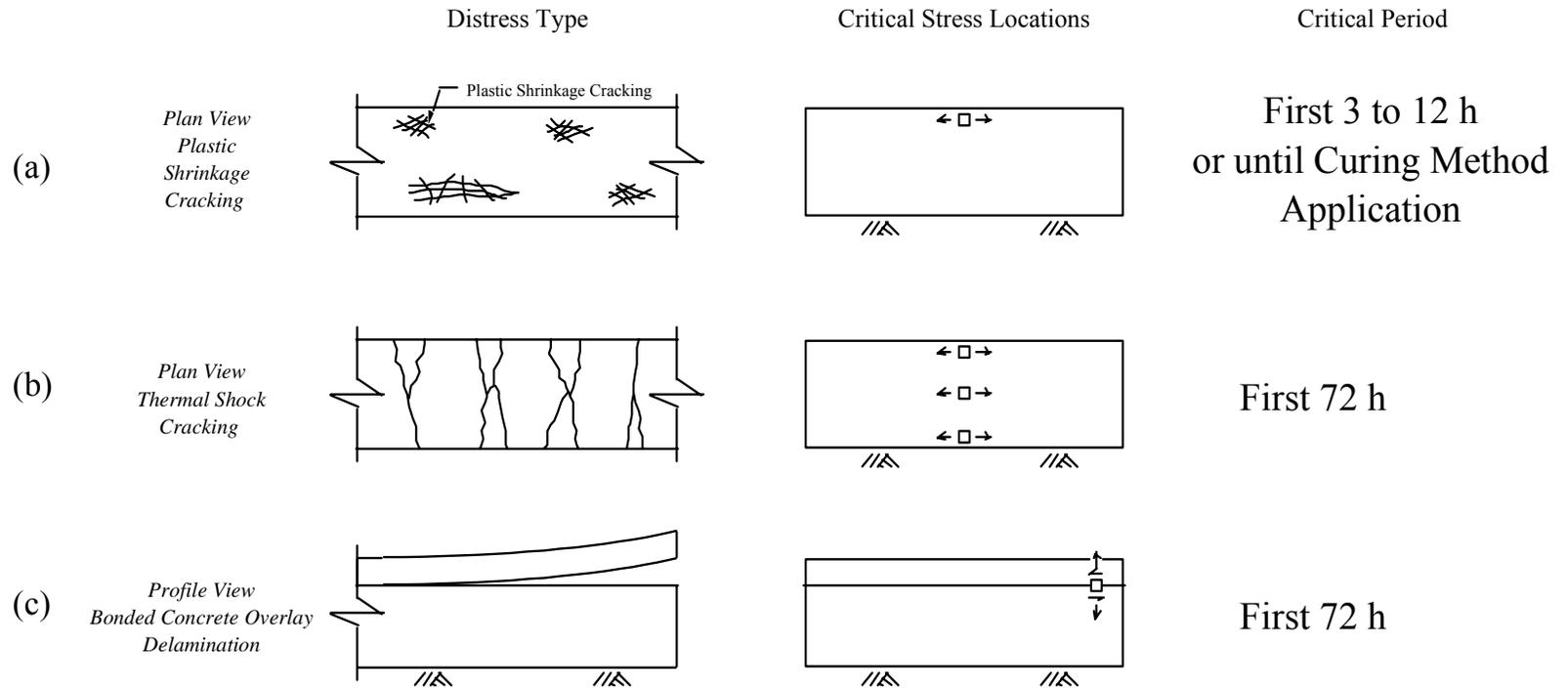
Figure 26. Graphical representation of distress models.

cracking which can occur in any exposed PCC surface during the very-early-age period (before final set).This type of distress is caused by excessive moisture loss at the surfaces of the pavement, and therefore the critical stress level is present at the surface as noted in the figure. The second form of distress is uncontrolled cracking of jointed concrete pavements. This distress is caused by volumetric changes due to temperature and moisture changes primarily in the early-age period. The critical stress can be at any depth in the pavement, as shown in the figure. The third mode of distress is specific to bonded concrete overlays: delamination. Delamination also occurs primarily during the early age period and can occur due to either excessive shear or tensile stresses at the interface of the existing PCCP and the BCO.

Sections 4.9.1 and 4.9.2 demonstrate the methods used to predict early-age cracking in PCCP and early-age delamination in BCO, respectively. Section 4.9.3 will then describe an additional method of early-age damage: plastic-shrinkage cracking.

4.9.1 Early-Age PCCP Cracking

Two possible scenarios of stress-versus-strength development can occur. Figures 27 and 28 graphically depicts these scenarios. The first scenario shows the stress maintaining a magnitude which is consistently lower than that of the strength, therefore early-age distress is not expected. The second scenario shows that stress development is at a much greater rate than strength development. At the point of intersection of these plots, a failure will occur in the form of a crack. The purpose of the HIPERPAV system is to derive a combination or combinations of inputs which can maintain a stress level which is lower than the strength level. The scenarios which achieve this goal can then be used as candidate design and construction methods. If they are in violation, then modifications must be made to the inputs to bring them into compliance. It should be noted that the strength curves in figures 27 and 28 represent the adjusted strength based on the level of reliability given. The mean strength curve would lie above that which is plotted in the figure (assuming a reliability level over 50% is selected).

4.9.2 Early-Age BCO Delamination

Delamination in the early-age BCO is the critical distress which is modeled by the HIPERBOND system. The delamination mechanisms were graphically depicted in figure 25. Two modes of failure are modeled by the guidelines: shear failure and tensile failure. A violation of the shear or tensile strength of the bond at any time can lead to delamination. The HIPERBOND delamination distress model simply compares the bond stresses with the bond strength.

Figures 29 and 30 demonstrate the concepts in this comparison process. The stresses and strengths in this figure represent the conditions at the "critical" bonded location which is defined as the location where the highest concentration of delamination stresses exist. Figure 29 demonstrates a set of conditions where the strength in shear and

tension remain above the stress levels at all times (during the early-age). Scenarios 2 and 3 in figure 30, however, show violations of the bond strength by shear and tension modes, respectively. Note that when delamination occurs, the stress level subsequently decreases in both shear and tension, thus a drop in the curves can be noted at these times. Scenario 4 in figure 30 demonstrates a very poor scenario where delamination occurs first in tension, and then later in shear. This scenario demonstrates the concept of progressive failure if the conditions causing the delamination are not countered.

Each of the latter three scenarios constitutes an early-age failure of the BCO system. A violation of either the shear or tensile strength can lead to delamination. Therefore, during the run-time of the HIPERBOND software, the user should note a violation (or near-violation) of both modes of failure.
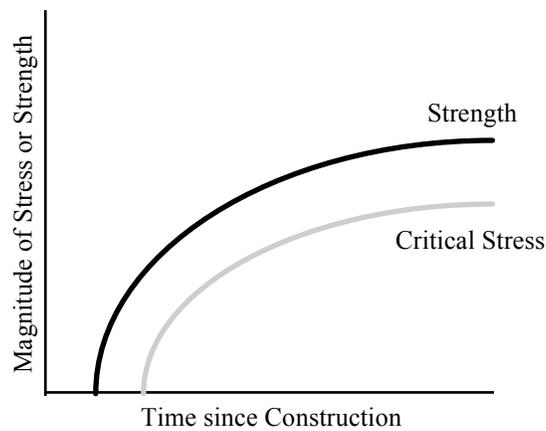
Scenario #1

Figure 27. Good stress and strength development scenarios.
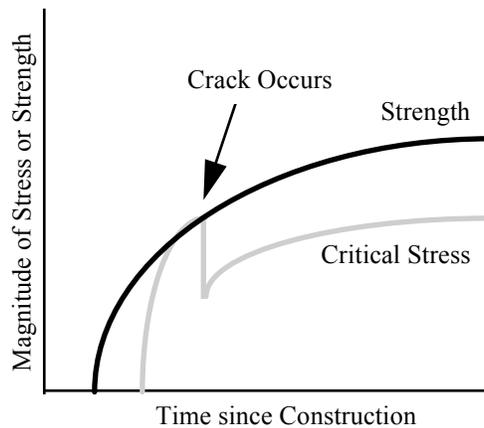
Scenario #2

Figure 28. Poor stress and strength development scenarios.

93
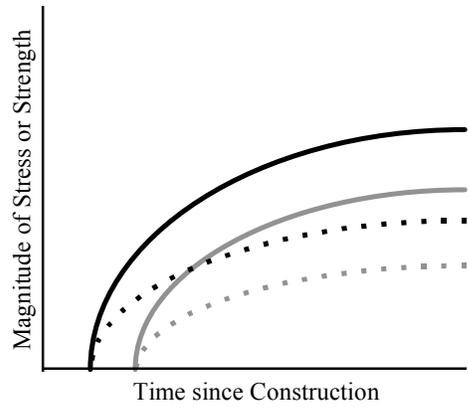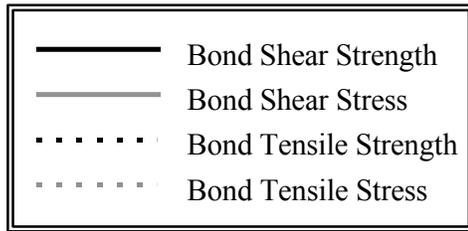
Figure 29. Good bond stress and strength development scenario.
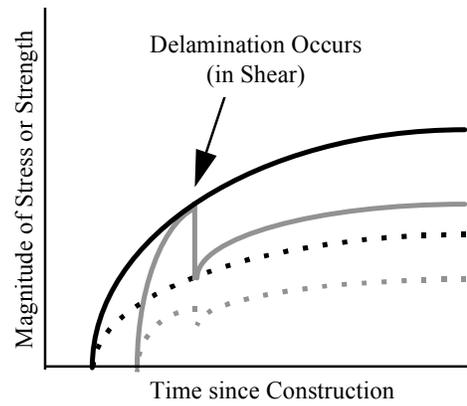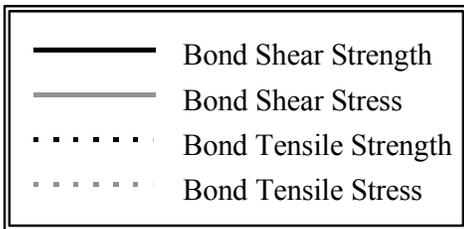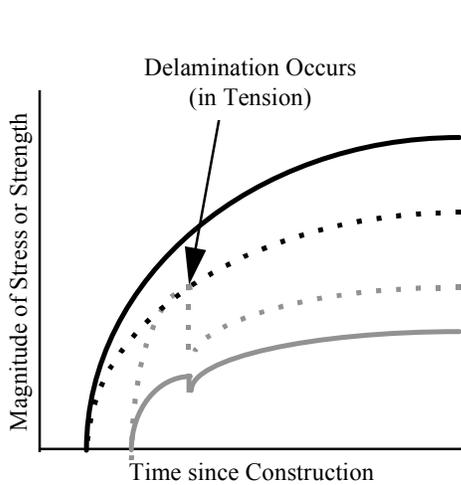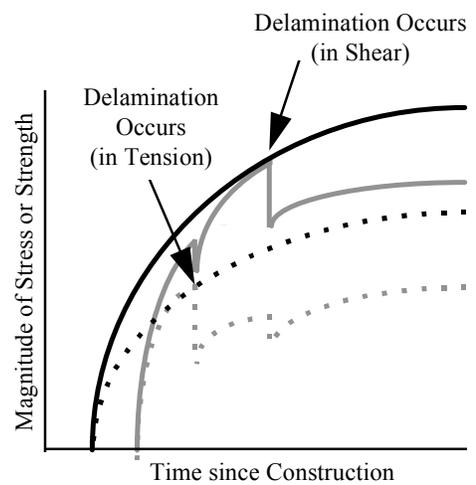
Figure 30. Poor bond stress and strength development scenarios.

4.9.3 *Plastic-Shrinkage Cracking*

Plastic shrinkage cracking has been found to be an important factor in determining the overall performance of either a PCCP or BCO. A simple model has been developed which estimates the evaporation of moisture from the surface of an exposed body of water. This model is currently the only one of its kind in widespread use. The model is as follows:

$$w = MAX \left\{ \begin{array}{l} \left[\left(5.86 + 0.0236 \dfrac{V_W}{1.609} \right) \bullet J \right] \\ 0.0 \end{array} \right. \tag{52}$$

where,

w = evaporation rate (kg/m²/h),
V_W = windspeed (km/h),
J = temperature-humidity coefficient, defined as:

$$J=\{0.000266*(T_{conc})2.2593-exp[-5.44+0.948*ln(RH)+0.033*(T_{air})]\}/1.17 \tag{53}$$

where,

T_{air} = ambient air temperature (°F), and
T_{conc} = concrete temperature (°F).
RH = ambient relative humidity (%),

It has been found from past experience that when the evaporation rate value exceeds 0.5 kg/m²/h (0.1 lb/ft²/h) that the potential for plastic shrinkage cracking of an exposed concrete surface is large, and when the value exceeds 1.0 kg/m²/h (0.2 lb/ft²/h), the probability is very high.[3] This rule must be used with caution, however, because it does not account for the additional variables involved in the curing of concrete. For example, the application of various curing method types can significantly affect the overall evaporation rate, and thus, the potential for plastic shrinkage cracking.

Appendix B describes in detail some work that has been done by the project staff in this area.

4.10 Calibration and Verification of Models

Several models have been presented in the previous sections that are related to stress and strength development in an early-age PCCP. The following sections describe calibration and verification efforts that were undertaken for these various models.

4.10.1 Slab Temperature Prediction Model

A similarity among many of the models used in the HIPERPAV/HIPERBOND system is their reliance on the temperature distribution model described in section 4.1. Because of this, calibration and verification of the temperature model was required to ensure an overall reliable product. In order to demonstrate the effectiveness of the temperature model in predicting slab temperature distributions, data from a PCCP section in Waller County, Texas, and a BCO section in Franklin County, Iowa were analyzed.

4.10.1.1 Waller County, Texas

The test section in Waller County, Texas constituted new pavement construction of an 28 cm (11 in) CRCP placed in June of 1995. A weather station was located on-site where temperature, humidity, windspeed, and solar radiation values were collected on June 15, 1995 to be used as inputs to the model. Figure 31 shows ambient air temperatures for the 24 h period from which the data was collected. The air temperatures during that period ranged from 18 to 29°C (65 to 85°F). Other environmental data such as solar radiation and wind velocity that were taken from the weather station are shown in figure 32. The solar radiation reached a maximum of 0.959 kW/m² at 12:00 P.M. and fell to zero at 9:00 P.M. Wind velocity ranged from 0.0 to 3.0 m/sec. The initial temperature of the concrete mix was 25°C (77°F).

Figures 33 to 35 show the measured and predicted temperatures of the concrete pavement structure at 2.54 cm (1 in) below the pavement surface, mid-depth, and at 1 inch above the bottom of the pavement, respectively. The maximum measured temperature was 49°C (121°F) at 2.54cm (1 in) below the pavement surface, 47°C (116°F) at mid-depth of PCCP, and 44°C (112°F) at 2.54cm (1 in) from the PCCP bottom. The maximum temperatures were predicted to be 47°C (116°F) at 2.54cm (1 in) below the pavement surface, 46°C (114°F) at mid-depth of the PCCP, and 43°C (110°F) at 2.54cm (1 in) from the PCCP bottom. Overall, the predicted temperature profile corresponded to the experimental data.
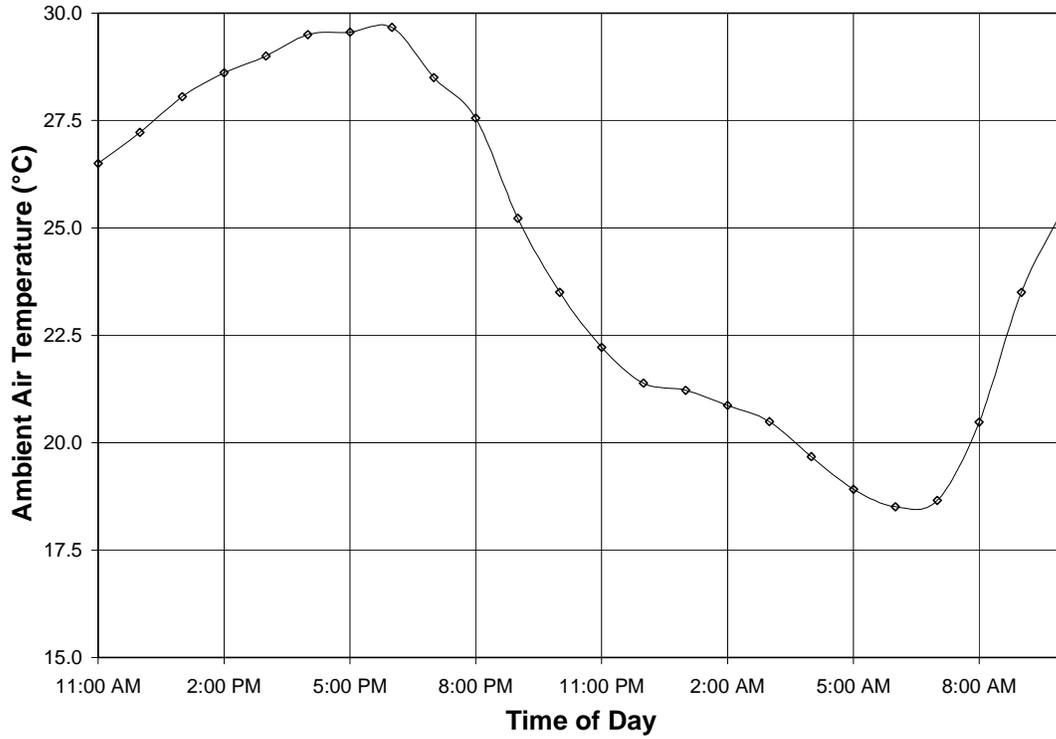
Figure 31. Hourly ambient air temperatures, Waller County PCCP.
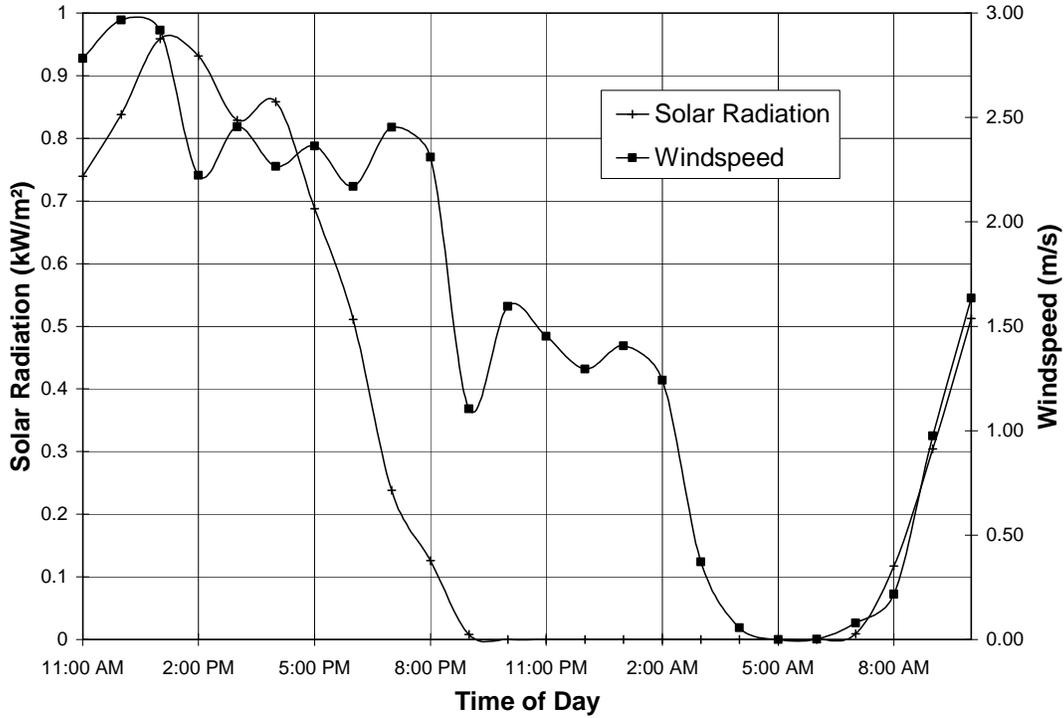
Figure 32. Hourly windspeeds and solar radiation values, Waller County PCCP.
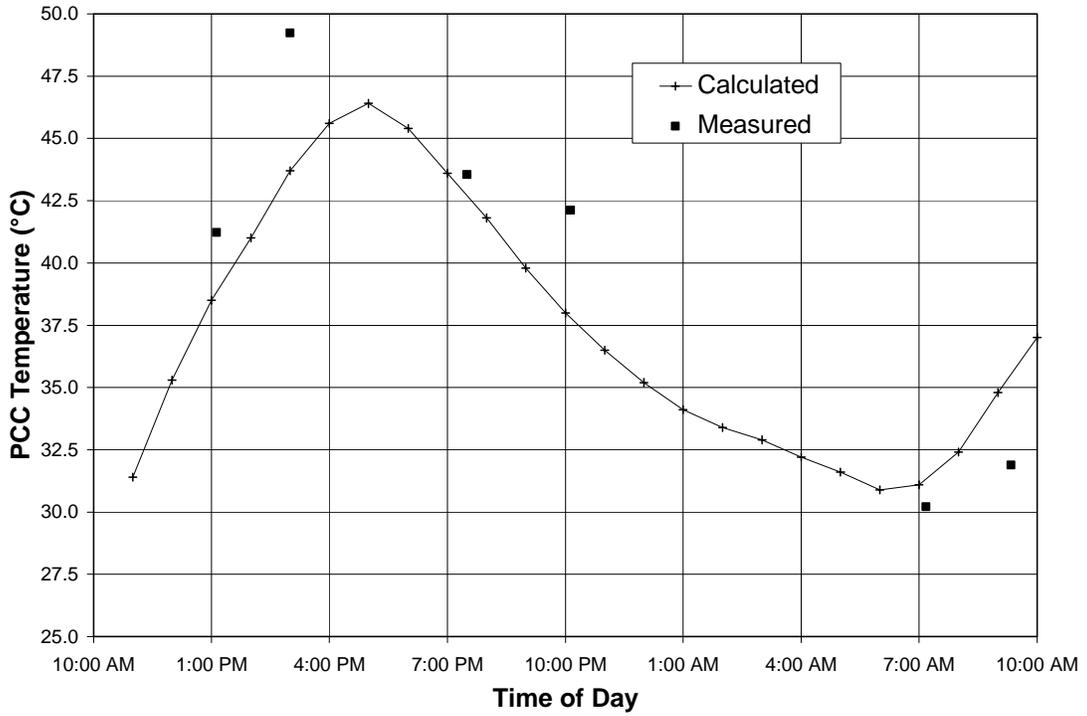
*Figure 33. PCCP temperatures at 2.54cm (1 in) below the surface,
Waller County PCCP.*
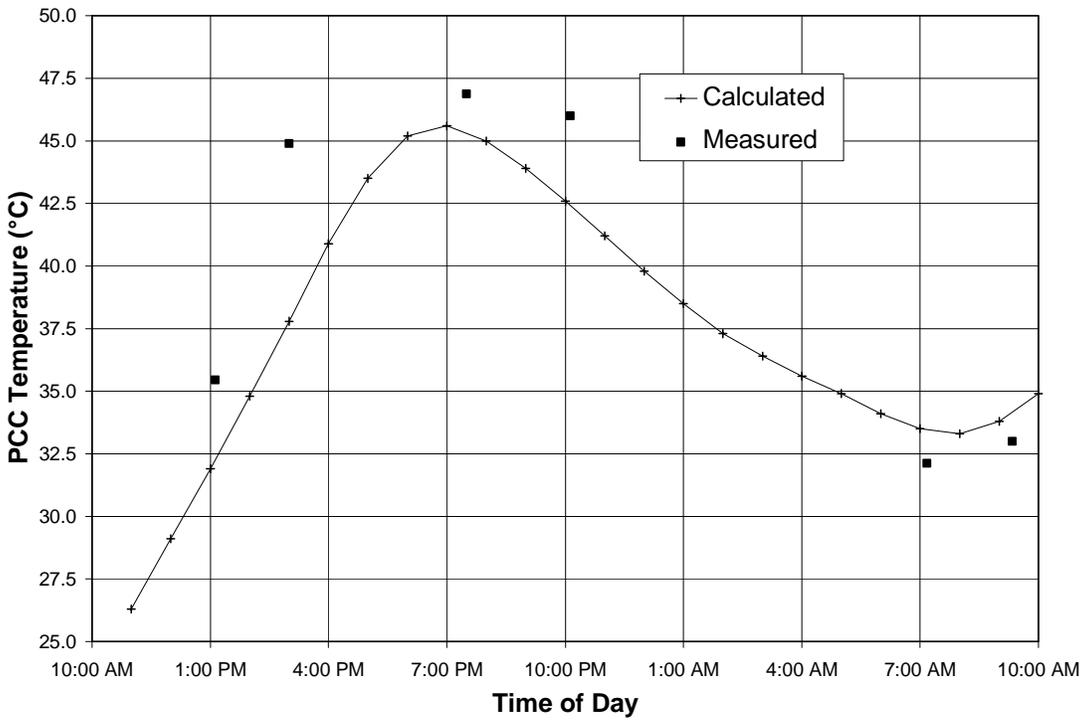
Figure 34. PCCP temperatures at mid-depth, Waller County PCCP.

98
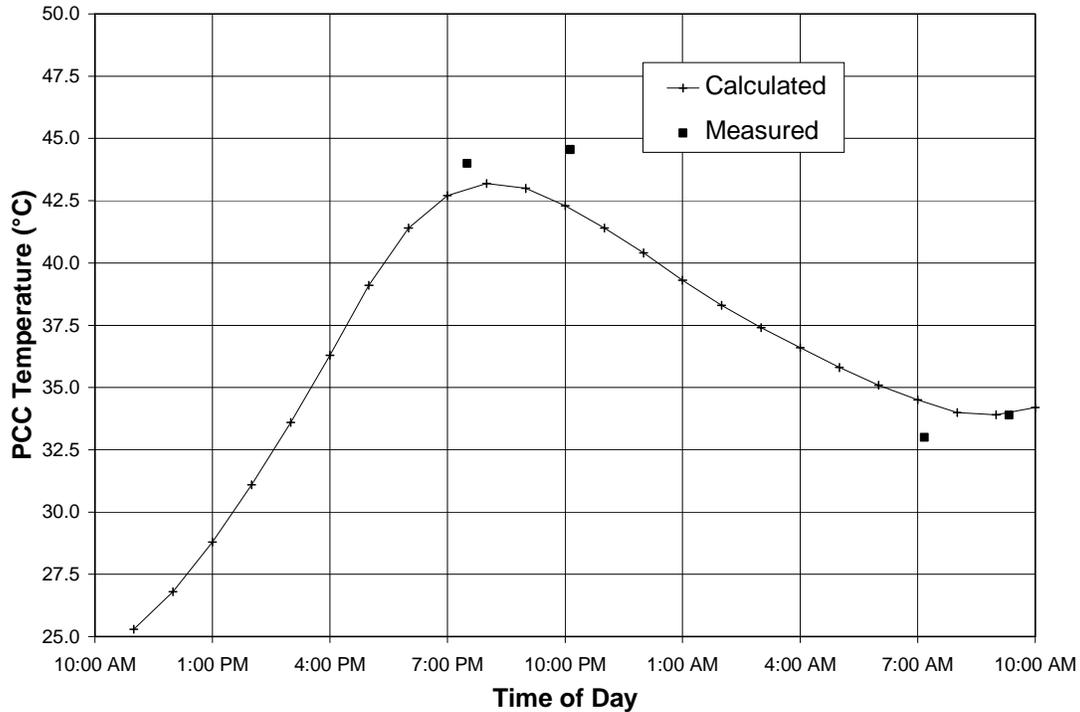
*Figure 35. PCCP temperatures at 2.54cm (1 in) above the bottom,
Waller County PCCP.*

4.10.1.2 Franklin County, Iowa

The Franklin County, Iowa project consisted of a fast-track bonded concrete overlay. The design thickness of the thin-bonded overlay was 7.5cm (3 in), and the total pavement width was 7.3m (24 ft). The new overlay was placed directly over an existing 20 cm (8 in) jointed plain concrete pavement (JPCP). Joints in the new overlay were sawed full depth directly over the joints in the existing JPCP. The majority of the construction occurred during September of 1994. The HIPERBOND software was used to predict the PCC temperature distribution in the overlay during the first 12 h. Figures 36, 37, and 38 compare these predicted values with the actual measured values at the top, middle, and bottom of the overlay, respectively.

Although some deviation can be observed, the general trend of the predicted versus the measured values is good. The differences can be explained by assumptions that had to be made for the model inputs. A more accurate assessment of the true inputs would result in a closer fit.
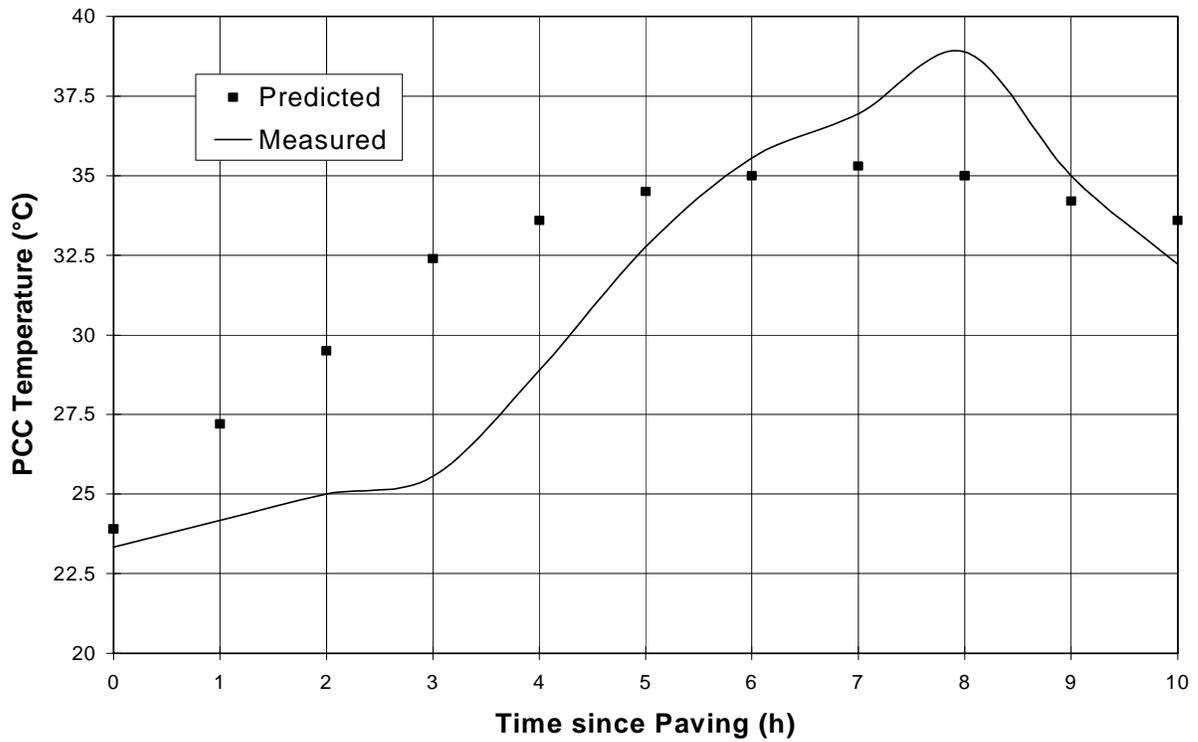
Figure 36. BCO temperatures at the top surface, Franklin County BCO.
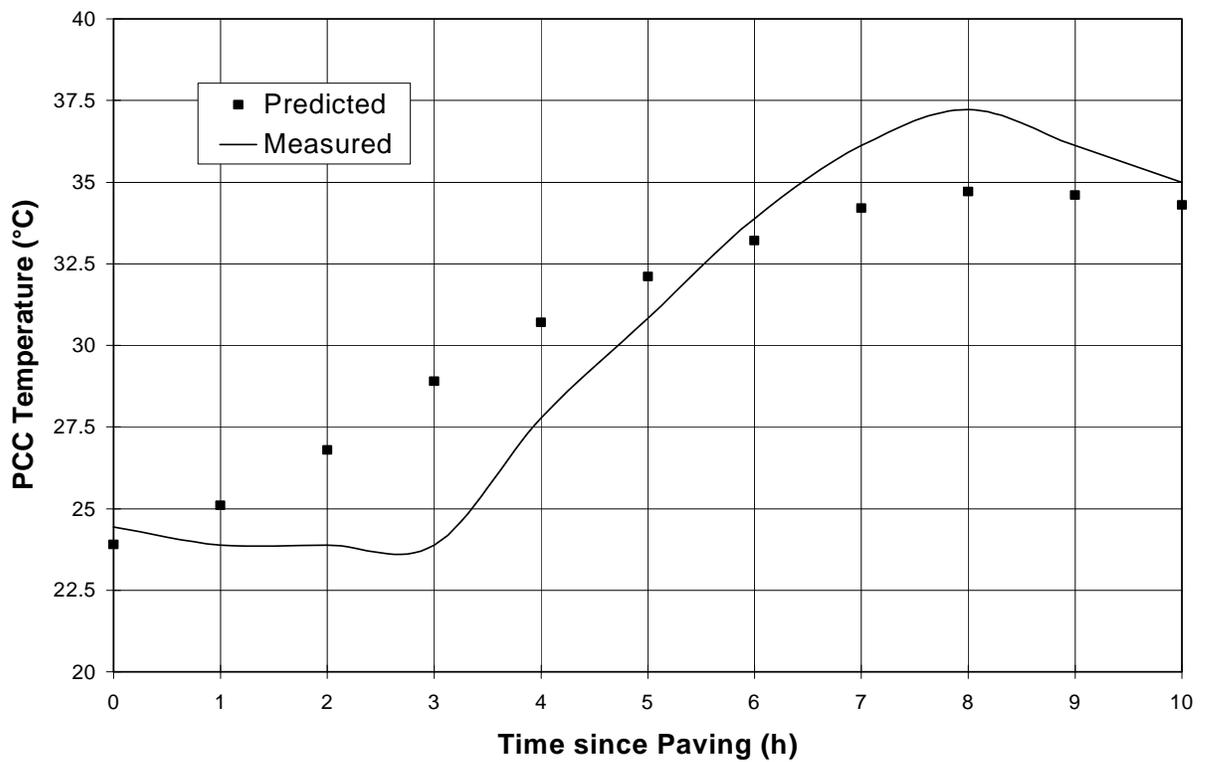
Figure 37. BCO temperatures at the middle, Franklin County BCO.
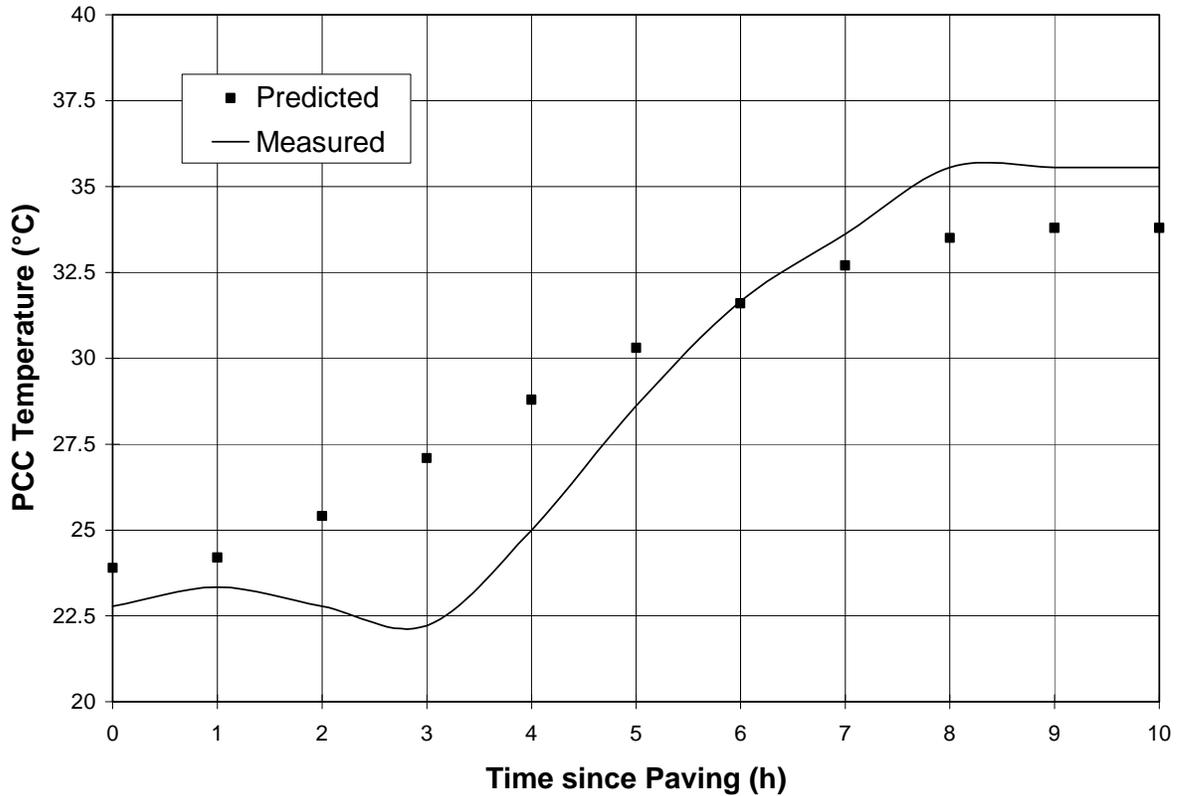
Figure 38. BCO temperatures at the BCO/existing PCCP interface,
Franklin County BCO.

4.10.2 PCC Strength Prediction Model

Another critical element for predicting early-age behavior of a PCCP is the strength prediction model. The methodology used for this modeling process is described in section 4.7. This section describes the predicted versus measured strengths at a test section in Puebla, Mexico.

Figure 39 demonstrates the ability of the strength model to predict the flexural strength of the PCC used in that test section. As can be observed, a good correlation exists between the predicted and the measured values.
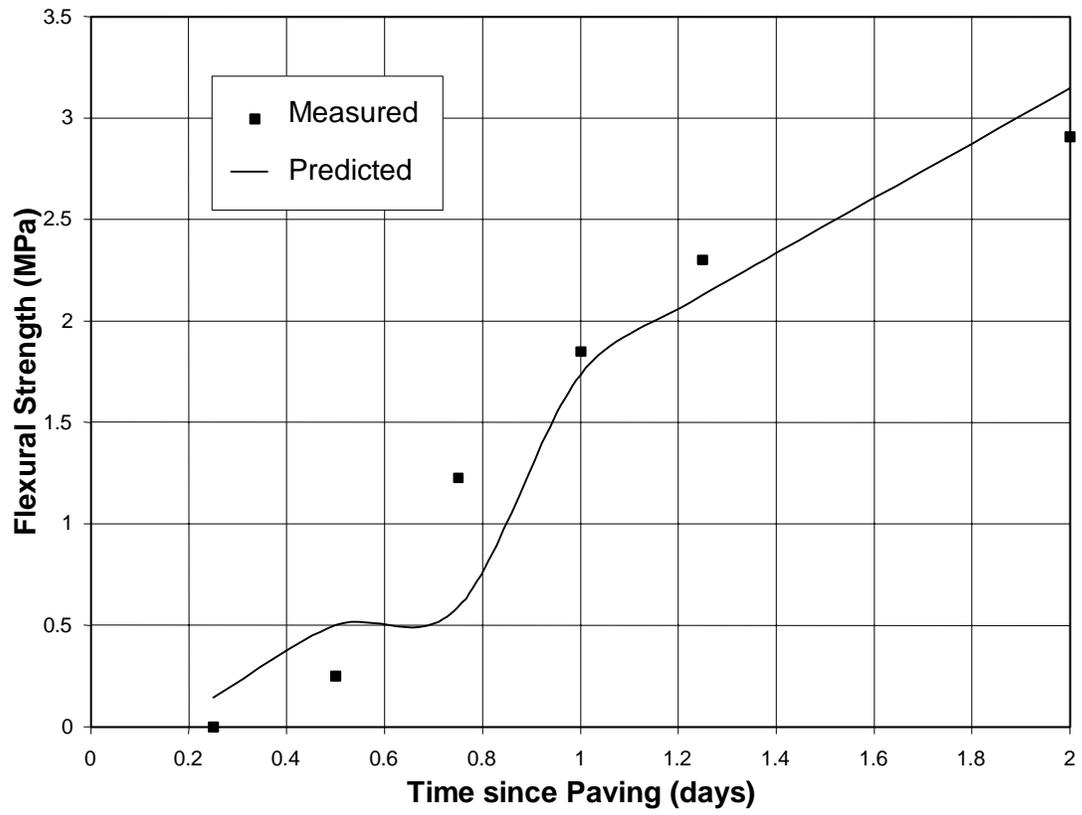
Figure 39. Predicted versus measured PCC flexural strengths; Puebla, Mexico test section.

CHAPTER 5   CONCLUSIONS AND RECOMMENDATIONS

The intent of this study was to develop a comprehensive set of guidelines to be used in predicting the early-age performance of jointed plain concrete pavements and bonded concrete overlays (BCOs). This objective was accomplished by two means: a qualitative set of guidelines, and a quantitative set of verification guidelines termed HIPERPAV (for early-age PCCP) and HIPERBOND (for early-age BCO).

5.1   Conclusions

A set of qualitative guidelines has been developed which detail the effects on the overall performance of both PCCP and BCO as a function of various inputs. These inputs are categorized into four general areas: mix design, construction, environmental conditions, and general pavement design. These guidelines could be used as a stand-alone product offering guidance toward better design and construction of high performance PCCP and BCO. These inputs consist of a conglomeration of past experiences with the design and construction of high performance PCCP and BCO.

A second product was developed for this study, however, which enhances the first: a computerized verification system termed HIPERPAV (HIgh PERformance PAVing - for new construction of PCCP) and HIPERBOND (HIgh PERformance BONDed concrete overlays).

HIPERPAV and HIPERBOND enable the engineer to investigate the direct impact on the early-age behavior of a PCCP and BCO as a function of the aforementioned four categories. Comprehensive models were developed which predict the critical stress levels in young pavements and overlays subjected to environmental and internal loading. Parallel models predict the pavement and bond strength during the early-age as a function of the heat development from the hydration process. The combination of these properties are then compared and the overall behavior can be predicted.

The need for this type of system is clear. Today, PCCP and BCO are being used more than ever due to their inherent durable nature and low life cycle costs. In addition, the increasing costs of interrupting traffic for maintenance activities is warranting the use of longer-lasting pavement alternatives that can be constructed quickly. The combination of these factors lead to the use of fast-track mixes which require early opening to traffic, and thus, high early-strength. The problems inherent with high early-strength mixes are the increased potential for early-age damage due to the restraint of large volumetric changes. The internal heat generated (and subsequent cooling) from a fast-track mix is sufficient enough to cause damage if measures are not taken to minimize it.

The large number of variables that can be modified in the design and construction of a fast-track mix have warranted the development of a set of guidelines to direct these activities.

The HIPERPAV and HIPERBOND systems meet this void by providing the engineer with an opportunity to predict the potential for damage in the early-age.

This study has met this objective and has provided an opportunity to enhance the state-of-the-art in fast-track paving and bonded concrete overlay construction. By providing the ability to predict the early-age behavior of a PCCP and/or BCO, a confidence level can be used during design and construction. It should be noted, however, that variability in the inputs and the unpredictable nature of some of the inputs (especially the environmental-related ones) can still lead to the potential for early-age cracking and delamination. It is important for the users of these systems to understand that these guidelines are not to be used as an end-all in making decisions regarding PCCP and BCO design and construction. It should be used in conjunction with engineering judgment and other considerations such as economic factors.

5.2   Recommendations

The products of this study have inherent assumptions. These were required in order to provide a tangible product. Because the number of factors that determine the overall behavior, and thus performance, of a PCCP or BCO system are too numerous to itemize, an attempt has been made to reduce the number of effects to those which are believed to be the most significant in the overall scheme. In doing this, the potential for error is created. The key to countering this problem is through the careful selection of the inputs to the guidelines as well as the careful interpretation of the results.

This project was, like all others, constrained by money and time. Additional effort can be made in enhancing all of the aspects of the products of this study. This section attempts to prioritize the areas of these products which could be enhanced. The following is a list of the components which can be enhanced, and the means by which this can be done (if applicable):

PAVEMENT MOISTURE MODELING - As the discussion in chapter 4 alluded to, the framework for a pavement moisture model has been developed during this study. A detailed description of this work can be found in appendix A of this report. The implementation of this model into the HIPERPAV and HIPERBOND systems was not warranted due to the premature nature of the model at the terminus of this study. However, it is highly recommended that additional efforts be made to finalize the model and incorporate it into the final system in future work. The result of this would be the ability to more accurately define the induced stresses due to moisture loss and movement within a pavement. In the early-age, the most important of these effects would be the loss of moisture and the resulting drying shrinkage-induced stresses. In addition, the model would provide a means to assess the stresses due to restrained moisture warping of the pavement. Finally, a mechanistic method of predicting plastic shrinkage cracking can be incorporated into the HIPERPAV and HIPERBOND systems as a result of the development of the moisture prediction model.

THERMAL COEFFICIENT OF EXPANSION MODEL - The model as it stands in the HIPERPAV and HIPERBOND systems is based upon a volumetric definition of the thermal coefficient of the various components of a concrete mixture (i.e. the aggregates and the paste). However, a comprehensive model to predict the thermal coefficient of the paste was never fully developed. A single relationship defining the thermal coefficient of the hydration paste is used in the HIPERPAV and HIPERBOND systems, but it may not provide enough accuracy to predict the exact value at early-ages. Further work is needed to enhance the existing model. A relationship between the thermal coefficient and the degree of hydration and the cement characteristics would be the ideal way to enhance this model.

CHARACTERIZATION OF CURING METHODS - The type of curing method used in the early-ages of a PCCP or BCO can significantly affect the overall behavior and performance. The HIPERPAV and HIPERBOND systems characterize the various curing methods by adjusting the heat convection coefficient based upon work done in this study. However, the effect of moisture flow and insolative properties was not fully addressed. It is therefore recommended that these factors be directly considered in future improvements.

CREEP RELAXATION MODEL - It has been demonstrated that creep relaxation is an important factor to characterize in early-age PCC. The model that is currently used in the HIPERPAV and HIPERBOND systems was selected from the literature due to its calibration with some early-age data. However, the validity of this model due to the types of loads experienced in a PCCP system has not been proven. It is therefore recommended that further work be done in verifying the validity of this model by calibrating it to in-service conditions.

APPENDIX A
MOISTURE DIFFUSION, DRYING SHRINKAGE, AND AN ASSESSMENT OF CURING EFFECTIVENESS OF CONCRETE

A.1   Introduction

The Request for Proposal for this study dealt primarily with the temperature aspects of PCC during its early life, while alluding to the moisture aspects. The models developed, therefore, concentrated on the temperature mechanisms while moisture variations are treated with less sophisticated models.

The properties and performance of concrete are in many ways linked to its moisture history at an early age. Materials research in concrete has shown that a correct prediction of the distribution and history of pore humidity at its early age is of major importance relative to the quality of curing, (i.e., properties of the concrete). Its understanding is necessary for a realistic determination of drying shrinkage, thermal expansion, strength, maturity and curing efficiency. Although some experimental data have been assembled over many years of research, little data on drying at early concrete ages is presently available.

The objective for the material presented herein is to demonstrate the need for more sophisticated modeling of the vertical moisture flow in order to more reliably predict concrete behavior.

The material presented in the following sections first covers the modeling of the vertical moisture flow in the concrete. Next, these concepts are explored with a laboratory testing program, and this is followed by a section which discusses the results in terms of a measure of the effectiveness of curing compounds, and finally the validation of the models.

A.2   Basis for Modeling Diffusivity of Concrete

Moisture in concrete materials is comprised of two parts - one referred to as structural or water chemically bound within the cement paste hydration products (w_n) and the other as water contained within the pore structure of the calcium silicate hydrate (C-S-H) (w_g). The sum of these portions equals the total water content (w) in the paste. One aspect of the effect of moisture in concrete pavement can be reflected in drying shrinkage and creep behavior. These behavioral characteristics are of concern with respect to concrete slab deflections and formation of cracks or development of delaminations in bonded concrete overlay systems. Materials-related moisture properties of concrete (permeability, diffusivity, slope of the moisture isotherm, etc.) play a key role in the mathematical modeling and representation of stress and strain due to drying shrinkage and creep under varying humidity conditions. Materials tests are necessary to determine these pertinent material properties. The properties are identified by moisture flow models which represent the variation of moisture with time. In terms of engineering

applications, an important need exists for the prediction of humidity and water diffusion in consideration of warping and other related stresses, strains, and deformations induced in concrete pavements.

Moisture properties affect how moisture is distributed in a concrete material either while hardening or in a mature state. There are trends in the drying characteristics of concrete, such as when drying develops in concrete materials where the remaining moisture in the paste moves or diffuses into the atmosphere at decreasing rates of flow with time. This is reflected in high initial diffusion rates followed by gradually lower moisture flow rates. This characteristic is inherently related to a material property referred to as the moisture diffusivity (D) which has been generally accepted to be dependent upon the pore water content of the paste. It has been observed that the value of D may change significantly with variations in the moisture content or the relative humidity (from 100 to 70 percent) of the concrete material. (See references 30, 31, 32, and 33)

Moisture in concrete materials has been measured in the past by actual weight measurements which reflect the remaining water in the bulk sample. Recently, moisture quantities have been estimated based on direct measurements using relative humidity sensors. Several papers have been published regarding moisture flow and diffusion in concrete materials. (See references 34, 35, 36, 37, and 38) Further elaboration on this topic will require discussion of diffusion mechanisms and the form of the diffusion equation or model in terms of basic physical principles.

The best way to describe and to understand the flow of moisture in concrete is by examination of the expressions relative to moisture transport in a porous medium such as concrete. The rate of moisture movement through concrete materials may be characterized by the velocity of flow (J) representing the mass of evaporable water (w_g) passing through a unit area perpendicular to the direction of flow per unit time. Darcy's Law inherently assumes that the driving force of the moisture flow is derived from energy gradients:

$$J = -C \cdot \nabla \mu \qquad (54)$$

where μ is Gibbs free energy (GFE) per unit mass of evaporable water. The relation shown in equation 54 is consequently restricted to small energy gradients and laminar flow conditions meeting Darcy's Law requirements. The coefficient (C) characterizes the permeability of the porous, concrete material. This relation is also a function, as is pointed out later, of temperature and evaporable water content. Assuming water vapor behaves as an ideal gas: [34]

$$\mu = (\frac{RT}{MV_w}) \cdot \ln h + \mu_{sat}(T) \qquad (55)$$

where,

μ = Gibbs free energy per mass of evaporable water,
R = universal gas constant (8.3143 J/mol-°K),
T = absolute temperature (°K),

108

M = molecular weight of water (18.015 g/mol),
V_w = specific volume of water (1 cm³/g),
h = pore humidity, and
μ_{sat} = Gibbs free energy per mass of saturated material.

It should be pointed out that at any point in a mass of concrete material, as measured by a relative humidity sensor, Gibbs Free Energy represents the state of stress or the tension within the various phases of pore water that is assumed to be translated into the measured resultant bulk relative humidity of the different phases of pore water. These phases, which consist of water vapor, capillary water, and unhindered adsorbed water are assumed to be in mutual thermodynamic equilibrium at any time. [34]

Substituting equation 55 into 54 and then rewriting equation 54 in terms of pore humidity (h) and temperature yields:

$$J = -c \cdot \nabla h \qquad (56)$$

where,

∇h = pore humidity at any vertical level from the surface, and

$$c = (\frac{RT}{MV_w}) \times (\frac{C}{h}) \qquad (57)$$

Therefore, the coefficient c, referred to as the permeability, is a function of humidity and temperature. Moisture diffusion through concrete typically is a slow process, particularly in the hardened or mature state which tends to verify that the pore water phase equilibrium described previously exists. The relationship between h and w at a constant temperature and the degree of hydration is described or governed by the desorption or sorption isotherms. [34] It is evident that the relationship between the moisture in the concrete and the measured relative humidity will vary as a function of the age. This is true, as will be subsequently shown, with respect to other moisture properties (such as diffusivity). These relationships, consequently, will need to be corrected as a function of time in analysis of the behavior of concrete while in the hardening stages.

The total mass of water per unit volume of concrete (w) can also be described in terms of the adsorbed water (w_a), the capillary water (w_c), and the non-evaporable water (w_n) which is, as pointed out before, water structurally bound in the hydrated cement paste products. The dependence of w on humidity (as a function of temperature) is a function of the porosity of the pore structure within the paste and is represented empirically in the form of desorption or sorption isotherms that are illustrated in figure 40. It should be noted that the isotherm for sorption is different from the isotherm for the preceding desorption. This characteristic may be due to the various states of equilibrium of the pore water. [34]
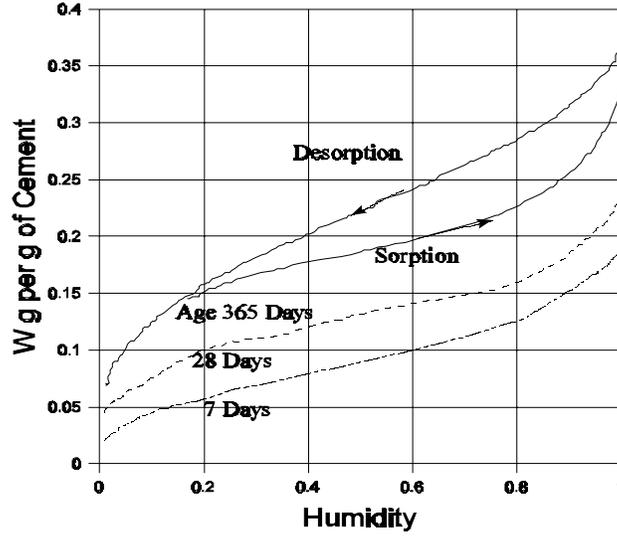
Figure 40. Desorption-sorption isotherms. [33]

An investigation recently completed by Parrot implied the significance of porosity with respect to the vertical position of the desorption/sorption isotherm. [35] His results indicated that a greater amount of moisture loss in drying specimens will occur in regions nearest to exposed drying surfaces which may also be regions of high porosity. Based on the experience of the authors, it is suggested that the porosity of the paste varies with distance from the exposed surface. Therefore, the data illustrated herein suggests there is a greater volume of coarse pores at positions nearer to an exposed surface, and consequently the h-w relationship will vary with respect to an exposed surface (i.e. paste porosity).

It should also be noted that the resulting desorption isotherm at any time during hydration of hardening concrete must be interpreted not only as a function of the degree of hydration, but also as a function of porosity. At a given porosity, the desorption isotherm may be expressed in the differential form as:

$$dh = kdw \qquad (58)$$

where,

$$k = \left(\frac{\partial h}{\partial w}\right) w \qquad (59)$$

The parameter k represents the slope of the moisture isotherm where the mass of water (w) is described as a function of relative humidity (h). Under variable temperature conditions, the calculation of humidity in hydrating concrete specimens requires additional terms to be added to equation 58 as follows:

$$dh = kdw + KdT + dh_s \qquad (60)$$

where,

$$K = (\frac{\partial h}{\partial T})_w \qquad (61)$$

where,

K   = hygrothermic coefficient, and
dh_s = change in h due to hydration at a constant (w) and time (t).

The term K in equation 60 represents the change in humidity (h) due to one degree change in temperature (T) at a constant mass of water (w) and a given level of hydration. It should be noted that the mass of water includes both the mass of evaporable (or capillary) water (w_c) and the mass of non-evaporable water (w_n). [34]

The flow of water mass per unit volume of concrete determined from the expression:

$$\frac{\partial w}{\partial t} = -\nabla \bullet J \qquad (62)$$

is based on the conservation of mass. Substituting (dw) from equation 58, (J) from equation 56 into equation 62 leads to: [34]

$$\frac{\partial h}{\partial t} = k \cdot \nabla \bullet (c \cdot \nabla h) + \frac{\partial h_s}{\partial t} + K \frac{\partial T}{\partial t} \qquad (63)$$

which is the diffusion equation for the drying of concrete under variable temperature conditions. Developing further,

$$\frac{\partial h}{\partial t} = kc \frac{\partial^2 h}{\partial z^2} + k \frac{\partial c}{\partial z} \frac{\partial h}{\partial z} + \frac{\partial h_s}{\partial t} + K \frac{\partial T}{\partial t} \qquad (64)$$

The above discussion implies that the permeability (c) is a function of the porosity and indirectly a function of the vertical position z. However, the calculated magnitude of the second term on the right side of equation 64 is insignificant compared to the other terms and therefore negligible, thus it is consequently dropped from the diffusion equation:

$$\frac{\partial h}{\partial t} = D \frac{\partial^2 h}{\partial z^2} + \frac{\partial h_s}{\partial t} + K \frac{\partial T}{\partial t} \qquad (65)$$

where,

$$D \quad = k \cdot c = \text{diffusion coefficient } (L^2/t).$$

Self-desiccation (h_s) which pertains to the structural water chemically bound within the cement paste and the diffusivity (D) depend on the degree of hydration of cement paste. The degree of hydration may be conveniently characterized by the equivalent curing period (t_e). [33,39] This variable, (t_e) is a function of both relative humidity (h) and temperature (T). The simplest possible relationship has the form:

$$dt_e = \beta_T \beta_H dt \tag{66}$$

where,

$$\beta_T \quad = \text{the degree of hydration based on temperature (T), and}$$
$$\beta_H \quad = \text{the degree of hydration based on humidity (h).}$$

The approximate dependence of β_H upon h can be expressed as: [33,39]

$$\beta_H \approx [1 + (7.5 - 7.5h)^4]^{-1} \tag{67}$$

The influence of T upon the rate hydration is known to obey the Arrhenius equation:

$$\beta_T = \exp(\frac{Q_h}{RT_0} - \frac{Q_h}{RT}) \tag{68}$$

where,

$$Q_h \quad = \text{activation energy for hydration, approximately } Q_h/R \approx 2500 \text{ °K } [40]$$

The characterization of diffusivity (D) is important in order to accurately model moisture flow in hardening concrete. At a constant w, diffusivity changes very little with time in a hardened concrete. However, dramatic changes occur in diffusivity during the early stages of hardening (during the first 24 h after placement). Through the use of inverse analysis, the drying diffusion equation can be manipulated to solve for diffusivity (D) by the use of a step by step differentiation process. [37] From this characterization of D, it is possible to account for varying moisture loss at an early age as an input to drying shrinkage strain prediction demonstrated by other studies. [38,39] Diffusivity has been found to be a function of humidity, concrete age, and paste porosity.

The rate of moisture exchange between the pavement surface and the environment can be characterized in a simple expression relative to the difference between the Gibbs free energies (GFE) per unit mass of water in concrete (h) and in the environment (h_{en}). For small rates of flow (J) across the concrete surface interface:

$$nJ = -B(\ln h_{en} - \ln h) \tag{69}$$

where,

       B   = the surface emissivity in units of area per length per unit time, and

       n   = unit outward normal at the surface.

The flow of moisture just below the surface (equation 56) can be assumed to be equivalent to the flow across the surface interface (equation 69). Therefore, equating equations 56 and 69:

$$d \cdot n \cdot \nabla h = \ln\left(\frac{h}{h_{en}}\right) \tag{70}$$

where,

$$d = \frac{c}{B} \tag{71}$$

Note that d is in units of vertical distance and may be used to represent the effectiveness of surface curing in terms of an equivalent thickness of concrete that numerically replaces the curing system (curing compound, polyethylene sheeting, mats, etc) used to retain moisture at the pavement surface. By using the measured values of relative humidity and temperature just above and below the pavement surface, equation 69 forms the basis for an estimate of d which should be very useful in monitoring the curing effectiveness during and immediately following the placement of the concrete slab.

A.3   Laboratory Investigation

A.3.1   *Lab Measurements of Moisture Movement*

After experimenting with several types of equipment, a sensor monitoring system was configured using currently available hardware (figure 41). The M200 moisture meter made by ATEK was used to determine the relative humidity of the curing concrete in field or laboratory instrumentation programs for the measurements of dry bulb temperature and dew point temperature. The moisture change at different depths below the exposed surface was measured in the laboratory by use of a specially designed cylindrical concrete specimen eight inches in diameter and twelve inches in height cast in a PVC tube. The bottom end of the tube was sealed to a PVC plate. Moisture sensor locations were 1, 3, and 5 in below the exposed surface of the specimen.
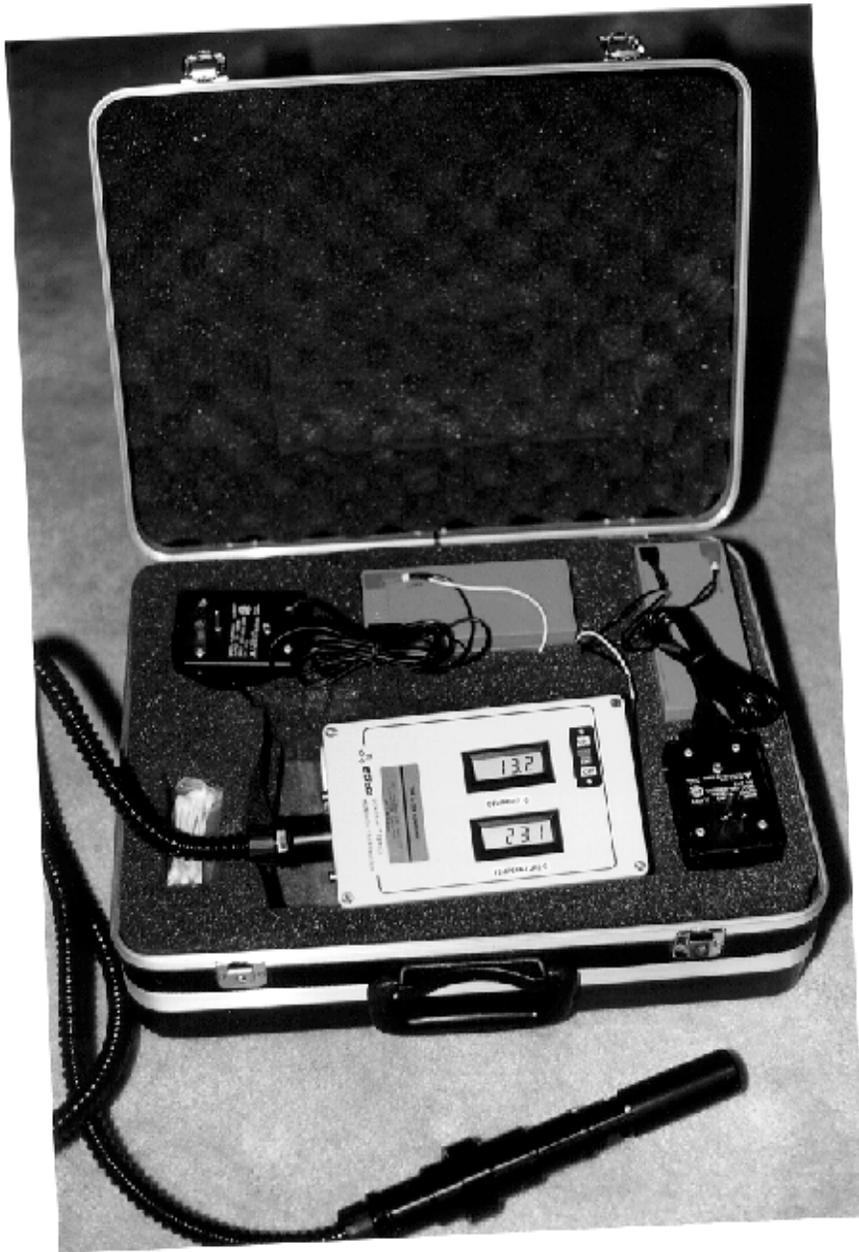
Figure 41. Moisture sensor.

After casting, the specimens were placed in an environmental chamber where the temperature and relative humidity were controlled at 32°C (90° F) and 50% respectively. The dew point and temperature data were recorded from the moisture sensor over a period of three days. The pore relative humidity 2.54, 7.62, and 12.7 cm (1, 3 and 5 in) below the surface of the

specimen were calculated from the dew point and temperature measurements. During the early age drying of concrete, the hydration heat changes the temperature of concrete. This temperature variation affects the readings of the relative humidity since relative humidity is a function of temperature. The relative humidity readings from the M200 moisture meter need to be corrected to those under a constant temperature through the psychrometric chart. Figure 42 shows the relative humidity vs. time data for a variable temperature (before correction), while figure 43 shows the one at a constant temperature (after correction). It can be seen that the greater the distance from the drying surface, the higher the pore relative humidity of the concrete.
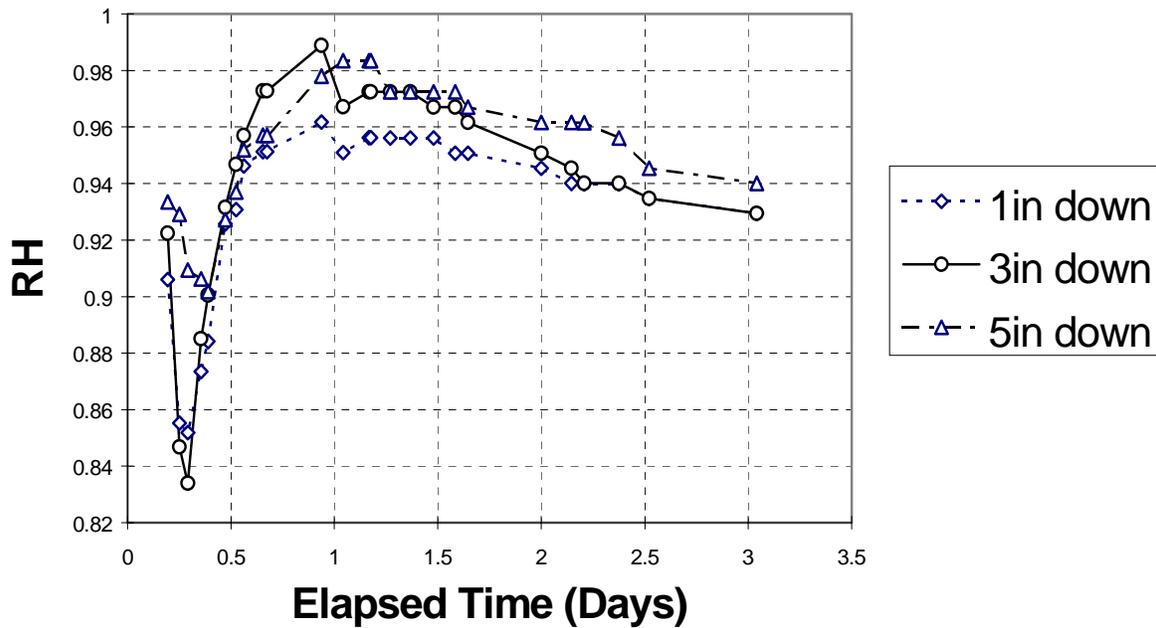
Figure 42. Uncorrected relative humidity versus elapsed time (variable temperature).
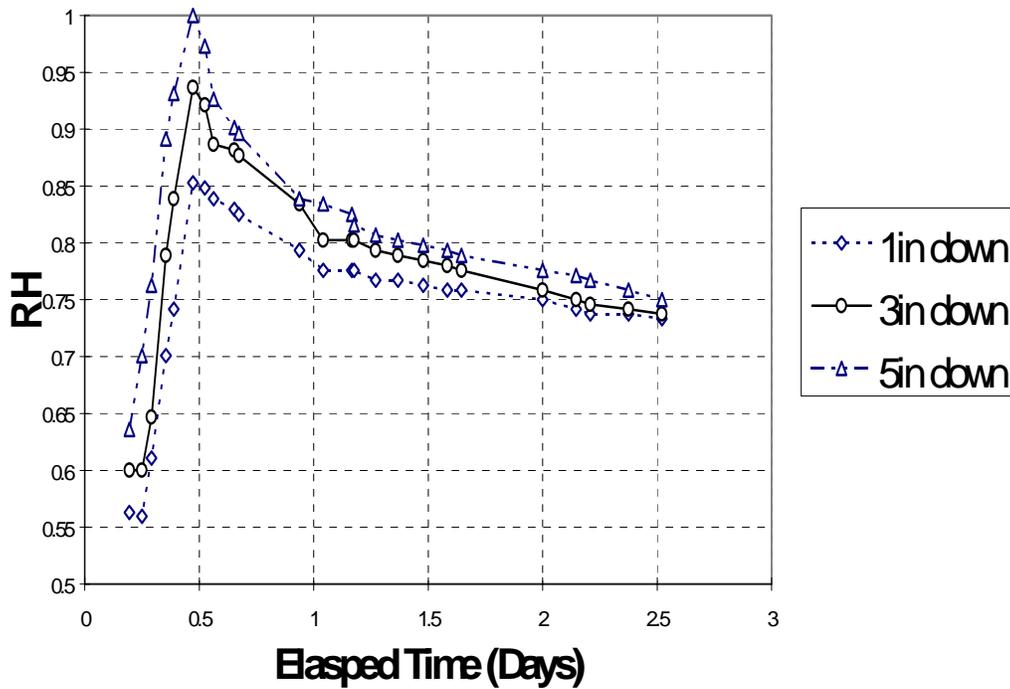
Figure 43. Corrected relative humidity versus elapsed time (constant temperature).

A.3.2   Data Analysis

When sufficient data are obtained from lab or field, the diffusivity value can be calculated directly from the estimated predicting equation for relative humidity. Having obtained the corrected relative humidity profile (figure 43), equivalent age (t_e) can be determined through equations 66-68. A mathematical equation which characterizes the moisture profile was developed through statistical software:

$$h = a + \frac{b}{1 + e^{-\frac{(t_e - f)}{g}}} \tag{72}$$

where,

$$a = e^{-0.682 + 0.229\left[1 + e^{-\frac{x - 3.314}{1.002}}\right]^{-1}} \tag{73}$$

$$b = \frac{1}{2.543 + \frac{0.139}{x^2}} - \frac{1}{2.543 + 0.139x^{-2}} \tag{74}$$

116

$$f = \left[0.057 + \frac{0.025}{\left(1 + e^{\frac{3.596-x}{0.962}} \right)} \right]^{0.5} \tag{75}$$

$$g = -0.003 - 0.050 \ln x + 0.058 x^{0.5} \tag{76}$$

where,

t_e = equivalent age (h), and
x = depth from drying surface (in).

In the analysis of diffusivity, the drop in h due to self-desiccation (h_s) was included in h, so we have $h_s = dh_s = 0$. The temperature was set to a constant value so that the relative humidity can be converted to those under this same temperature, we have $dT = 0$ in equation 57, then equation 65 becomes:

$$D = \frac{\frac{\partial h}{\partial t_e} \frac{\partial t_e}{\partial t}}{\frac{\partial^2 h}{\partial x^2}} \tag{77}$$

The diffusivity was determined and shown in figure 44. One equation for calculating the relative humidity at different times and different depths from the drying surface has been proposed by Parrot as: [35]

$$\text{Predicted RH} = \text{rha} + (100\text{-rha})f(t) \tag{78}$$

where,

rha = ambient relative humidity,
$f(t)$ = $1/(1+t/b)$,
t = drying time,
b = $35d^{1.35}(w\text{-}0.19)/4$,
d = depth from drying surface, and
w/cm = water/cement ratio.
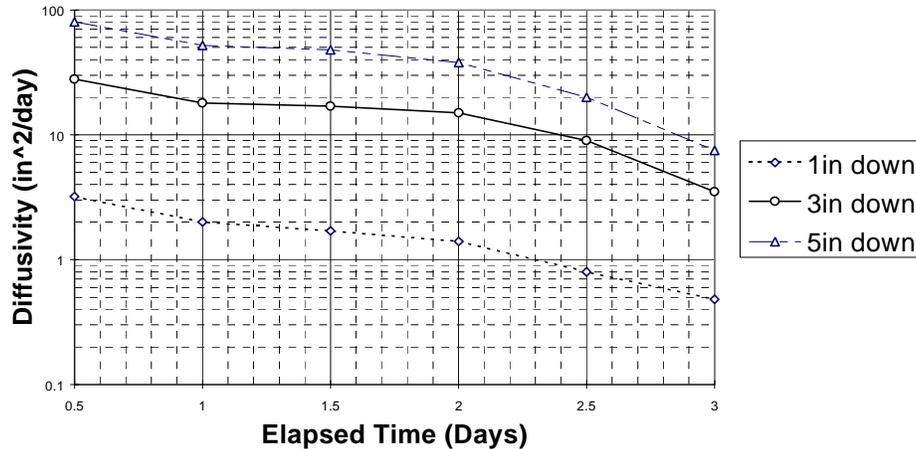
Figure 44. Diffusivity versus elapsed time.

This empirical equation is applicable only within the scope of the reported experimental condition.

A.4   Discussion of Results

This section covers the application of the results in terms of an implementation and then validation. The implementation is in terms of developing a methodology for assessing the curing effectiveness of curing methods. The second part addresses the validation of the models developed in section A.2.

A.4.1   *Assessment of the Curing Effectiveness*

The object of curing is to provide an environment in which the concrete can be kept as close to saturation as possible until the volume of water-filled space in the fresh cement paste has become substantially reduced. Both concrete strength, and more importantly durability, can be significantly impaired if correct attention is not paid to curing. It is the surface layer (i.e. the top 30 - 50 mm, 1.2 - 2.0 in), of the concrete that is most sensitive to lack of adequate curing. A high rate of evaporation of water from the surface leads to insufficient hydration resulting in a porous, permeable and weak surface layer, as has been evidenced by a systematic increase in concrete strength from the pavement surface to the pavement bottom. Although the importance of curing is well recognized, it is frequently neglected or carried out inadequately by contractors on site because of the following reasons:

(1) Lack of adequate attention to curing during construction,
(2) Lack of a simple field test to determine if curing has been carried out adequately, and
(3) The effects of poor curing are not apparent at early ages.

118

The measurement of relative humidity can be used as a way to assess the curing effectiveness. Three cylindrical concrete specimens of the same mix were cast in PVC tubes, each eight inches in diameter and twelve inches in height. Immediately after the specimens were moved to the environmental chamber (see section A.3.1), a Type II curing compound was applied on two specimens on the upper surfaces, one at a density according to TxDOT standard specification of 3.8 liters/16.8 m^2 (1 gallon/180 ft^2), the other at a density about three times that of the standard density (as shown later, this amount of curing compound may be approximately equivalent to perfect curing). The upper end of the third specimen was left exposed to the air as a control specimen. The dew point and temperature data were also recorded from the moisture sensor over a period of three days.

The pore relative humidity 2.54 cm (1 in) below the surface of each specimen was calculated from the dew point and temperature measurements, and is shown in figure 45. The relative humidity of the control (uncured) specimen dropped to nearly 85 percent during the hardening process. The relative humidity of the specimen with the standard curing application had dropped to 92 percent during the hardening of the concrete and prior to adding the curing compound. After the compound was added, the relative humidity increased to 97 percent, dropped briefly then climbed to a steady state. In contrast, the relative humidity of the highly cured specimen did not drop during the hardening, but increased to a steady state of 98 percent. The increase of concrete strength reportedly stops when the relative humidity drops to 80 percent. The control specimen (no curing compound), therefore, approached a zero strength increase condition although the stresses were building rapidly due to moisture loss. In addition, the data demonstrates that the high density curing compound prevents moisture evaporation more efficiently than the standard dose.
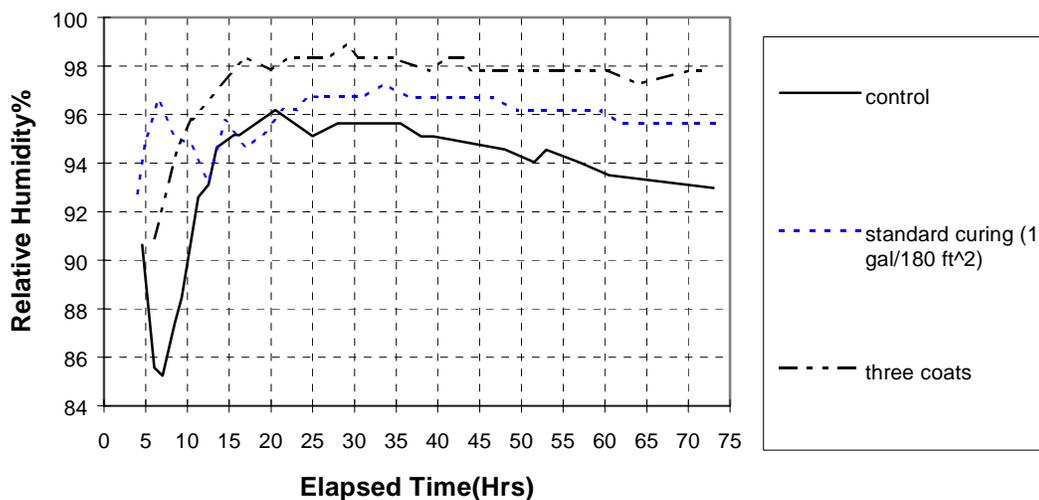
Figure 45. Effects of curing on the relative humidity 1 inch below surface.

These results imply that the method of measuring the relative humidity can also be used to assess the curing effectiveness of either different curing compounds or different curing methods. The relative humidity of the hardening concrete at a depth of 7.62 cm (3 in) is shown

in figure 46 for each method of curing. Note at this depth below the surface of the concrete that after a period of 10 to 12 h, the quality of curing is nearly equivalent between all three methods of curing, whereas this condition was never achieved near the surface (figure 45). It is also worth noting, that current maturity meter technology does not include the effect of moisture on strength gain of concrete but it is now apparent that with these advancements, it is now possible to upgrade maturity technology to account for both moisture levels and the quality of curing.
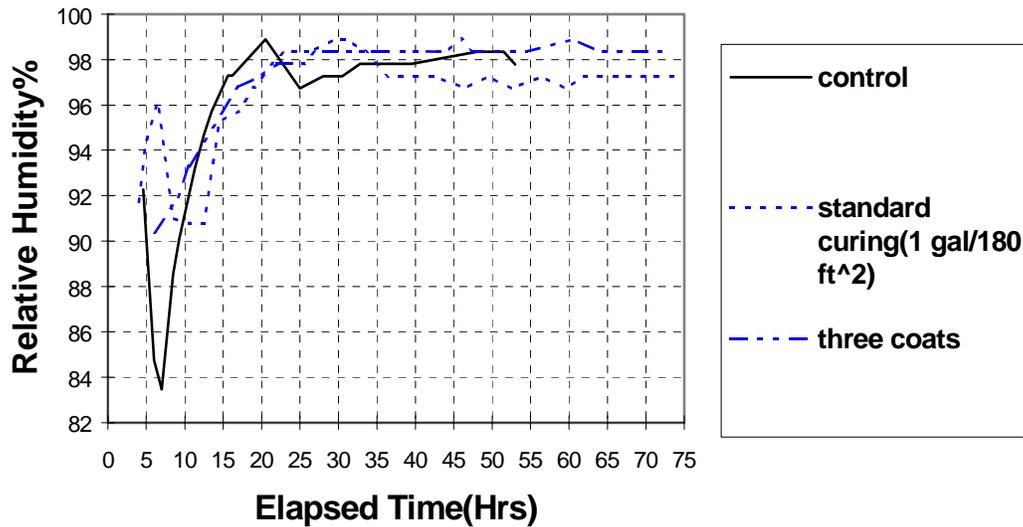
Figure 46. Effects of curing on the relative humidity 3 inches below the surface.

A framework for assessing the effectiveness of curing considering the equivalent thickness parameter as originally outlined by Bazant and Najjar is shown in equations 68 and 69. [34] The parameter, d, has the dimension of vertical distance; thus one can simply consider d to be the effective thickness of the curing membrane. Having defined the equivalent thickness (d), different curing conditions can be considered as having different degrees of curing effectiveness and thought of in terms of different effective or equivalent concrete thickness (d) superimposed upon the surface of the concrete pavement. An equivalent thickness versus elapsed time chart characterizing the curing conditions for the three curing conditions previously described is shown in figure 47. The data shows for the curing temperatures utilized in this experiment that the standard curing is equivalent to an effective thickness of concrete 1.3 cm (1/2 in) thicker than the control curing, while the improved curing technique (i.e. three coats of curing compound) is equivalent to a 6.35 cm (2.5 in) effective thickness of concrete added to the specimen. Based on these test results and the effective curing thickness shown in figure 47, the following can be concluded:

1) It appears that three coats of Type II curing compound provide an effective curing for the temperature and humidity conditions during testing (see section A.3.1). The relative humidity at one inch below the specimen surface was nearly equivalent to the relative humidity 7.62 cm (3 in) below the surface.

2) Since the moisture level at a depth of 7.62 cm (3 in) in the highly cured concrete maintained greater moisture levels prior to a period of 10 to 12 h into the curing process and since all the curing methods shown in figure 46 were similar after a period of 10 to 12h, the effective thickness of the curing compound should be between 5 to 7.6 cm (2 to 3 in).

3) The effective thickness of three coats of curing compound is 6.35 cm (2.5 in) which is consistent with the observations noted with the previous conclusion. Consequently, the concept of effective curing thickness appears to be valid and shows good potential as a QC/QA parameter for construction quality control.
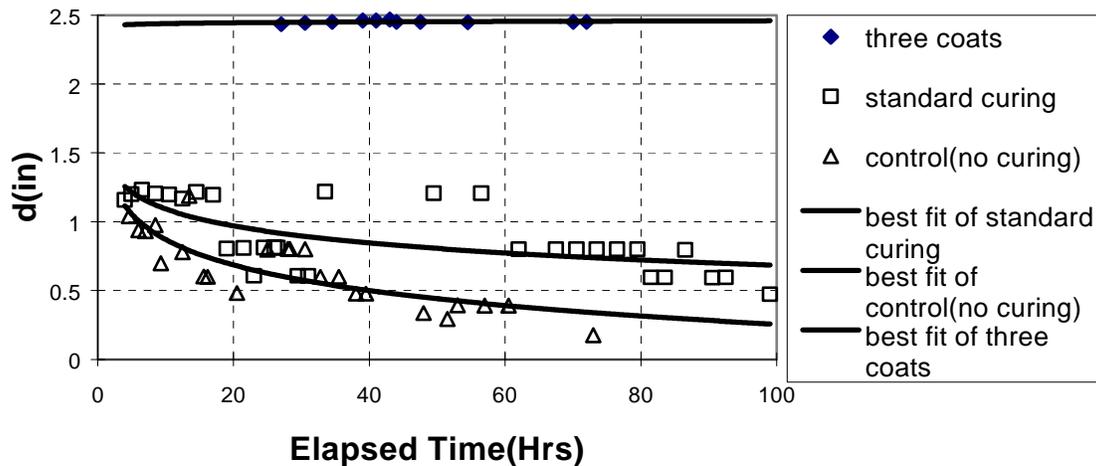
Figure 47. Equivalent thickness versus elapsed time.

Effects of the curing methods on the dew point are shown in figure 48. These data were obtained in the overlay test section at the Texas A&M University Riverside campus, Bryan, Texas. The overlay was 2.54 cm (1 in) thick, and three curing methods were applied: control (with no curing compound, poly sheeting or cotton mat covering), Type-I curing compound, and a cover consisting of a sheet of polyethylene and cotton mat above the polyethylene sheet. Figure 48 is a close look at the data for the fourth day. It shows that the polyethylene sheet plus cotton mat protected moisture from evaporating more efficiently than the curing compound.
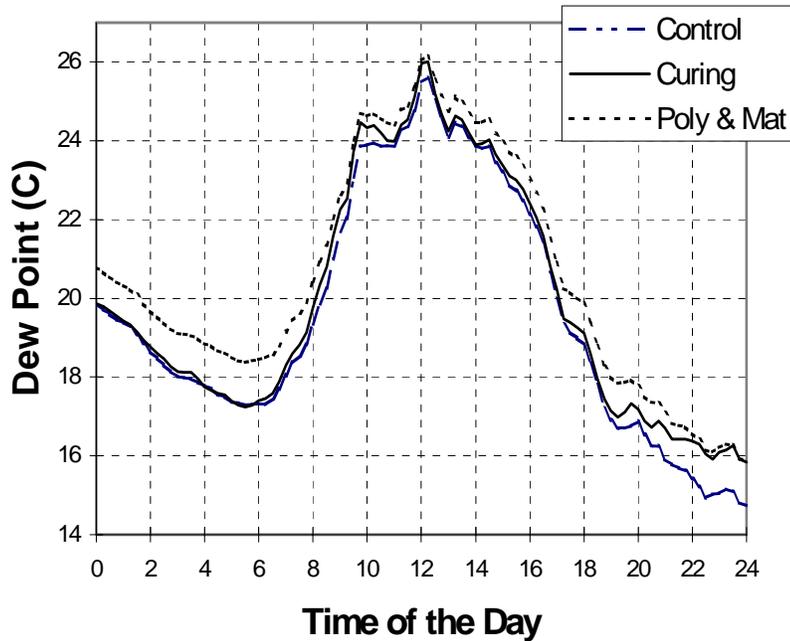
Figure 48. A field investigation of dew point versus hour of day during the fourth day after implementation.

A.4.2 Lab Strain Measurement

The measurements of strain are made with the moisture measurements through the use of the vibrating wire strain gauges. Two vibrating wire strain gages were embedded in the specimen in diametrical directions at the 2.54 cm and 12.7 cm (1 and 5-in) depths where strains inside the specimen were monitored. Temperature and dew point at different levels were also read from the M200 meter. Figures 49, 50 and 51 show the readings of strain, temperature and dew point respectively. From these three figures, it can be observed that the concrete expansion does not exactly correspond to the hydration temperature increase. These data imply that not only temperature but also moisture affects the early age strain.
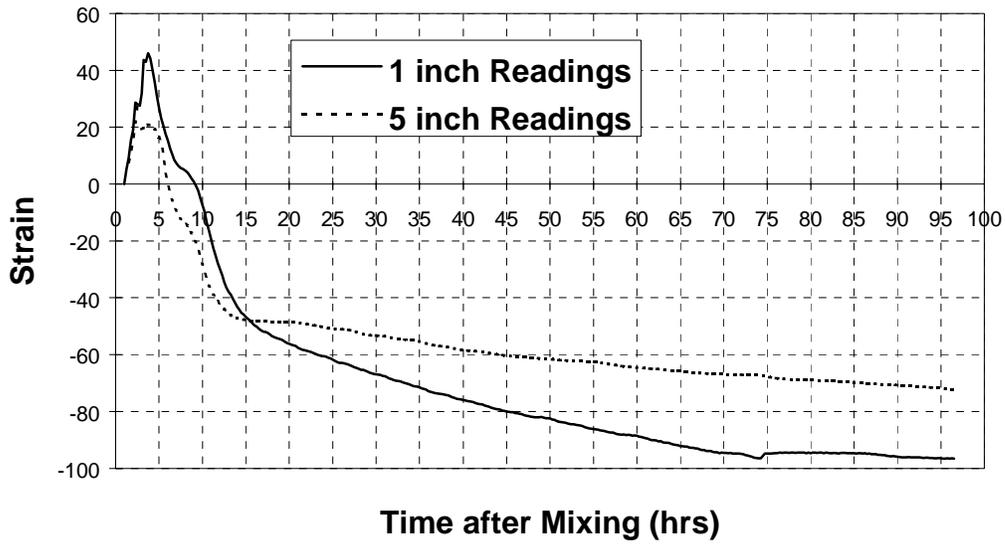
Figure 49. Strain versus time at different vertical positions.
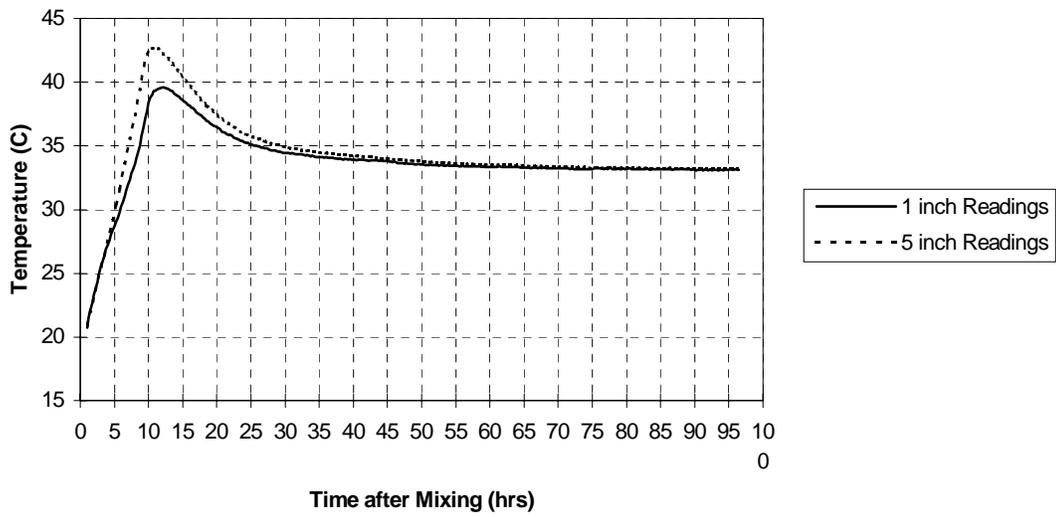
Figure 50. Temperature versus time at different vertical positions.

123
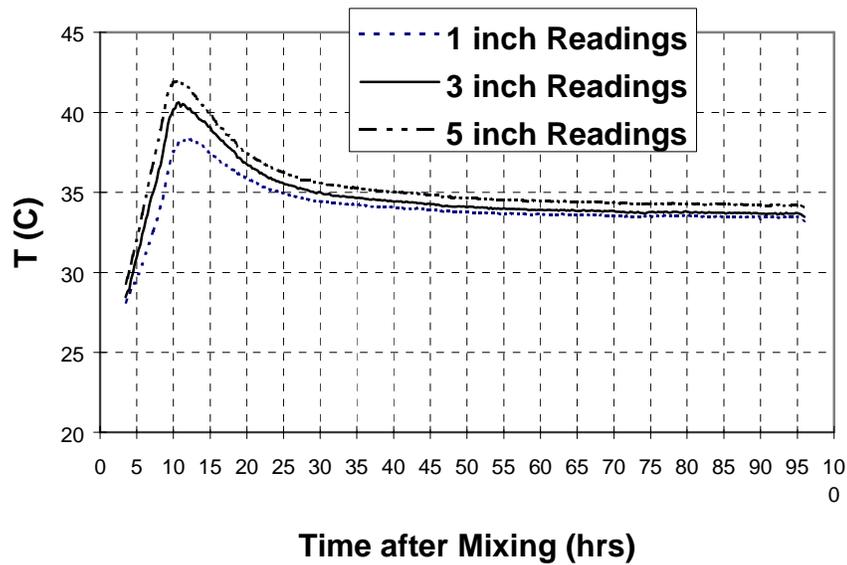
Figure 51. Dew point versus time at different vertical positions.

Figure 52 describes the whole process of the test of drying, environmental rewetting and surface water rewetting. The curve indicates the dew point at the 2.54 cm (1-in) depth. The strain change at the same depth is approximately inversely proportional to the change in the dew point. At 98 h after casting, the relative humidity of the environmental chamber was raised to 100 percent and remained so for the next 64 h. At 162 h, a saturated towel was placed on the upper end of the specimen. The environmental relative humidity seemed to have no apparent influence on the shrinkage during the period of time, while the wet towel dramatically increased the expansion of the specimen at the 2.54 cm (1-in) depth. Figure 53 illustrates the relative humidity result for a concrete that had been dried for 160 h at 94 percent before being exposed to a water-saturated towel for 50 h. It can be seen that the 1 inch relative humidity and dew point (figure 54) both went up during the process while the temperature readings (figure 55) did not change much. What is interesting is that the 2.54 cm (1 in) relative humidity went up from 94 percent to 97 percent similar to the relative humidity at the 12.7 cm (5 in) level. The rate of rewetting of concrete after periods of drying is relevant to corrosion of reinforcing steel and many other aspects of concrete durability. The kinetics of rewetting might also prove to be a useful general indicator of the diffusion resistance of concrete cover. The data of figures 53, 54 , 55 and 56 are recorded during the same period of time and clearly show how the moisture change is affecting the strain of concrete.

Drying Test-1 inch Dew Point-Transit Mix-Nov 13-22,1995
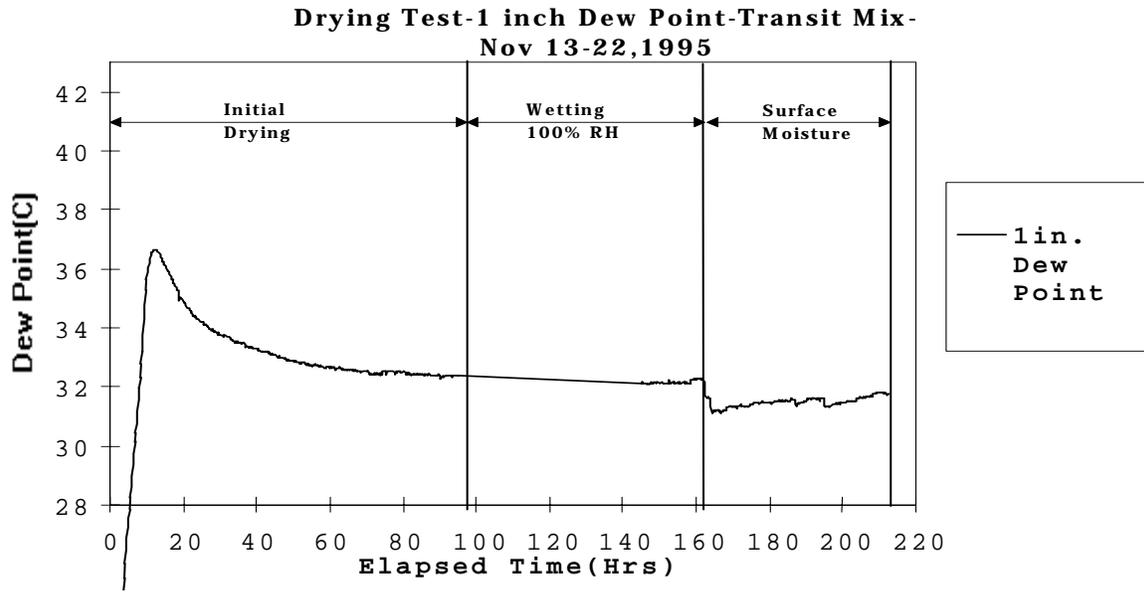
Figure 52. Test description.
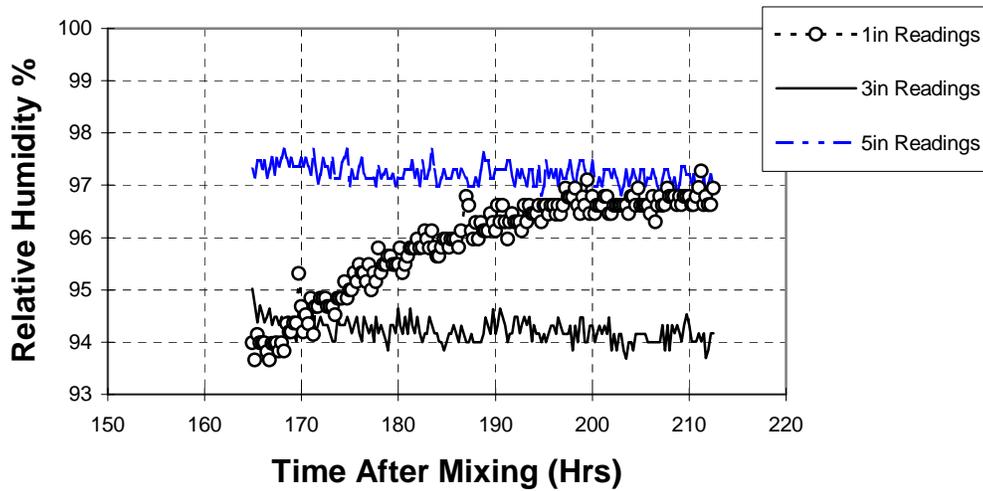
Figure 53. Effects of surface water on relative humidity.
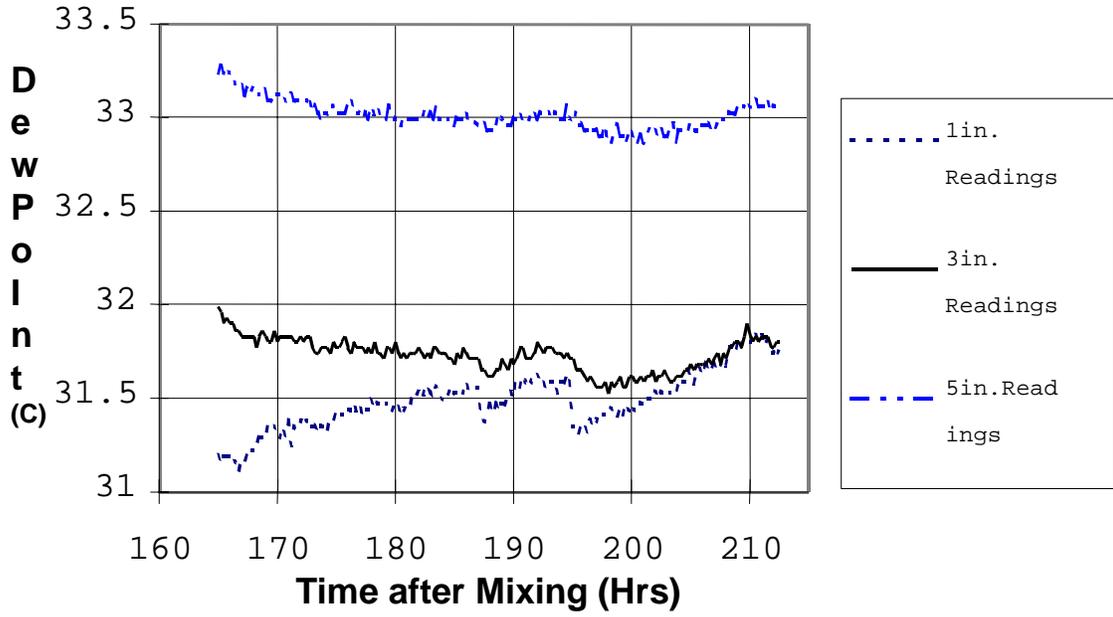
Figure 54. Effects of surface water on dew point.
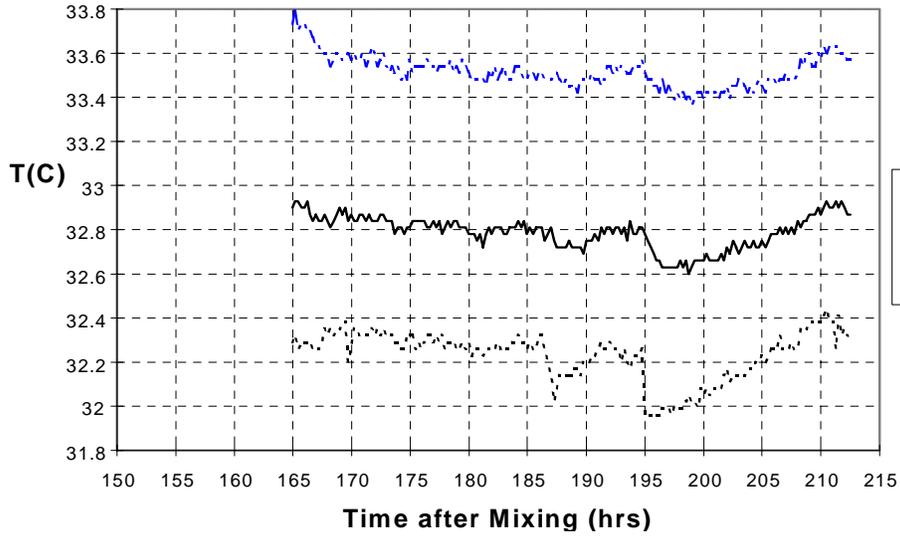
Figure 55. Effects of surface water on temperature.
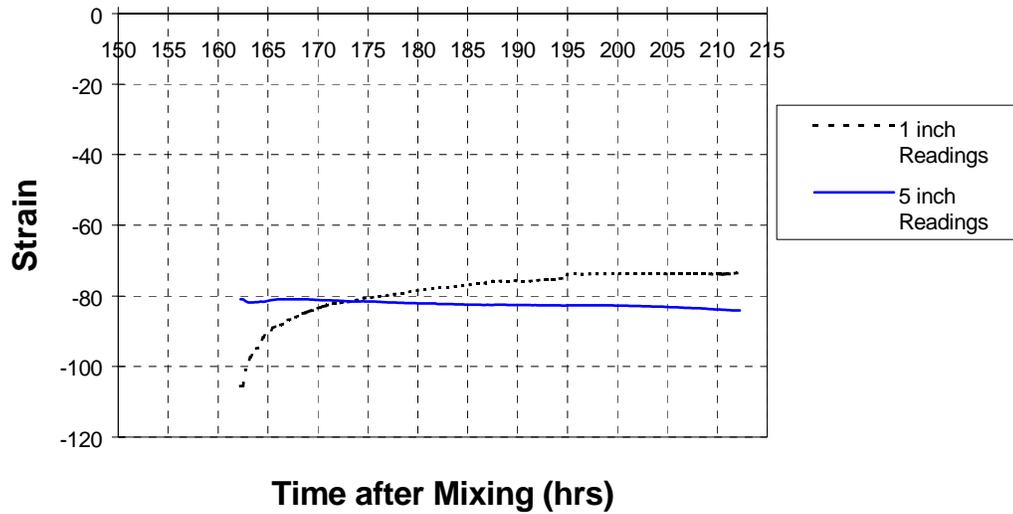
Figure 56. Effects of surface water on strain (10^{-6} microstrain).

The concrete mix design and the ambient condition of the test is shown in tables 16 and 17.

Table 16. Mix design (1 cubic yard, or 0.765m3, of concrete).

Material	Weight or Volume
GH Servtex Limestone (Well Graded)	1788 1b (812 kg)
GH Jones Sand	1178 1b (535 kg)
Cement	564 1b (256 kg)
Water	229 1b (104 kg)
A/E Agent	6.00 oz-US
Water Reducer	27.00 oz-US

Table 17. Ambient conditions.

Room Temperature	32°C
Room Relative Humidity	50%
Curing Compound	No

A.5　Summary

This study developed models for simulating the vertical distribution of moisture in concrete, and coupled these models with the temperature models. A full implementation of the moisture models with the sophisticated temperature models will provide an improved estimate of the concrete properties development and behavior during the early age.

APPENDIX B

CORRELATION OF PLASTIC SHRINKAGE CRACKING WITH EVAPORATION RATE

This appendix discusses the methods of data collection, assessment and analysis used for a correlation of the observed level of plastic shrinkage with the conditions of construction. To complete such an analysis, several components are required. These components include extensive construction data, environmental data, and the assessment of apparent plastic shrinkage. This appendix addresses these issues and discusses results of an analysis that has been performed from an actual field condition survey. The prediction of plastic shrinkage cracking potential via the calculation of the evaporation rate is an integral component of the HIPERPAV software.

B.1 Introduction

Plastic shrinkage cracks occur in the surface of freshly mixed concrete soon after it has been placed, and often while it is still being finished. Though shrinkage cracking is often associated with hot weather concrete placement, it will occur whenever ambient conditions are right to yield a rapid evaporation of moisture from the surface of the concrete. This cracking, then, occurs when water at the concrete surface evaporates more quickly than it is being replenished from the bleeding process. This rapid evaporation causes rapid drying shrinkage and tensile stresses at the surface, resulting in short, irregular, often parallel cracks. Plastic shrinkage cracking is promoted by high wind speeds, low humidity, and high air or concrete temperatures. The Portland Cement Association has established an evaporation rate limit of 0.98 kg/m^2/h (0.2 lb/ft^2/h), above which precautionary measures are strongly recommended [3].

In order to demonstrate the validity of the correlation between plastic shrinkage cracking and the measured pan evaporation rate during construction, an example analysis is given here. This analysis is based upon a survey performed on PCCP at McCarran International Airport in Las Vegas in 1996. This example can be used as a model for this type of correlation analysis procedure. The following sections identify the key tasks which were performed during this analysis.

B.2 Collect Data

The concrete pavement slabs at McCarran International Airport exhibited various degrees of plastic shrinkage cracking. A survey of selected PCC pavement section was undertaken to quantify the extent and level of the distress. The following sections describe the sources of this and other data used in the analysis procedure.

B.2.1   Construction Data

Condition surveys were completed in six locations at McCarran International Airport on May 28-30, 1996. Three of these sections were:

Site 1: Cargo Terminal Apron

Site 2: East end Runway 7L-25R

Site 3: West end Runway 7L-25R

In order to complete the analyses, specific types of construction data were required. These data included:

• Concrete temperatures at time of placement (measured for each batch at the truck),

• Exact dates of construction for each paving lane,

• Paving directions for each lane, and

• Lane numbering or panel labeling.

B.2.2   Environmental Data

All environmental records were received through the National Climatic Data Center. Hourly data reports were required in order to acquire the precision of the windspeed and temperature readings necessary for this type of analysis. The parameters used in the analysis included the ambient temperatures, concrete temperatures, wind speed, humidity, and any precipitation. These readings were taken at the data collection center located on-site at the airport.

B.2.3   Distress Data

The quantification of any visually measured pavement distress is always a difficult task. To minimize the subjectivity of the evaluation, field personnel took several steps to standardize their operations. For example, the same two personnel surveyed all six sections together, thereby minimizing any variability between surveyors. Also, these six sections comprised approximately 280,000 m^2 (3'000,000 ft^3) of pavement, providing a statistically sound sample size for the analyses. Third, both personnel standardized their quantification to the Strategic Highway Research Program Distress Identification Manual [41].

Extensive and detailed data were collected from each of the sections. The level of plastic shrinkage cracking on each panel was assigned an index value from 0 to 6, respectively ranking the condition from "no apparent cracking" to "high severity cracking."

B.3   Data Analysis

B.3.1   Theoretical Background

The first evaporation nomograph was developed by Menzel in 1954 [42] and was considered very complicated. The nomograph was revised six years later by the National Ready Mix Concrete Association [42], and then became adopted internationally. However, with the proliferation of modern computers and calculators, this nomograph actually became a limitation, thereby creating an incentive to redevelop the analytical approach.

Menzel's original equation, which served as a basis for developing the evaporation nomograph, employed the use of Dalton's Law, which is based on the fundamental physics of the evaporation process. Menzel's equation, however, requires two vapor pressures as inputs. In meteorological practice, it is difficult to measure vapor pressures directly at a site. Instead, both the dry-bulb and wet-bulb temperatures are commonly measured to give the relative humidity. Given the relationship between vapor pressures and humidity, Menzel's equation was rewritten to allow the use of humidity inputs for vapor pressure inputs. This modified equation was then combined with Teten's 1930 equation [42] relating saturated vapor pressure over a pure water surface and temperature. The resulting equation requires input variables of wind speed, relative humidity, air temperature, and concrete temperature. These are the same inputs for the nomograph. This yields an evaporation rate that serves as a surrogate measure for the actual evaporation rate in the same climatic conditions. This equation, used for the following analyses, has been tested and verified by the Center for Transportation Research at the University of Texas at Austin [42].

B.3.2   Analysis Procedure

The data collected from the condition survey were first entered into a database format. Next, from the construction records received, concrete placement log data were used to match concrete placement times and locations against ambient environmental conditions in a panel-by-panel order. The placement time of each panel was, therefore, estimated to the nearest hour, based on available information. It should also be noted that the curing method used on these slabs was specified as a single-application of liquid membrane. Using the climatic data, concrete temperatures, and placement hour as inputs, a resultant evaporation rate was computed. This evaporation rate was then compared to the corresponding plastic shrinkage level observed. The charts and figures in the next section illustrate this relationship.

B.4   Analysis Results

The results of the analyses of the three pavement sections follow.

East end, 7L-25R

The development of a statistically sound correlation is dependent upon the availability of a wide range of pavement conditions and corresponding evaporation rates. Of the three sections surveyed, the east end of Runway 7L-25R provided some of the most varied pavement conditions. The surveyed area was broken down by construction date and analyzed by lane. An example of the varied pavement conditions and their corresponding evaporation rates is shown in figure 57. The figure represents the sampling of Lane 8, which was paved February 11-12, 1994. For each panel, a shrinkage cracking index was assigned depending on the severity of cracking observed. An index value of zero indicates the presence of no plastic shrinkage cracking and a value of 5 indicates very severe plastic shrinkage cracking.
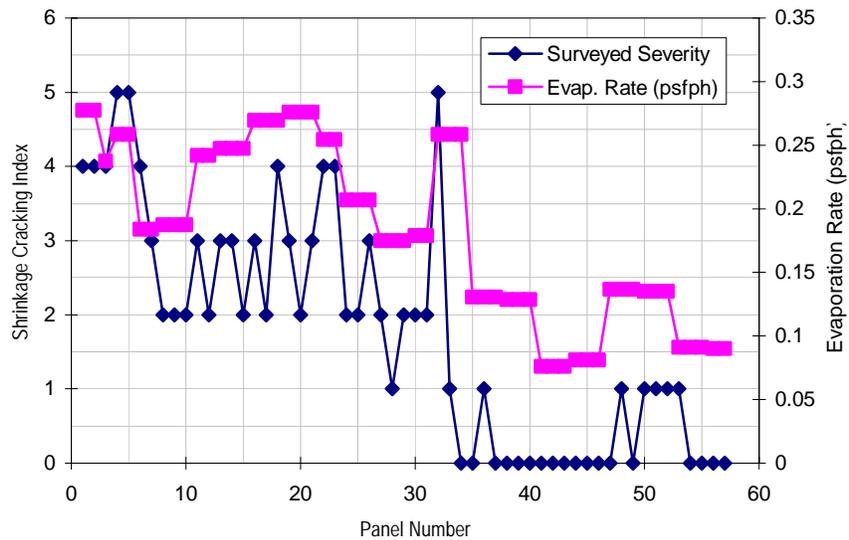
Figure 57. Calculated evaporation rate and observed plastic shrinkage cracking of Lane 8, east end 7L-25R

Because of the similar environmental conditions on February 11 and 12, the figure includes both days. As the figure illustrates, the observed changes in plastic shrinkage cracking severity follows the changing evaporation rate, calculated based on temperatures and wind speeds.

West end, 7L-25R

The majority of the panels surveyed in the West end of the runway were evaluated as having "no apparent" to "very low" levels of plastic shrinkage cracking (index values of 0 and 1, respectively). One lane, however, provided a wide range of cracking levels. This second sample of the condition survey results is presented below. This sample, from Lane 22 of the West end of runway 7L-25R was paved on April 22, 1994. As figure 58 illustrates, three panels showed severe shrinkage cracking, with a corresponding evaporation rate nearing 1.5 kg/m^2/h (0.30 lb/ft^2/h). These panels, incidentally, are currently not under traffic.
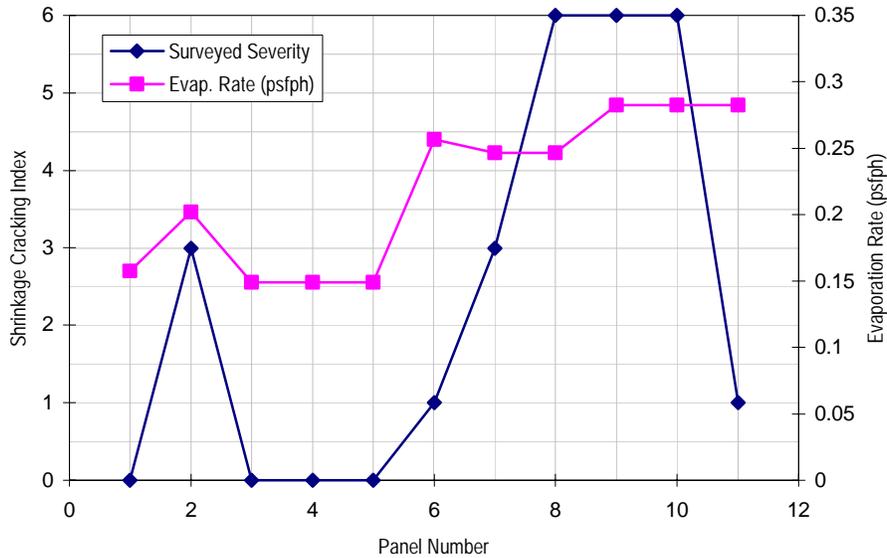
Figure 58. Sample of evaporation rate with observed plastic shrinkage cracking of Lane 22, west end 7L-25R

Cargo Terminal

The cargo terminal apron was at the very low range of shrinkage cracking observed by field personnel. Figure 59 is a sample of the data recorded in the condition survey, along with the corresponding evaporation rates. This sample is from Lane 2 of the cargo apron, which was paved on April 20, 1994. This figure shows that as the evaporation rate stays relatively constant at a low level, so too does the level of plastic shrinkage.
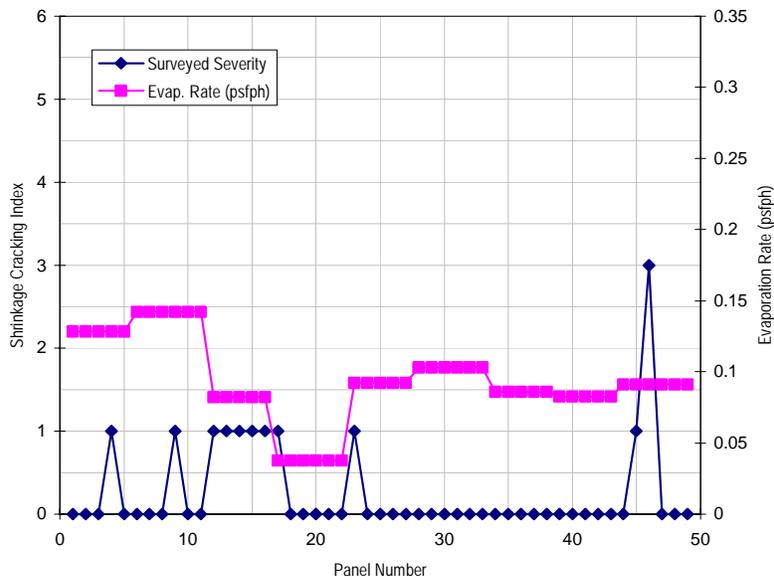
Figure 59. Sample of evaporation rate with observed plastic shrinkage cracking of Lane 2, cargo terminal

133

B.5   Discussion of Results

From both the condition survey and the subsequent analyses of the construction data as presented in the previous sections, certain observations can be made. Each of the previous figures, while presenting differing conditions and levels from different pavement sections, all converge toward a common threshold value. Figure 60 below charts all non-heavy traffic panels surveyed at the East end of Runway 7L-25R, totaling over 840 panels. The figure plots the cumulative frequencies of evaporation rates for each category of shrinkage cracking. For example, as illustrated by this figure, some 90 percent of the panels that were observed to have "very low" severity cracking were constructed in conditions where the evaporation rate did not exceed 0.98 kg/m^2/h (0.20 lb/ft²/h). Alternatively, some 90 percent of the panels that were observed to have "moderate" severity cracking were constructed in conditions where the evaporation rate did not fall below 1.5 kg/m^2/h (0.30 lb/ft^2/h). From this sizable set of data, it is conclusive that these data converge about the rate of 0.98 kg/m^2/h (0.20 lb/ft²/h) as a statistically sound threshold value. This preliminary threshold value is of unique value to the construction of concrete pavements at McCarran International Airport. Since it is site-specific for the Airport, it can be successfully and accurately used as a construction guideline in regards to placement and curing techniques. At the time and location of future construction, real-time weather data and concrete temperatures can be computed into a precise real-time evaporation rate for the concrete. This real-time evaporation rate can then be used to determine which type of curing method should be employed.
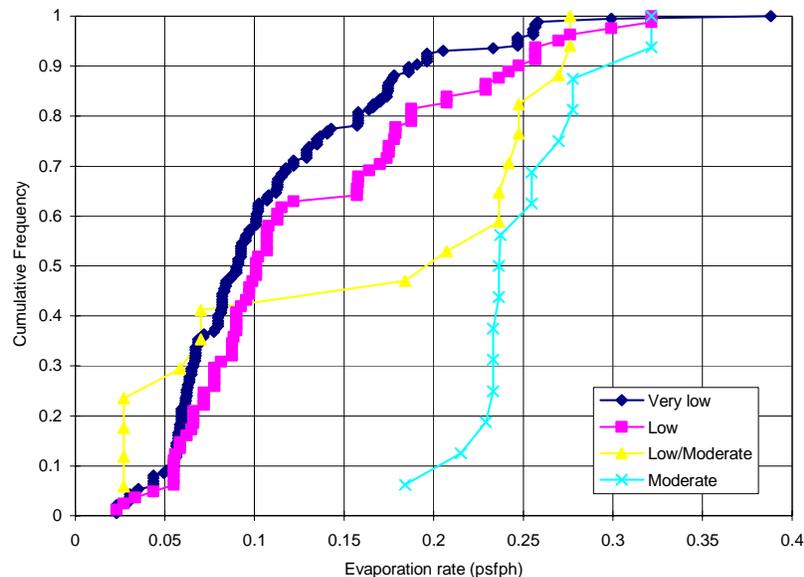
Figure 60. Cumulative frequency of evaporation rates by shrinkage severity

Some construction specifications state that as the evaporation rate increases, increasing levels of moisture loss prevention are recommended. A practical approach to decreasing this moisture loss is multiple applications of curing compound. For example, if the prevailing

134

evaporation rate exceeds a pre-determined limit, two passes of membrane curing compound may be required. A recent joint study conducted by the Center for Transportation Research and the Texas Transportation Institute for the Texas Department of Transportation included the effectiveness testing and measurement of multiple curing applications on jointed concrete pavements [37]. In this study, moisture loss protection was measured as the effective thickness through which moisture must travel to reach the evaporative surface. A larger effective thickness, therefore, translates into greater moisture loss protection. Figure 61 displays the results of the investigation. As the figure shows, when compared to non-cured pavement, a single pass of membrane curing compound increases the effective thickness. Three passes, however, significantly increase the moisture protection of the pavement, with little appreciable decline in protection over time.
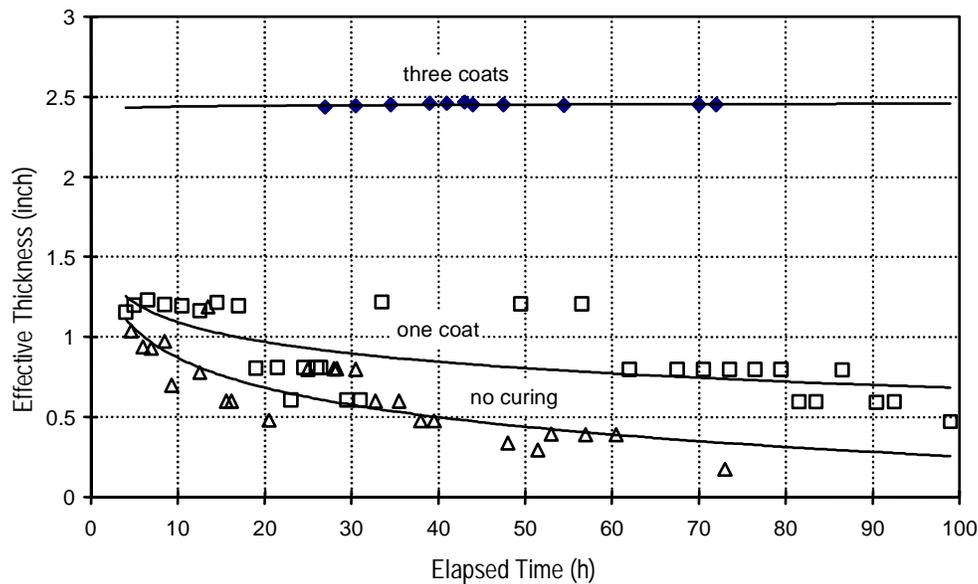
Figure 61. Comparison of effective thickness values between varying numbers of curing coats

The following conclusion can be drawn from this analysis: from these three differing pavement sections, a common threshold evaporation rate of 0.98 kg/m^2/h (0.2 lb/ft²/h) was determined. This preliminary result is the same evaporation rate used in the construction specifications. This rate is also commonly held as a threshold value by the Portland Cement Association [3].

This procedure can be used by any agency or institution which desires to determine at which evaporation rate plastic shrinkage cracking can be expected for the local construction and environmental conditions. Knowledge of this can lead to better PCCP performance.

APPENDIX C

TEST SECTIONS OF FAST TRACK PAVING OPERATIONS

This appendix discusses the methods of test site administration, instrumentation, and data collection for studying the behavior of fast track paving operations. Presented below are the test sites used for the calibration and validation efforts for this project. This appendix addresses these issues and presents the results of the data collection activities.

C.1 Chambers County, Texas

The test sections on McCarthy Road in Houston, Texas were paved at 3:30 pm, on September 24, 1994. They were opened to traffic at 12:00 pm the following day. The purpose of the field investigation was to detect factors which affect strength gains and drying processes at an early age for this jointed concrete pavement (JCP). These test sections are jointed reinforced concrete pavement (JRCP) placed 25.4 cm (10 in) thick. The test sections consist of four different curing sections with the same concrete mix design for monitoring temperature and moisture variations in newly placed JCP. Figure 62 shows a plan view of the test section in Chambers County, Texas providing the locations of the sawcuts and the instrumentation installed in the pavement. Plots of the data collected from the investigation are shown in figures 63 through 77, and the concrete mix design is described in tables 18 and 19.
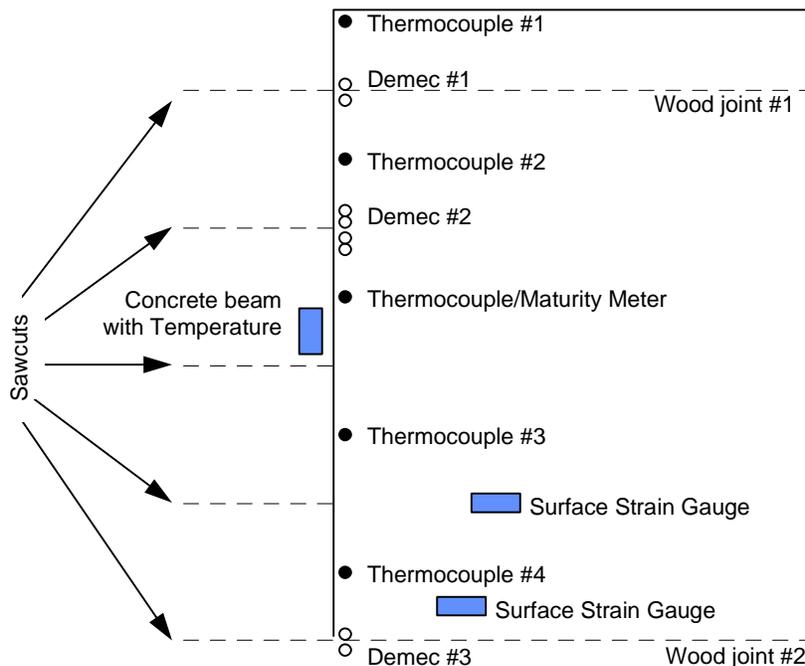
Figure 62. Site map of Chambers County, Texas test section.

137

Figure 64. Slab temperature differentials at station no. 1.

Figure 63. Slab and air temperatures at station no. 1.

138
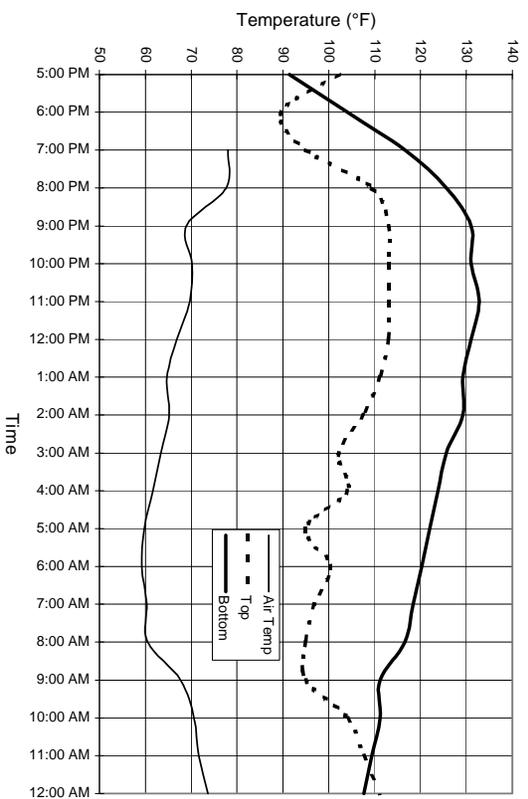
Figure 65. Slab and air temperatures at station no. 2.
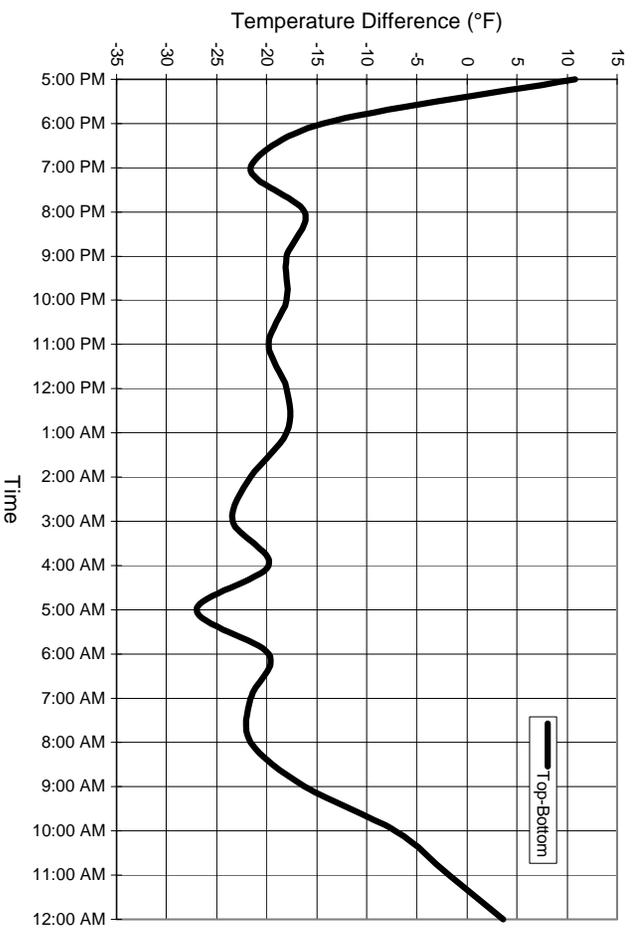
Figure 66. Slab temperature differential at station no. 2.

139
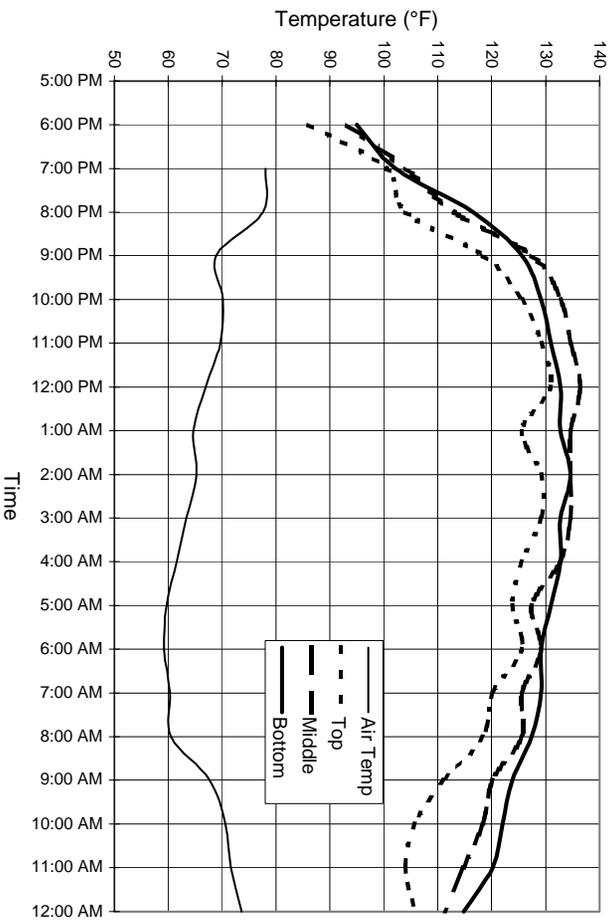
Figure 67. Slab and air temperatures at station no. 3.
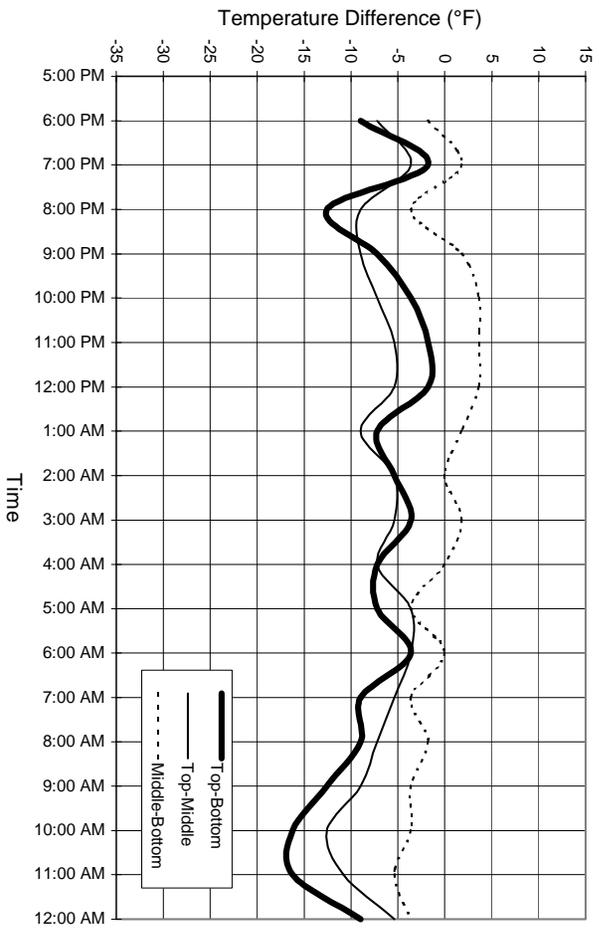
Figure 68. Slab temperature differentials at station no. 3.

140
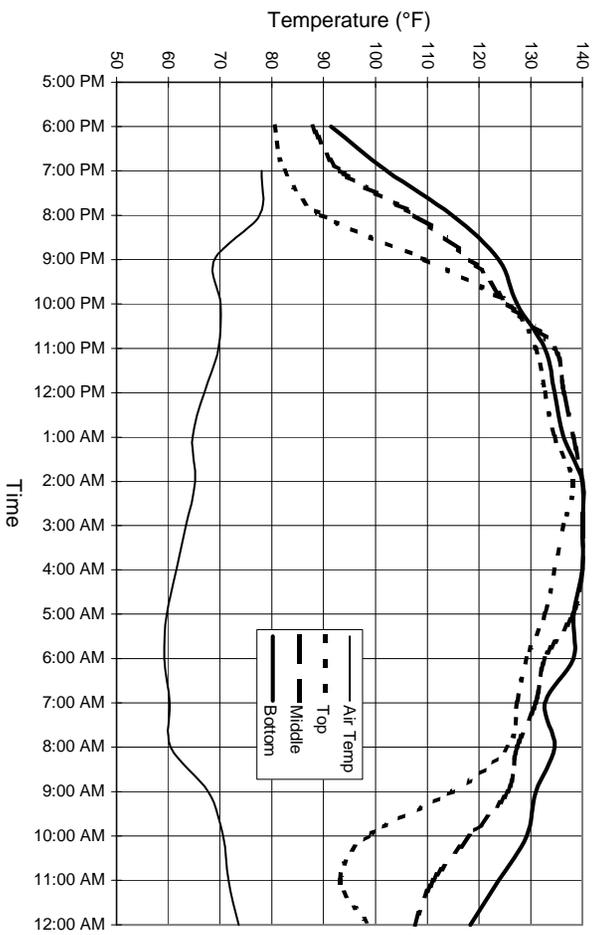
Figure 69. Slab and air temperatures at station no. 4.
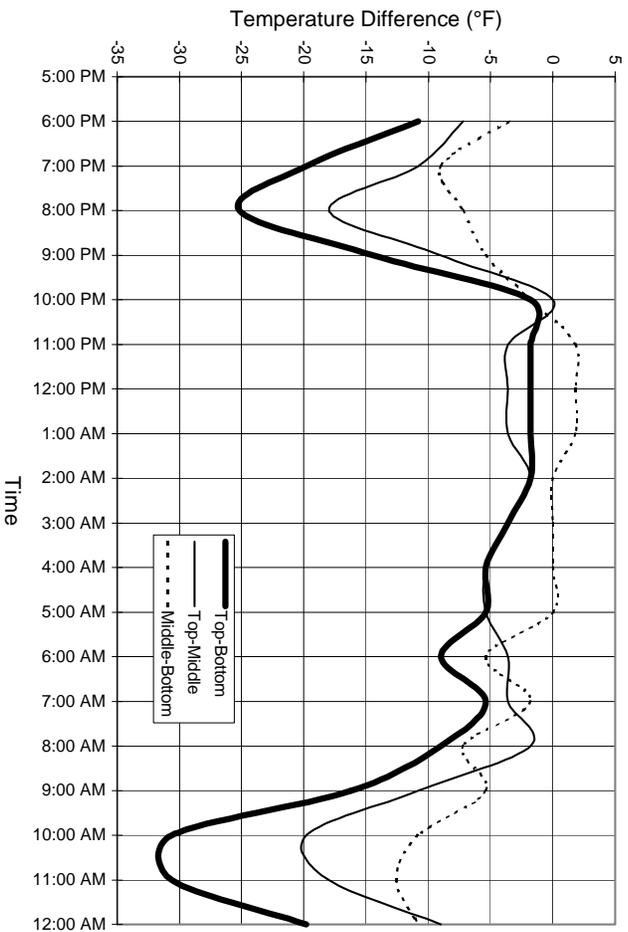
Figure 70. Slab temperature differentials at station no. 4.

141
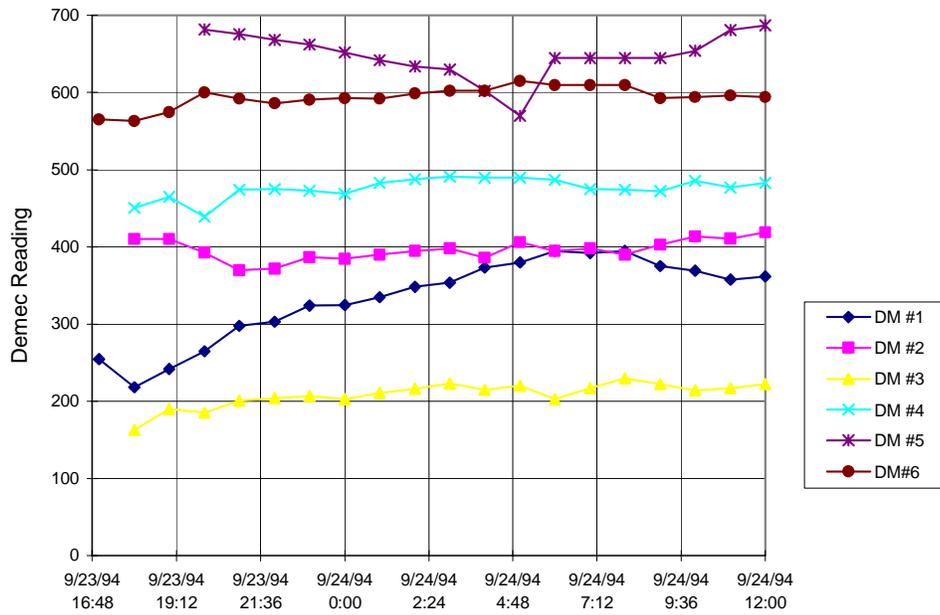
Figure 71. Construction joint movements using demec points.
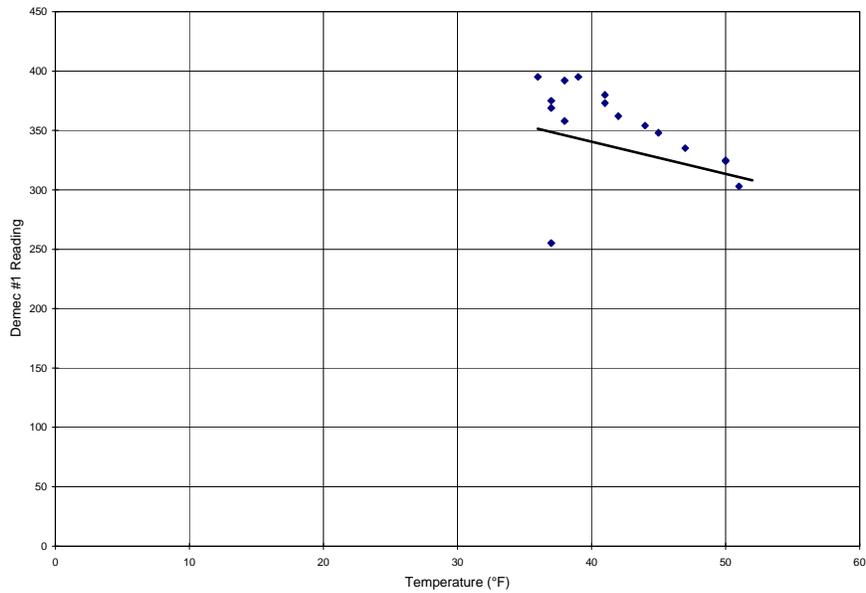
Figure 72. Construction joint movement at demec no. 1.
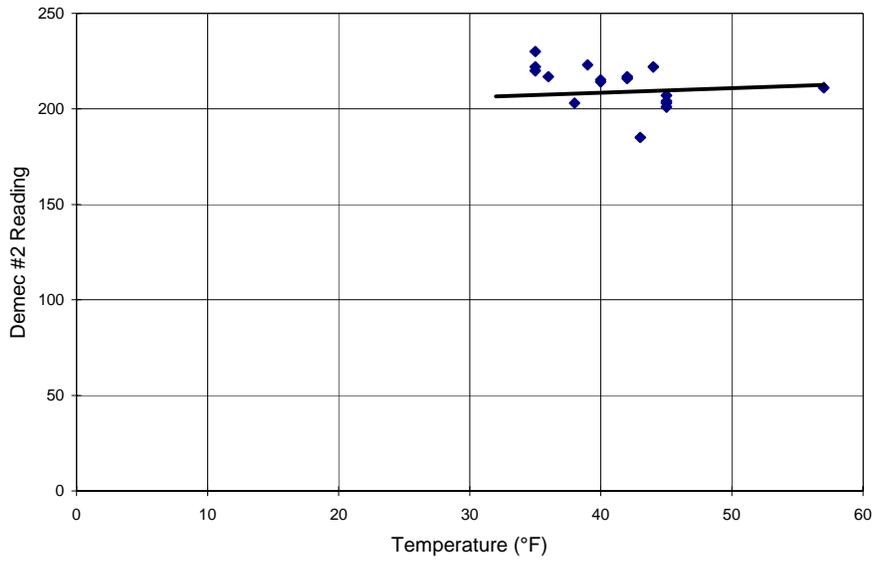
Figure 73. Construction joint movement at demec no. 2.
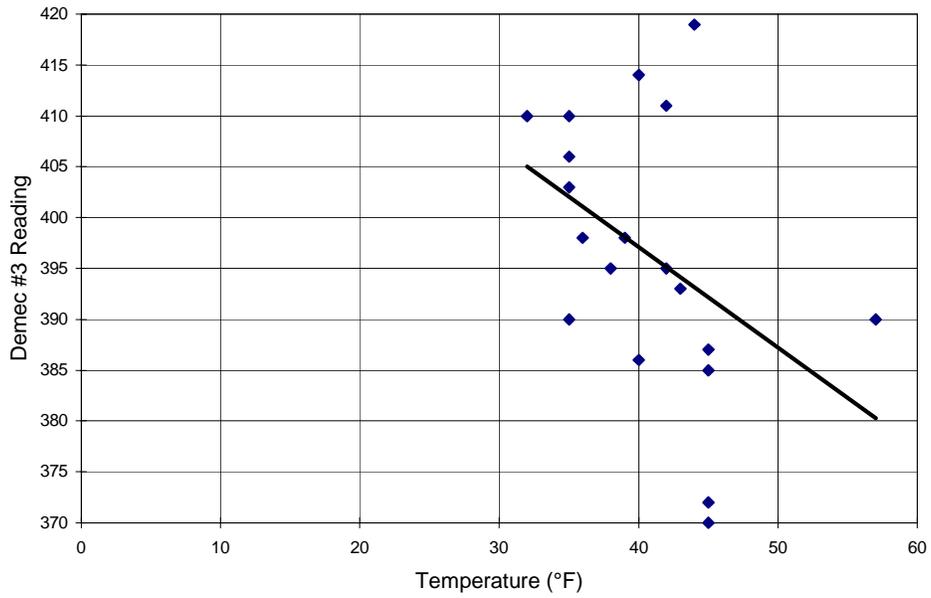
Figure 74. Construction joint movement at demec location no. 3.
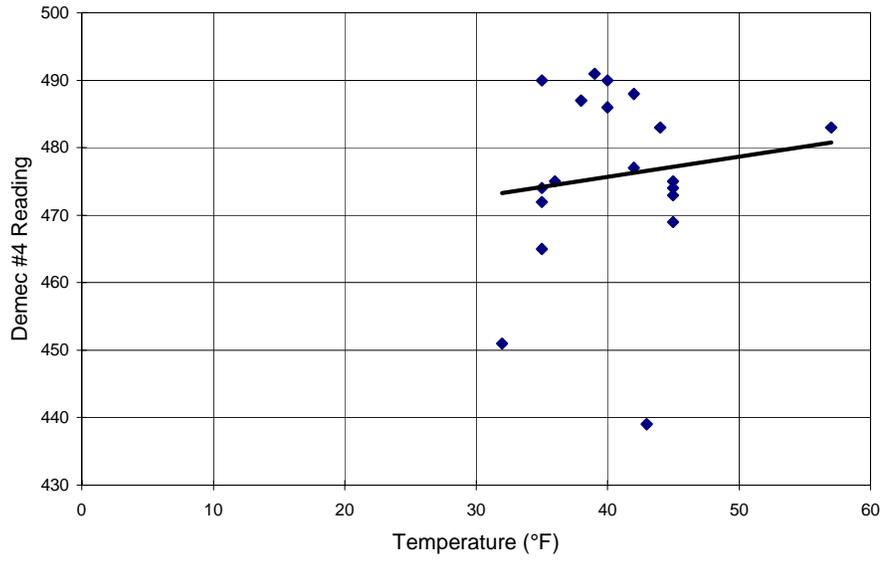
Figure 75. Construction joint movement at demec location no. 4.

Figure 76. Construction joint movement at demec location no. 5.

144
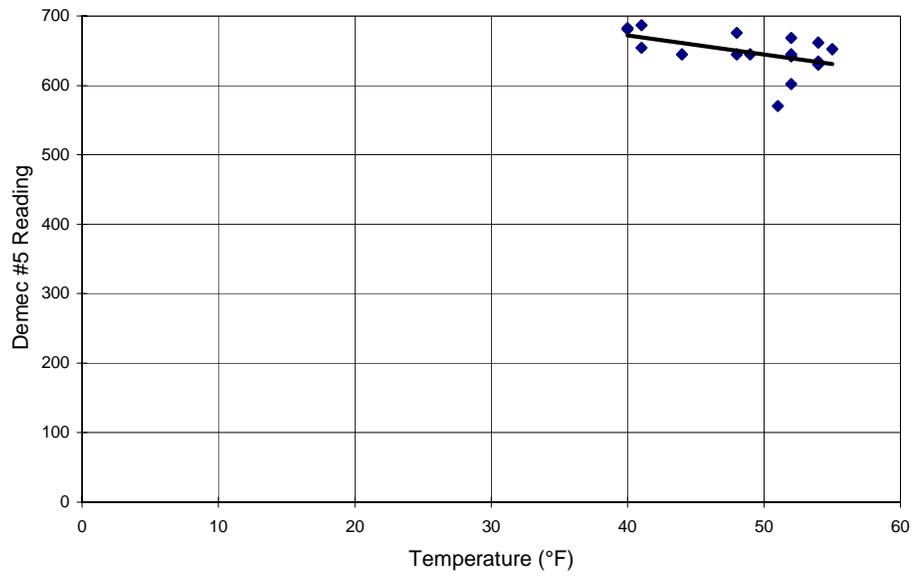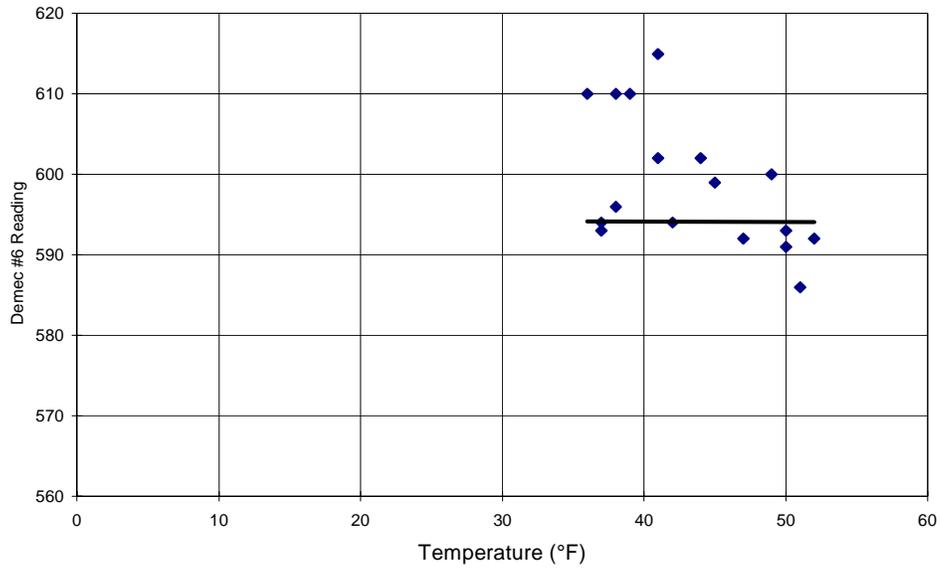
Figure 77. Construction joint movement at demec no. 6.

Tables 18 and 19. Mix design and cement properties specifications.

Mix Design, Houston	
Material	**Weight or Volume**
Gulf Coast Cement, Type I	705 lb (320 kg)
Redland Worth Crushed Limestone	1863 lb (845 kg)
Dolen Sand	975 lb (442 kg)
Water	263 lb (119 kg)
Total Air	4.30%
Amex-210	2.0 oz-US (0.06 kg)
Rheobuild 1000	70.5 oz-US (2.034 kg)
Water/Cement Ratio	0.37
Slump	1.0 in (25 mm)
Concrete Unit Weight	141.2 pcf (2259 kg/m3)
Total Yield	**27.00 cf (0.765 m3)**

Cement Properties, Houston	
Property (see eq. 5 - chap. 4)	**Value**
Φ (kJ/mol)	44.873
λ_1	0.1
t_1	500
κ_1	0.8
Hu (J/g)	496.8

C.2   Puebla, Mexico

This section reviews the experimental design and investigation of concrete pavement behavior and performance on roads constructed near Tepeaca, Puebla in Mexico. For this experiment, two concrete slabs, each 23 cm (9 in) in thickness, were instrumented to monitor the stresses and deformations caused by environmental factors and traffic loads. Prior to concrete placement, the subbase was cleared and prepared. Following the subbase preparation, the entire test section was fitted with instrumentation prior to paving.

Both slabs were placed on December 16, 1994. The first slab was paved at noon with an average ambient temperature of 21°C (69°F), humidity of 19%, wind velocity 6.2 kph (3.9 mi/h), and concrete temperature of 24°C (75°F). The second slab was placed at 1:15 pm with an average air temperature of 21.9°C (71.5°F), a relative humidity of 16%, a wind velocity of 6.4 kph (4.0 mi/h) and a concrete temperature of 24°C (75.2°F). From the environmental conditions, an average evaporation rate of 0.49 kg/m^2/h (0.1 lb/ft^2/h) was estimated. No evidence of plastic shrinkage was noted.

This section describes the instrumentation of several testing procedures. These tests included Demec measurements of joint movement, temperature measurements, horizontal strain measurements, moisture sensors, and maturity meters.

Two *Roctest em-5* vibrating steel wire strain gauges were installed in half-cylinders at both ends of the slab. These cylinders were placed near the edge of the slab (figure 78). Four

additional sets of gauges were installed throughout the slab. Each set consisted of a top gauge (21 cm or 8.3 in from subbase), a middle gauge (12 cm 4.7 in from subbase), and a bottom gauge (2 cm or 0.8 in from subbase). A second set of instruments installed at the site included multidepth temperature probes. Two sets of four-depth temperature probes were installed. Additionally, four moisture sensor cans were installed to evaluate the relative humidity inside the concrete at different depths.

The test sections included two different curing methods used to measure the temperature effects of curing. A standard membrane curing compound was sprayed over the surface. In addition to the curing compound, black polyethylene sheeting was placed over the first slab. Following is a layout of the instrumentation installed (figure 78), plots of the data collected from the investigation (figures 79 through 91), and the mix design of the concrete used (tables 20 and 21).
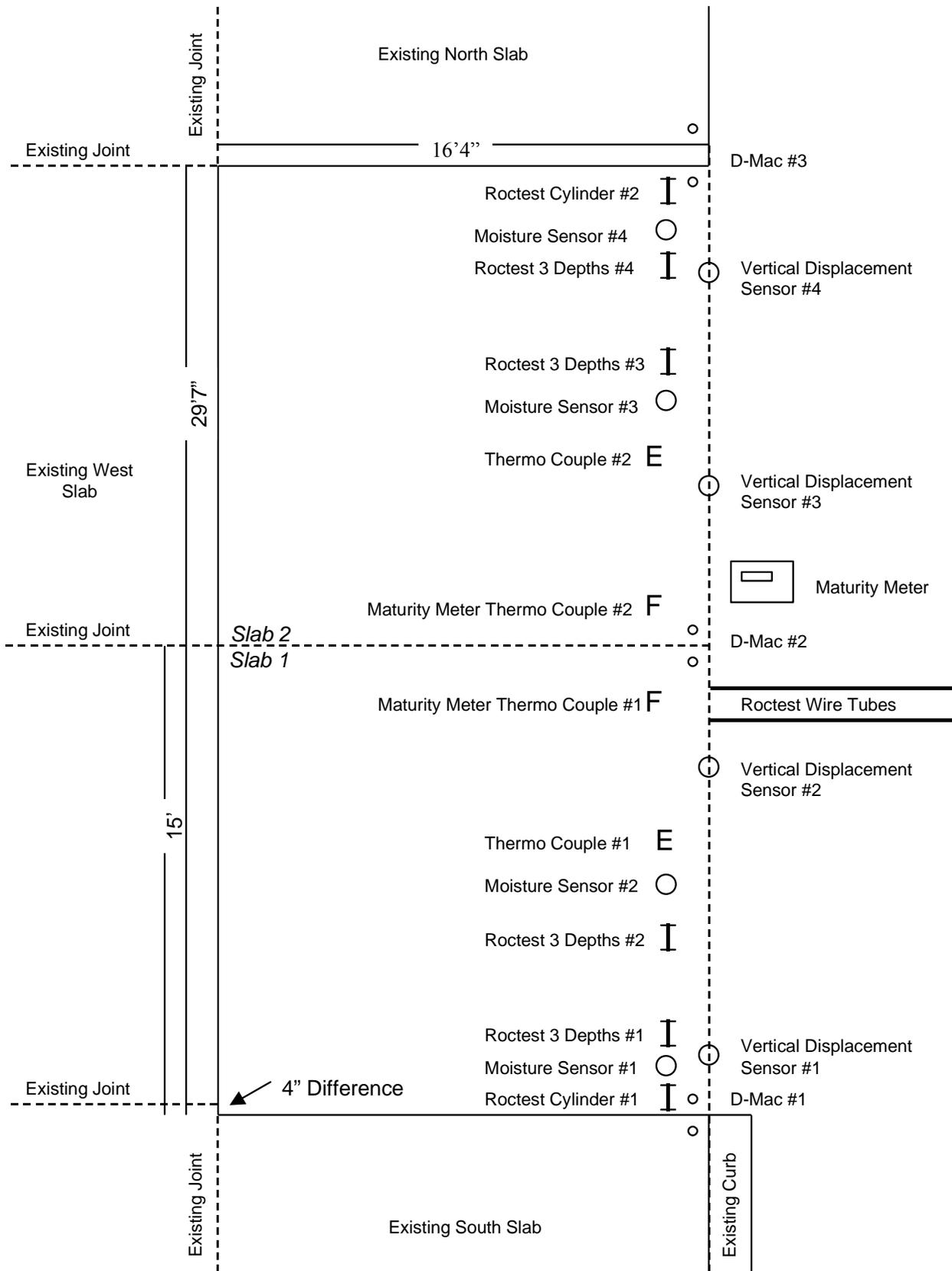
Figure 78. Site map of Puebla, Mexico test section.
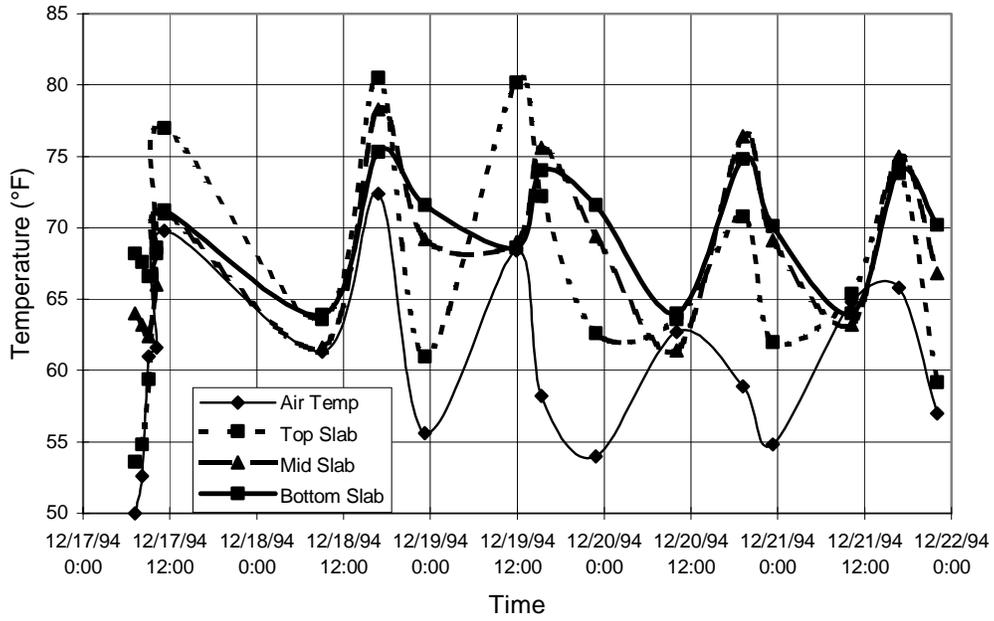
Figure 79. Concrete temperatures (w/o poly sheeting) in Tepeaca, Mexico.
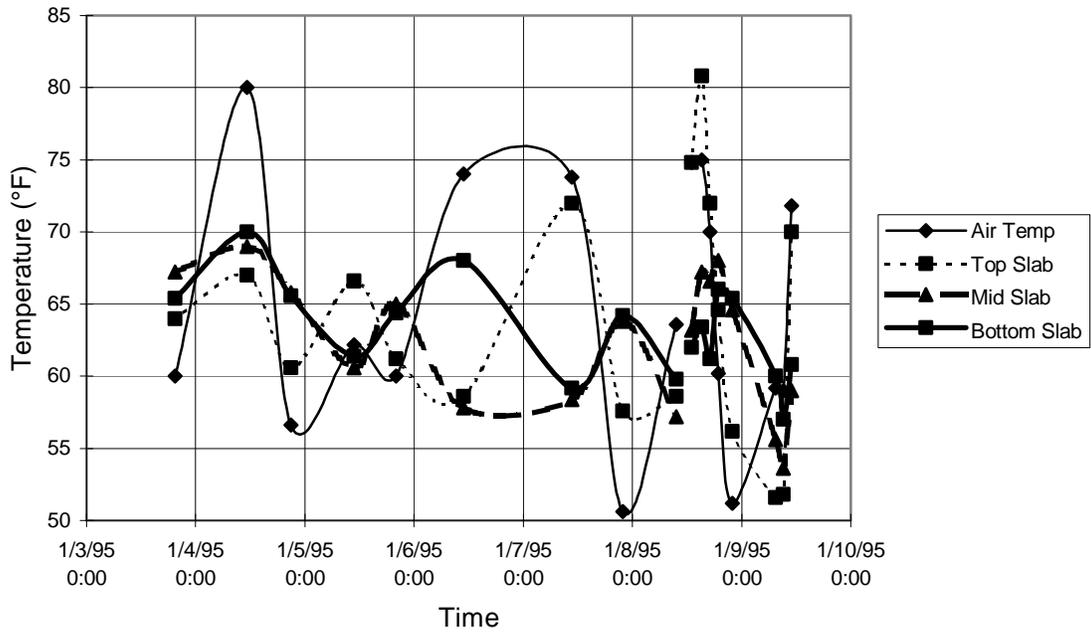
Figure 80. Concrete temperatures in Tepeaca, Mexico two weeks after placement.

149
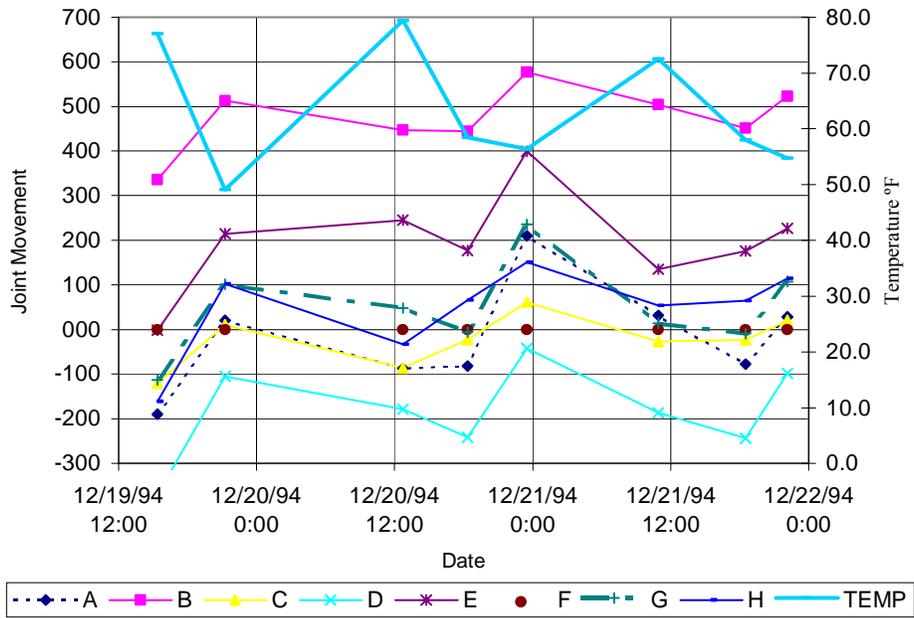
Figure 81. Joint movement at each of eight locations.
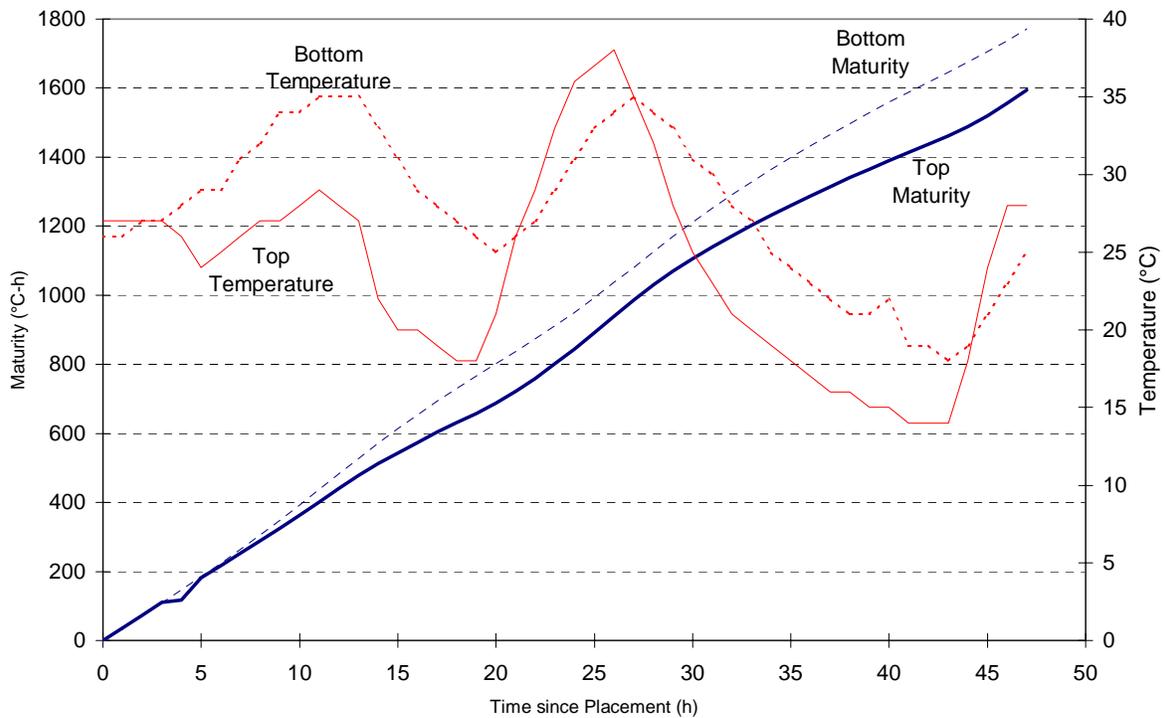
Figure 82. Slab temperature and slab maturity at two depths (w/ poly sheeting).

150
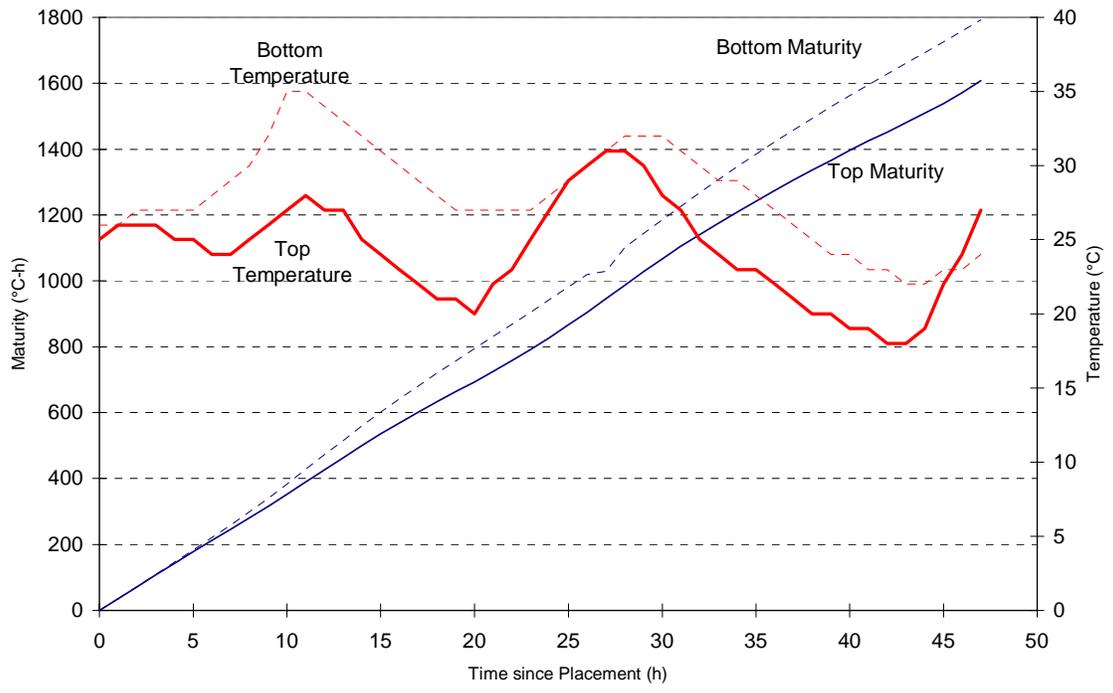
Figure 83. Slab temperature and slab maturity at slab age.
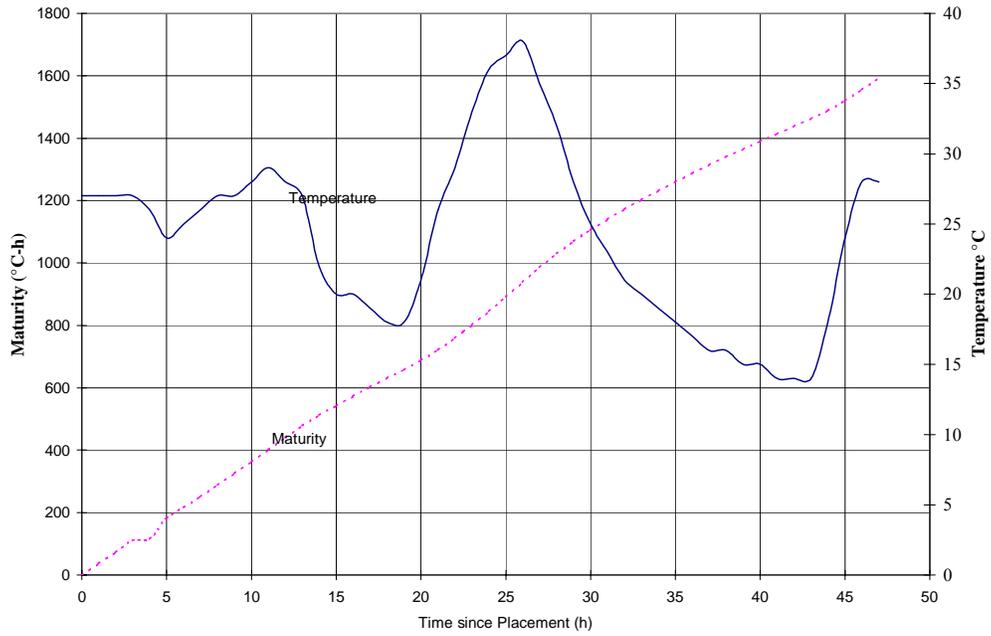
Figure 84. Slab temperature and maturity at channel no. 1.

151
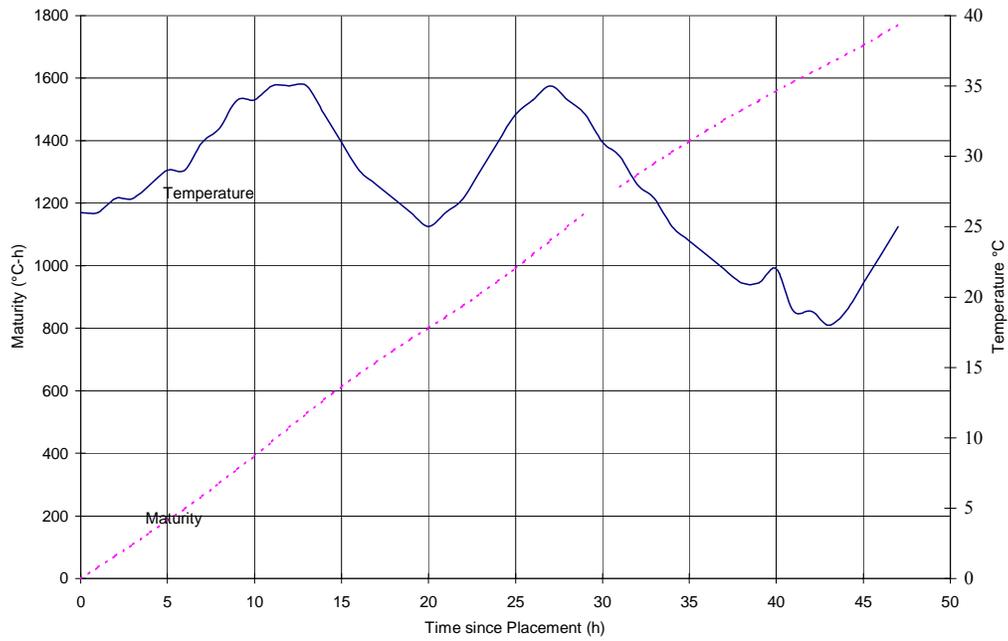
Figure 85. Slab temperature and maturity at channel no. 2.
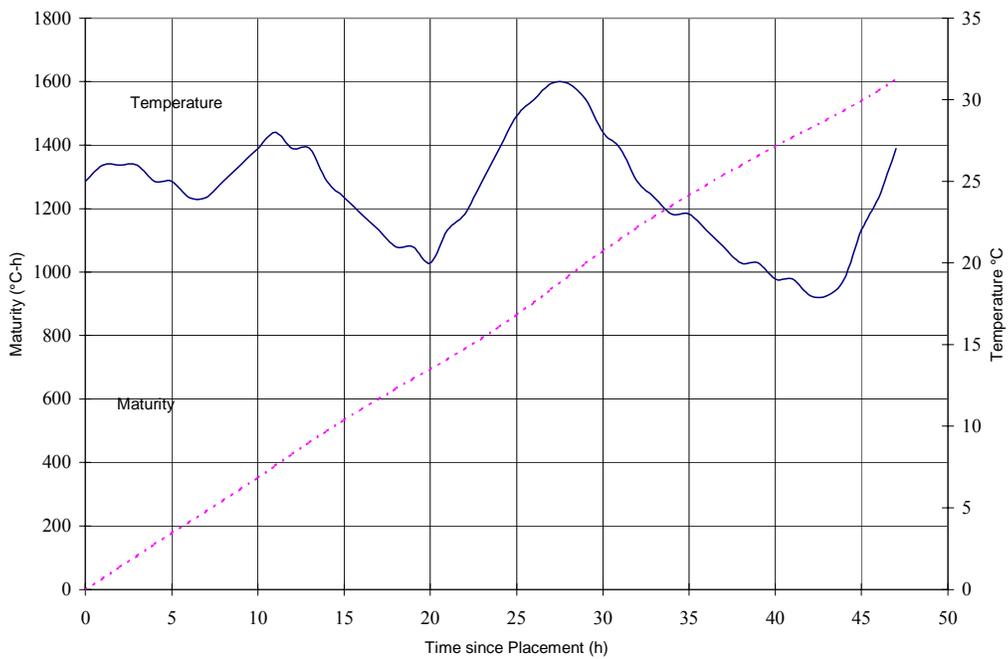
Figure 86. Slab temperature and maturity at channel no. 3.

152
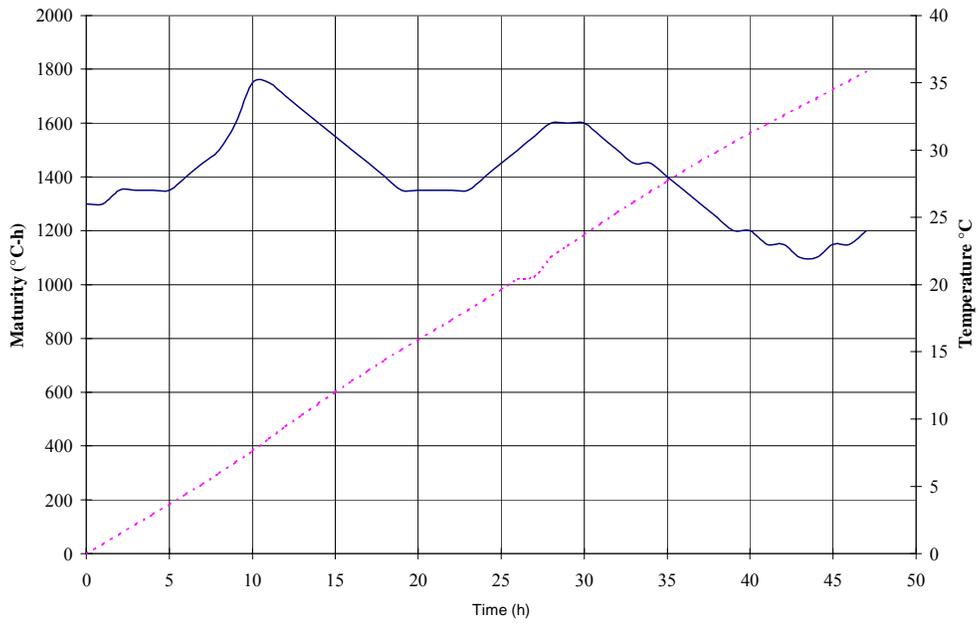
Figure 87. Slab temperature and maturity at channel no. 4.
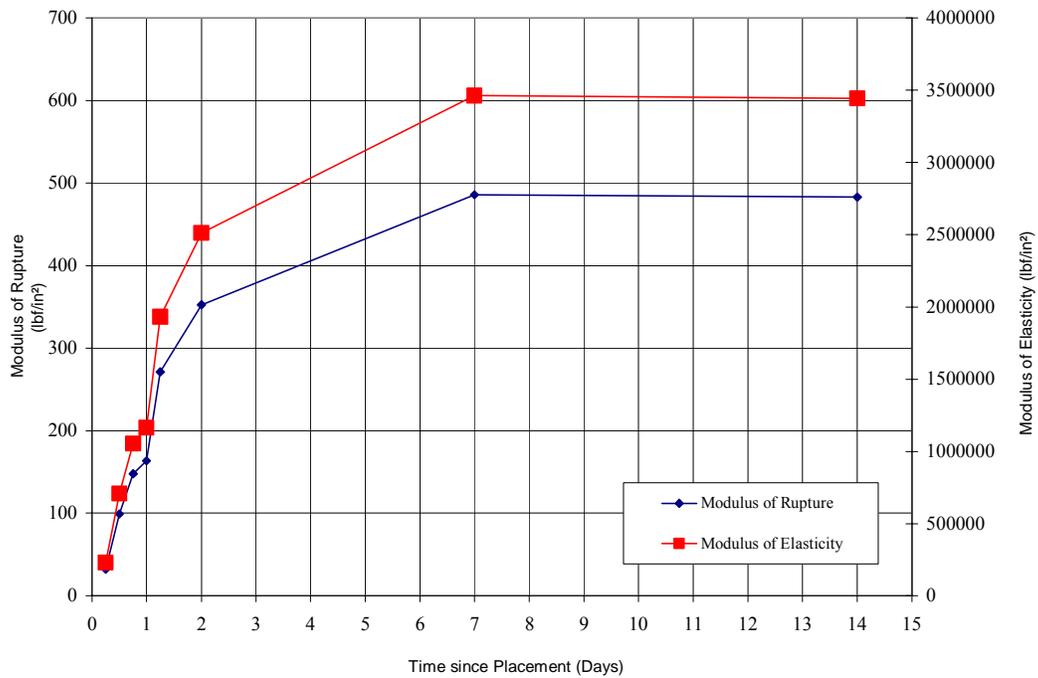
Figure 88. Measured moduli of rupture and elasticity for membrane-cured section.

153
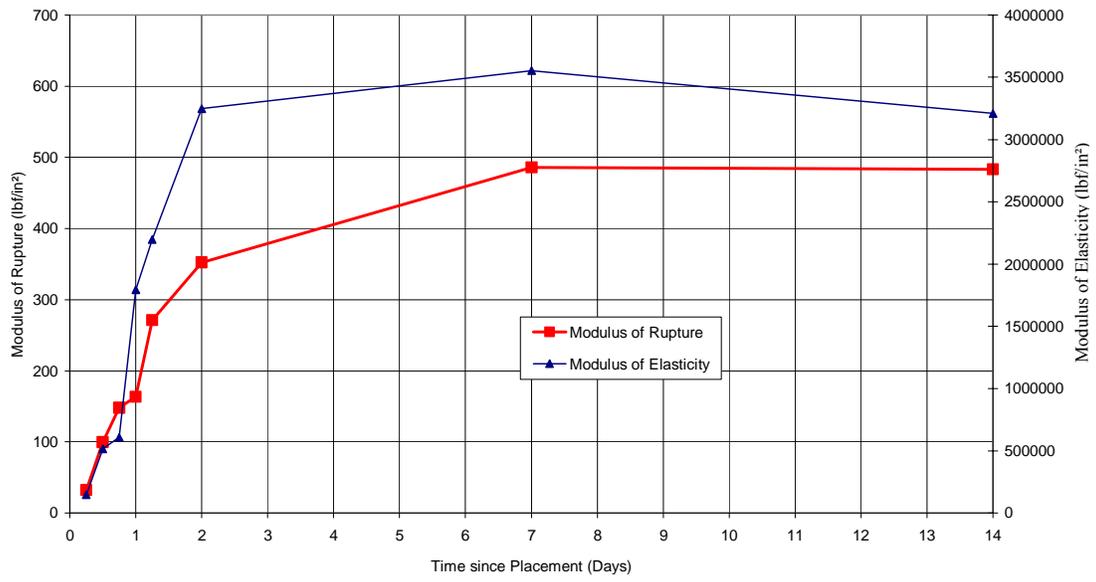
Figure 89. Measured moduli of rupture and elasticity for polyethylene-cured section.
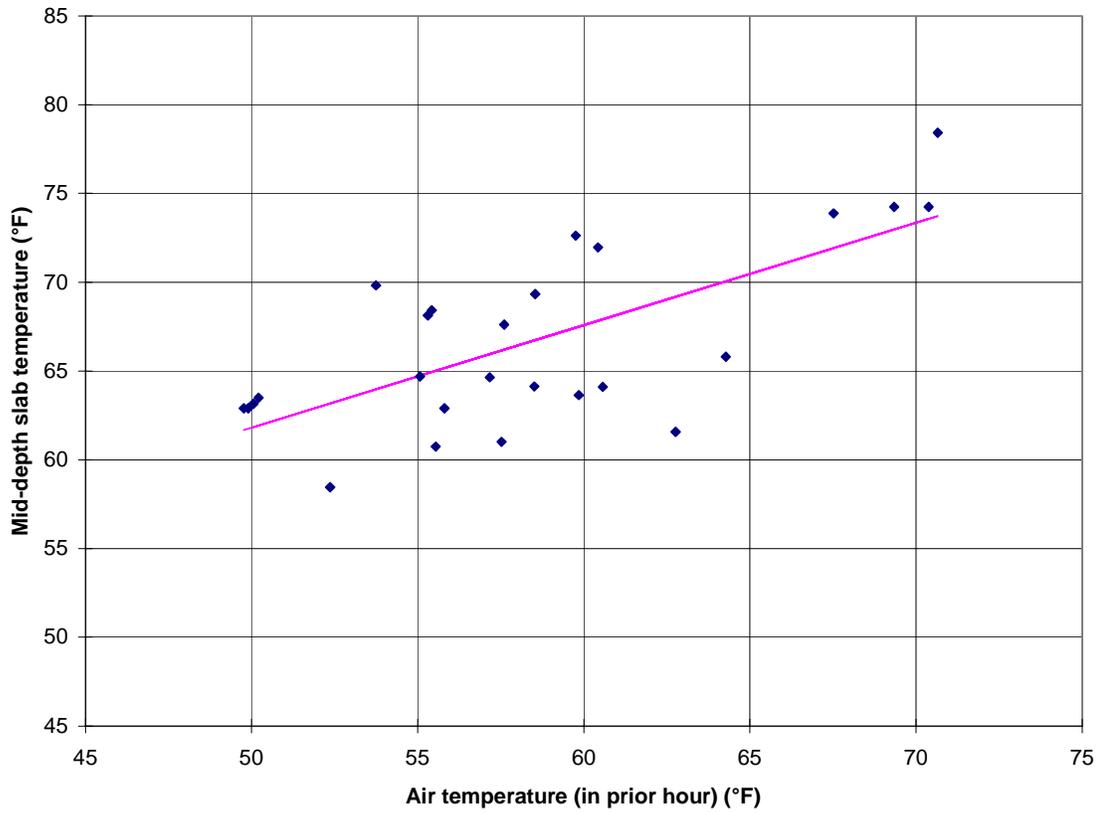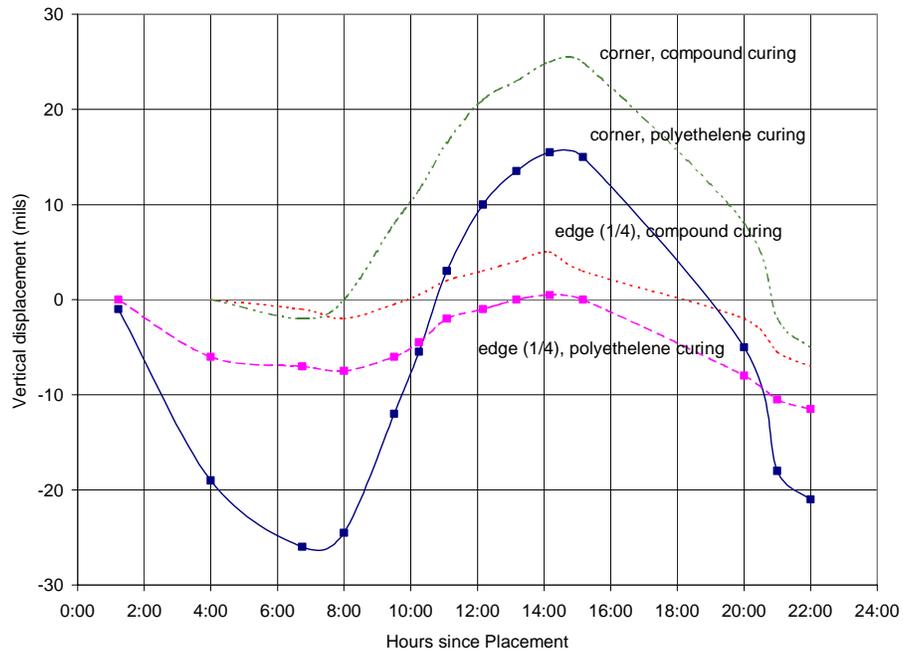
Figure 91. Vertical displacement, corner and edge.

Tables 20 and 21. Mix design and cement properties specifications.

Mix Design, Tepeaca	
Material	**Weight or Volume**
Cement	641 lb (291 kg)
Gravel, 1 1/2"	756 lb (343 kg)
Gravel, 3/4"	756 lb (343 kg)
Sand	1239 lb (562 kg)
Water	260 lb (118 kg)
A/E Agent	4.6 oz-US (0.131 kg)
Water Reducer	15.3 oz-US (0.436 kg)
Water-Cement Ratio	0.41
Concrete Unit Weight	135.4 pcf (2166 kg/m3)
Total Yield	**27.00 cf (0.765 m3)**

Cement Properties, Tepeaca	
Property (see eq. 5 - chap. 4)	**Value**
Φ (kJ/mol)	35.956
λ_1	0.69
t_1	21
κ_1	1.39
Hu (J/g)	468.3

C.3   Waller County, Texas

The test sections in Hempstead, Texas were placed from May 30 through June 15, 1995. These sections employed continuously reinforced concrete pavement with an 28 cm (11 in) thickness. The mix designs varied in the type of coarse aggregate used: siliceous river gravel, crushed limestone, and a blend of both. The pavement sections included #5 reinforcing longitudinal steel, and #6 reinforcing transverse steel. Transverse and longitudinal rebar was placed at mid-depth of the pavement. Longitudinal rebar was spaced at 20 cm (8 in), and transverse rebar was spaced at 0.9 m (3 ft) on center. One percent steel was used in the test sections. Figures 92 and 93 are plots of the data collected from the investigation and tables 22 and 23 describe one of the mix designs used (using 100% limestone coarse aggregate). Standard liquid membrane curing was used.
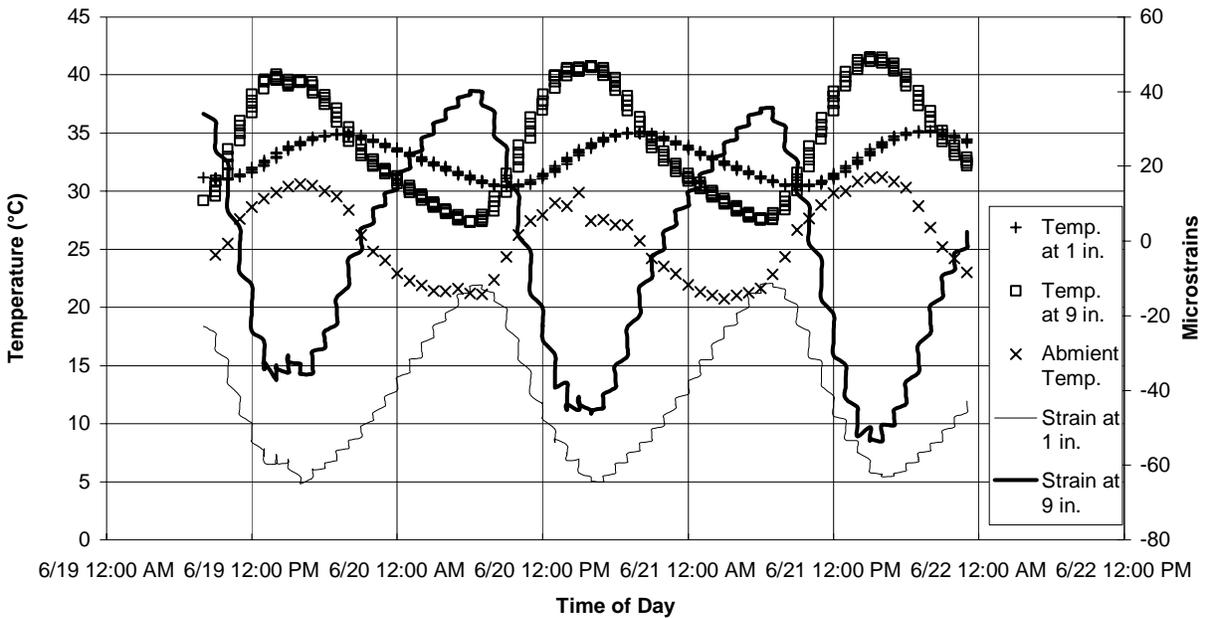
Figure 92. Roctest strain gauge readings at early age.
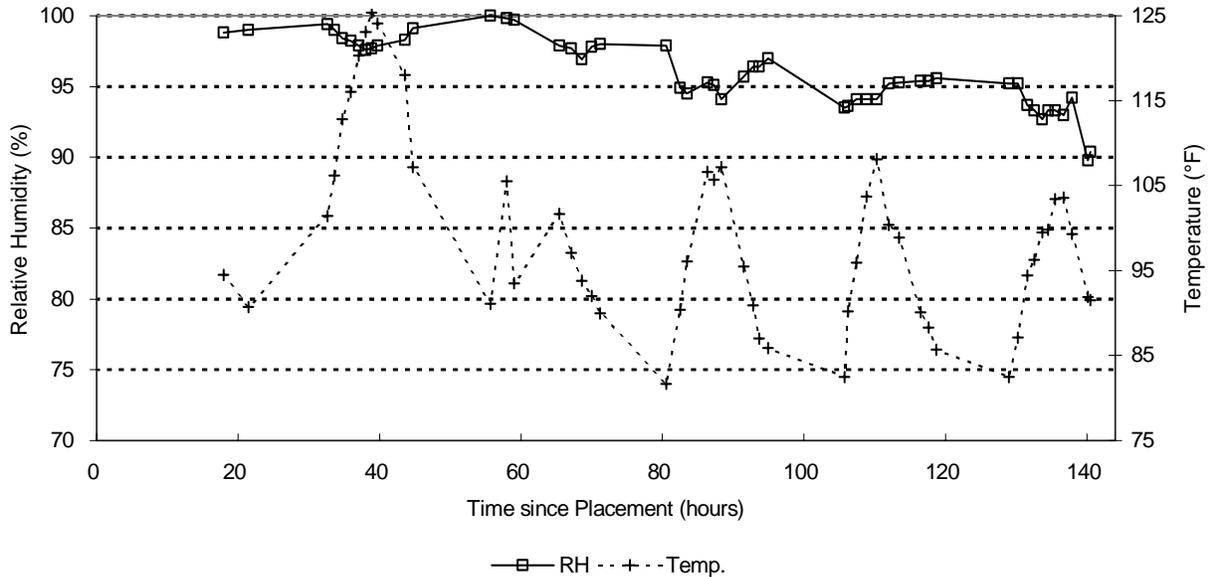
Figure 93. Relative humidity in concrete at mid-depth.

Tables 22 and 23. Mix design and cement properties specifications.

Mix Design, Hempstead	
Material	**Weight or Volume**
Cement, Type I	423 lb (192 kg)
Fly Ash, Type C	115 lb (52 kg)
Crushed Limestone	1153 lb (523 kg)
Siliceous Sand (Intermediate Aggregate)	673 lb (305 kg)
Siliceous Sand, (Fine Aggregate)	1289 lb (585 kg)
Water	227 lb (103 kg)
Total Air	5.0 percent
Water-Cement Ratio	0.42
Slump	2.0 in (50.8 mm)
Concrete Unit Weight	143.6 pcf (2301 kg/m3)
Total Yield	**27.00 cf (0.765 m3)**

Cement Properties, Hempstead	
Property	**Value**
AE (kJ/mol)	47.755
λ_1	1.65
t_1	13
κ_1	1.21
Hu (J/g)	483

C.4   Brazos County, Texas

The test sections at the Texas A&M University Riverside "Annex" Campus were paved August 16, 1996 at approximately 1:00 pm. Each of the two slabs was 3 m by 3.8 m (10 ft by 12 ft by 5 in). These non-trafficked sections were used to investigate the effects of thermal shock on several properties. Both slabs were paved simultaneously, then cured. Membrane curing was applied to both slabs. One slab, to be thermal shocked, was additionally covered with both clear poly sheeting and cotton mats. This section was kept insulated until the concrete reached a calculated flexural strength of approximately 2,760 ksi (400 lbf/in^2). This strength was reached at approximately 1:00 am on the morning of August 17, 1996. As the temperature and vertical deflection charts confirm, the effect of insulation removal was significant. Although significant differences in the temperature profiles are not evident, the measured vertical deflections show significant differences.

The properties measured throughout the survey included concrete temperature, maturity, concrete moisture (relative humidity), vertical deflection, compressive strength, and strain. Figure 94 below illustrates the layout of the instrumentation. Figures 95 through 107 are plots of measurements taken from the various instruments on this test section during Summer of 1995.
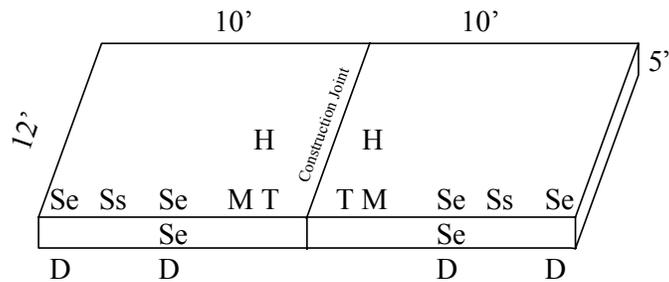
Figure 94. Schematic of instrumentation at TTI annex site.

Where,

Se: embedded strain gauge   H: moisture sensor installation
Ss: surface-mounted strain gauge   M: maturity meter
D: vertical deflection gauge assembly T: temperature meter
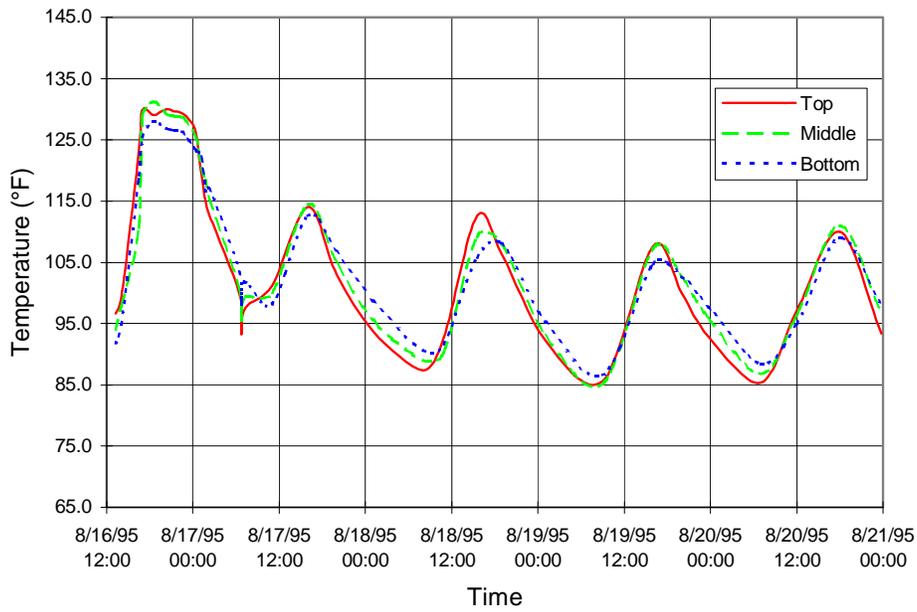
Figure 95. Temperature in concrete slab subjected to thermal shock.
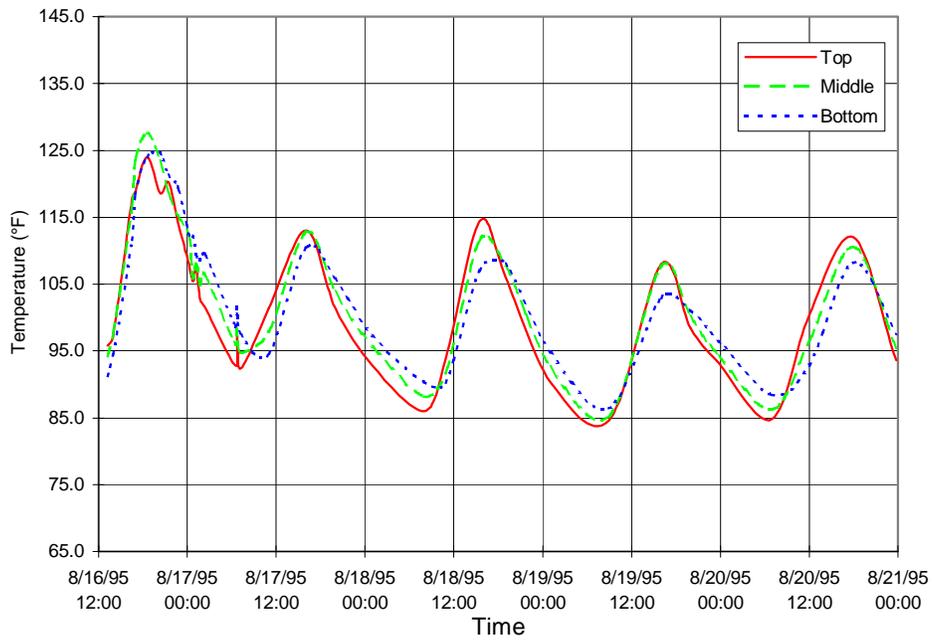
Figure 96. Temperature in concrete slab not subjected to thermal shock.
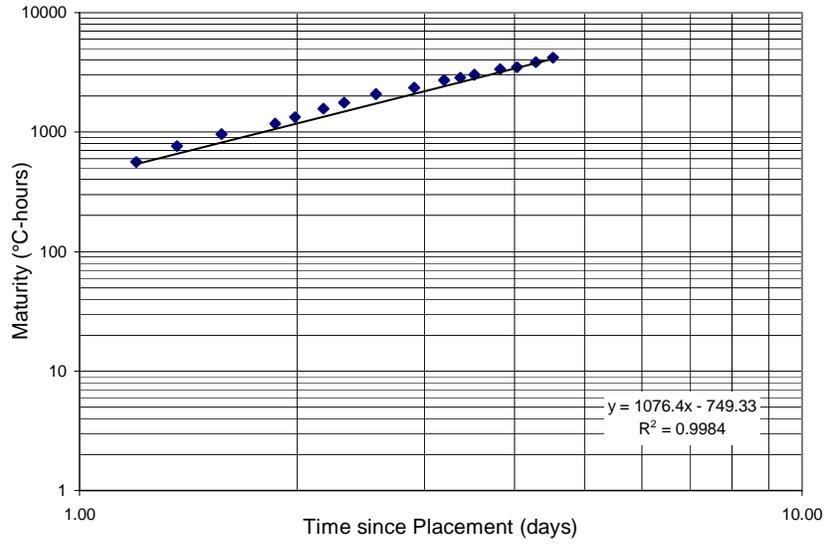
Figure 97. Maturity of shocked slab.
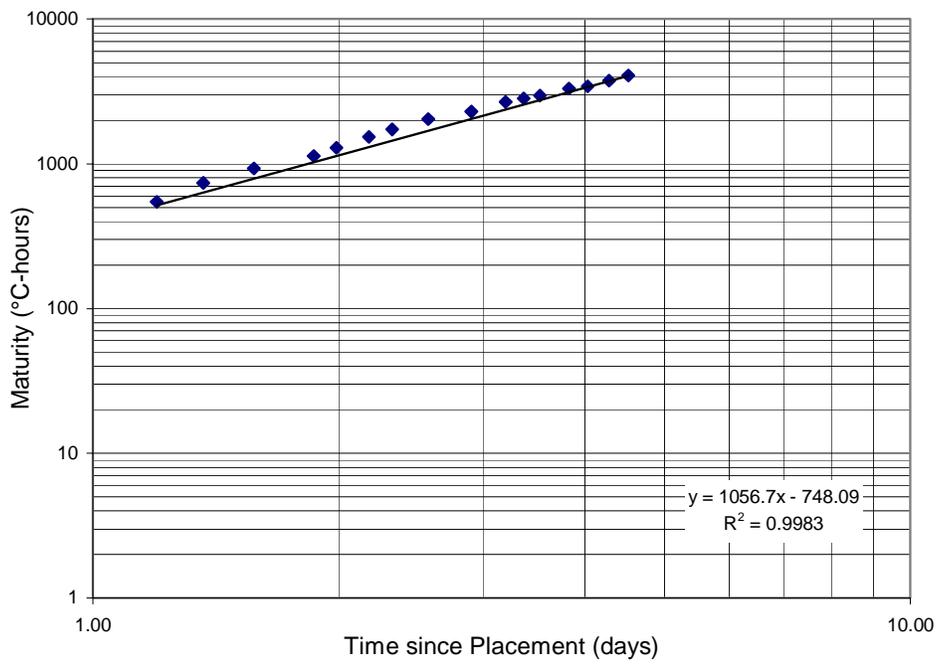
Figure 98. Maturity of unshocked slab.

160
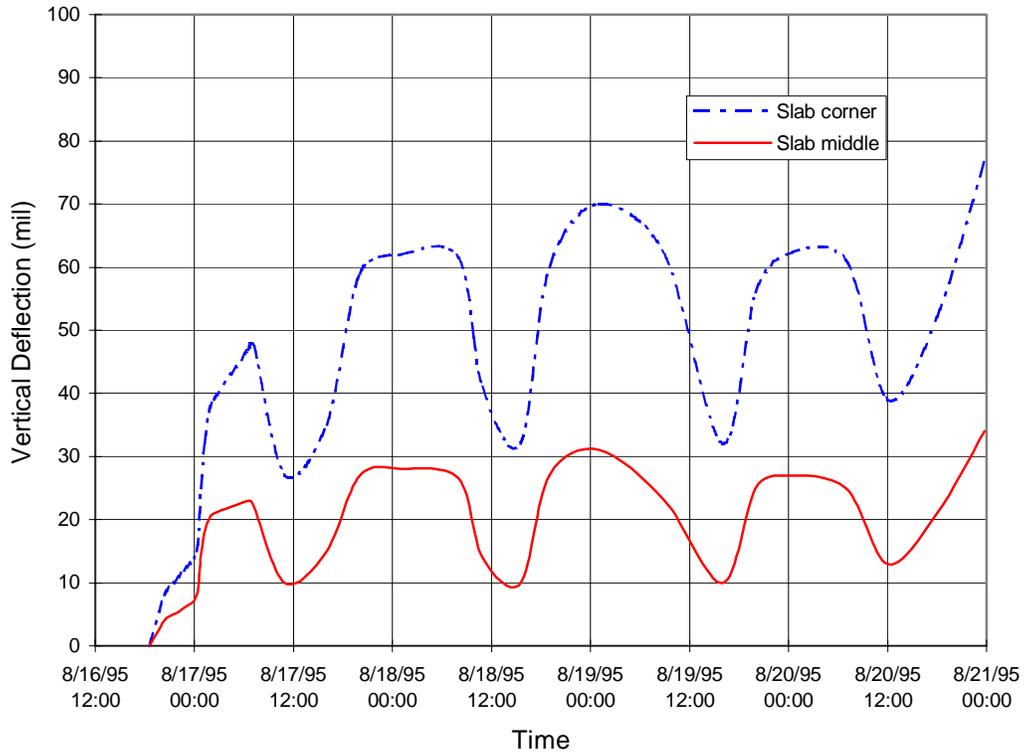
Figure 99. Vertical deflection in concrete slab subjected to thermal shock.
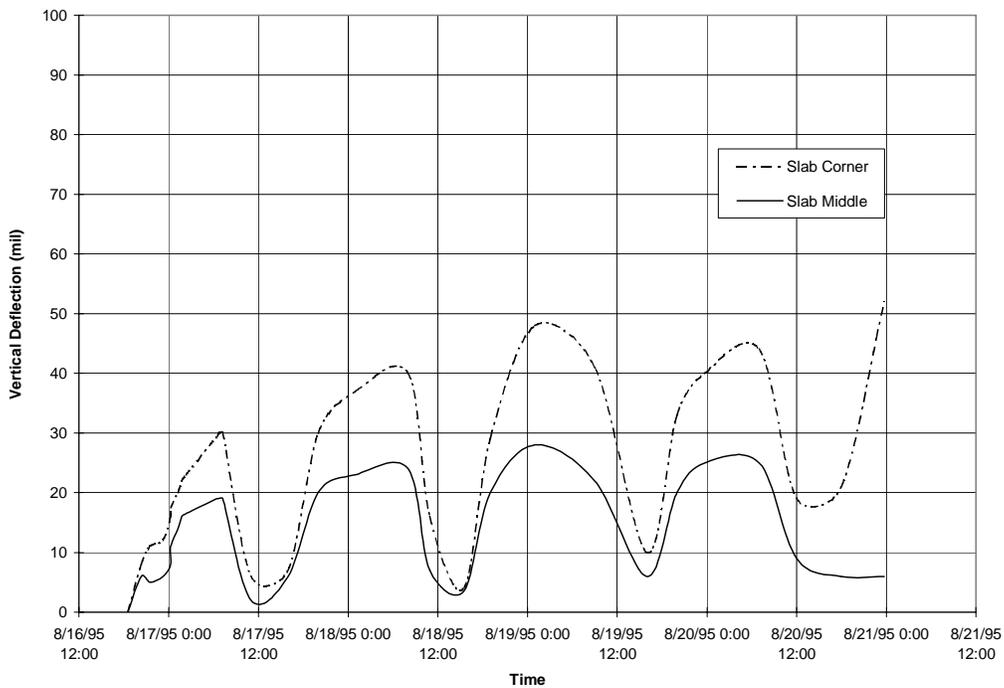
Figure 100. Vertical deflection in concrete slab not subjected to thermal shock.

161
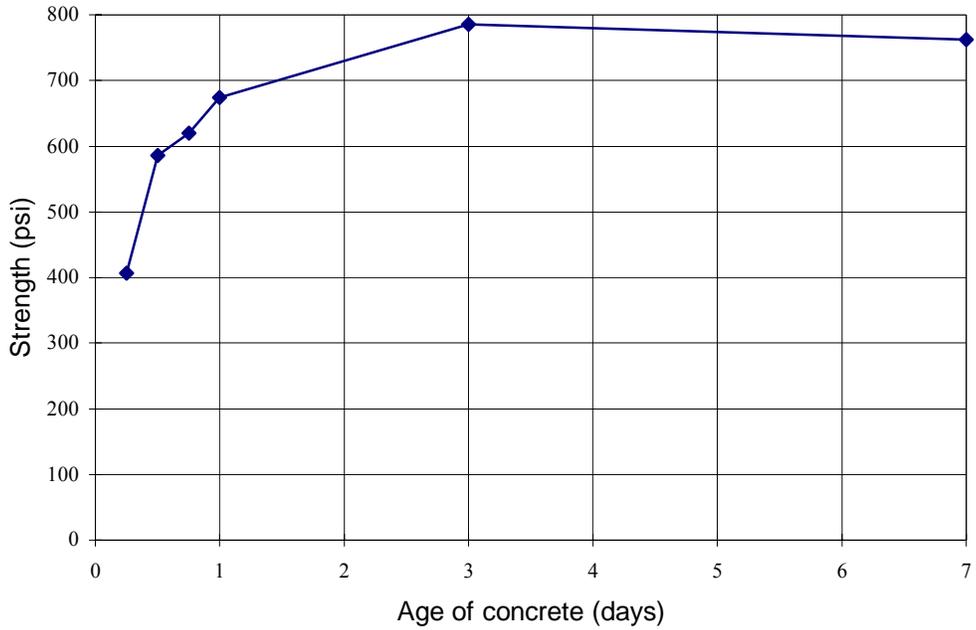
Figure 101. Flexural strength development of test specimens.
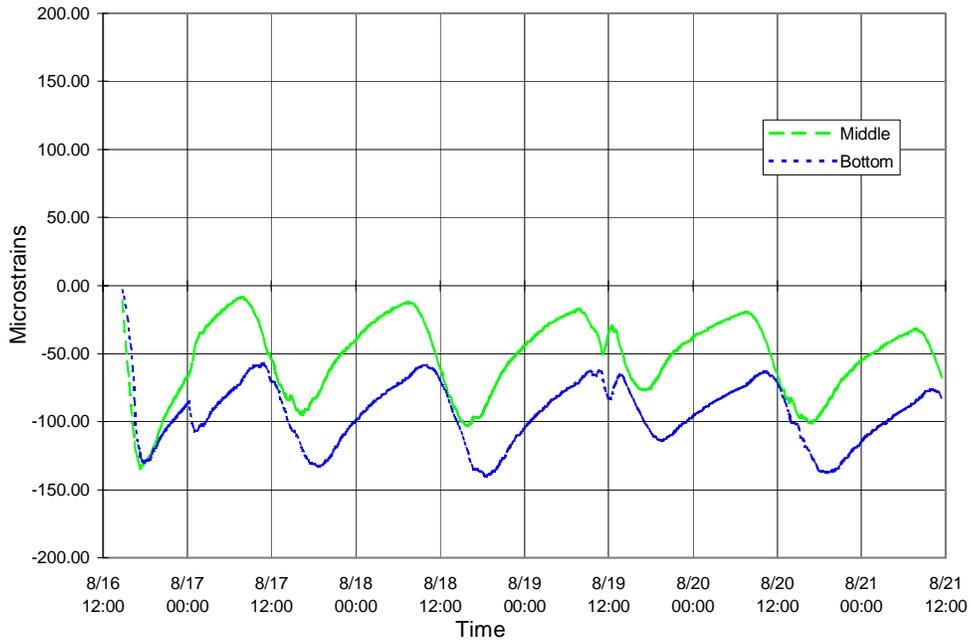
Figure 102. Vibrating wire strain gauge readings in thermal shock section.
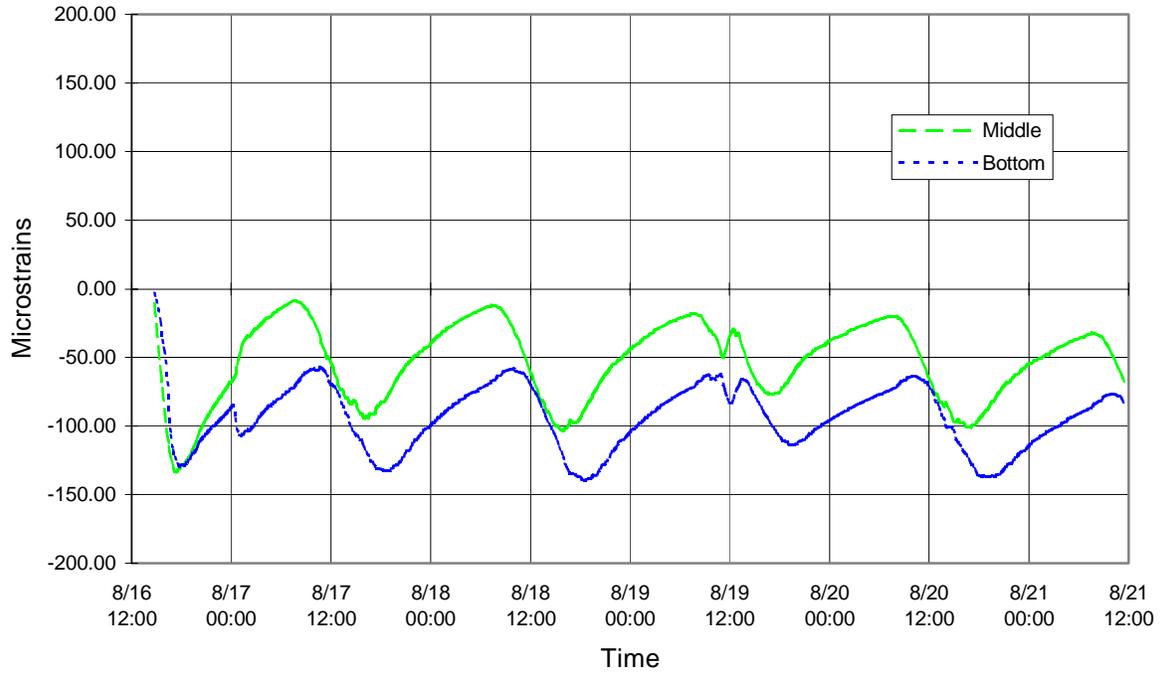
Figure 103. Vibrating wire strain gauge readings in non-shocked slab.
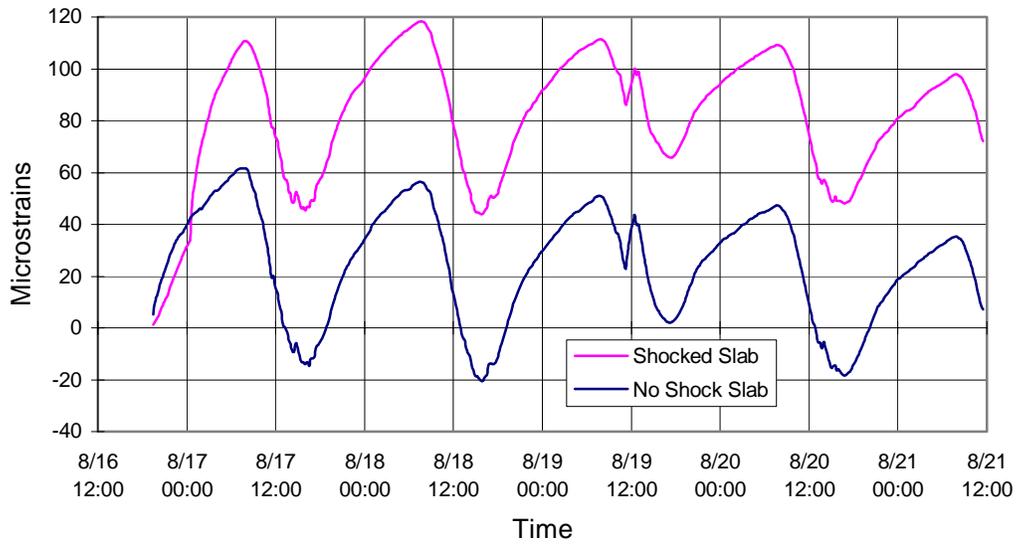
Figure 104. Vibrating wire strain gauge readings in half-cylinders.

163
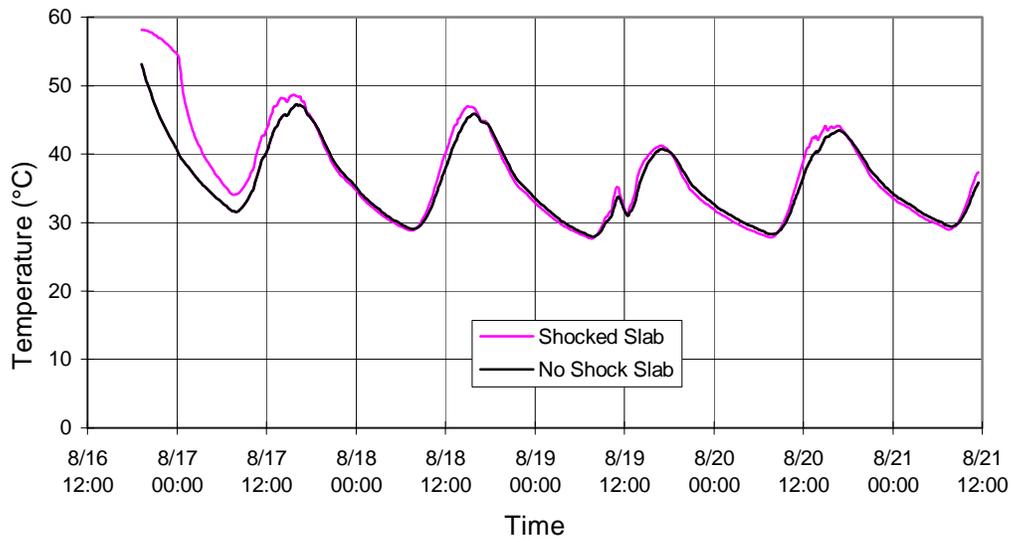
Figure 105. Vibrating wire strain gauges in half-cylinders.
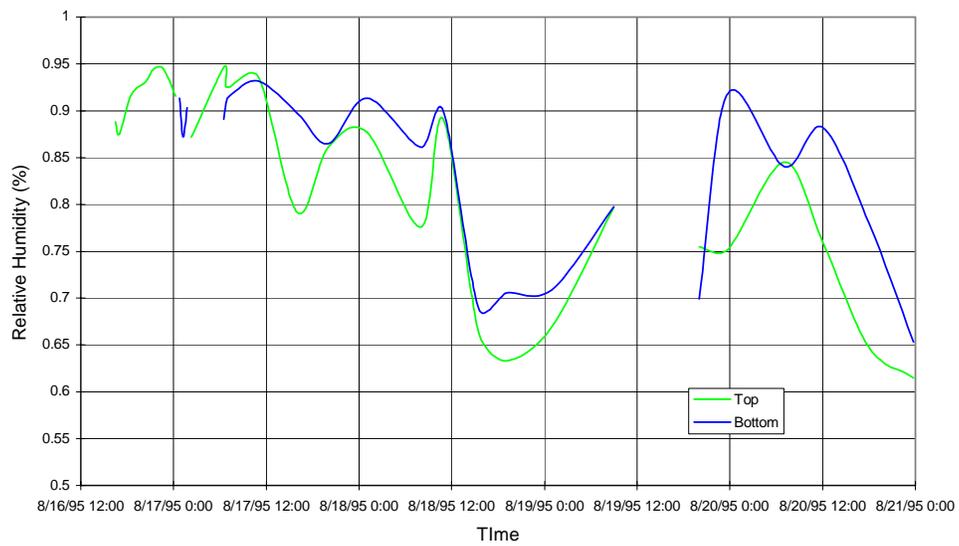
Figure 106. Moisture gauge readings at two depths in shocked slab.

164
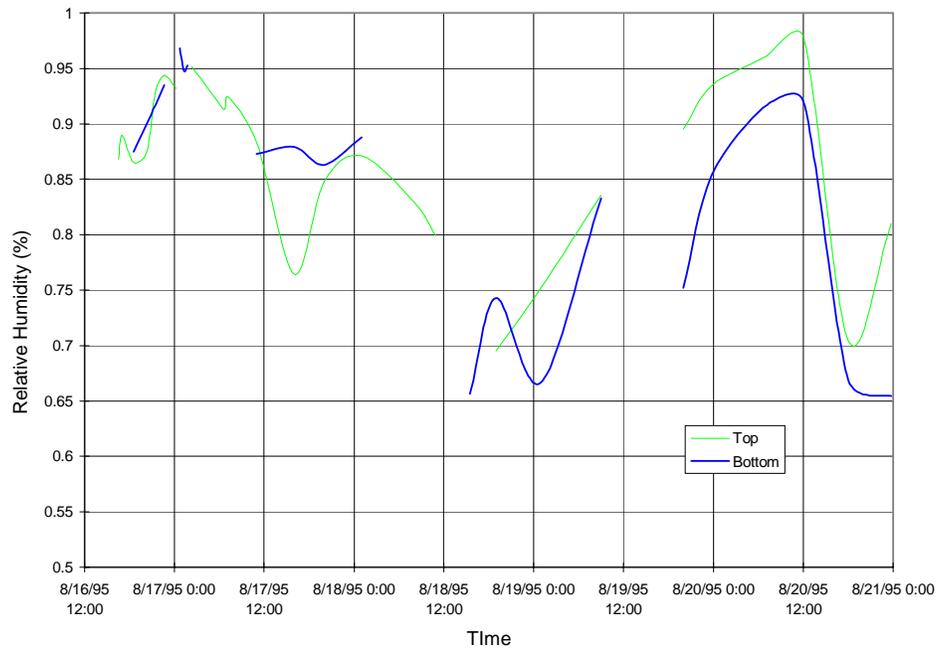
Figure 107. Moisture gauge readings at two depths in non-shocked slab.

APPENDIX D
TEST SECTIONS OF BONDED CONCRETE OVERLAY CONSTRUCTION OPERATIONS

This appendix discusses the methods of test site administration, instrumentation, and data collection for studying the behavior of bonded concrete overlays. Presented below are the test sites used for the calibration and validation efforts of this project. This appendix addresses these issues and presents the results of the data collection activities.

D.1   Franklin County, Iowa

The initial field experimentation was performed on an Iowa project on State Highway 3, about 1.0 mi west of Interstate 35 in Franklin County, Iowa. This location included several interesting construction implications that may be factors in the performance responses to date. The test site included two sections. This first section was originally constructed in 1963 as part of a relocation of Iowa State Highway 3 and the construction of the I-35 interchange. The pavement was built on a clay subgrade with no special drainage layers or longitudinal subdrains. This resulted in some pavement faulting and joint deterioration over the life of the pavement (which was repaired prior overlay construction). The second test section was originally constructed in 1931, and was reconstructed in 1969. The total length of the project was 4,296 m (2.67 mi).

The project consisted of a fast-track, thin-bonded concrete overlay. The design thickness of the thin-bonded overlay was 7.62 cm (3 in), and the total pavement width was 7.3 m (24 ft). The new overlay was placed directly over the existing 20 cm (8 in) jointed plain concrete pavement (JPCP). Joints in the new overlay were sawed full depth directly over the joints in the existing JPCP. As a result, all load transfer across the transverse joints was provided by the existing JPCP and none was provided by the new overlay. This project provided vital information and data for the investigative portions of Task C.

This project was constructed under a fast track paving schedule. In order to achieve release strengths in as little as 6 h, a Type III high early strength cement was used as well as insulated curing blankets. In order to accurately monitor the buildup of concrete strength over time, a sophisticated system of non-destructive testing techniques was used. This included pulse velocity tests at 61 m (200 ft) intervals, and maturity meters placed at 152 m (500 ft) intervals.

Three sites were selected for instrumentation on the project to measure pavement temperatures, longitudinal, transverse, and vertical strains, and bond development. The first of the two sections provided opportunity for the study of three types of bonding procedures: the use of Type II grout, Type III grout, and no grout. The mix design used (tables 24 and 25) and the results of the tests conducted at the test sites are included below (figures 108 through 117).
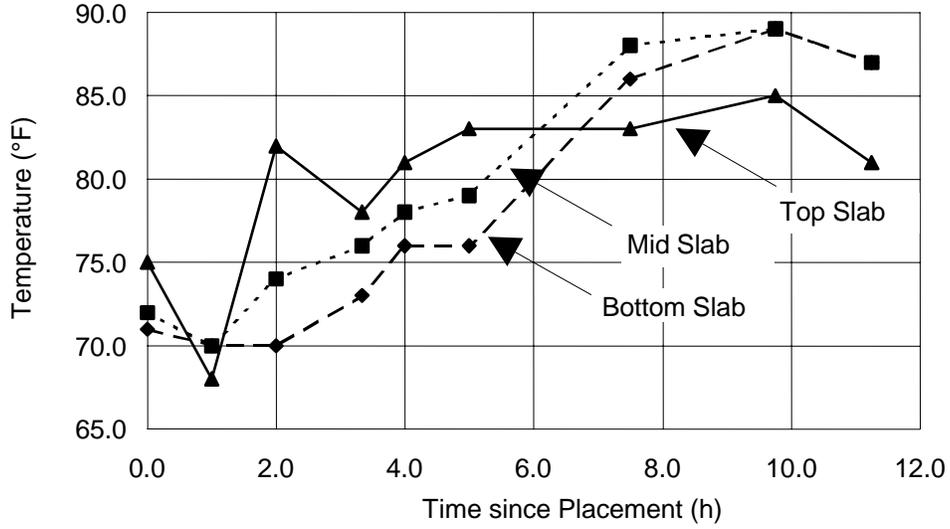
Figure 108. Slab temperatures in section using type II grout and clear polyethylene sheeting.
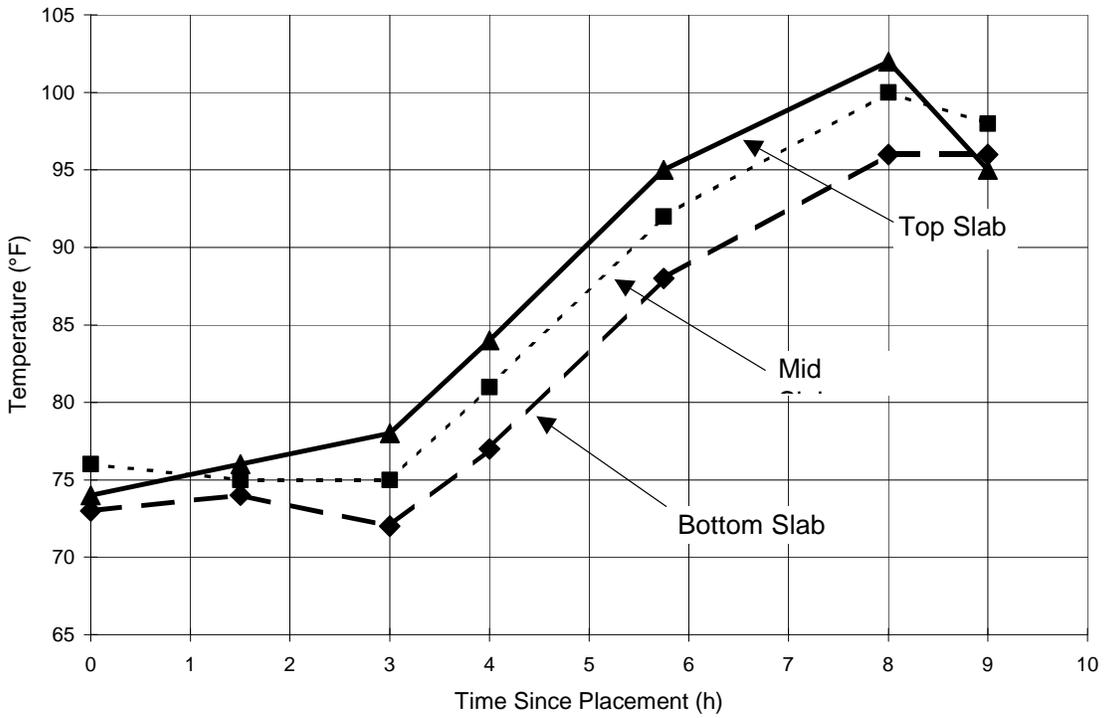

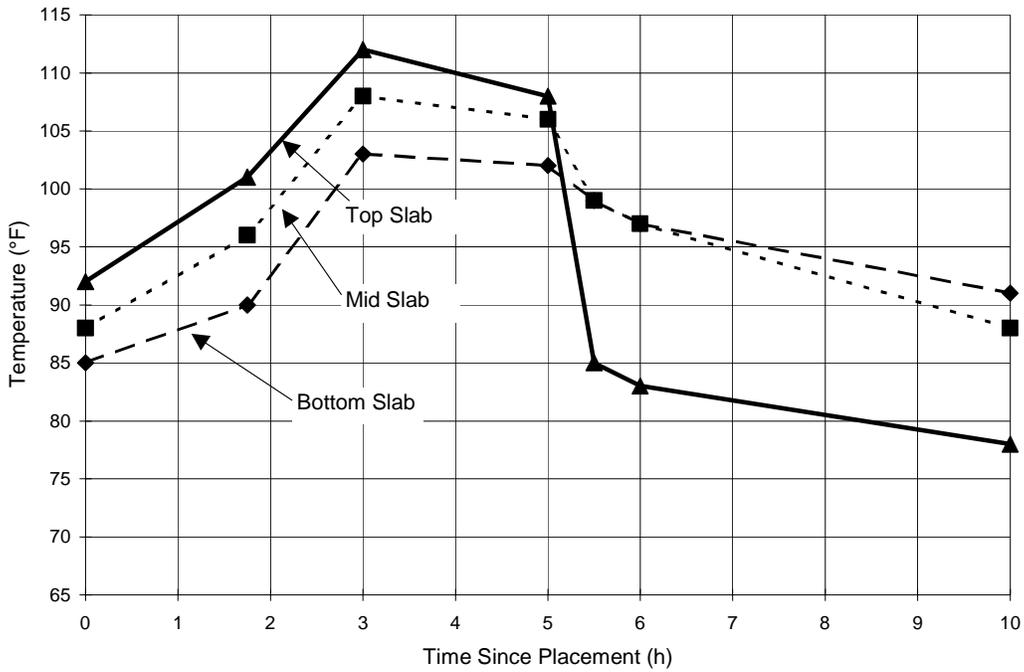*Figure 109. Slab temperatures in section using type II grout and white insulated curing blanket.*

168

Figure 110. Slab temperatures in section using type II grout and black insulated curing blanket.
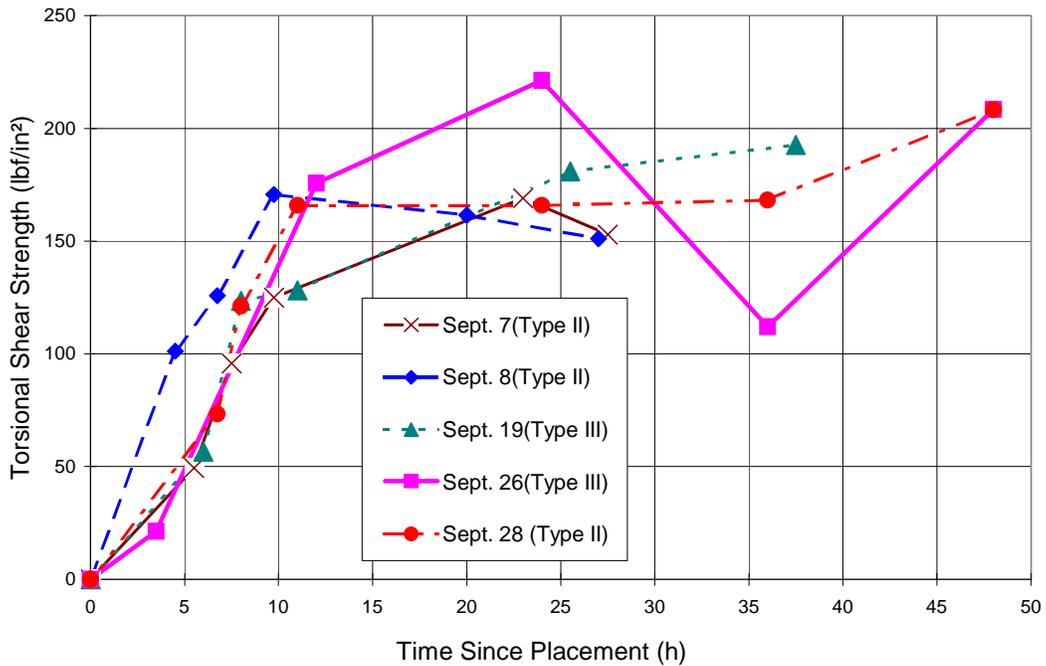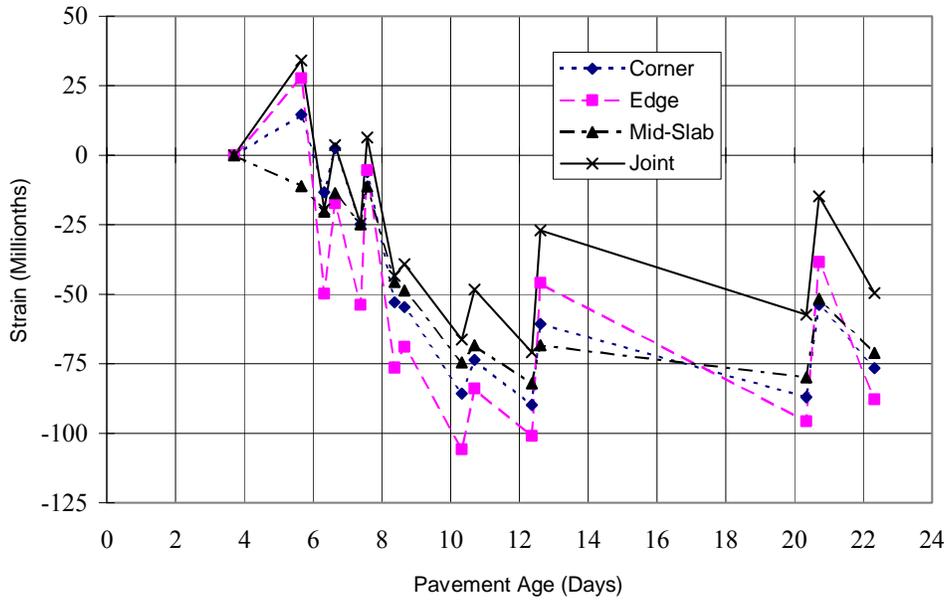
Figure 112. Total horizontal strain at station 661+25.
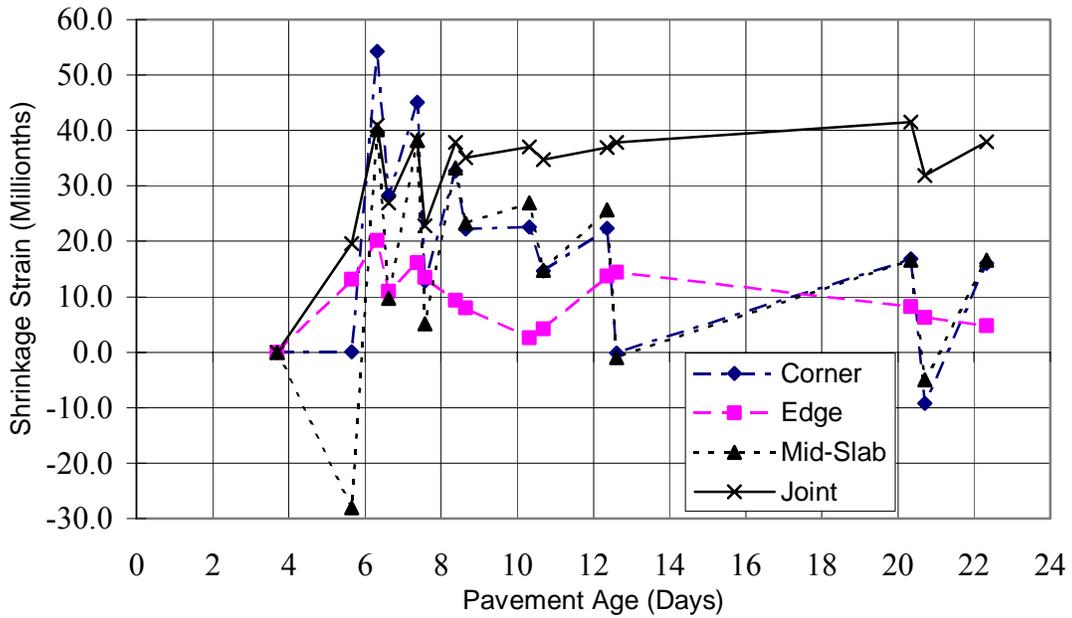
Figure 113. Shrinkage strain at station 661+25.
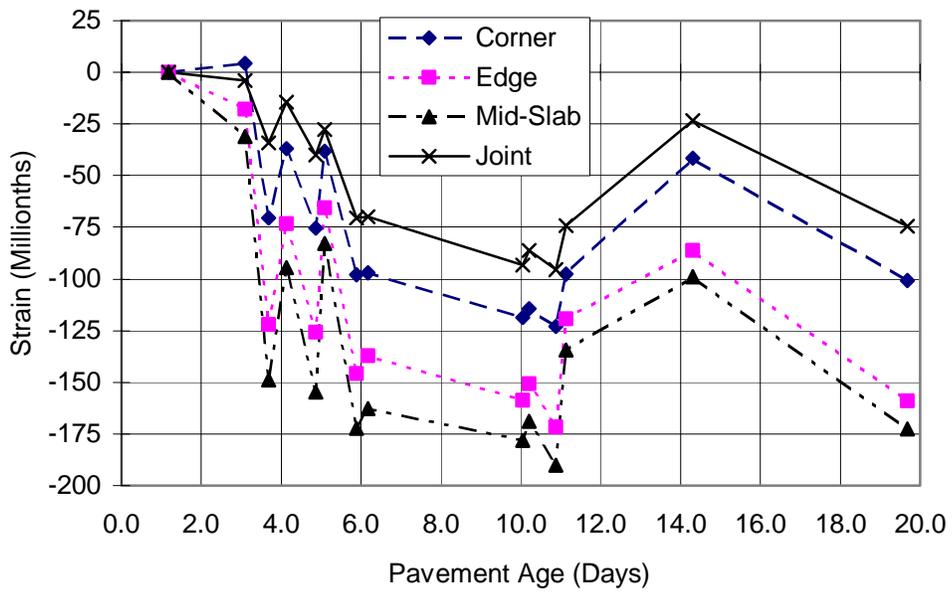
170
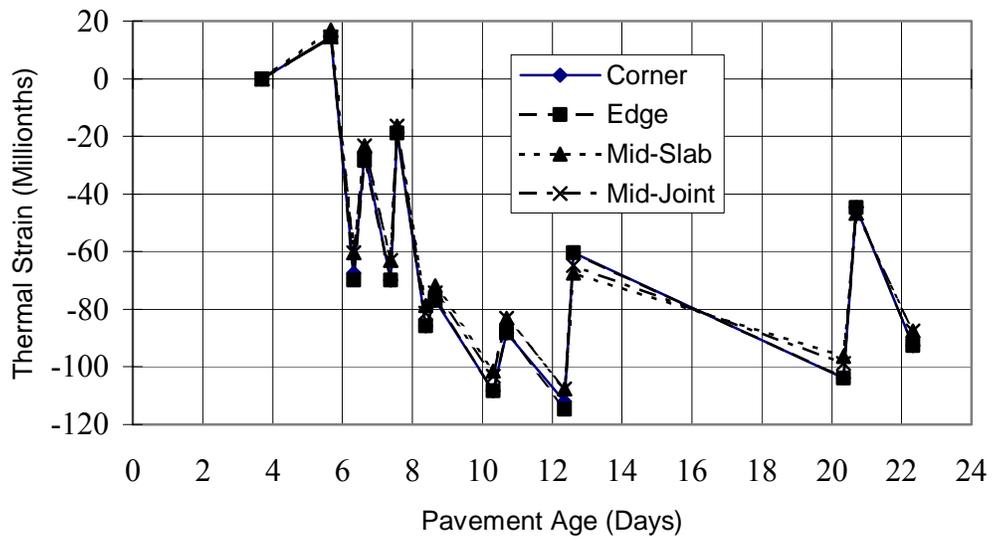
Figure 114. Thermal strain at station 661+25.

Figure 115. Total horizontal strain at station 701+50.
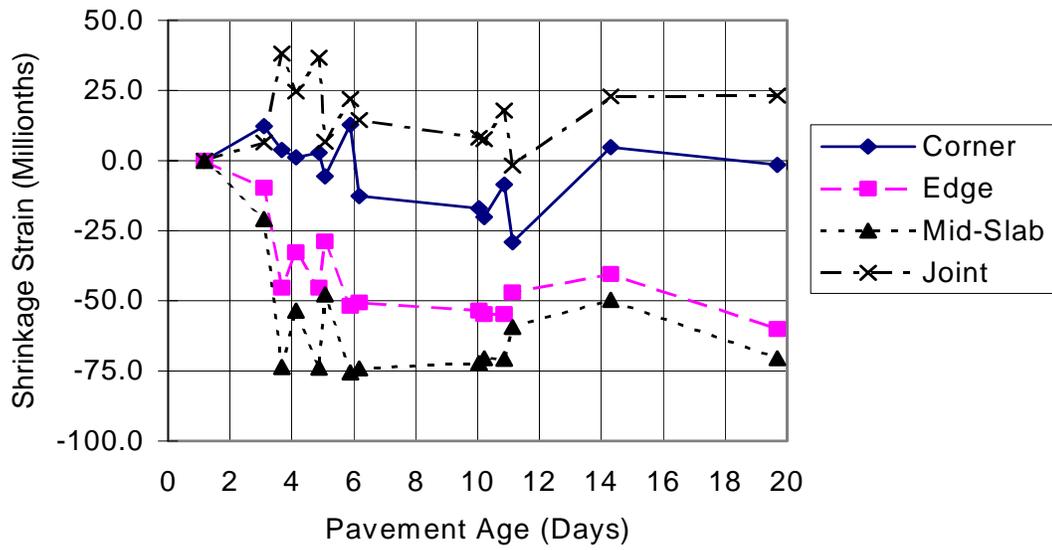
Figure 116. Shrinkage strain at station 701+50.
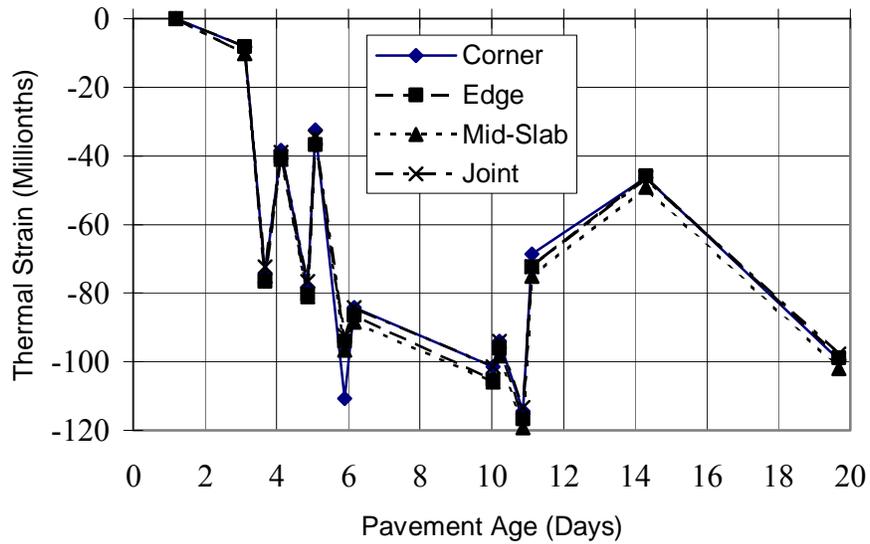
Figure 117. Thermal strain at station 701+50.

172

Tables 24. and 25. Mix design and cement properties specifications.

Mix Design, Iowa	
Material	**Weight or Volume**
Lehigh Cement, Type III	737 lb (334 kg)
Deal #4 Fly Ash	79.4lb (34 kg)
Alden Crushed Limestone	1282 lb (582 kg)
Anderson Sand	1322 lb (600 kg)
Water	330 lb (150 kg)
A/E Agent	0.87 oz-US (0.025 kg)
Water Reducer, WRDA 82	1.15 oz-US (0.033 kg)
Water-Cement Materials Ratio	0.4
Concrete Unit Weight	138.9 pcf (2222 kg/m3)
Total Yield	**27.00 cf (0.765 m3)**

Cement Properties, Iowa	
Property	**Value**
AE (kJ/mol)	33.423
λ_1	1.77
t_1	8.7
κ_1	1.83
Hu (J/g)	-

D.2   El Paso County, Texas

Several different designs for overlay test sections were constructed on an aggregate plant haul road in El Paso, Texas on June 22 1995. On May 1 1995, a continuously reinforced concrete pavement base slab 137.2 m (450 ft) in length had been constructed to simulate the existing condition of IH-10. The pavement was 203 mm (8 in) thick and 3.66 m (12 ft) wide. The original mix design was duplicated as closely as possible with the available cement and aggregates. During base slab construction several different curing methods were tested, with the idea of using the most successful method for the overlay construction. However, the humidity was unseasonably high and the wind speed was low, so evaporation was not severe (0.73 to 1.22 kg/m^2/h, or 0.15 to 0.25 lb/ft^2/h). No difference between the alternatives could be observed. It was decided that a TxDOT approved white pigmented membrane-forming curing compound should be used.

Aggregate trucks were allowed to use the pavement over the next month. On June 13, sawcuts were made 5 cm (2 in) deep and 1.52 m (5 ft) apart in the base slab, to simulate the cracking on IH-10 that had been mapped under the TxDOT 1957 study (no existing cracks were present). Over the next two days the surface was prepared for the overlay, using two different methods (shotblasting and hydrocleaning, discussed below). On June 17 and 18 Hilti nails and anchor bolts (discussed below) were installed, and a concrete debonding agent used in precast construction was applied to one end and one edge of each test section to cause overlay delamination in selected areas. This was done to attempt to detect and map these delaminations using nondestructive methods, and investigate whether the delaminations spread under traffic loading. The overlay constructed at 6.5 in thick. The results of the tests conducted at the test site are presented in figures 118 through 128.
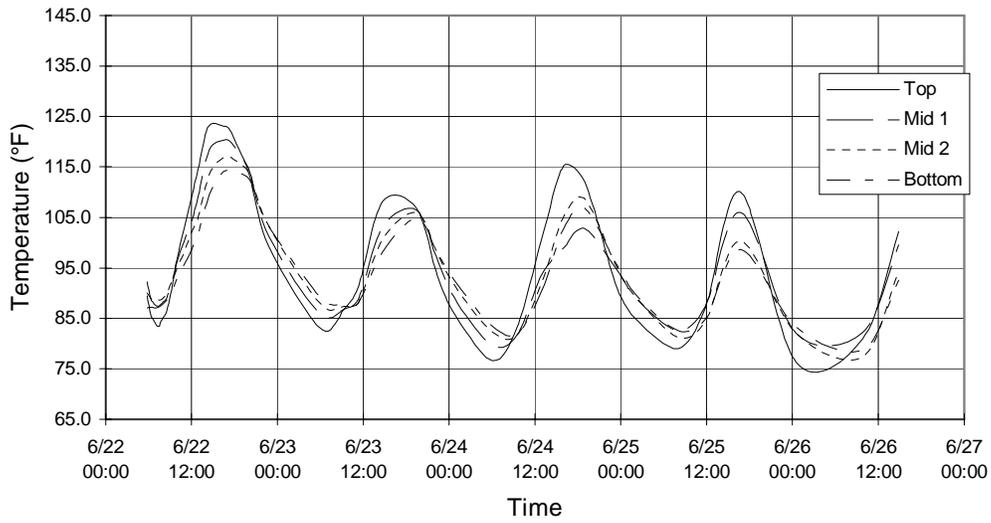
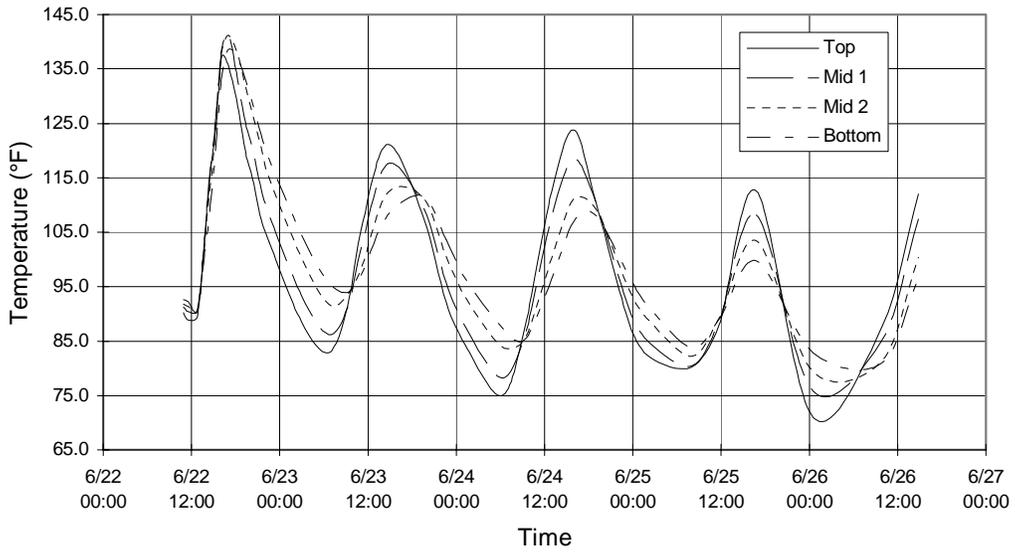*Figure 118. Slab temperature at four depths, thermocouple no. 1.*

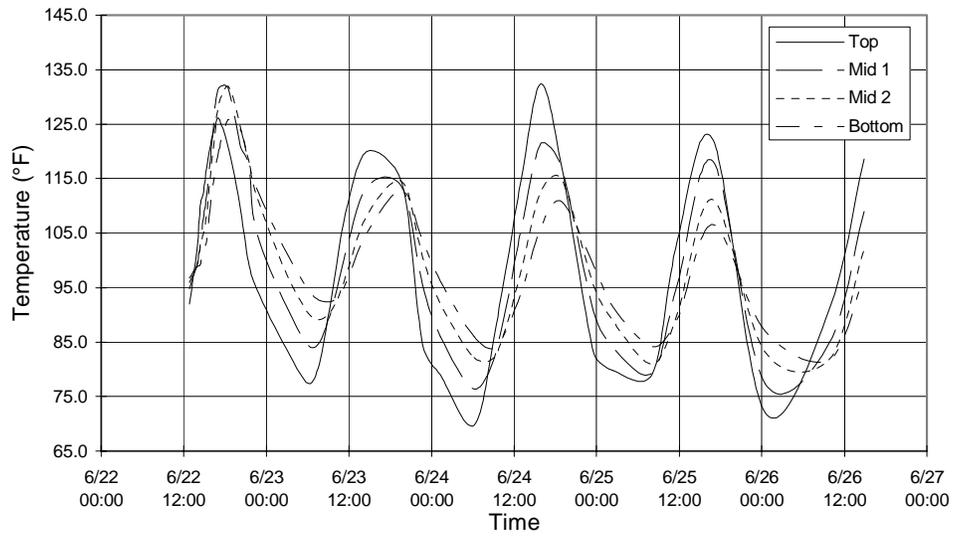*Figure 119. Slab temperature at four depths, thermocouple no. 2.*

174

Figure 120. Slab temperature at four depths, thermocouple no. 3.
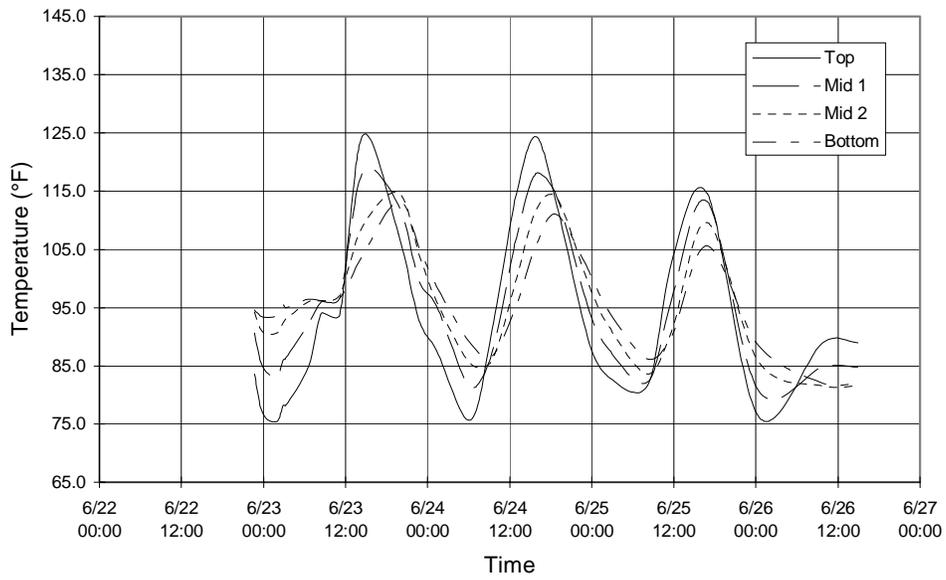

Figure 121. Slab temperature at four depths, thermocouple no. 4.
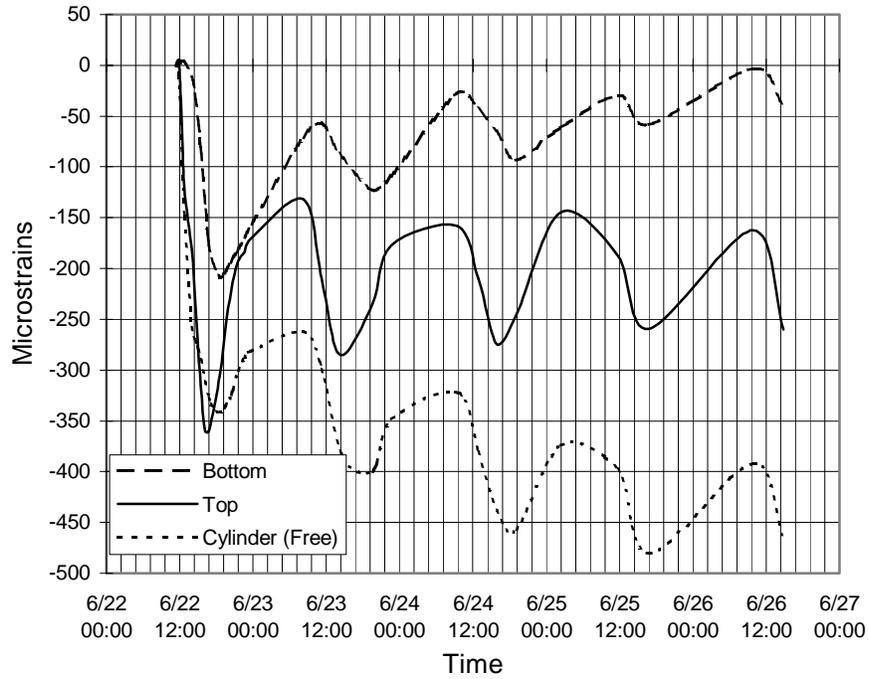
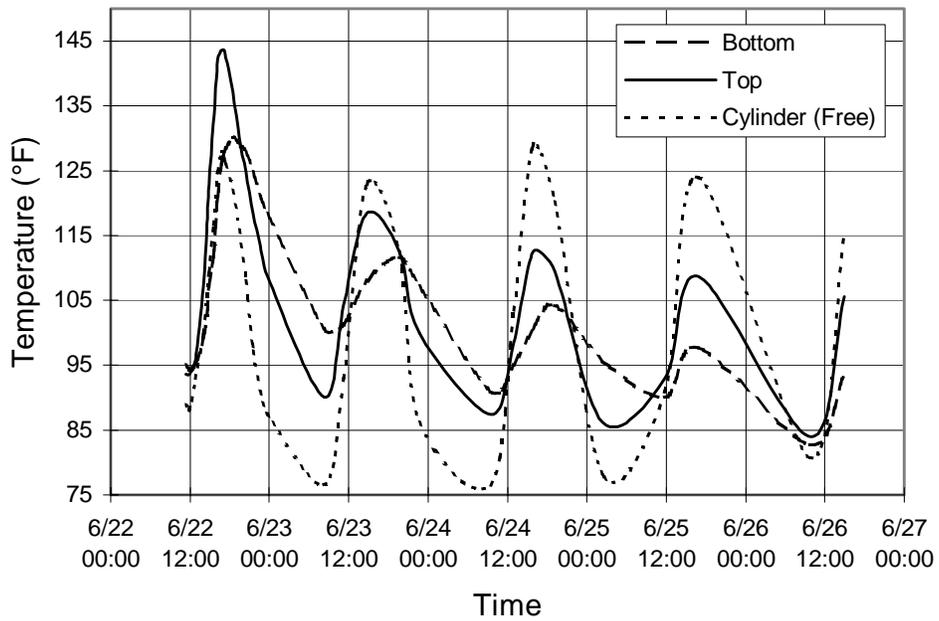175

Figure 122. Vibrating wire strain gauges in test slab.
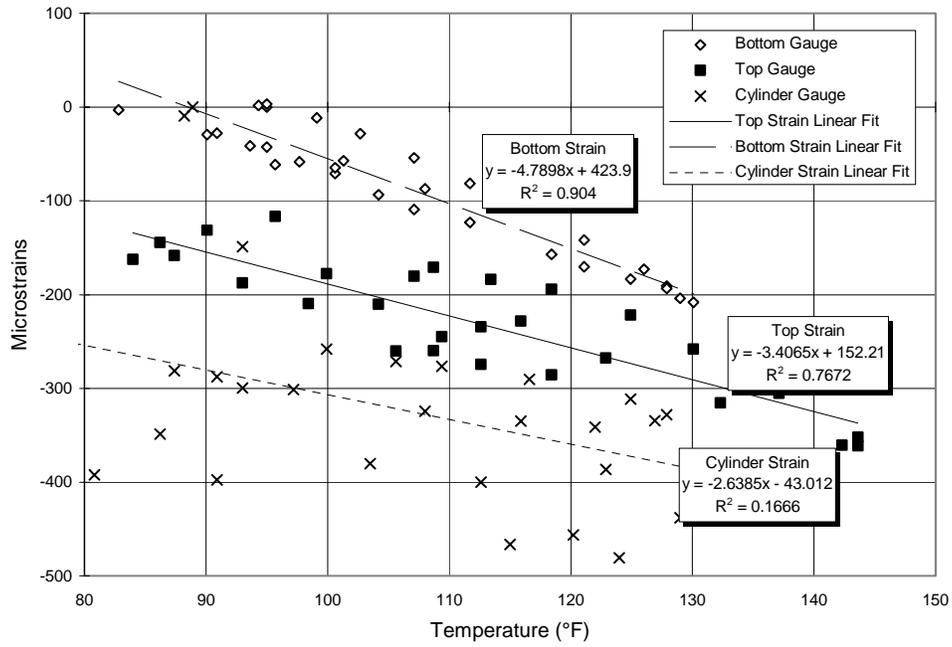

Figure 123. Vibrating wire strain gauges.

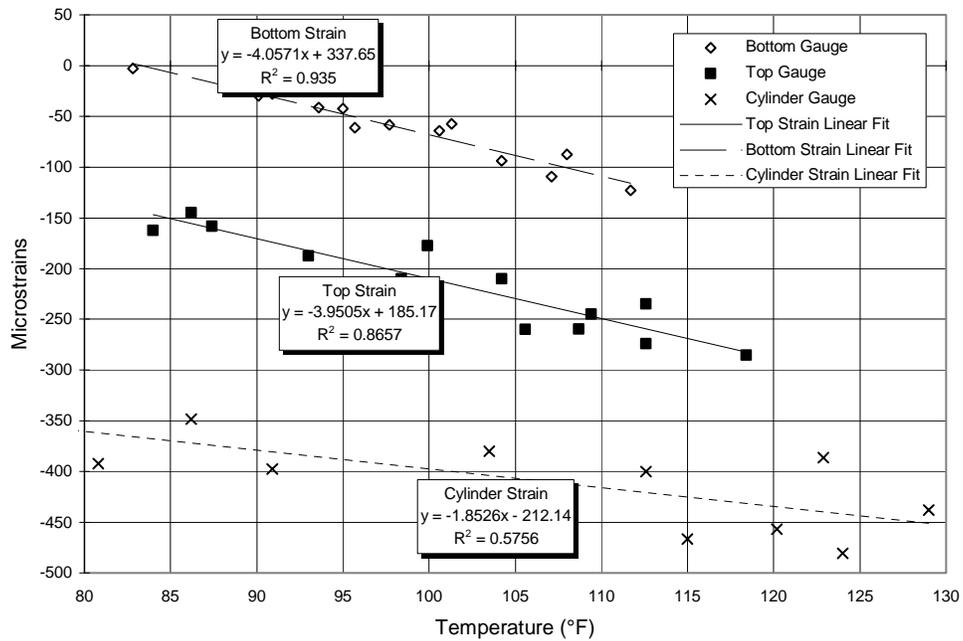*Figure 124. Strain versus temperature in first 24 h.*
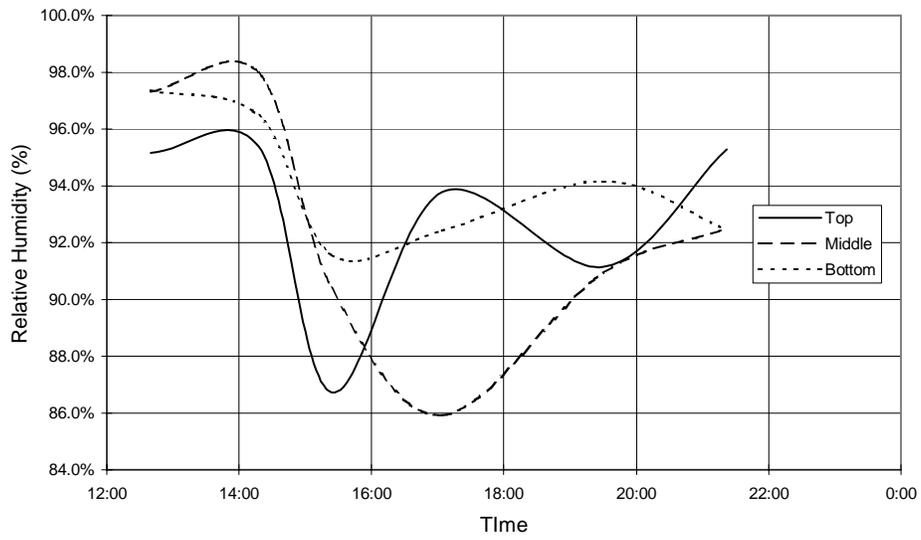

Figure 125. Strain versus temperature after 24 h.

177

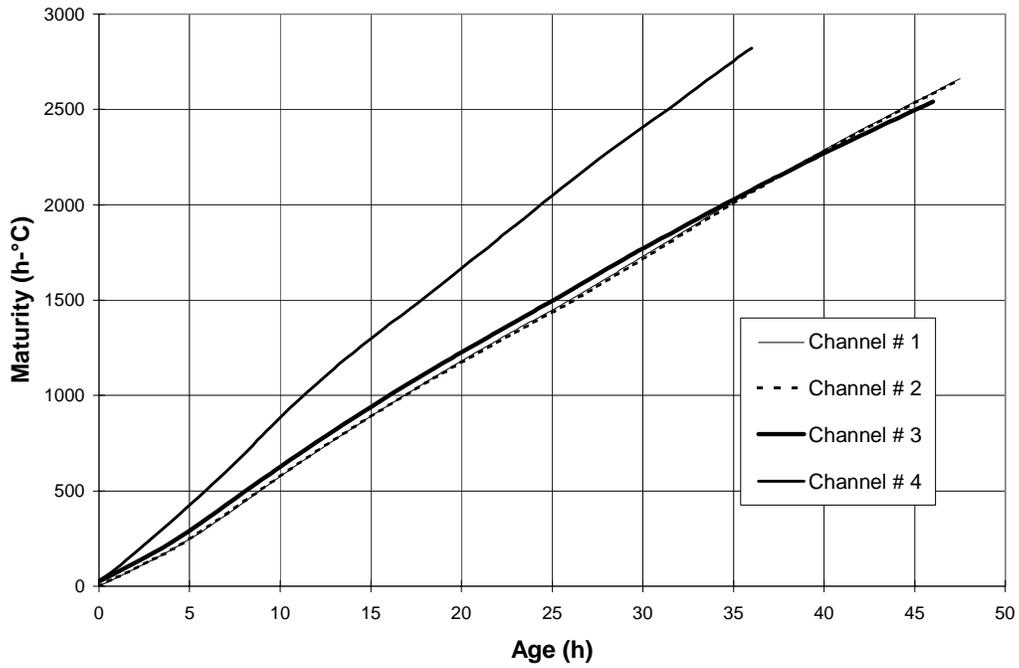*Figure 126. Moisture readings in concrete at three depths, June 22, 1994.*
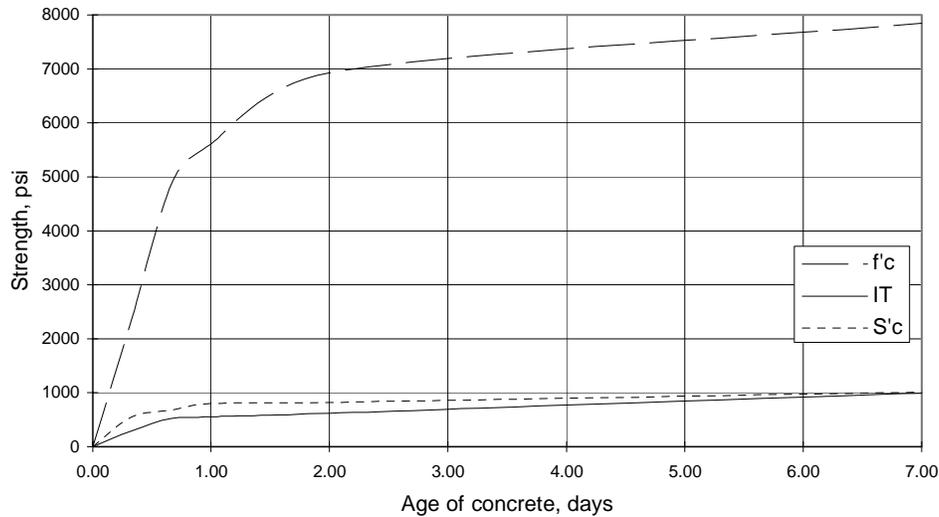

Figure 127. Maturity versus age in test slab.

178

Figure 128. Strength development in concrete test specimens.

D.3   Brazos County, Texas

Phase I, November 1994

The laboratory bond tests were performed at the Texas Transportation Institute Annex, at the Texas A&M University Riverside campus. The Riverside campus is an old military airfield managed by the Texas A&M University System for research purposes. The first phase of testing at the Annex was performed in November of 1994. During this phase of testing, significant information was attained regarding the methods available for isolating a test specimen insitu. This was largely a trial and error process. Of all the methods investigated, the PVC ring with dual tapered sides proved to be the most effective. Figure 129 shows the results of torsional shear strength testing from the first phase of testing at the TTI annex. These results were similar to the Iowa field tests in that the torsional shear strength increased gradually during the first 24 h after construction. This was followed by a "flattening" of the strength gain curve over the next seven days. There was actually a slight drop in bond strength as measured in the field. However, this drop may have been variability in the testing apparatus. Only a fraction of the prepared surface at the Annex was used for these tests. Figure 130 shows the results of the break off tests that were performed concurrently with the torsional shear tests. The missing data points were the result of difficulties encountered in trying to isolate test specimens insitu. Figures 131 and 132 show the corresponding compressive and flexural strength test results for the concrete used in the bond tests.
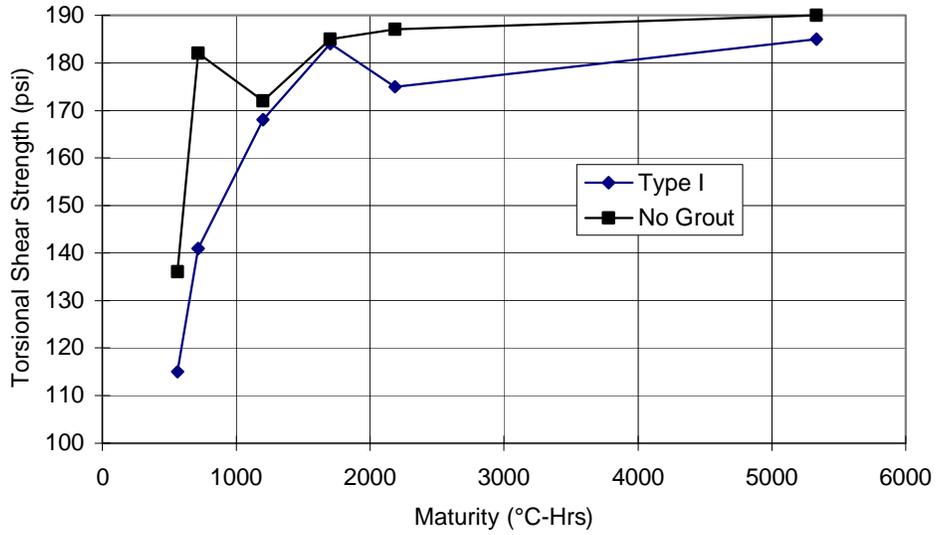
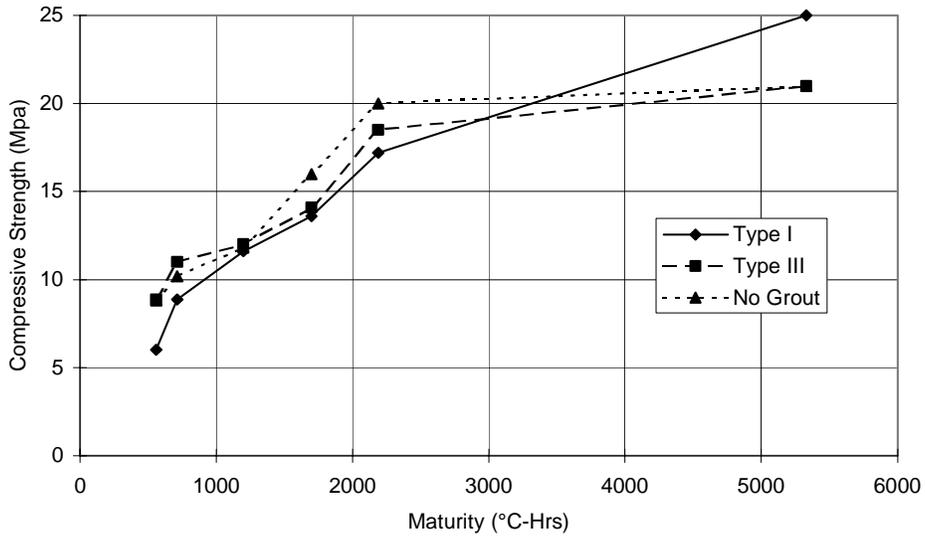*Figure 129. Torsion shear tests, November 15, 1994.*
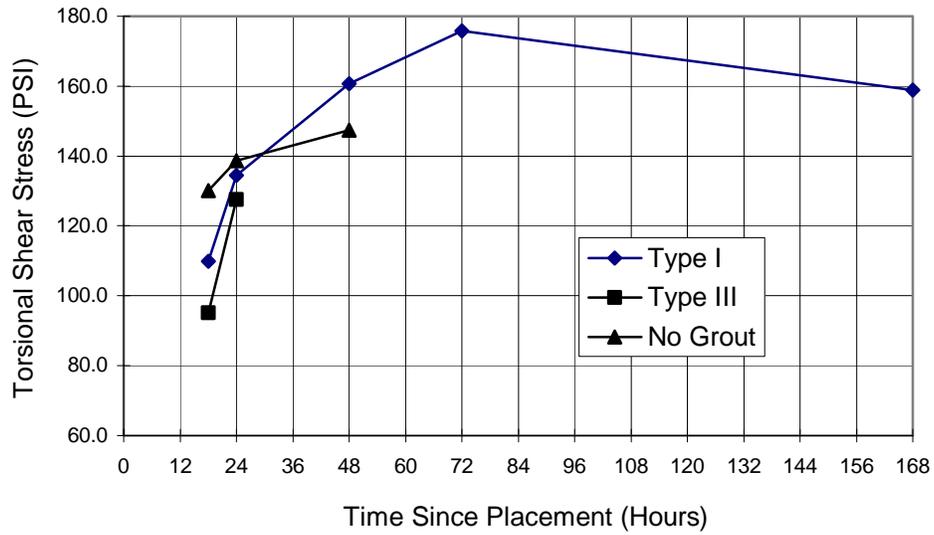

Figure 130. Break off tests, November 15, 1994.

180

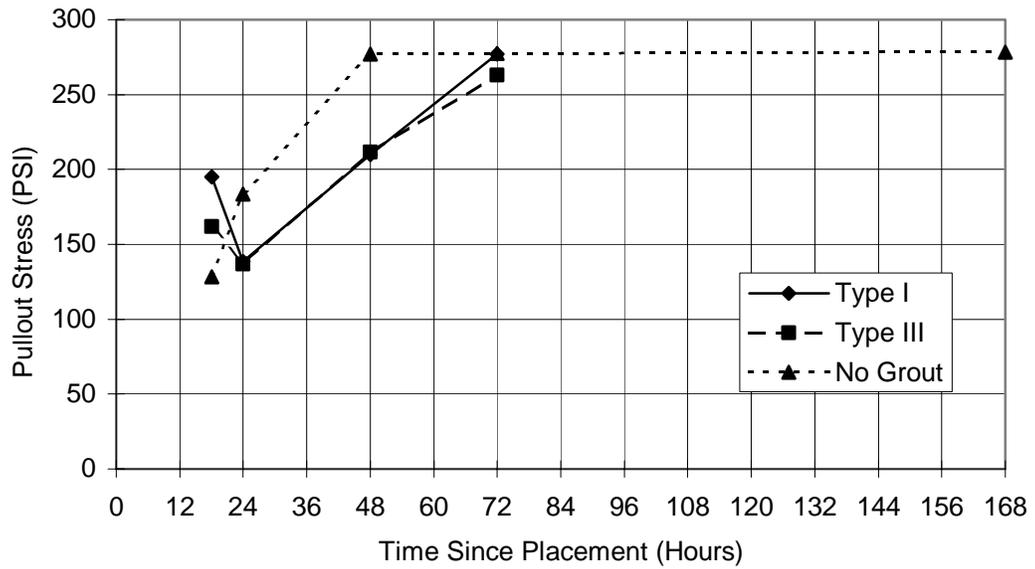*Figure 131. Torsion shear test, November 15, 1994.*

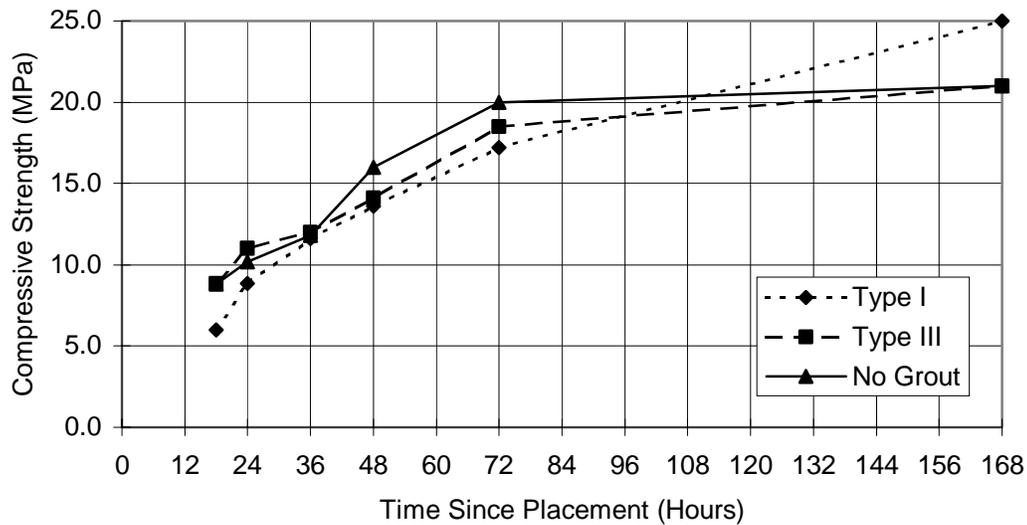*Figure 132. Pullout test results, November 15, 1994.*

Figure 133. Break off test results, November 15, 1994.

Phase II, July 1995

Using the knowledge that was gained from the first round of testing at the Annex, phase II testing was planned for the following summer. This round of testing was performed during the month of July 1995. For this phase of testing, the torsional shear and break off tests were selected for bond strength tests due to the numerous advantages over all other forms of testing.

During this phase of testing, three grout types were again investigated. All sections were cured with an insulated cotton mat followed by a polyethylene sheet. For each data point, two specimens were tested and the average was recorded. These averages are plotted in Figure 134. While the general strength gain patterns were similar for these test techniques, there were some differences. The type III cement grout section resulted in a slight decrease in strength of approximately 1900 degree-h after placement. Subsequently, the type III grout sections showed a gradual increase in strength. The type I cement grout section resulted in a more uniform strength gain pattern during the first 3500 degree-h (≈48 h) after placement. However, this data suggested a slight drop in bond strength at 4000 degree h (≈56 h) after placement. The "no-grout" section provided a uniform increase in strength through 6000 degree-h. This was followed by slight reduction in bond strength.

This data would suggest that the type I cement grout does not significantly increase bond strength at early ages in the pavements life. Additional testing would be required to develop results for periods greater than the first 72 h after construction. The results of the tests conducted are presented in figures 134 through 138.
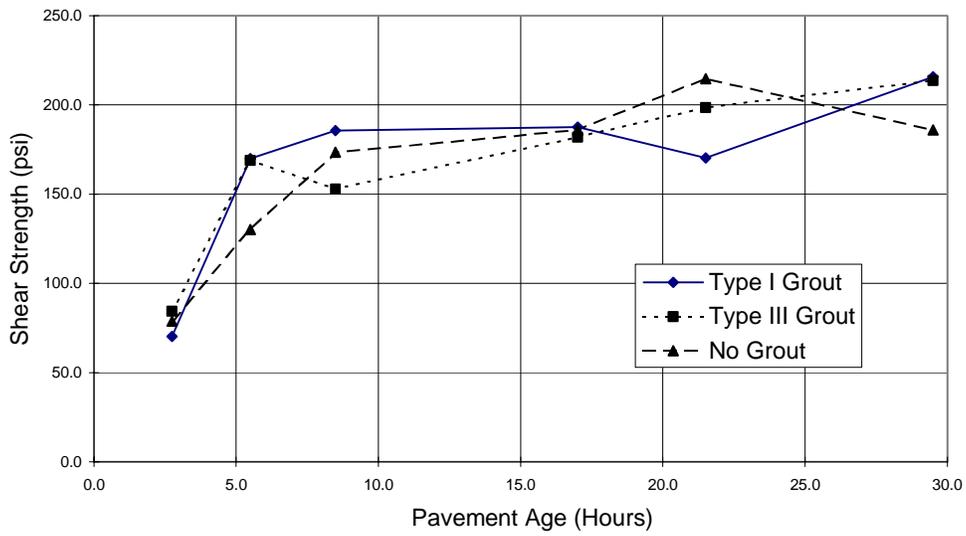
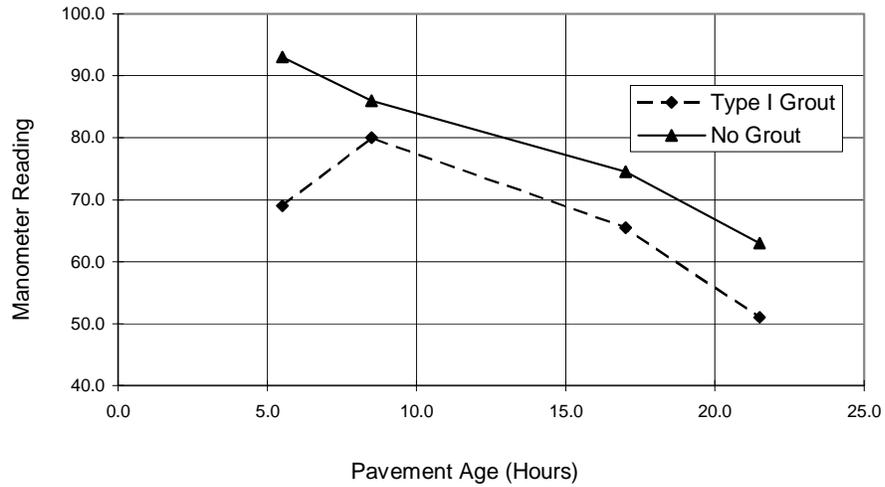*Figure 134. Torsion shear strength versus pavement age.*

Figure 135. Break-off manometer readings versus pavement age.
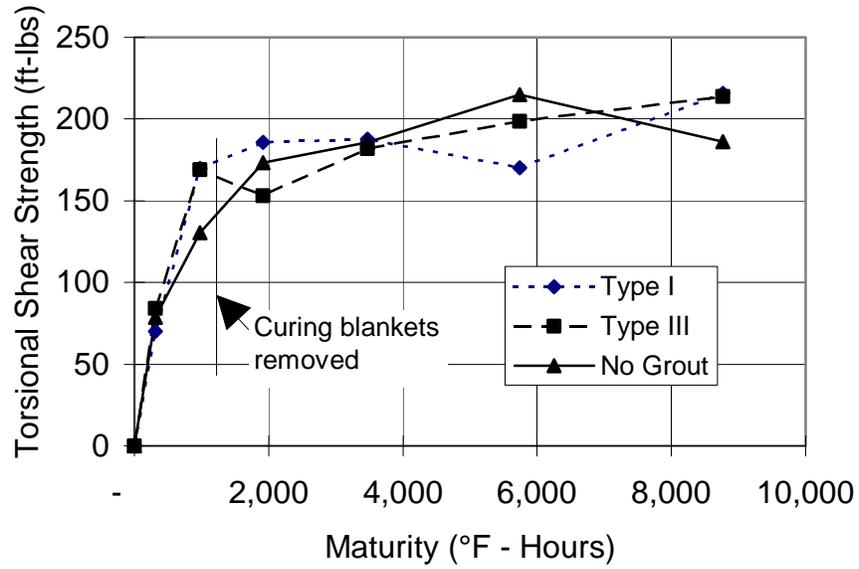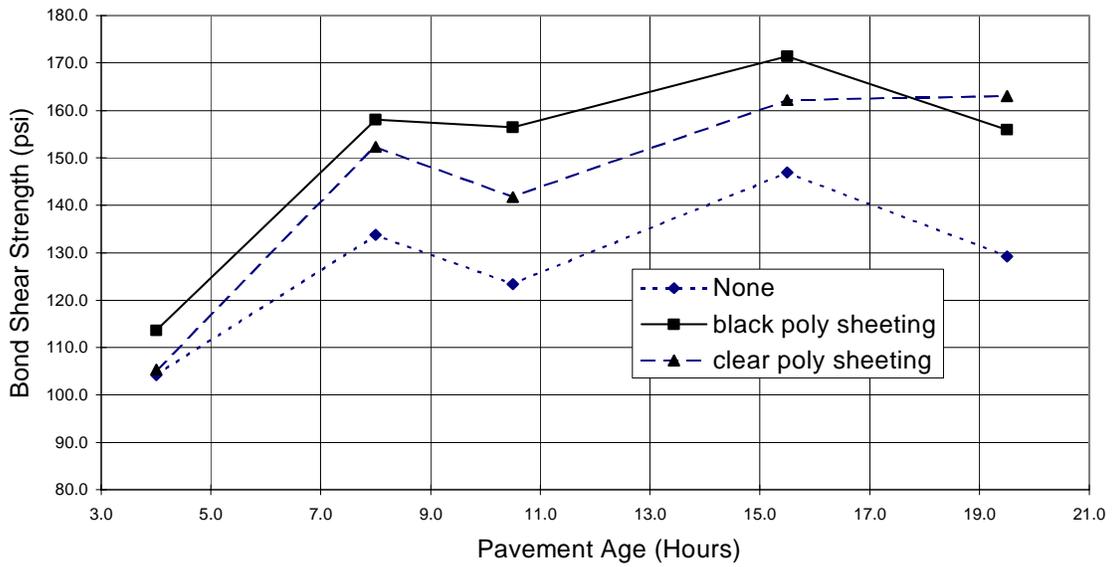
Figure 136. Torsional shear strength versus maturity.

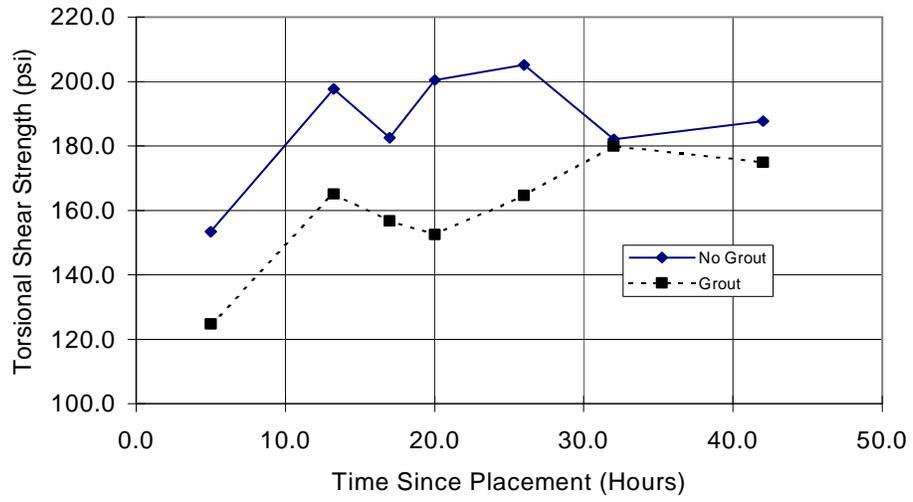*Figure 137. Bond strength versus pavement age, 3000 lbf/in² mix.*

184

Figure 138. Torsion shear tests on grout and no grout sections, July 28, 1995.

REFERENCES

(1) Senadheera, S. P., and D. G. Zollinger, *Influence of Coarse Aggregate in Portland Cement Concrete on Spalling of Concrete Pavements*, Research Report 1244-11, Texas Transportation Institute, College Station, Texas, 1994.

(2) *"Structure and Performance of Cements,"* edited by P. Barnes, Applied Sciences Publishers.

(3) Kosmatka, Steven H., and Panarese, William C**.. Design and Control of Concrete Mixtures, 13th ed.** Portland Cement Association, 1988.

(4) Richardson, J.M. and Armaghani, J.M., "*Stress Caused by Temperature Gradient in Portland Cement Concrete Pavements,"* **TRR** No. 1121, Transportation Research Board, Washington, D.C., 1987.

(5) Okamoto, P.A., et. al. *Guidelines for Timing Contraction Joint Sawing and Earliest Loading for Concrete Pavements*, FHWA Publication Nos. FHWA-RD-91-079 and FHWA-RD-91-080, Volumes I and II, 1994.

(6) Zollinger, D. G., and E. J. Barenberg, *Continuously Reinforced Pavements: Punchouts and Other Distresses and Implications for Design*, Project IHR - 518, Illinois Cooperative Highway Research Program, University of Illinois, Urbana, Ill., 1990.

(7) Koesno, K, and B. F. McCullough, *"Evaluation of the Performance of the Bonded Concrete Overlay on Interstate Highway 610 North, Houston, Texas,"* Research Report 920-2, Center for Transportation Research, The University of Texas at Austin, December, 1987.

(8) Reynolds, William C., and Perkins, Henry C., **Engineering Thermodynamics**, McGraw-Hill, New York, 1977.

(9) Emborg, M., *"Thermal Stresses in Concrete Structures at Early Ages,"* Doctoral Thesis, Lulea University of Technology, Sweden, 1989.

(10) Trinhztfy, H. W., Blaauwendraad J., and Jongendijk, J. *"Temperature Development in Concrete Structures Taking Account of State Dependent Properties,"* **Proceedings from RILEM International Conference on Concrete at Early Ages, Vol. I**. Paris, 1982, pp. 211-218.

(11) **Computer Interactive Maturity System**. Operating Manual. Digital Site Systems, Inc., Pittsburgh, 1988.

(12)   Hsieh, C.K., Qin, C., and Ryder, E.E., *"Development of Computer Modeling for Prediction of Temperature Distribution inside Concrete Pavements,"* Mechanical Engineering Department, University of Florida, Report FL/DOT/SMO/90-374, Gainesville, Florida, 1989.

(13)   Truman, K.Z., Petruska, D.T., and Norman, C.D., *"Creep, Shrinkage, and Thermal Effects on Mass Concrete Structure,"* **Journal of Engineering Mechanics** Vol. 117, No. 6, June 1991, pp. 1274-1288.

(14)   Yargicoglu, A. and Johnson, C.P., *"Temperature Induced Stresses in Highway Bridges by Finite Element Analysis and Field Tests,"* Research Report 23-3F, Center for Transportation Research, The University of Texas at Austin, July 1978.

(15)   Byfers, J., *"Plain Concrete at Early Ages,"* Research 3:80, Swedish Cement and Concrete Research Institute, Stockholm, Sweden, 1980.

(16)   Ndon, U. J., and K. L. Bergeson, *Thermal Expansion of Concretes: Case Study in Iowa*, Journal of Materials in Civil Engineering, Vol. 7, No. 4, November 1995.

(17)   Breugel, K.V., *"Simulation of Hydration and Formulation of Structure in Hardening Cement-based Materials,"* Delft University of Technology, Netherlands, Nov. 1991.

(18)   Emanuel, J.H. and Hulsey, J.L., *"Prediction of the Thermal Coefficient of Expansion of Cement,"* **ACI Journal.** Vol: 74, No. 4, Apr. 1977, pp. 149-154.

(19)   Mindess, S. and Young, T.F.. **Concrete.** Prentice-Hall Inc., Englewood Cliffs, New Jersey, 1981.

(20)   Green, W. J., R. L. Carrasquillo, and B. F. McCullough, Coarse Aggregate for PCC -- Pilot Study Evaluation, Research Report 422-1, Center for Transportation Research, The University of Texas at Austin, September, 1987.

(21)   Bazant, Z. P. and Baweja, Sandeep, *"Creep and Shrinkage Prediction Model for Analysis and Design of Concrete Structures - Model B_3,"* **RILEM Materials and Structures**, Vol 28, 1995, pp. 357-365.

(22)   Westergaard, H. M., *"Analysis of Stresses in Concrete Pavements Due to Variations of Temperature,"* Proceedings of the Sixth Annual Meeting, Highway Research Board, 1927.

(23)   Bradbury, R. D., **Reinforced Concrete Pavements,** Wire Reinforcement Institute, Washington, D. C., 1938.

(24)   Carino, N. J., and Tank, R. C*., "Maturity Functions for Concretes Made with Various Cements and Admixtures,"* **ACI Materials Journal**, Vol. 89, No. 2, 1992, pp. 188-196.

(25)   Umehara, H., et. al., *"Effect of Creep in Concrete at Early Ages on Thermal Stress,"* **RILEM Thermal Cracking in Concrete at Early Ages**, ed. by Springenschmid, R., 1994, pp. 79-86.

(26)   Xin, Dapeng, Zollinger, Dan G., and James, Ray W., *"One-Dimensional Model for Analysis of CRC Pavement Growth,"* **ASCE Journal of Transportation Engineering**, Vol. 118, Number 4, July/August 1992, pp. 557-575.

(27)   Wimsatt, Andrew W., McCullough, B. Frank, and Burns, Ned H., *"Methods of Analyzing and Factors Influencing Frictional Effects of Subbases,"* Research Report 459-2F, Center for Transporttion Research, Austin, 1987.

(28)   Rostasy, F.S., Gutsch, A., and Laube, M., *"Creep and Relaxation of Concrete at Early Ages - Experiments and Mathematical Modeling,"* **RILEM Thermal Cracking in Concrete at Early Ages**, ed. by Springenschmid, R., 1994, pp. 453-458.

(29)   Chen, Du, Cheng, Shun, and Gerhardt, T.D., *"Thermal Stresses in laminated Beams,"* **Journal of Thermal Stresses**, Vol 5, 1982, pp. 67-82.

(30)   Pihlajavaara, S.E., *"Introductory Bibliography for Research on Drying of Concrete,"* The State Institute for Technical Research, Helsinki, 1964.

(31)   Kasi, S.S.H., and Pihlajavaara, S.E., *"An Approximate Solution of a Quasi-Linear Diffusion Problem,"* Publication No. 153, The Station Institute for Technical Research, Helsinki, 1969.

(32)   Bazant, Z.P., *"Constitutive Equation for Concrete Creep and Shrinkage Based on Thermodynamics of Multiphase Systems,"* **Materials and Structures** (RILEM), Vol. 3, No.13, 1970, pp. 3-36.

(33)   Bazant and Najjar, L.J., *"Nonlinear Water Diffusion in Nonsaturated Concrete,"* **Materials and Structures** (RILEM), Vol. 5, No. 25, 1972.

(34)   Parrot, L.J., *"Moisture Profiles in Drying Concrete,"* **Advances in Cement Research**, Vol. 1, No. 3, July 1988.

(35)   Parrot, L.J., *"Factors Influencing Relative Humidity in Concrete,"* **Magazine of Concrete Research**, Vol. 43, No. 154, March 1991.

(36)   Xin, Dapeng and Zollinger, D.G., *"Calibration of Diffusibility Based on Measured Humidity Profiles in hardening Concrete,"* **Advanced Cement Based Materials**, Draft.

(37)   Buch, Neeraj and Zollinger, D.G., *"Preliminary Investigation of Effects of Moisture on Concrete Pavement Strength and Behavior,"* **TRR** No. 1382, Transportation Research Board, Washington, D.C., 1993.

(38)   Bazant, Z.P., *"Thermodynamic Theory of Deformation of Concrete with Explanation of Drying Creep,"* **American Concrete Institute Symposium on Designing for Effects of Creep, Shrinkage and Temperature**, SP 27, p. 411.

(39)   Copeland, L.E., Kantro, D.L., and Verbeck, G*., "Chemistry of hydration of Portland Cement in: Chemistry of Cement,"* **Proceedings of 4th International Symposium,** Washington, D.C., 1960, National Bureau of Standards, Monograph 43, Vol. I, Paper IV-3, 429-465 (PCA Bulletin 153).

(40)   **Distress Identification Manual for the Long-Term Pavement Performance Project**. Strategic Highway Research Program, Federal Highway Administration, SHRP-P-338, 1993.

(41)   Hwang, Tony, and Weissmann, Jose*, "A Study of the Evaporation Rates for the El Paso BCO Project,"* Technical Memorandum 2911-45, Center for Transportation Research, 1995.